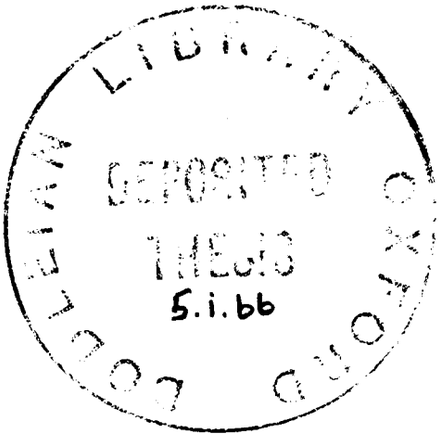
SOME STUDIES OF

CHARGE TRANSFER COMPLEXES.



A thesis submitted by

J.D. WRIGHT

of

MAGDALEN COLLEGE

for the degree of

DOCTOR OF PHILOSOPHY.

July 1965.

(LIBRARY COPY).

ACKNOWLEDGMENTS.

The author wishes to express his thanks to:-

Dr. R.J.P. Williams, for his continued guidance and encouragement during the supervision of this work,

Drs. C.K. Prout and B. Kamenar, for their enthusiasm and assistance in the crystallographic part of the work,

Dr. A.S. Bailey and co-workers, for providing many of the electron acceptors used,

The Science Research Council (DSIR), for financial assistance,

The staff of the Inorganic Chemistry Laboratory,

and numerous others, particularly those mentioned at appropriate points in the text, without whose co-operation this work could not have been carried out.

NOTE.

Apart from minor references to work submitted for Part II of the Final Honour School of Chemistry, June, 1963, (whose origin is clearly stated at the appropriate places), none of the work included in this thesis has been submitted, or is being submitted, for any other degree in this or any other University.

INDEX.

Chapter. Page.

1. INTRODUCTION. 1

2. MATERIALS.

2.1. Choice of materials. 3

2.2. Preparations. 5

2.2.1. Starting materials. 5

2.2.2. Molecular complexes. 6

2.2.3. Donor properties of metal complexes with other ligands. 12

2.2.4. Preparations leading to further reactions. 15

2.2.5. Conditions for growing large crystals of the complexes. 16

2.3. Analysis. 17

2.3.1. Carbon, hydrogen, nitrogen and chlorine. 17

2.3.2. Copper. 17

2.3.3. Palladium. 18

2.3.4. Analysis for copper in copper-doped crystals of palladium 8-hydroxyquinolinate/chloranil. 18

3. CRYSTAL STRUCTURES.

3.1. Introduction. 24

3.2. Structural principles of the complexes. 39

4. SPECTRA.

4.1. Theory. 48

Chapter. Page.

4.1.1. Molecular orbital and valence bond approaches to bonding and spectra in molecular complexes. 48

4.1.2. Shape and intensity of charge transfer absorption bands. 55

4.1.3. Appearance of several charge transfer bands. 57

4.1.4. Polarization of charge transfer bands. 57

4.2. Experimental methods. 58

4.3. Results. 60

4.3.1. Molecular complex spectra. 60

4.3.2. Spectroscopic studies of the reactions between strong donors and strong acceptors. 71

4.4. Discussion. 76

4.4.1. Validity of the theories of charge transfer spectra for complexes with metal chelates as donors. 76

4.4.2. Ionization potentials, electron affinities and orbital energies from spectra. 88

4.4.3. Infra-red spectra. 95

5. ELECTRON SPIN RESONANCE.

5.1. Introduction. 97

5.2. Experimental. 98

5.3. Results and discussion. 100

6. ELECTRICAL CONDUCTIVITY.

6.1. Introduction. 110

Chapter. Page.

6.2. Apparatus and techniques. 110

6.2.1. Apparatus for electrical measurements. 110

6.2.2. Apparatus for illuminating the sample. 115

6.2.3. Technique. 120

6.3. Results. 122

6.3.1. Tests of the apparatus. 122

6.3.2. Investigations of photoconductivity in molecular complexes of 8-hydroxyquinoline and its metal complexes with electron acceptors. 129

6.3.3. Photoconductivity of palladium 8-hydroxyquinolinate/chloranil complexes doped with copper 8-hydroxyquinolinate/chloranil. 151

6.3.4. Photoconductivity of copper and palladium 8-hydroxyquinolinates. 155

6.4. Discussion. 162

6.4.1. Summary of facts deduced from experimental results. 162

6.4.2. Mechanisms of photoconduction in molecular complexes. 163

6.4.3. Interpretation of resistivity data for copper-doped palladium 8-hydroxyquinolinate/chloranil complexes. 170

6.4.4. Photoconduction in metal 8-hydroxyquinolinate crystals. 173

6.4.5. Photovoltaic effects. 174

6.4.6. Relevance to the role of quinones in chloroplasts. 175

Chapter. Page.

APPENDIX A. DETERMINATION OF THE CRYSTAL STRUCTURES OF THE COMPLEXES OF bis-8-HYDROXYQUINOLINATO PALLADIUM^{II} WITH CHLORANIL AND 1,2,4,5-TETRACYANOBENZENE. 176

A.1. X-ray photography. 176

A.2. Cell dimensions and crystal data. 177

A.3. Optical goniometry. 178

A.4. Calculations. 181

A.4.1. Palladium 8-hydroxyquinolinate/chloranil. 181

A.4.2. Pd 8-hydroxyquinolinate/1,2,4,5-tetracyanobenzene. 186

A.5. Description of the Pd 8-hydroxyquinolinate/chloranil structure. 187

A.6. Description of the palladium 8-hydroxyquinolinate/1,2,4,5-tetracyanobenzene structure. 188

APPENDIX B. TECHNIQUES OF SOLID STATE SPECTROSCOPY. 228

REFERENCES. 231

ABSTRACT. 236

CHAPTER 1.

INTRODUCTION.

Charge transfer complexes between organic π electron donors and acceptor molecules have been known for many years, and have been extensively studied[1], both in solution and in the solid state, by many techniques. These studies have clarified the nature of charge transfer processes in organic molecules, particularly in aromatic molecules, and have provided a method for studying the effect of substituents on orbital energies.

In the present work, these studies have been extended to organometallic complexes of a similar type, in which the organic π electron donor is replaced by a planar metal complex with an aromatic ligand. The main objectives of the work are as follows:

(i) To study the effects of different metal ions on the energy levels of the ligand π orbitals.

(ii) To investigate the inter-relation between ligand-metal charge transfer processes and those involving charge transfer from filled ligand π-donor orbitals to vacant π orbitals of electron acceptor molecules.

(iii) To study the crystal structures of compounds of this type, to determine what new structural principles apply when charge transfer complexes contain metal ions, and to investigate the effect of structure on physical properties of the complexes.

(iv) To investigate the relation between charge transfer over short distances (of the order of the dimensions of a single molecule of the complex) and charge transfer over much longer distances through a crystal lattice, and to bring to light any cases where the presence of a particular metal ion produces anomalous differences between these two types of charge transfer.

(v) To relate these results to redox reactions of the systems, where charge transfer is complete, to discover the factors conducive to complete electron transfer.

(vi) To discover whether these simple systems have any relevance in understanding the role of certain quinones, such as plastoquinone, which appear in association with chlorophyll in chloroplasts playing a key role in the energy conversion processes of photosynthesis[2].

To simplify the interpretation of results, most of the techniques used have been concerned with the solid state, where the environment is fixed and may be determined precisely by X-ray crystallography. Thus, there is a possibility of separating electronic and environmental effects on charge transfer processes, which is the key to full understanding of these processes. The widespread importance of charge transfer phenomena, both in the bonding and reactions of inorganic complexes, gives considerable significance to any systems such as those used here, which provide fresh experimental results on problems of theoretical interest.

CHAPTER 2.

MATERIALS.

2.1. Choice of Materials.

If an inorganic complex is to form crystalline molecular complexes with electron acceptors, it must satisfy the following requirements:

(i) The ligand must be aromatic or highly conjugated.

(ii) It must form planar complexes with a variety of metals, or the characteristic plane-to-plane stacking of molecules in the lattice of a molecular complex will not be possible. (Large structural variations thus produced may influence other physical properties and prevent valid comparisons with normal complexes.)

(iii) The complexes must be reasonably stable to oxidation, or many of the common electron acceptor molecules will induce complete electron transfer and oxidation of the donor, possibly followed by further reactions, instead of forming a stable molecular complex.

(iv) The complexes must be soluble in solvents which will also dissolve electron acceptor molecules, and the solubility relationship between the donor and acceptor molecules and the solid complex of the two must be such that conditions can be arranged in which the complex will crystallise free from the components.

(v) If possible, the ligand should be capable of modification (e.g. by substituents) while still satisfying the above conditions, so that small electronic changes can be produced easily.

8-hydroxyquinoline is a common ligand satisfying all these requirements, and was therefore chosen for this work. Its complexes with copper, palladium and nickel also satisfy the requirements.

The requirements for suitable electron acceptor molecules are:

(i) The solubility must fit in with criterion (iv) above, for donor molecules.

(ii) The molecule must posses a low energy vacant π orbital of the correct symmetry to receive an electron from one of the filled π orbitals of the donor molecule.

(iii) It must not present excessive steric hindrance to donor molecules approaching to a plane-to-plane position, nor should it be so large that an economical lattice packing in the crystal is difficult.

Research by many workers on organic molecular complexes[1] has produced a large number of suitable molecules of this type, with the result that complexes of 8-hydroxyquinoline and its metal complexes with 13 electron acceptors have been prepared.

2.2. Preparations.

2.2.1. Starting materials.

(a) Acceptor molecules.

Thanks are due to Dr. A.S. Bailey for providing samples of benzotrifuroxan, benzotrifurazan, nitrobenzodifuroxan, dinitrobenzfuroxan, dichloronitrobenzfuroxan, picryl azide and 1,2,4,5-tetracyanobenzene. These were prepared and purified by the published methods[3]. A further supply of tetracyanobenzene was prepared by the author in the same way, and additional samples of benzotrifuroxan were kindly donated by Dr. G. Morpurgo.

Laboratory reagent grade 1,3,5,-trinitrobenzene, 2,4,7-trinitrofluorenone, chloranil and dichlorodicyanoquinone were purified by recrystallisation from ethanol (nitro compounds) or dioxan (quinones).

Tetracyanoethylene was used as supplied by Kodak Ltd.

(b) Donor molecules.

B.D.H. AnalaR 8-hydroxyquinoline was used as a donor without further purification, and was also used to prepare copper(II), palladium(II) and nickel(II) chelates, as follows:

Copper: 8-hydroxyquinoline (3 gm.) in warm ethyl alcohol (30 ml.) was added to a solution of AnalaR copper acetate (2 gm.) in hot distilled water (150 ml,), with stirring. The solid

was collected, washed well with hot distilled water, and dried for several hours at 140°C.

Palladium: $Pd(NH_3)_2Cl_2$ (0·21 gm.) was dissolved in hot distilled water and filtered into a solution of 8-hydroxyquinoline (0·3 gm.) in AnalaR glacial acetic acid. The yellow solid was washed well with hot distilled water and dried for several hours at 120°C.

Nickel: 8-hydroxyquinoline (3 gm.) in warm ethyl alcohol (30 ml.) was added to an acidic solution of AnalaR $NiCl_2.6H_2O$ (2·4 gm.) with stirring. The solid was collected, washed well with hot distilled water, and dried for several hours at 140°C.

Several other complexes were prepared, to test their suitability as donors in molecular complexes, and the results of these experiments are described in section 2.2.3, below.

2.2.2. Molecular complexes.

Molecular complexes of 8-hydroxyquinoline and its metal complexes were prepared by dissolving the donor compound in a slight excess of the hot solvent (usually distilled chloroform) and adding the calculated quantity of the solid acceptor compound. the solution was then warmed, filtered, and allowed to crystallise slowly. Picryl azide complexes were prepared at temperatures below 40°C, to avoid decomposition of the azide. The complexes were washed with a little of the cold solvent and dried in a dessicator.

8-hydroxyquinoline complexes.

(i) With benzotrifuroxan[4].

Pale yellow plates from n-propanol.

(Found: C, 52·9; H, 2·6; N, 21·0 % .

$(C_9H_7NO)_2C_6N_6O_6$ requires C, 52·1; H, 2·6; N, 20·7 %).

(ii) With trinitrobenzene.

Yellow needles from chloroform.

(Found: C, 50·5; H, 2·7; N, 16·0 % .

$C_9H_7NO.C_6H_3N_3O_6$ requires C, 50·3; H, 2·8; N, 15·6 %).

(iii) With picryl azide.

Yellow needles from ethanol.

(Found: C, 45·5; H, 2·3; N, 24·7 % .

$C_9H_7NO.C_6H_2N_6O_6$ requires C, 45·1; H, 2·3; N, 24·6 %).

(iv) With trinitrofluorenone.

Fine orange needles from chloroform.

(Found: C, 61·6; H, 3·2; N, 11·6 % .

$(C_9H_7NO)_2.C_{13}H_5N_3O_7$ requires C, 61·5; H, 3·2; N, 11·6 %).

(v) With tetracyanobenzene.

Yellow needles from glacial acetic acid.

(Found: C, 70·0; H, 2·8; N, 21·9 % .

$C_9H_7NO.C_{10}H_2N_4$ requires C, 70·6; H, 2·8; N, 21·7 %).

Bis 8-hydroxyquinolinato copper (II) complexes.

(i) With benzotrifuroxan[4].

Brown prisms from chloroform.

(Found: Cu, 10·3; C, 47·4; H, 2·1; N, 19·2 % .

$Cu(C_9H_6NO)_2.C_6N_6O_6$ requires Cu, 10·5; C, 47·7; H, 2·0; N, 18·6 %).

(ii) With dinitrobenzfuroxan.

Brown microcrystals from chloroform.

(Found: Cu, 10·4; C, 50·0; H, 3·2; N, 14·7 % .

$Cu(C_9H_6NO)_2.C_6H_2N_4O_6$ requires Cu, 11·0; C, 49·9; H, 2·4; N, 14·5 %).

(iii) With trinitrobenzene.

Dark red needles from tetrachlorethane.

(Found: Cu, 8·1; C, 46·3; H, 2·7; N, 14·3 % .

$Cu(C_9H_6NO)_2.2C_6H_3N_3O_6$ requires Cu, 8·2; C, 46·3; H, 2·3; N, 14·4 %).

(iv) With picryl azide.

Dark red needles from tetrachlorethane.

(Found: Cu, 7·3; C, 41·7; H, 2·1; N, 23·0 % .

$Cu(C_9H_6NO)_2.2C_6H_2N_6O_6$ requires Cu, 7·4; C, 41·9; H, 1·9; N, 22·8 %).

(v) With trinitrofluorenone.

Brown microcrystals from $CHCl_3$ + $C_2H_2Cl_4$.

(Found: Cu, 9·2; C, 56·2; H, 3·0; N, 10·3 % .

$Cu(C_9H_6NO)_2.C_{13}H_5N_3O_7$ requires Cu, 9·5; C, 55·8; H, 2·6; N, 10·5 %).

(vi) With tetracyanobenzene.[4]

Black needles from chloroform.

(Found: Cu, 8·9; C, 64·0; H, 1·8; N, 20·4 % .

$Cu(C_9H_6NO)_2.2C_{10}H_2N_4$ requires Cu, 9·0; C, 64·5; H, 2·5; N, 19·8 %).

(vii) With chloranil.

Blue-violet needles from chloroform.

(Found: Cu, 10·5; C, 48·5; H, 2·4; N, 5·1; Cl, 23·8 % .

$Cu(C_9H_6NO)_2.C_6O_2Cl_4$ requires Cu, 10·6; C, 48·2; H, 2·0;
N, 4·7; Cl, 23·7 %).

(viii) With dichlorodicyanoquinone.

Dark green microcrystals from chloroform.

(Found: Cu, 11·0; C, 53·9; H, 2·1; N, 9·0; Cl, 12·0 % .

$Cu(C_9H_6NO)_2.C_8N_2O_2Cl_2$ requires Cu, 11·0; C, 53·9; H, 2·1;
N, 9·7; Cl, 12·2 % .)

Bis 8-hydroxyquinolinato palladium (II) complexes.

(i) With benzotrifuroxan.

Scarlet needles from chloroform.

(Found: Pd, 16·4; C, 44·5; H, 1·9; N, 17·5 % .

$Pd(C_9H_6NO)_2.C_6N_6O_6$ requires Pd, 16·5; C, 44·5; H, 1·9; N, 17·3 % .)

(ii) With dinitrobenzfuroxan.

Brown microcrystals from chloroform.

(Found: Pd, 16·0; C, 45·0; H, 3·1; N, 13·3 % .

$Pd(C_9H_6NO)_2.C_6H_2N_4O_6$ requires Pd, 17·1; C, 46·4; H, 2·3; N, 13·5 %).

(iii) With trinitrofluorenone.

Brown microcrystals from chloroform.

(Found: Pd, 15·0; C, 52·0; H, 2·3; N, 9·8 % .

$Pd(C_9H_6NO)_2.C_{13}H_5N_3O_7$ requires Pd, 15·0; C, 52·4; H, 2·4; N, 9·9 %).

(iv) With tetracyanobenzene.

Very dark red prisms from chloroform.

(Found: Pd, 18·1; C, 58·5; H, 2·5; N, 14·8 % .

$Pd(C_9H_6NO)_2.C_{10}H_2N_4$ requires Pd, 18·6; C, 58·7; H, 2·5; N, 14·7 %).

(v) With Chloranil.

Very dark green needles from chloroform.

(Found: Pd, 16·3; C, 46·0; H, 2·0; N, 4·5; Cl, 22·3 % .

$Pd(C_9H_6NO)_2.C_6O_2Cl_4$ requires Pd, 16·6; C, 45·0; H, 1·9;
N, 4·4; Cl, 22·1 %).

(vi) With dichlorodicyanoquinone.

Dark blue-green powder from chloroform.

(Found: Pd, 16·9; C, 50·2; H, 2·2; N, 7·6; Cl, 11·8 % .

$Pd(C_9H_6NO)_2.C_8N_2O_2Cl_2$ requires Pd, 17·1; C, 50·2; H, 1·9;
N, 9·0; Cl, 11·4 %).

Thanks are due to Miss J.M. Evans for preparing the complexes of benzotrifurazan, and to Miss F. Pick for preparing the complexes of dichloronitrobenzfuroxan, with copper and palladium 8-hydroxyquinolinates and with pyrene and other organic donors. Details of these preparations are recorded elsewhere[3, 5].

The complexes of copper 8-hydroxyquinolinate with benzotrifuroxan and tetracyanobenzene, and of 8-hydroxyquinoline with benzotrifuroxan, have been described previously (see reference 4 - the author's Part II thesis).

The preparation of the copper 8-hydroxyquinolinate complex of tetracyanoquinodimethane has recently been reported[6].

The following complexes could not be prepared in a pure state, owing to unfavourable solubility relationships: palladium 8-hydroxyquinolinate complexes of trinitrobenzene, picryl azide, nitrobenzodifuroxan and tetracyanoethylene; copper 8-hydroxyquinolinate complexes of nitrobenzodifuroxan, tetracyanoethylene, benzoquinone and 1,2,4,5-benzenetetracarboxylic anhydride.

Bis 8-hydroxyquinolinato nickel (II) complexes.

Attempts to prepare these complexes as pure solids failed, owing to the poor solubility of the nickel complex relative to the electron acceptors and the molecular complexes, in all available organic solvents. However, impure complexes, containing some of the free components, have been isolated with benzotrifuroxan, tetracyanoethylene and chloranil, from o-dichlorobenzene. Charge transfer interactions definitely exist in solution, as shown by the spectra.

Complexes with organic donors, used in the spectroscopic work, have been described elsewhere[3-5].

2.2.3. Donor properties of metal complexes with other ligands.

(The majority of these complexes are not of great interest in the present work, but details are given here for the benefit of future workers in this field.)

Small samples of the crystalline complexes of palladium and copper 5-methyl-8-hydroxyquinolinates with chloranil were prepared for spectroscopic work, from chloroform solution, by methods identical to those used for the corresponding 8-hydroxyquinolinate complexes. Attempts to prepare similar complexes from nickel 5-methyl-8-hydroxyquinolinate failed, for solubility reasons.

Copper complexes of 5-fluoro- and 5-cyano-8-hydroxyquinoline were soluble in chloroform, but did not form isolable chloranil complexes.

Copper complexes of 5-aldoxime- and 5,7-di-iodo-8-hydroxyquinoline were prepared, but were insoluble or only very slightly soluble in all available solvents.

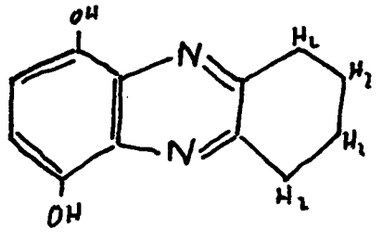
The attempted preparation of the copper complex of 5-amino-8-hydroxyquinoline led to oxidation of the ligand, owing to enhancement of ligand-metal charge transfer by the amino substituent.

The following metal complexes were tested for ability to form molecular complexes, but proved of no use, either because

they were insoluble or did not form complexes when mixed with electron acceptors in solution:

8-hydroxyquinoline complexes of Ag(I), Mg, Mn(II), Cd, Co(II), and Zn;

Copper complexes of salicylaldehyde, 5-chlorosalicylaldehyde-imine, α-nitroso-β-naphthol, o-hydroxyacetophenone, dibenzoylmethane, acetaldehyde benzoic hydrazone, nicotinic acid, and



(The behaviour of the last of these ligands is interesting. In cool dilute solution it forms a black crystalline solid with copper salts. In hot, more concentrated solutions a purple powder is produced. On warming this purple solid in tetrachlorethane, a proportion dissolves, giving a black residue and a brown solution. The black solid from cool solutions is insoluble in all common solvents. The two products may be different coordination polymers, with large delocalised π electron systems, and the electrical properties of the solids would be interesting if larger crystals could be prepared.)

8-mercaptoquinoline complexes of copper, palladium and nickel were prepared on a small scale from a sample of the sodium salt of the ligand, kindly donated by Dr. Quintus Fernando[7]. No

complexes with electron acceptors were obtained when procedures similar to those used for corresponding 8-hydroxyquinoline complexes were applied, but experiments on larger quantities of materials than were available might prove more succesful, as the metal complexes appear to be slightly soluble in chloroform.

Investigations were carried out to test the possibility of forming complexes between metal complexes with neutral ligands, such as stilbene diamine and o-phenanthroline, and anionic electron acceptors, such as the picrate anion. Previous work on materials of a similar type has included the preparation of $Co(NH_3)_6$ picrate and $Co(en)_3$ picrate[8], bis(3-nitrosalicylaldehyde)-2,2'bipyridyl Cu^{II}/picric acid complex[9], and bis aquo acetyl-acetonato Cu^{II}picrate[10], but no complexes in which the metal is surrounded by uncharged aromatic ligands in a plane, with picrate anion above the ligands in a plane-to-plane arrangement, completing the coordination sphere of the metal ion, have as yet been reported.

o-phenanthroline was shown to form a yellow crystalline complex with picric acid, from ethanol. In an attempt to prepare Cu^{II} o-phenanthroline picrate, the calculated quantity of o-phenanthroline was dissolved in ethanol and added to a solution of AnalaR $CuCl_2.2H_2O$ + picric acid in hot ethanol (yellow), with stirring. The solution turned a vivid green, and was allowed to stand in the dark. Green crystals (plates) formed, and were

filtered and dried in a dessicator. A corresponding preparation was carried out with nickel chloride. The spectra of the products showed bands at 425-450 mμ, where the bis o-phenanthroline bis chloride complexes do not show strong bands, but these bands are virtually identical to the new bands in the o-phenanthroline/picric acid complex. It may therefore be concluded that in this system, metal ions are not producing a large perturbation of the ligand orbital energies. (The spectrum shows bands characteristic of the metal o-phenanthroline complex, showing that the product is not simply the o-phenanthroline/picric acid complex.)

An attempt was made to prepare (copper bis stilbene diamine)$^{2+}$ $(picrate)_2^-$ by adding an alcoholic solution of picric acid, neutralised with alcoholic NaOH, to an alcoholic solution of Cu bis stilbene diamine bis chloride (kindly supplied by Dr. I.R. Gordon). The blue copper complex solution changed to a greenish colour on adding the yellow picrate solution, but no complex separated.

This line of investigation was therefore not pursued further, although work with anions of stronger acceptors (such as $TCNQ^-$ [6]) might provide examples of materials of this type with more interesting properties.

2.2.4. Preparations leading to further reactions.

When a chloroform solution of dichlorodicyanoquinone is

added to solutions of 8-hydroxyquinoline or its nickel complex in chloroform, the solutions first become dark coloured (deep olive green and magenta, respectively), when hot. However, these solutions do not give crystalline molecular complexes, as further reaction takes place, giving green-yellow precipitates and a rapid fading of the transient charge-transfer colour. A similar reaction occurs between 8-hydroxyquinoline and tetracyanoethylene in ethyl acetate solution. Reactions of a similar type between tetramethyl p-phenylenediamine and dichloroquinone have been reported recently by Foster and Thomson[11]. These reactions may be due to complete electron transfer, followed by further reaction[11] or to Diels-Alder type reactions assisted by the formation of the molecular complex as a transient species[12].

Spectroscopic work on these systems is reported in section 4.3.

2.2.5. Conditions for growing large crystals of the complexes.

For electrical conductivity and electron spin resonance work, large crystals of the complexes are required. Experience has shown that these can be produced in favourable cases by slow crystallisation from dilute solutions of the mixed components, over a period of about one week. Essential precautions are:

(i) The use of distilled solvents and dry materials

(ii) The careful filtration of the solutions before leaving

them to stand, and

(iii) The use of carefully cleaned flasks for the crystallisation.

These conditions give a low concentration of nucleating centres which can initiate crystallisation, and, provided the solutions are not disturbed, they are likely to produce crystals of any complex in which the solubility relationships between the donor, acceptor, and complex are correct. Slow crystallisation was particularly valuable in the preparation of a series of complexes of palladium 8-hydroxyquinolinate with chloranil, in which varying percentages of the palladium complex were replaced by the copper complex in the preparation. These complexes incorporate the copper-containing molecule into the same lattice as the pure palladium complex, as shown by optical goniometry (see chapter 3), and slow crystallisation ensures near-equilibrium conditions for this process throughout the growth time of the crystals.

2.3. Analysis.

2.3.1. Carbon, hydrogen, nitrogen and chlorine were analysed by Drs. Weiler and Strauss, of Oxford, or by Alfred Bernhardt, of the Microanalytical Laboratory, Max Planck Institut für Kohlenforschung, Mülheim, Germany.

2.3.2. Copper was analysed by colourimetric microanalysis, using biquinolyl as the reagent, by the method described in Sandell's

"Colourimetric determination of traces of metals" (3rd. edition, 1959), p. 453. A standard calibration curve was prepared using eight solutions containing up to 80 micrograms of copper in 40 ml., prepared from a stock solution made by dissolving a weighed amount of pure copper metal in dilute nitric acid. Beer's law was obeyed in the conditions used. The samples for analysis were weighed, fumed down with a mixture of concentrated sulphuric acid plus a little concentrated nitric acid, and diluted to a known volume for use in the analytical method. Each analysis was repeated three times.

2.3.3. Palladium was analysed by colourimetric microanalysis, using the p-nitrosodimethylaniline method described by Overholser and Yoe (J. Amer. Chem. Soc. 63 3224 (1941)). Johnson Matthey "Specpure" $(NH_4)_2PdCl_4$ was used in preparing a standard calibration curve for the method. It was necessary to keep the solutions acidic before use, to prevent hydrolysis, and to adjust to the correct pH with a little sodium hydroxide solution immediately before adding the reagent. Beer's law was obeyed in the conditions used. The samples for analysis were weighed, fumed down with equal volumes of concentrated perchloric and hydrochloric acids, and diluted to a known volume for analysis. Each analysis was repeated three times.

2.3.4. Analysis for copper in copper doped crystals of palladium 8-hydroxyquinolinate/chloranil.

The concentrations of copper in the particular crystals which were used in electrical conductivity measurements must be determined before interpretations of the measurements can be attempted. It cannot be assumed that the percentages of copper used in the preparations and present in the resulting crystals are the same, or that all crystals from any one preparation contain identical percentages of copper. Therefore, a method for determining copper concentrations of less than 3 % in small single crystals is required.

Direct chemical analysis of such small quantities is difficult. The samples were therefore analysed by the X-ray fluorescence method. The apparatus used incorporated a curved diffracting crystal to provide sharply focussed monochromatic X-rays on a very small area of the sample[13]. This area was smaller than the crystal, so the intensity of the fluorescence was dependent only on copper concentration and not on crystal size. The intensity of the first order Cu K_α line of the fluorescence was measured using an automatic counter, and taking counts over 40 seconds. Table 2.1 shows the count rates obtained for crystals of ten different compositions. The likely errors in count due to statistical fluctuations of the process are approximately equal to $\pm \sqrt{\text{count-rate}}$.

Thanks are due to Miss Julia Stern, who carried out the measurements, and to Dr. D.T. Hall, for providing facilities for this work.

TABLE 2.1.

Analysis for copper in copper-doped palladium 8-hydroxyquinolinate/chloranil complexes. X-ray fluorescence ($Cu\ K_\alpha$) data.

Percent of copper complex in the preparation.	Intensity of Cu K_α X-ray fluoreseence. (counts/sec.)
100	2150
30	920
27	705
24	660
22	590
16	350
10	250
5	230
1	56
0 (background)	25

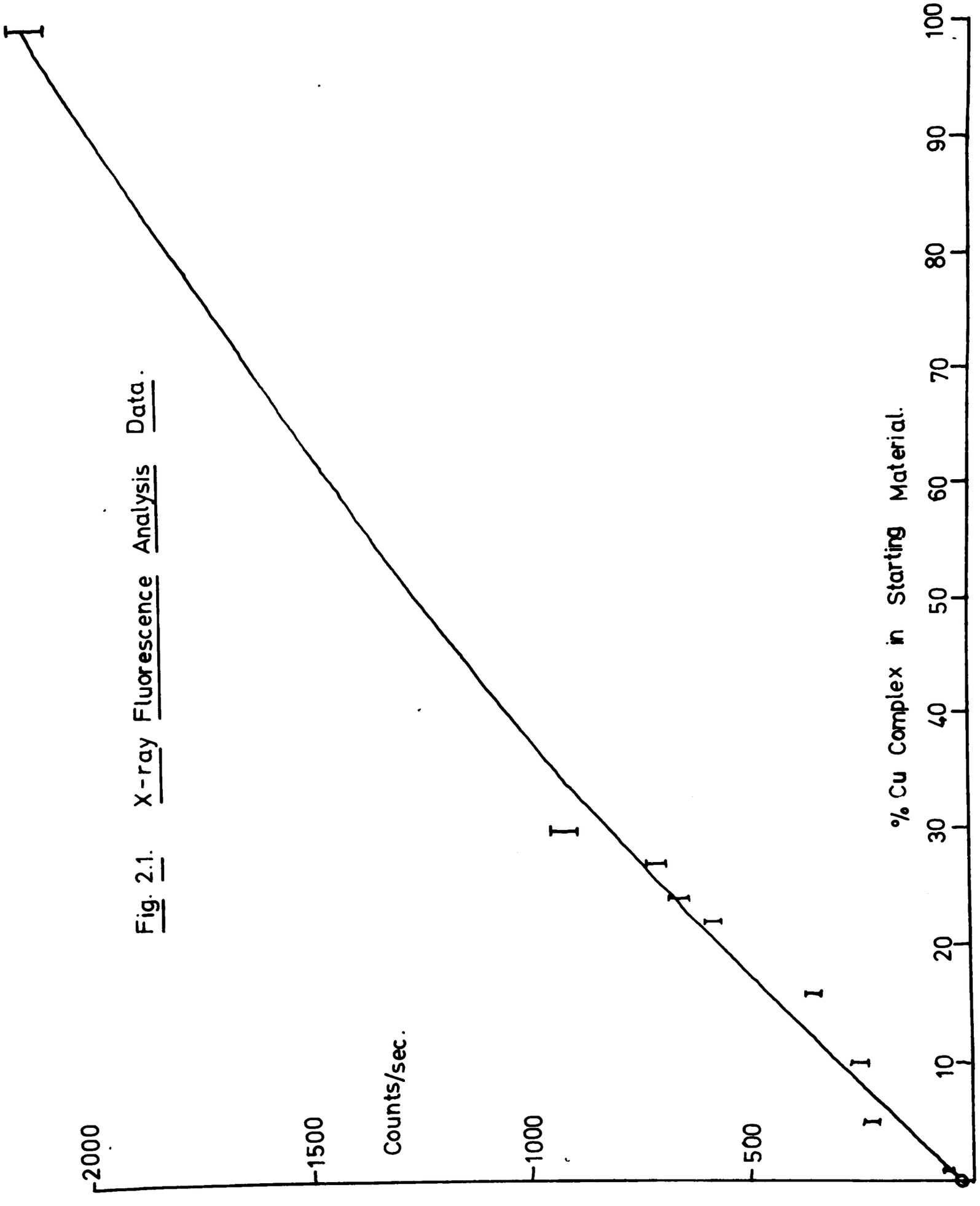


Fig. 2.1. X-ray Fluorescence Analysis Data.

The geometry of the apparatus prevented measurements of the first order K_α line for palladium, and the second order line was too weak for reliable measurement. This prevented measurement of the copper:palladium ratios directly. A plot of the percentage of copper complex in the preparation against the count for the Cu K_α fluorescence was therefore prepared (figure 2.1) to obtain an estimate of the deviation of the copper concentration in the crystals used for conductivity measurements from that in the starting material of the preparation. From this plot, it can be seen that all the crystals are within about 2·5 % of the actual percentage of copper complex used in the preparation. The deviations may be real differences of composition, or they may represent errors due to slight mis-alignment of the crystals in the X-ray fluorescence measurements. To distinguish between these two alternatives, chemical analysis for copper in the complex prepared with 30 % of copper complex in the starting material was carried out, using the biquinolyl method described above (2.3.2.). (This method uses a cuprous complex, and is therefore free from interference by palladium). The crystals contained 2·9(5) percent of copper. Since the molecular weights of the copper and palladium complexes are 597·5 and 640·4 respectively, the percentage of copper complex in the sample is given by x, where:

$$2{\cdot}9 = \frac{(x/100)(63{\cdot}5)(100)}{597{\cdot}5x/100 + 640{\cdot}4(100-x)/100}$$

x is therefore found to be 29·2 % , which means that, allowing for experimental error, the percentage of copper complex in this crystal is essentially the same as in the starting material.

This suggests that deviations from the line in figure 2.1 are probably due to mis-alignment of the crystals in the fluorescence apparatus, and to other experimental error. These two analytical results therefore indicate that meaningful qualitative (but not quantitative) discussions can be attempted for the relationships between conductivity properties and the percentages of copper complex in the crystals, while making the approximation that the percentage of copper in the crystals of a complex is the same as used in the preparation of the solution from which the crystals were obtained. In view of the similarity of shape and orbital energies of the copper and palladium complexes (c.f. chapters 3 and 4), this result is to be expected.

CHAPTER 3.

CRYSTAL STRUCTURES.

3.1. Introduction.

The objects of determining the crystal structures of the complexes used in this work are as follows:

(i) To show if the complexes are of the same general structural type as organic molecular complexes, and, if so, to test the validity of Mulliken's "Overlap and Orientation Principle" [14] for these compounds.

(ii) To investigate the possibility of specific interactions between the metal atom and particular parts of the electron acceptor molecule.

(iii) To determine bond lengths and angles of the molecules involved, particularly of the acceptor molecules.

(iv) To show if the complexes have structures which are of several different types, and, if so, to uncover any important structural differences between types which might lead to differences in other physical properties.

(v) To discover any evidence provided by the structures on why some complexes are 1:1, while others have a 1:2 donor: acceptor ratio.

The complexes are particularly suitable for study by

the x-ray diffraction technique, because

(i) they can be obtained as well-formed single crystals which are stable in the x-ray beam in air,

(ii) they contain a heavy atom, which dominates the phases of the reflections and simplifies the computation required, and (iii) they give sharp diffraction patterns, observed to the Cu K_α limit, giving a high observation:parameter ratio.

Appendix A gives details of the methods used and the results obtained for the three-dimensional structures of the complexes of palladium 8-hydroxyquinolinate with chloranil and 1,2,4,5-tetracyanobenzene. These structures have been determined by the author, working with Drs. C.K. Prout and B. Kamenar. (Appendix A contains a statement concerning the actual portions of the work carried out by the author). Dr. Prout, with Professor H.M. Powell, Drs. A.S. Bailey and B. Kamenar, and Mr. T.S. Cameron, has also determined the crystal structures of the complexes of copper 8-hydroxyquinolinate with picryl azide[15] and benzotrifuroxan[16], and of palladium 8-hydroxyquinolinate with benzotrifurazan[17]. This chapter consists of a discussion of the structural principles which can be deduced from these five structures, and of their relevance to other parts of the work.

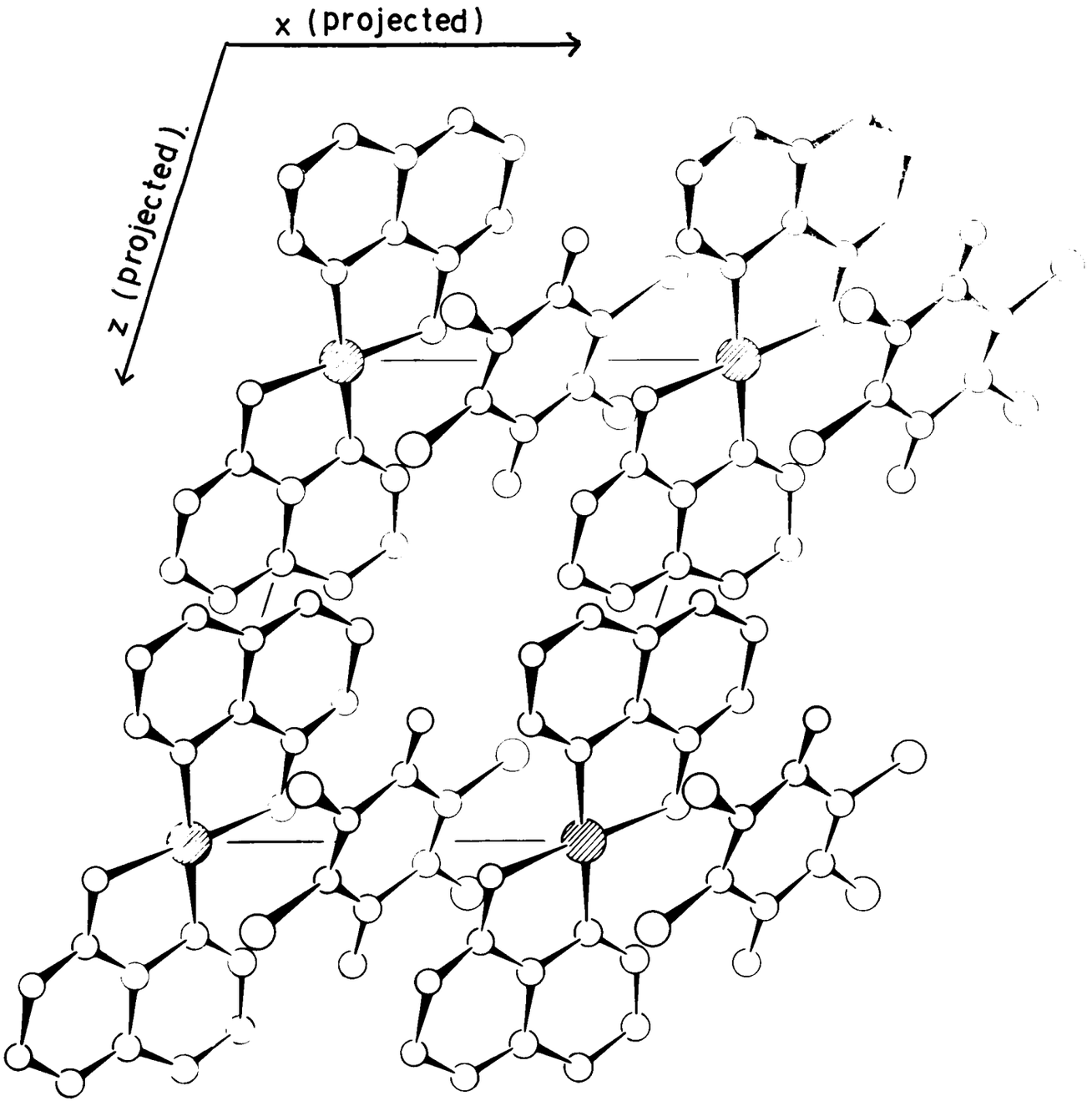


FIGURE 3.1.

Palladium 8-hydroxyquinolinate/chloranil.

(Projected down the b axis).

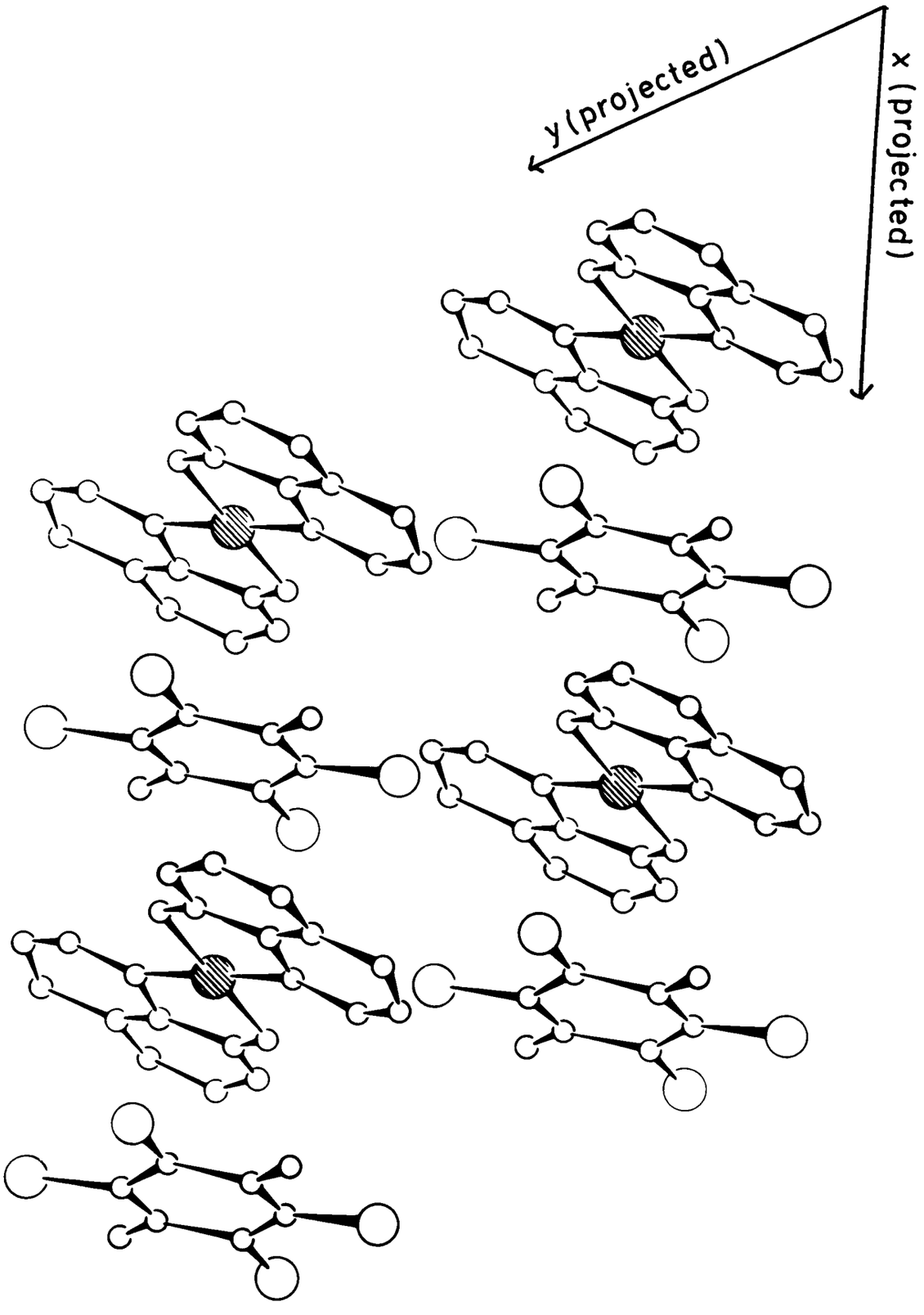


FIGURE 3.2.

Palladium 8-hydroxyquinolinate/chloranil.

(Projected down the c axis).

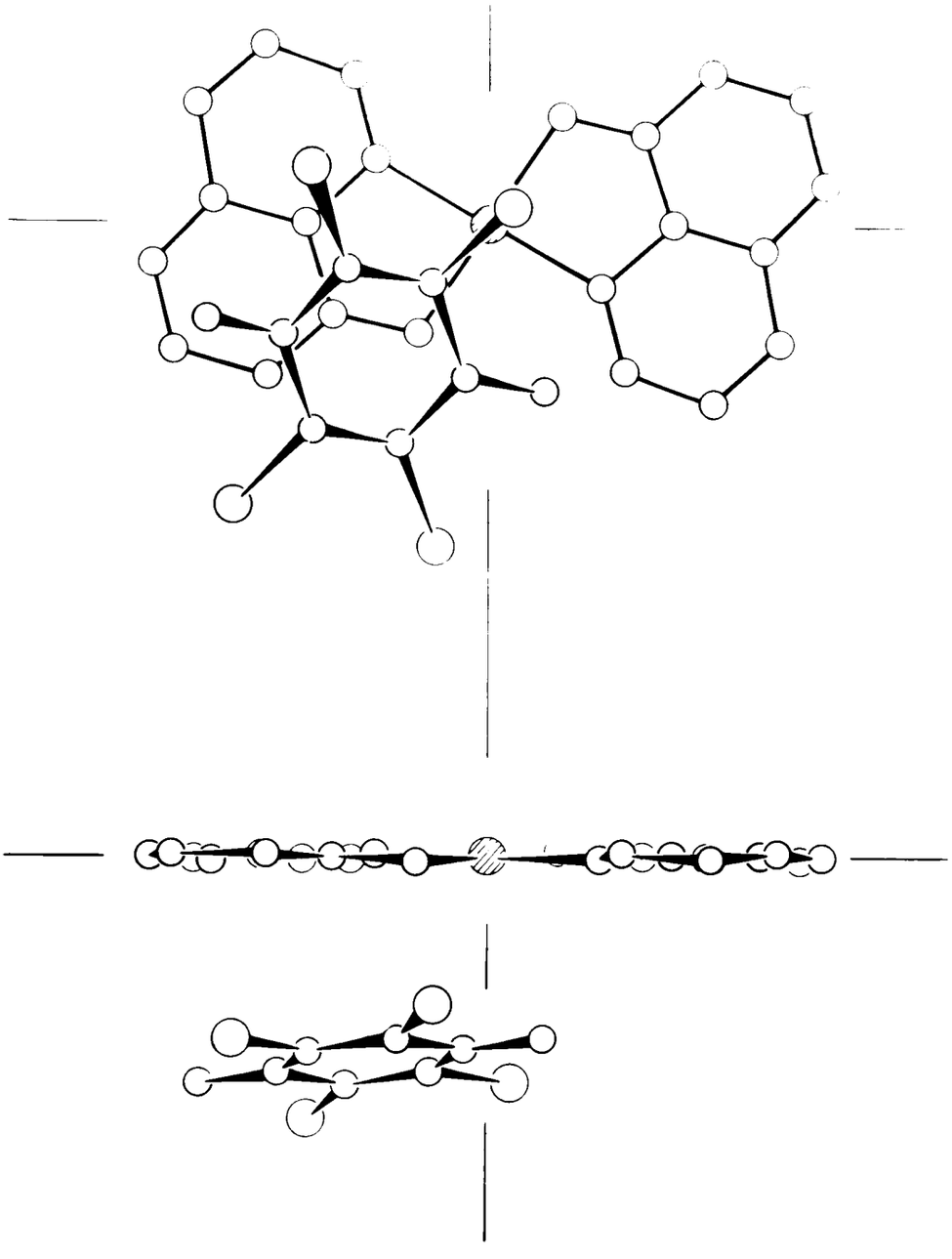


FIGURE 3.3.

Palladium 8-hydroxyquinolinate/chloranil.

(Projected parallel and perpendicular to the least-squares best plane of the Pd 8-hydroxyquinolinate molecule).

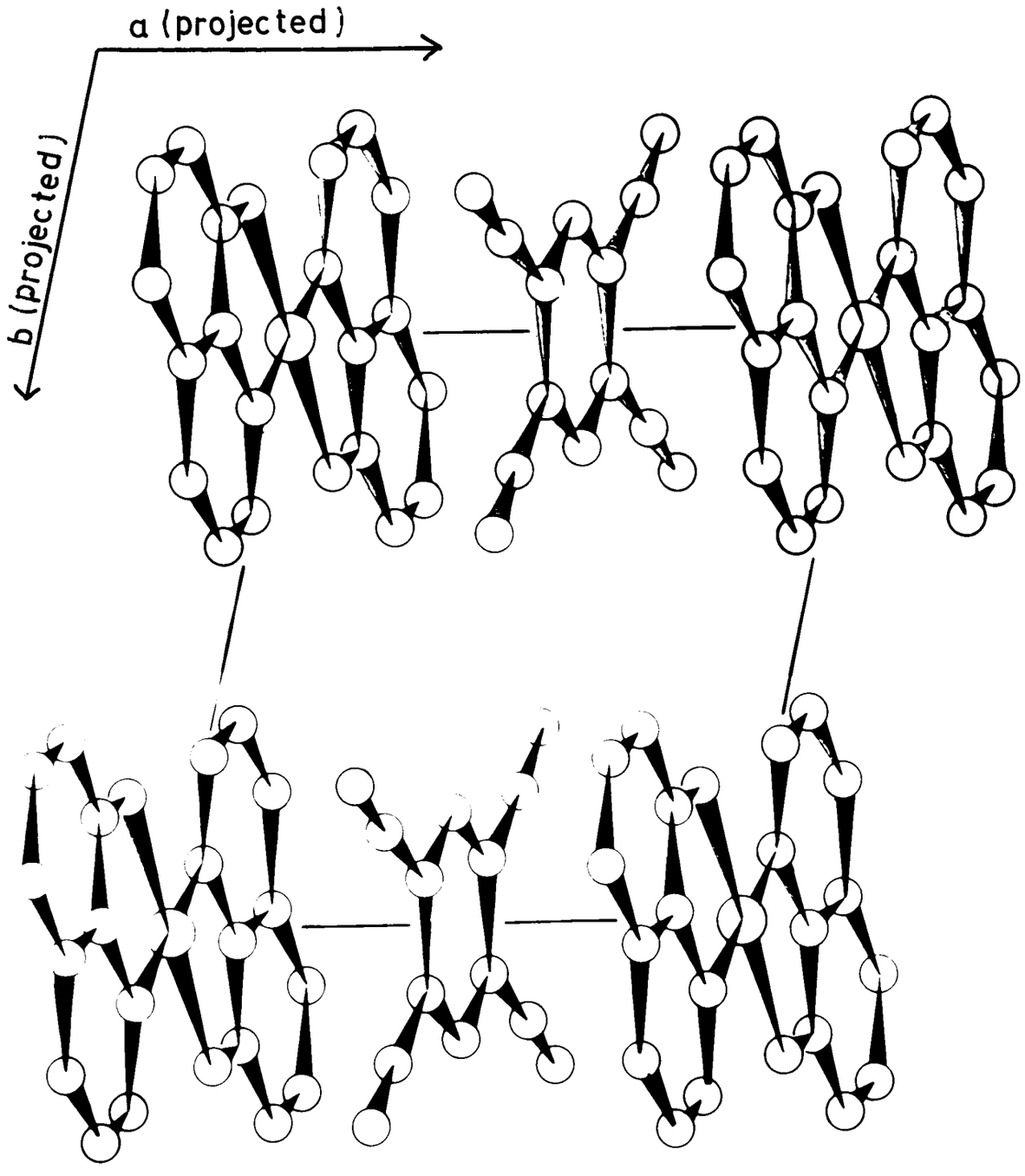


FIGURE 3.4.

Palladium 8-hydroxyquinolinate/tetracyanobenzene.

(Projected down the c axis).

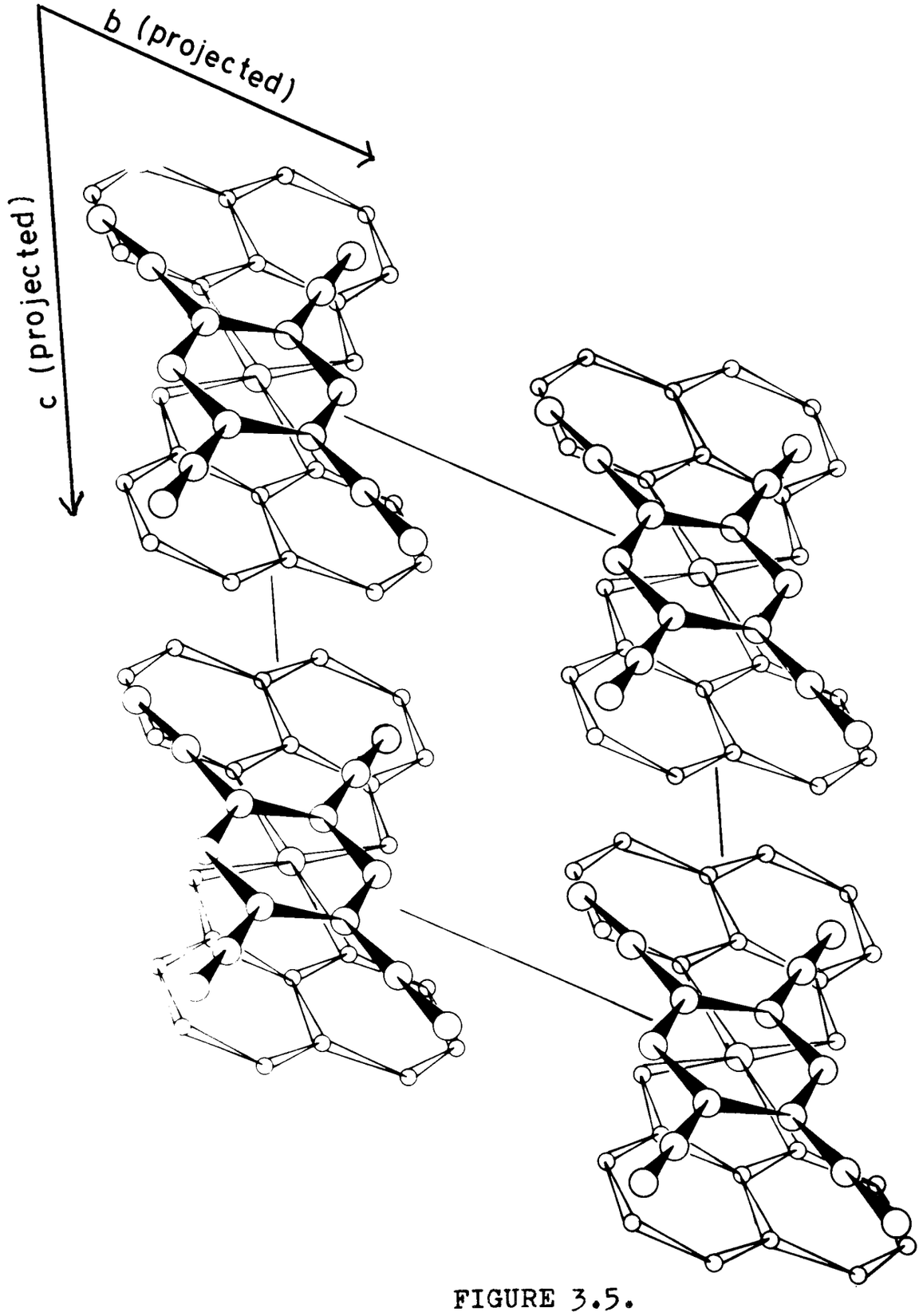


FIGURE 3.5.

Palladium 8-hydroxyquinolinate/tetracyanobenzene.

(Projected down the a axis).

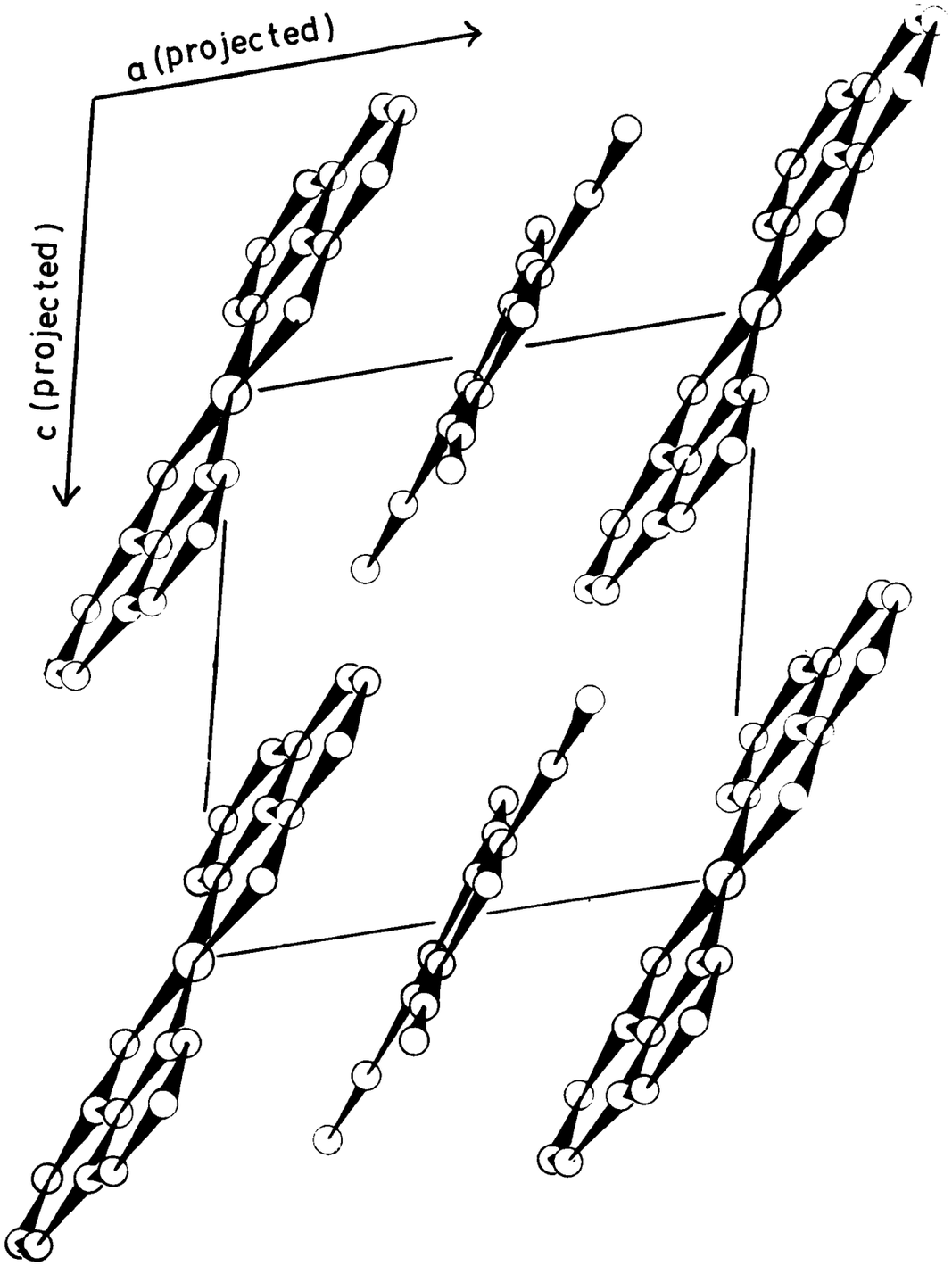


FIGURE 3.6.

Palladium 8-hydroxyquinolinate/tetracyanobenzene.

(Projected down the b axis).

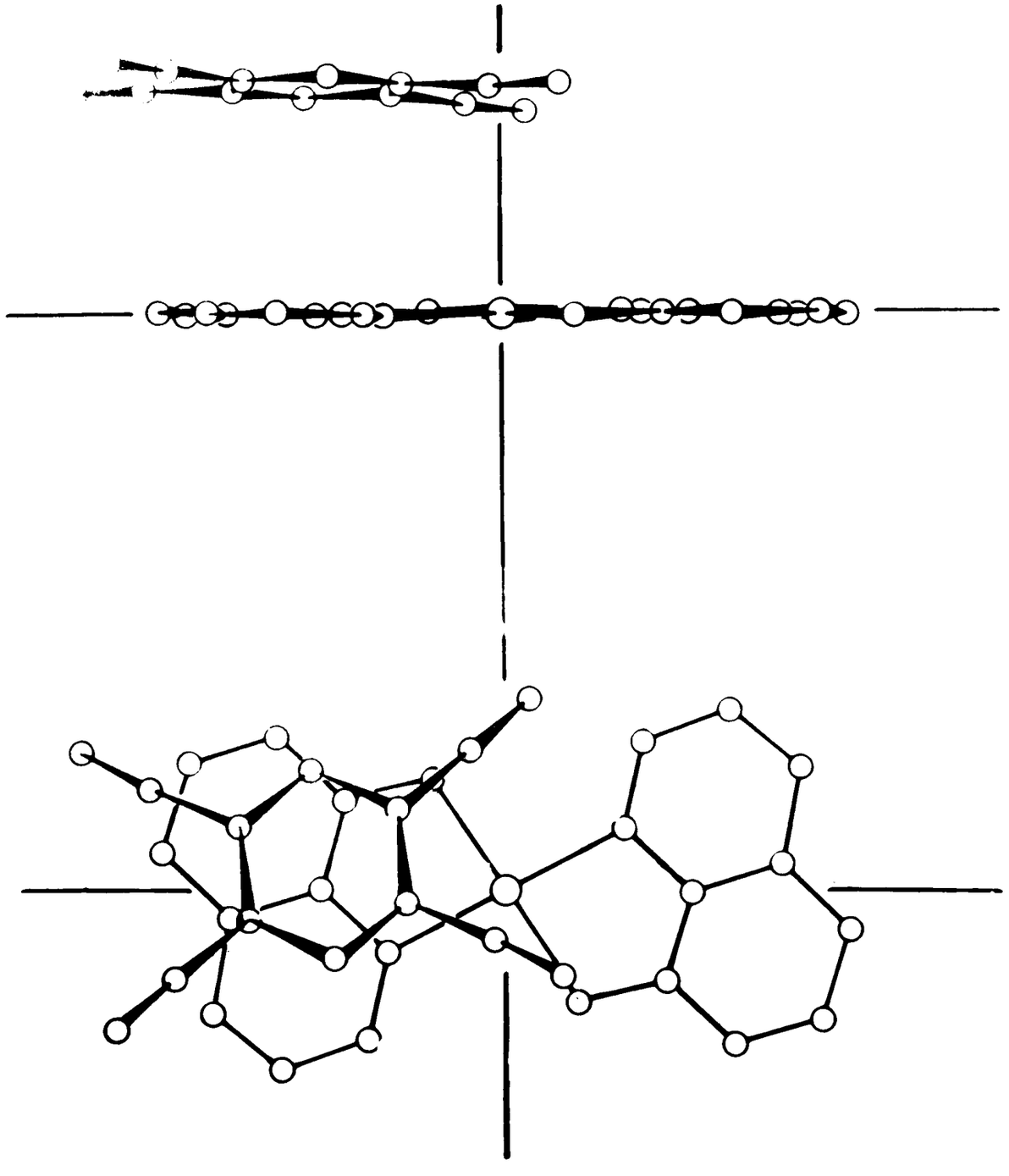


FIGURE 3.7.

Palladium 8-hydroxyquinolinate/tetracyanobenzene.
(Projected parallel and perpendicular to the least-squares best plane of the Pd 8-hydroxyquinolinate molecule.)

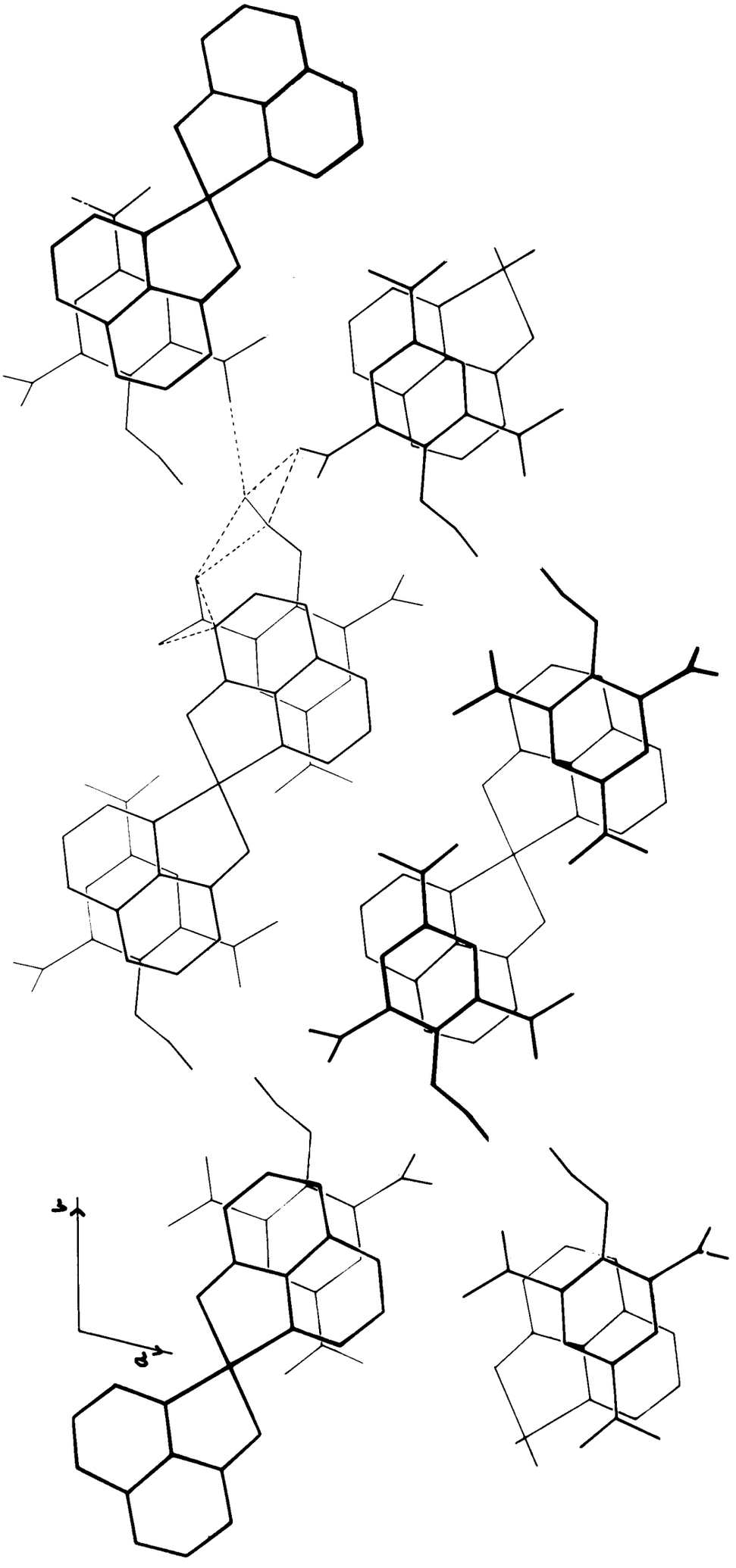


Fig. 3.8. Cu 8-hydroxyquinolinate/picryl azide. (Projected down the c axis.)

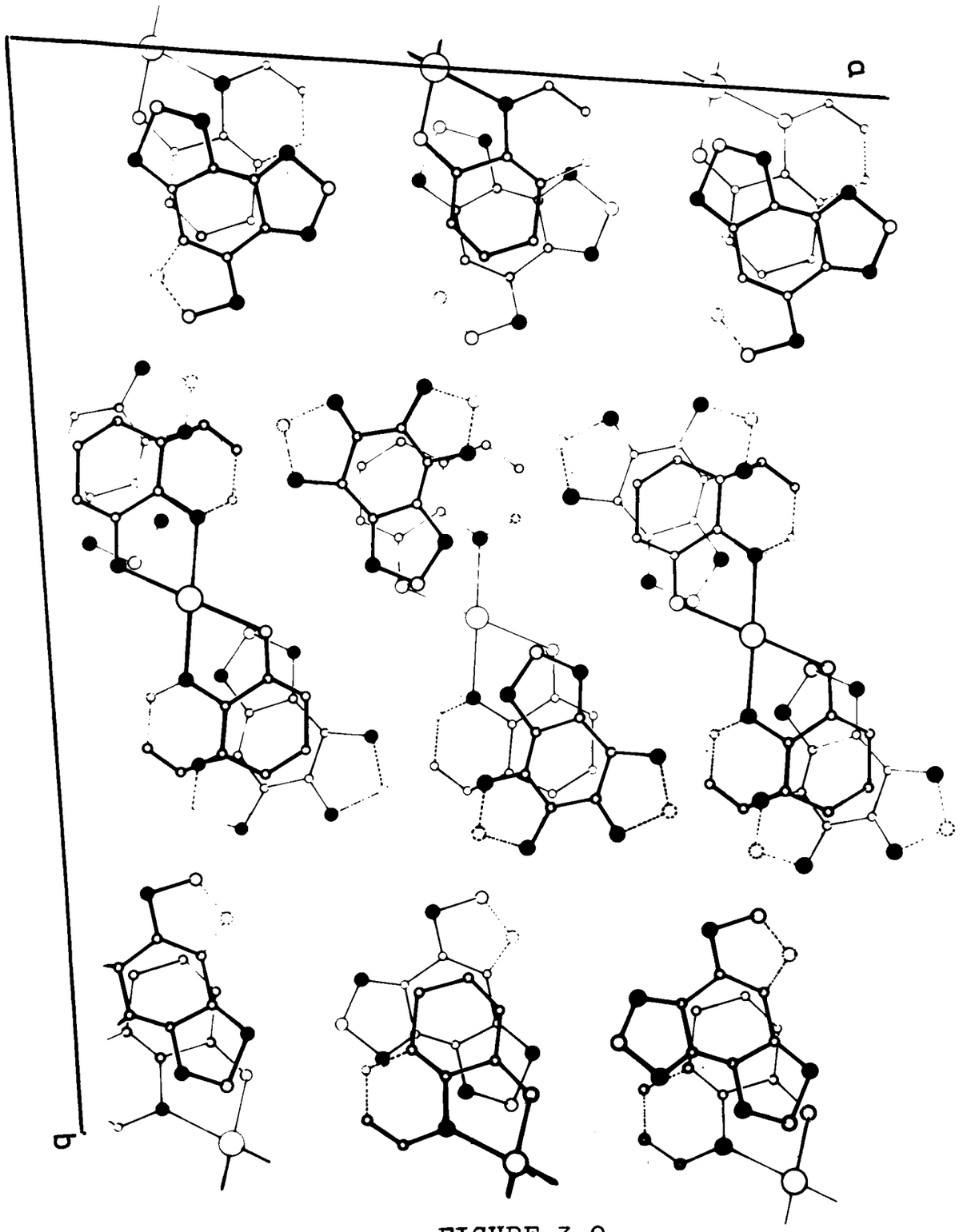


FIGURE 3.9.

Copper 8-hydroxyquinolinate/benzotrifurazan.

(Projected down the c axis).

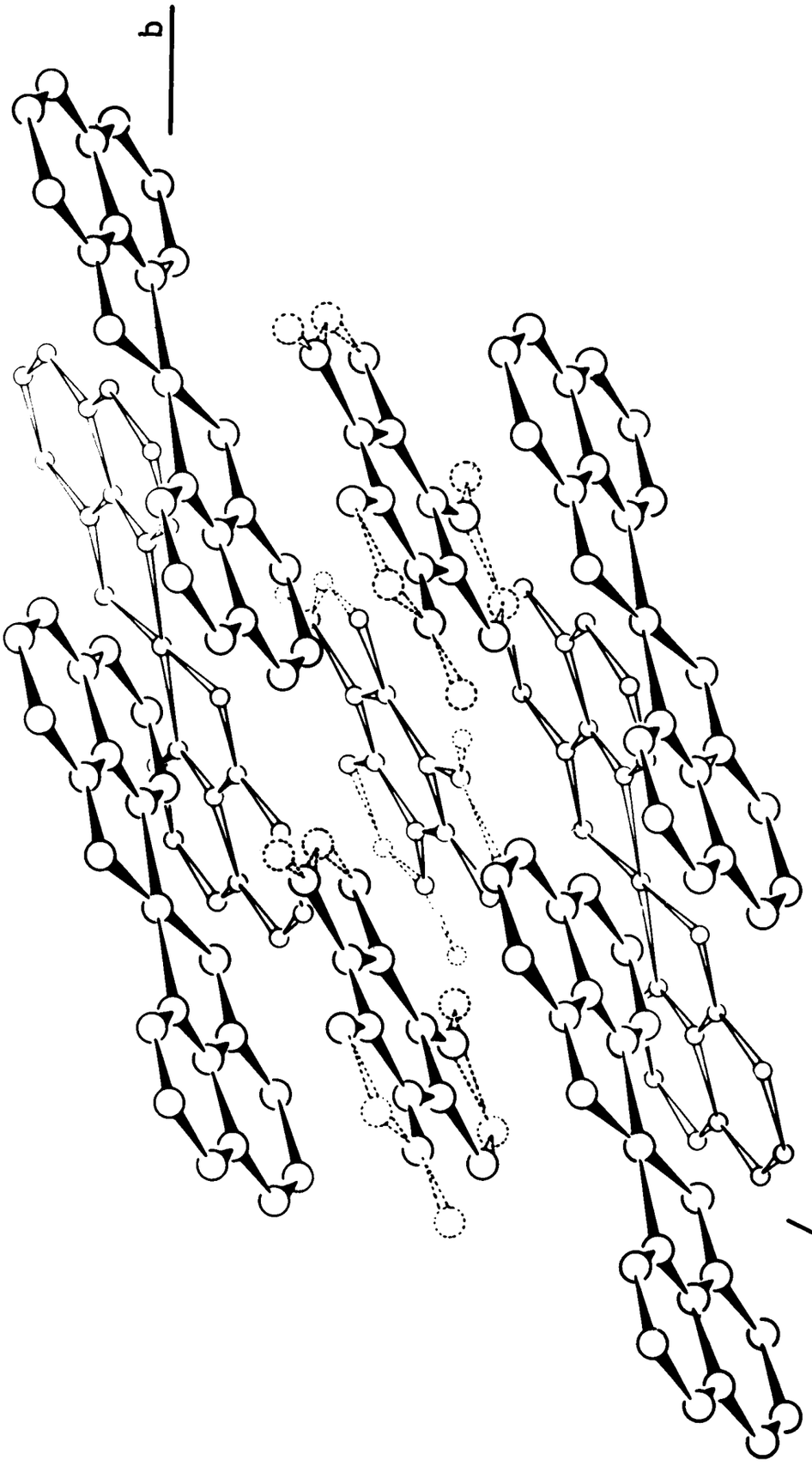


Fig. 3.10. Cu 8-hydroxyquinolinate/benzotrifuroxan.

(Projected perpendicular to the (100) planes)

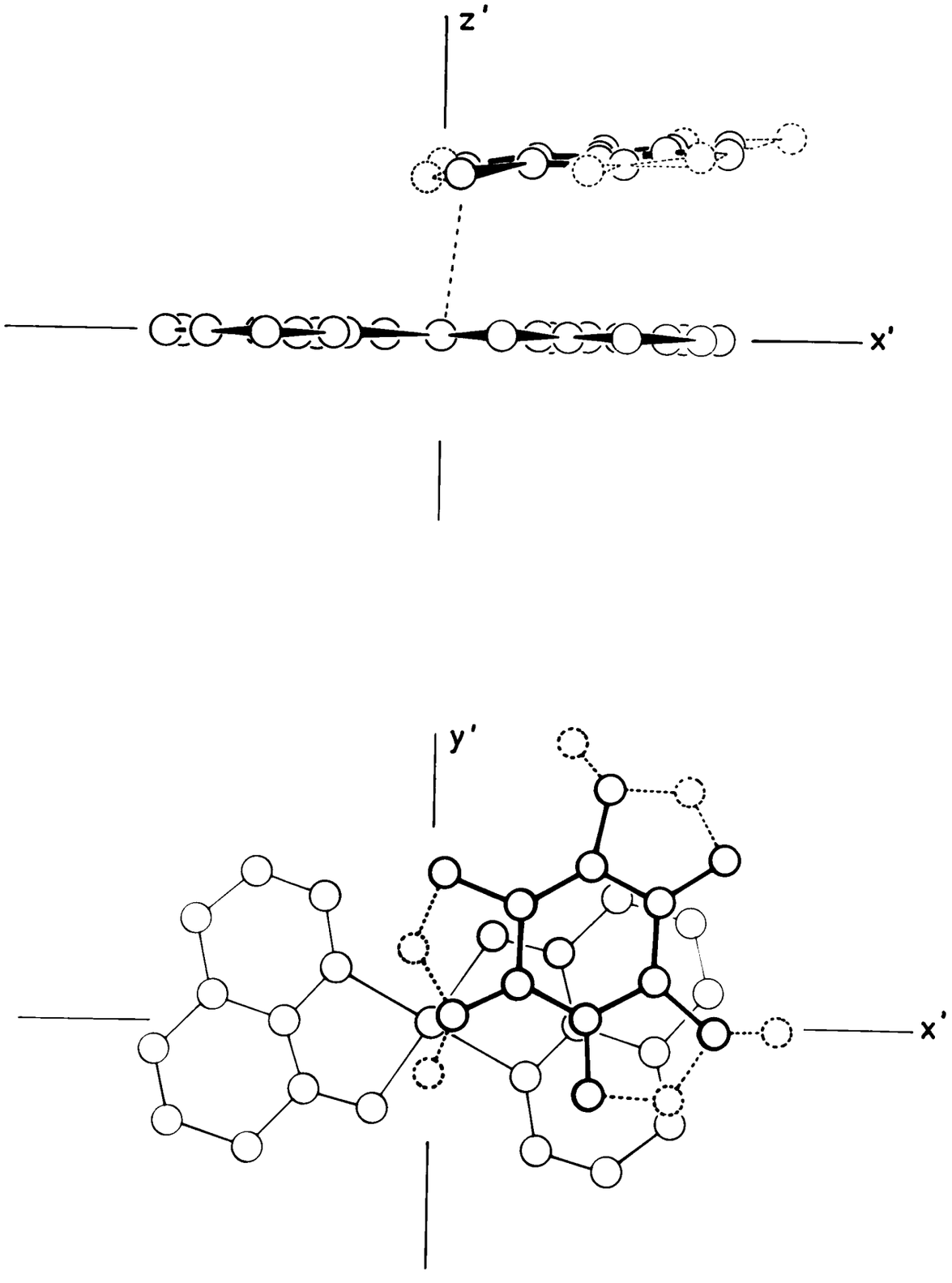
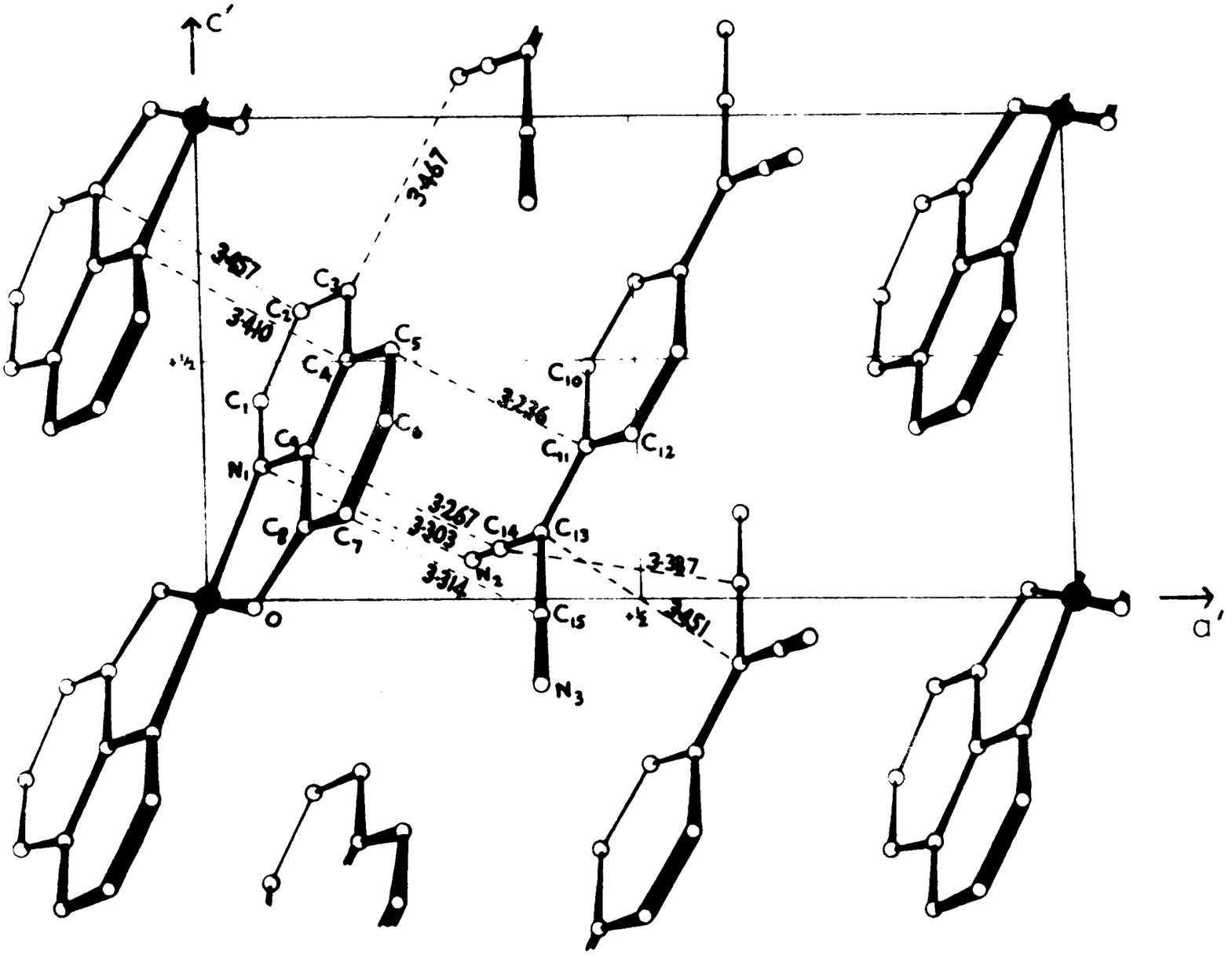


FIGURE 3.11.

Copper 8-hydroxyquinolinate/benzotrifuroxan.
(Projected parallel and perpendicular to the least-squares best plane of the Cu 8-hydroxyquinolinate molecule.)



View of the structure projected along the b axis.

Fig. 3.12. Cu 8-hydroxyquinolinate/ TCNQ.

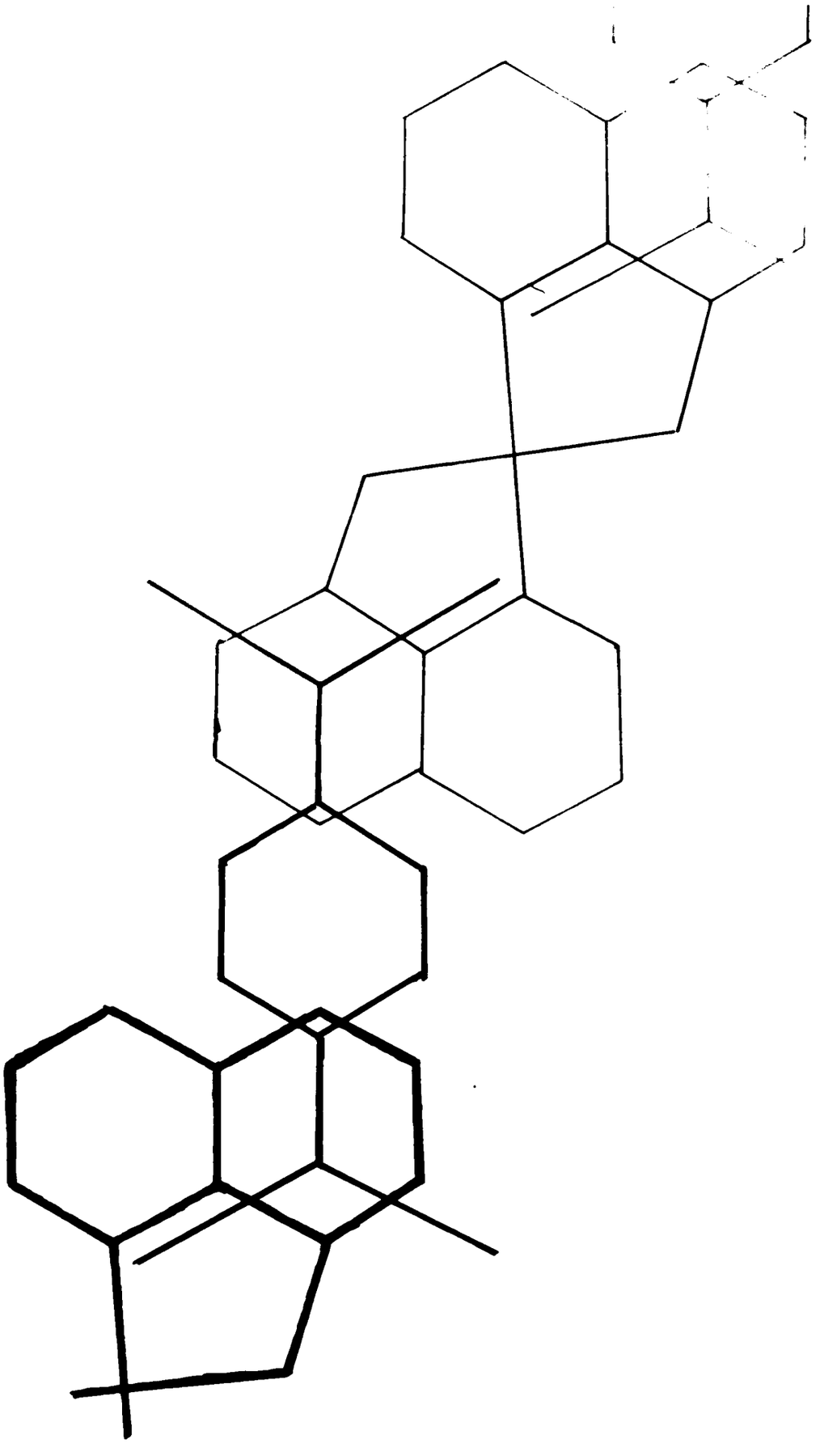


Fig. 3.13. Cu 8-hydroxyquinolinate/ TCNQ.

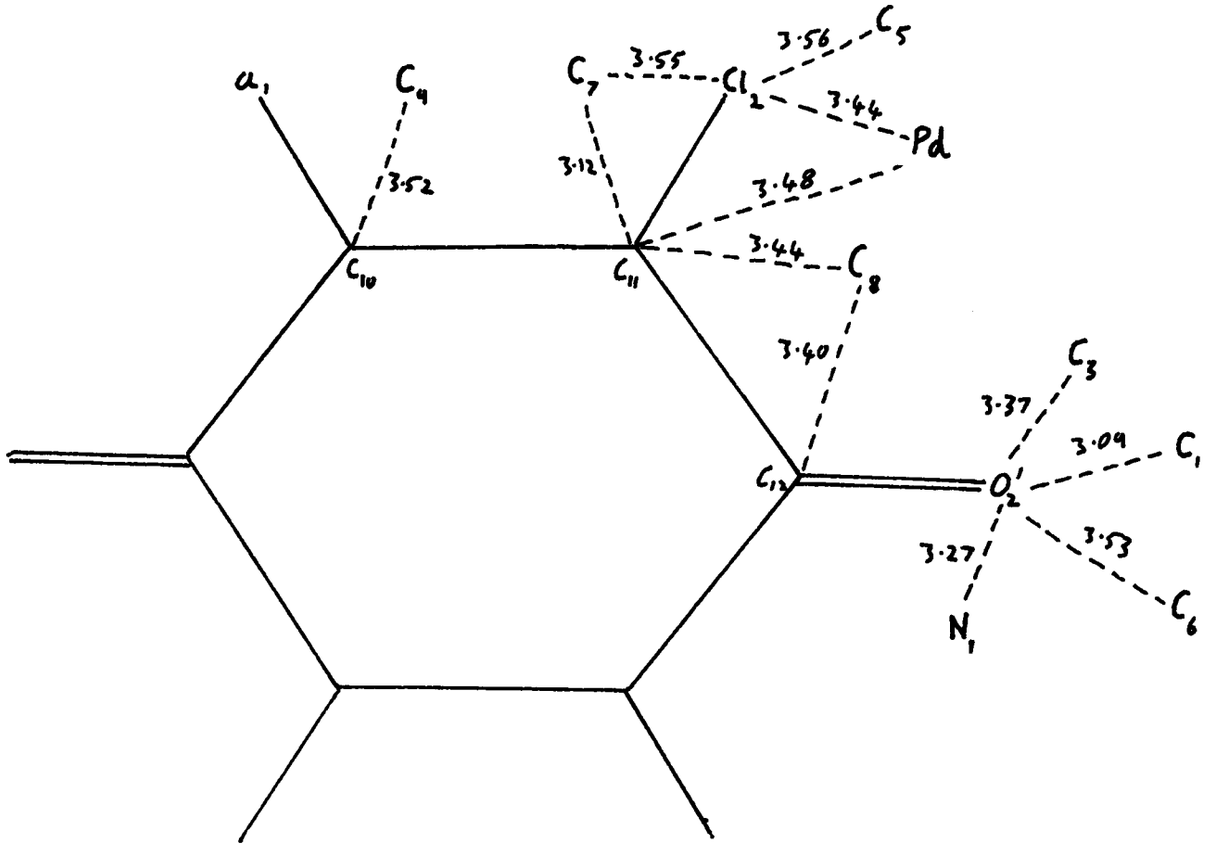
Projection onto 8-hydroxyquinolinate plane.

3·2. Structural principles of the complexes.

Figures 3.1 to 3.13 show various projections of the available structures. The main features of these are discussed below.

1) The lattice is always composed of stacks of alternate donor and acceptor molecules in an approximate plane-to-plane arrangement. This is characteristic of all molecular complexes.

2) The mean distance of the acceptor molecule from the plane of the donor molecule is close to the interplanar distance of 3·40 Å found in aromatic hydrocarbons, where the attractive forces are of the van der Waals type. For example, in the Pd 8-hydroxyquinolinate/chloranil complex, the close contacts between atoms of the acceptor and near neighbours in the donor are as shown in the figure below:



3) Molecules in adjacent stacks frequently form sheets, which are approximately planar. In the palladium 8-hydroxyquinolinate complexes with chloranil and tetracyanobenzene, there are close-packed sheets containing equal numbers of donor and acceptor molecules. In the Pd 8-hydroxyquinolinate/benzotrifurazan complex, the sheets are still close-packed, but contain two acceptor molecules for every one donor molecule. In the copper 8-hydroxyquinolinate/picryl azide complex, the sheets are not close-packed, molecules which would complete the close-packed layers forming a second set of layers separated from the first by 1/6 of the unit cell length, due to the bulk of the picryl azide molecule. The copper 8-hydroxyquinolinate/benzotrifuroxan complex, which forms a "herringbone" type of lattice, is an exception, and does not contain these sheets.

This suggests that lattice packing is an important structure-determining factor.

4) The planes of the donor and acceptor molecules are always somewhat inclined towards each other, because of

(a) steric repulsions between parts of the two molecules

or (b) specific attractions to the metal atom, which are very largely van der Waals interactions (see (5) below).

The angles of tilt for some of the complexes are as follows:

Pd 8-hydroxyquinolinate/chloranil	15·5°
Pd 8-hydroxyquinolinate/tetracyanobenzene	4·5°
Cu 8-hydroxyquinolinate/benzotrifuroxan	10°
Cu 8-hydroxyquinolinate/picryl azide	2°

5) The dominating interaction stabilising these complexes might be expected to be that between the metal atom, which has residual positive charge, and the polarisable acceptor molecule. The following evidence suggests that this is not so:

(a) Complexes exist in which no part of the acceptor molecule is close to the metal atom (e.g. the Cu 8-hydroxyquinolinate/picryl azide complex). Such an interaction cannot therefore be of key importance in these complexes.

(b) In the Pd 8-hydroxyquinolinate/chloranil complex, it is the chlorine atom of the acceptor and not an oxygen atom which lies over the palladium atom. Since the oxygen atoms of a quinone are expected to have larger residual negative charge than the chlorine atoms, this shows that van der Waals interactions are more important than electrostatic interactions with the residual positive charge on the metal atom, in this case.

(c) The contact distances between atoms of the acceptor molecule near the metal atom and the metal atom itself are close to the van der Waals contact distances. Thus, in the palladium 8-hydroxyquinolinate/tetracyanobenzene complex, there is a contact of 3·5Å between the palladium atom and a carbon atom (C14) of the acceptor. Taking the van der Waals radius of carbon as half the interplanar distance in aromatic hydrocarbons, i.e. as 1·7Å, and assuming that the interaction in this case is purely of the van der Waals type, we obtain a

van der Waals radius of 1·8Å for palladium. The van der Waals radius of copper will be rather smaller than this. (For example, in copper 8-hydroxyquinolinate itself, there is a copper-oxygen contact of 2·83Å[18], and, subtracting Pauling's estimated van der Waals radius for oxygen of 1·40Å[19], this gives a value of 1·43Å as the van der Waals radius of copper.) Using these values, and Pauling's van der Waals radii for chlorine (1·80Å) and nitrogen (1·50Å)[19], gives values of 3·60 and 2·93Å for the van der Waals contact distances for Pd-Cl and Cu-N, respectively. The observed distances are 3·44 and 3·06Å, which is in good agreement, suggesting only small electrostatic interactions in addition to the van der Waals interactions. The other contact distances, for example those shown in (2) above, are also very close to the sums of the van der Waals radii of the atoms involved.

These facts do not eliminate the possibility of other interactions, such as ion-dipole or -induced dipole forces between the metal atom and the acceptor, and electrostatic interactions due to the small percentage of charge-transfer state mixed into the ground state of complexes of this type (c.f. chapter 4). Such interactions are known to be small (e.g. the heats of formation of similar organic complexes are of the order of 5 kcal./mole[20]), and the repulsion energy increases very rapidly as the molecules are brought closer together than the equilibrium van der Waals distance. Weak interactions of these types will therefore not produce a marked effect

on the structures of the complexes. However, the van der Waals attraction term may be large for acceptors in which atoms can approach the heavy metal atom easily. Thus, Mulliken's overlap and orientation principle will be most likely to be obeyed in complexes where no atom of the acceptor can approach closely to the metal atom.

The overlap and orientation principle states that the partners in a donor-acceptor complex tend to assume a relative orientation such that the overlap integral between the donor orbital from which an electron is removed and the acceptor orbital to which it is transferred is maximised. From figure 3.8 it is clear that in the picryl azide complex, where no atom of the acceptor is near the copper atom, this principle is obeyed. On the other hand, in the complexes, such as the chloranil complex, where there is an atom of the acceptor close to the metal atom, this principle is not obeyed, and the acceptor lies far from the position of best overlap with the metal complex π orbitals. However, in these cases, the acceptor always lies over the side of the ligand which has the largest π electron density (the oxygen side[21]).

The actual orientation in these compounds is therefore controlled by the balance between the energies of

(i) an orientation giving maximum overlap with the π electrons of the ligand, but no interaction with the metal

and (ii) an orientation giving direct interaction with the metal atom and overlap with the electron-rich region of the ligand, but not maximum overlap with the ligand π electron cloud.

(The exact position of the acceptor will be determined by lattice repulsions, as in (3) and (4) above.)

The structures so far determined support the conclusion that case (ii) is always more favourable than case (i) if the shape of the acceptor permits this orientation.

6) The stoichiometry of the complex is influenced by the possibility of specific interactions between the acceptor and the metal atom. If such interactions give a more stable lattice, structures allowing the interaction will be favoured. Since two atoms cannot occupy the same site, complexes involving specific interaction with the metal atom are 1:1 complexes. Complexes of other acceptors are 2:1, provided that two acceptor molecules can be accommodated on the same side of the donor molecule. This gives more stability than the alternative with only one acceptor per donor in such cases.

Thus, 1:1 complexes include those with benzotrifuroxan, dinitrobenzfuroxan, chloranil and dichlorodicyanobenzoquinone (all of which can adopt orientations allowing specific interaction with the metal atom). 2:1 complexes include those with picryl azide, trinitrobenzene, and benzotrifurazan (which cannot give this interaction so easily.) Trinitrofluorenone is too large a molecule to form a 2:1 complex with these donors. The cyano-substituted acceptors, tetracyanoquinodimethane (TCNQ) and tetracyanobenzene (TCNB) are interesting exceptions to this rule. TCNQ forms a 1:1 complex with copper 8-hydroxyquinolinate, but the cyanide groups

are too far from the metal atom to give any significant specific interaction (c.f. figures 3.12 and 3.13[22]). This is because the two ends of the acceptor molecule are acting as separate acceptors, so that a 1:1 complex has the same effect on the lattice energy as a 2:1 complex of any other acceptor. The complexes of TCNB with palladium and copper 8-hydroxyquinolinates appear to be anomalous, since the former is 1:1, while the latter is 2:1. This is the only case where the stoicheiometries of these two donors with a common acceptor are not the same. The full crystal structure of the copper complex has not yet been determined, but preliminary Weissenberg photography shows that the unit cell dimensions are approximately 7·5 x 7·4 x 14·0Å, corresponding to a cell volume of about 780Å^3. This is much nearer the volume of the 2:1 picryl azide complex (830Å^3) than to the volume of the Pd 8-hydroxyquinolinate/chloranil complex (546Å^3, 1:1). The lattice energy differences between 1:1 and 2:1 complexes of these two donors with TCNB are clearly small, and discussion of this anomaly must therefore await the determination of the Cu 8-hydroxyquinolinate/TCNB structure.

The stoicheiometries of the 8-hydroxyquinoline complexes follow those of the metal complexes, if the metal chelate is regarded as the donor equivalent of two 8-hydroxyquinoline molecules. This suggests that the above discussion does not represent the only factor determining stoicheiometry, since specific interactions with central heavy atoms cannot be invoked in the case of complexes with the free ligand.

An alternative interpretation, not involving these specific interactions is based on the strength of the complexes formed. All the acceptors forming complexes with a 1:1 ratio with metal complex donors are strong acceptors[1,3], with the exception of trinitrofluorenone (where the size of the acceptor is the domonating factor), whereas the 2:1 complexes are formed by acceptors which form complexes with low formation constants[3]. Thus, strong acceptors may be capable of binding a greater number of donor molecules in the lattice than weak acceptors. The possibility of specific interactions between the acceptor and the metal atom may therefore be regarded as a factor increasing the formation constant of the complex rather than as one which controls the stoicheiometry directly.

On present evidence, therefore, the stoicheiometry of a complex is determined by a combination of the following three factors:

(i) The magnitude of the complexing ability of the acceptor molecule,

(ii) The possibility of specific interaction between the acceptor molecule and the metal atom,

and (iii) The relative lattice packing efficiencies of 1:1 and 2:1 complexes.

The above generalisations show that these structures cannot be regarded as metal 8-hydroxyquinolinate lattices with acceptor

molecules taking the place of some metal complex molecules in a regular way. The complexes crystallise from solution as a result of charge-transfer interactions, and the structure is determined by factors (1) to (6) above, as well as by the requirement that the free space in the lattice shall be minimised. The combination of these effects is very different from the factors controlling the formation of crystals of the donor or acceptor compounds, so it is not surprising that the structures of the complexes are not directly related to those of the parent compounds.

Several of the points made above apply equally to organic molecular complexes, and, apart from the modifications caused by the presence of the metal atom, the complexes are of the same basic type, structurally, as purely organic molecular complexes[e.g.27].

Structural modifications caused by the presence of heavy metal atoms are unlikely to produce large effects on spectroscopic properties, since they produce a small change in what is already a small perturbation of the donor and acceptor energy levels (c.f. chapter 4, section 4). They may, however, produce a larger effect on electronic properties involving movement of charge through the entire lattice (i.e. on electrical conductivity properties.)

CHAPTER 4.

SPECTRA.

4.1 Theory.

4.1.1. Molecular Orbital and Valence Bond approaches to bonding and spectra in molecular complexes.

The theory of bonding and spectra in molecular complexes was first formalised by R.S. Mulliken[14, 24, 29], in terms of a model similar to the valence bond theory. More recently, M.J.S. Dewar[25] has used concepts more akin to molecular orbital theory, although basically similar to those used by Mulliken.

When an electron donor (D) encounters an electron acceptor (A), there may be no movement of charge, or charge may move from D to A, or, (less frequently, by the definitions of D and A) from A to D. Mulliken's theory states that the interaction between D and A is made up of contributions from all of these situations.

For the state involving no movement of charge, all the classical intermolecular forces (e.g. dipole-dipole, ion-dipole, dipole-induced dipole, london forces and H-bonding) may be included for simplicity in one wave function ψ_0.

For charge transfer from D to A, the forces between the molecules now include ion-ion forces if D and A were initially uncharged, and forces due to the possibility of weak chemical bonding between the odd electrons on the components. All these

forces may be included in a second function ψ_1 .

There is a corresponding wave function ψ_2 for the case involving charge transfer from A to D.

ψ_0 is known as the no-bond function, and ψ_1 and ψ_2 are dative-bond functions.

The Mulliken theory states that the ground state of the complex is made up of a combination of the three states, so that the ground state wave function is

$$\psi_N(D,A) = a\,\psi_0(DA) + b\,\psi_1(D^+A^-) + c\,\psi_2(D^-A^+) \qquad (4.1)$$

where $a \gg b \gg c$, normally.

Similarly, for an electronically excited state, the excited state wave function is

$$\psi_E(D,A) = a'\,\psi_0(DA) + b'\,\psi_1(D^+A^-) + c'\,\psi_2(D^-A^+) \qquad (4.2)$$

where now $b' \gg a' \gg c'$, normally.

Wave mechanical principles[26] imply that:

(i) ψ_0 , ψ_1 and ψ_2 must have correct symmetry for mixing, and (ii) The partners in the complex will tend to assume the orientation which maximises the overlap integral between the highest energy filled orbital of the donor and the lowest energy vacant orbital of the acceptor, in the absence of other polarisation forces or steric requirements. This is the "overlap and orientation principle", whose influence was discussed in chapter 3.

The energy levels represented by these wave functions may

also be thought of in terms of sums of contributions from the different components of the combined wave functions.

Thus, the energy of the ground state W_N

$$= W_\infty - \Delta H_f$$

$$= W_\infty + G_o - X_o$$

$$= W_o - X_o \qquad (4.3)$$

where W_∞ = total energy of the separated molecules,

$-\Delta H_f$ = enthalpy of formation of the complex,

X_o = resonance energy gained by mixing ψ_1 and ψ_L with ψ_o,

and G_o = sum of the energy terms due to electrostatic interactions, van der Waals energy etc. (contributions from ψ_o, ψ_1 and ψ_L).

In a weak complex, the electrostatic term G_o may be much more important in stabilising the complex than the resonance term X_o, and, if this is so, the term "charge transfer complex" is not appropriate. Molecular complex or π complex is then a better term. On the other hand, in strong complexes the donor-acceptor separation may be less than the van der Waals distance, so that G_o represents a repulsion force and X_o is made much more important, due to improved overlap of orbitals. Thus, strong complexes may justly be called charge transfer complexes.

In the case of the excited state, the energy W_E

$$= W_\infty + I_D^v - E_A^v - G_1 + X_1$$

$$= W_1 + X_1 \qquad (4.4)$$

where I_D^v = vertical ionisation potential of the isolated donor

E_A^v = vertical electron affinity of the isolated acceptor

X_1 = the resonance energy gained by mixing ψ_1 with ψ_0 and ψ_2

and G_1 = the sum of the large electrostatic interaction energy of D^+ and A^-, the small valence energy of the dative D^+-A^- bond, and a correction for the influence of environment on the energy of D^+ and A^-.

Thus, electronic charge-transfer transitions from the ground state to an excited charge-transfer state give rise to absorption of energy of amount

$$\begin{aligned} h\nu_{C.T.} &= W_E - W_N \\ &= (W_1 - W_0) + (X_1 - X_0) \\ &= I_D^v - (E_A^v + G_1 + G_0) + (X_1 - X_0) \end{aligned} \qquad (4.5)$$

This equation could be used to predict the position of charge transfer bands if the energies W_E and W_N could be calculated from ψ_E and ψ_N. In practice, this is too complex, and simplifications are needed, as follows:

(i) For a series of complexes of a given acceptor with various donors, the term $(E_A^v + G_1 + G_0)$ is assumed constant.

(ii) The assumption is made that for weak complexes, perturbation theory is valid, so that

$$X_1 - X_0 = \frac{\beta_0^2 + \beta_1^2}{W_1 - W_0} \qquad (4.6)$$

(where $\beta_o = H_{o1} - W_o S_{o1} = \int \psi_o H \psi_1 \, d\nu - W_o \int \psi_o \psi_1 \, d\nu$

and $\beta_1 = H_{o1} - W_1 S_{o1}$.)

It is further assumed that $(\beta_o^2 + \beta_1^2)$ is constant for a series of complexes with a common donor or acceptor.

(It is interesting to notice that, since W_1 is usually greater than W_o, this means that $X_1 > X_o$, so that the destabilization of the excited state by resonance is greater than the stabilization of the ground state.)

Using these assumptions, equation 4.5 may be simplified:

$$h\nu_{C.T.} = I_D^v - (E_A^v + G_1 + G_o) + (X_1 - X_o)$$

$$= I_D^v - c_1 + \frac{c_2}{W_1 - W_o} \qquad \text{(using eqn. 4.6)}$$

$$= I_D^v - c_1 + \frac{c_2}{I_D^v - c_1} \qquad \text{(using eqns. 4.3 and 4.4)} \qquad (4.7)$$

where c_1 and c_2 are constants.

This relationship has the form of a curve, with a linear region over the ionization potential range 7-12 eV. It is approximate, and liable to break down to the extent that the approximations are invalid, particularly in the case of strong complexes. However, the expression is still rather cumbersome to use for predicting positions of charge transfer bands from ionization potential data, or vice versa, so it is usual to simplify it still

further to $$h\nu_{C.T.} = k_1 I_D^v + k_2 \qquad (4.8)$$

This is useful, despite the approximations, because:

(a) Ionization potentials of aromatic donors are usually in the range 7-8·5 eV., which is within the linear region of equation 4.7,

and (b) the error introduced by the approximations is in any case less than the differences between experimental values of ionization potentials obtained by different methods not involving these assumptions.

Particular care must be taken in interpreting any anomalous values obtained using 4.7 or 4.8, especially when strong complexes are being studied, or when literature values of ionization potentials measured under adiabatic, as opposed to vertical, conditions are being used. k_1 and k_2 in equation 4.8 are empirical constants with no physical significance.

An analogous expression,

$$h\nu_{C.T.} = k_1' - k_2' E_A^v \qquad (4.9)$$

may be derived, relating charge transfer absorption maxima to electron affinity for a series of complexes of a common donor with different acceptors.

The Molecular Orbital approach of Dewar[25] differs from Mulliken's approach in emphasis rather than in the actual form

of the mathematical treatment. Whereas the Mulliken theory considers the approach of two initially isolated molecules, the molecular orbital theory regards the two molecules as a single complex, within which there are three possible sets of electronic transitions:

(a) Two sets of internal electronic transitions of the donor and acceptor molecules,

(b) A set of transitions between filled orbitals of the donor and vacant orbitals of the acceptor.

The simplest molecular orbital approach begins by making the assumption (implicit in the approximations given in the development of the Mulliken theory) that perturbations of the energy levels of orbitals of the donor or acceptor in the complex are negligible, so that simple molecular orbital expressions for the orbital energies in the isolated molecules can be used for the molecules in the complex.

Hückel theory for the energy of an orbital (i) of an aromatic hydrocarbon, gives the expression

$$E = \alpha + \chi_i \beta \qquad (4.10)$$

where α = Coulomb integral for carbon,

β = carbon-carbon resonance integral

and χ_i = a term characteristic of the $i^{th.}$ orbital, calculated by wave mechanics.

Calculated values of χ for various orbitals of many aromatic compounds have been tabulated[27], and form what is in effect a calculated ionization potential series.

Using the calculated value of χ_i for the highest occupied orbital of the donor, we have, assuming no perturbations,

Energy of charge transfer transition $h\nu_{C.T.} = E_\pi$

$$= A_j - \alpha - \chi\beta \qquad (4.11)$$

where A_j is the eneggy of the lowest vacant orbital of the acceptor. For complexes of a common acceptor, $(A_j - \alpha)$ and β are constant, so the expression becomes

$$E_\pi = a + b\chi \qquad (4.12)$$

which is analogous to equation 4.8. In this case, if the approximations are valid, a is equal to $(A_j - \alpha)$ and b is equal to $-\beta$. β has been estimated by other means, so this provides a method for estimating the extent of perturbation effects.

4.1.2. Shape and Intensity of Charge Transfer Absorption Bands.

The ground state of a molecular complex involves only a few percent of charge transfer character (as implied by $a \gg b \gg c$ in eqn. 4.1), as shown by the small dipole moment (e.g. chloranil/dimethylaniline 2·64D[28]). The excited state is much more polar, and therefore more rigidly held in position. Thus, the potential energy curve for the ground state is shallow, whereas that for the excited state is usually much steeper, as shown in figure 4.1[29]. Vertical transitions, in the Franck-Condon sense, from two vibrational levels of the shallow ground state may therefore produce absorption of widely differing energy (e.g. transitions 1 and 2 in figure 4.1),

so that, even at room temperature, the absorption bands produced will be very broad.

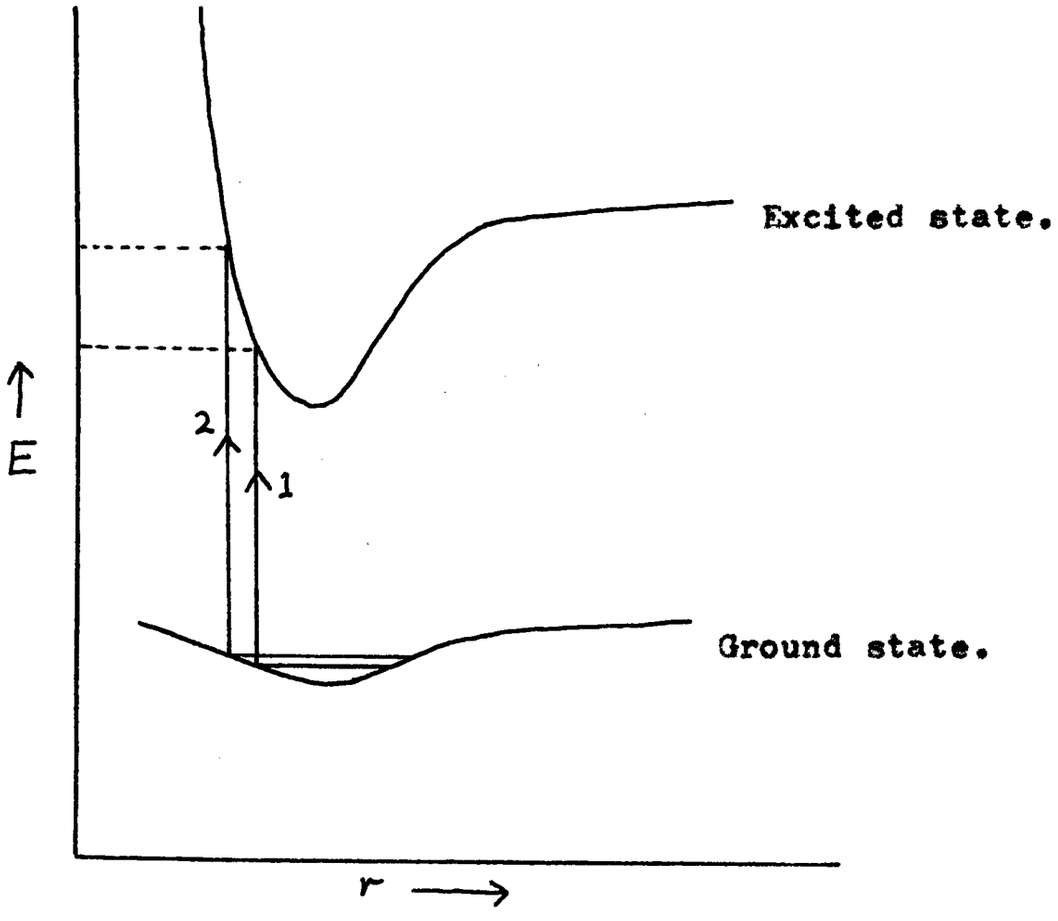


Figure 4.1.

The large dipole change on going to the excited state means that the transition moment of the excitation is large, so that the absorption intensity is also large. The intensity of charge transfer absorption may depend on the structure of the complex as well as on the concentration of donor-acceptor pairs. The most striking examples of this occur when contact charge transfer is involved[30]. This can give rise to an increase in absorption coefficient as temperature is raised, and to different absorption coefficients in different environments, such as solid and solution.

To eliminate any confusion in interpretation which this effect might cause, spectra of solids have been recorded where possible.

4.1.3. Appearance of several charge transfer bands.

If orbitals other than the highest filled donor orbital and lowest vacant acceptor orbital can be involved in charge transfer transitions, several new bands due to charge transfer may appear in the spectrum. This can occur in two ways:

(a) From transitions from a single donor orbital to several vacant acceptor orbitals

(b) From transitions from several filled donor orbitals to a single vacant acceptor orbital.

Overlap considerations favour (a) slightly, but (b) also produces several bands (e.g. in complexes where there are no low-lying vacant acceptor orbitals of correct symmetry near the first vacant orbital, as is the case with tetracyanoethylene[31]). The multiple bands observed in tetracyanobenzene complexes with organic electron donors (see table 4.2) have been shown to be of type (a)[4,32].

4.1.4. Polarization of charge transfer bands.

The transition involving charge transfer from donor to acceptor is strongly polarised, although not necessarily in a direction perpendicular to the planes of the aromatic systems of the donor and acceptor. Thus, in the pyrene/TCNE complex[33a] and in quinhydrone[33b], the direction of polarization of the absorbed light is found to lie along the vector joining the

centres of the molecules.

This polarization is due to the strong directional character of the transition moment. It is interesting to note that charge transfer emission occurs as well as absorption, and that polarization ratios for emitted light are roughly 3 times as great as for absorbed light[34]. This is interpreted as due to induced polarization in neighbouring molecules around each of the strongly dipolar excited charge transfer complex molecules, leading to an extra field polarising the emission process more strongly.

4.2. Experimental Methods.

Solid state spectroscopy was used in preference to solution spectroscopy in this work, for the reasons mentioned in the Introduction (Chapter 1), and because it gives the following advantage over solution work:

In solution, a molecular complex is in equilibrium with its components. This means that the ratios of observed intensities of the charge transfer band and the bands characteristic of the components are always less than in the pure solid complex. In cases where charge transfer bands overlap these component bands partially, the solid state spectrum therefore provides the most favourable conditions for separation of the two bands.

Appendix B describes the various methods available for obtaining spectra of solid samples. Molecular complexes show strong

absorption bands in the visible and ultraviolet regions of the spectrum. Transmission spectra of mulls, pellets, films and single crystals are therefore difficult to obtain satisfactorily. Reflectance spectra require carefully constructed and tested equipment, which was not available.

The spectra in this work were therefore obtained largely by reflection spectroscopy. The dilution technique was found very valuable because:

(i) The complexes are relatively soft, and easily form a thin film over the surface of particles of the diluting material. This gives most effective dilution and least modification of the regular component of the reflectance of the diluent, which is also used as the reference.

(ii) The choice of diluent is easy, because the complexes are not reactive and do not require especially inert diluents. AnalaR KBr was chosen as a suitable inert, transparent, non-hygroscopic, easily-ground diluent.

(iii) The intense transitions due to charge transfer show greatly improved resolution when diluted samples, as opposed to undiluted samples of the complex, are used.

(Experiments to determine the best grinding conditions for the samples, and examples of the improvement in resolution for organic complexes of this type, were described in the author's Part II thesis, 1963, (reference 4).)

Dilutions of 1000:1, and grinding times of about 10 minutes

with hand-grinding were found to give spectra of satisfactory resolution. All solid spectra were recorded on a manual Unicam SP500 spectrophotometer, with reflection attachment.

4.3. Results.

4.3.1. Molecular complex spectra.

Absorption due to the following types of transitions occurs in the visible and ultraviolet spectra of molecular complexes between transition metal complexes with aromatic ligands and organic electron acceptor molecules:

(i) π-π^* transitions of the ligand and electron acceptor molecules.

(ii) π-π^* transitions perturbed by ligand-metal charge transfer.

(iii) Electronic transitions involving charge transfer from π orbitals of the metal complex to vacant π orbitals of the electron acceptor.

(iv) Weak d-d transitions of the transition metal ion.

Transitions of type (iii) only appear in the spectrum of the complex, whereas the other transitions also occur in the free donor and acceptor molecules. Type (iii) transitions are broad, intense bands (c.f. section 4.1.2.), and may therefore be distinguished from the narrower intense bands produced by type (i) and (ii) transitions and the weaker type (iv) bands. In some cases, their width, plus the fact that transitions of the components are shifted in the complex (due to charge transfer perturbations),

means that it is difficult to locate band maxima of type (iii) transitions located near component transitions. However, in most cases it is possible to identify separated new absorption bands of the complex, not present in the spectra of the components, as due to charge transfer from the metal complex to the acceptor molecule.

Tables 4.1 - 4.3 give band maxima for these inter-molecular charge transfer bands for the new complexes studied in this work.

Ligand-to-metal charge transfer bands for some 8-hydroxyquinoline complexes with copper, palladium and nickel are tabulated in table 4.4. Some of these bands have been assigned by other workers[35], and those for other complexes prepared were assigned by analogy.

The weak d-d transitions of the metal ions are nearly always partially or completely obscured by strong charge transfer bands in these complexes, so they cannot be studied directly. d-d bands in the π complexes and in the free metal complex will differ, for two reasons:

(i) The environment of the metal ion will be different, depending on the presence or absence of atoms in the two out-of-plane positions completing the octahedron about the metal atom. (e.g. The d-d bands in the essentially square planar Cu 8-hydroxyquinolinate/picryl azide complex will differ from the corresponding bands in the benzotrifuroxan complex, where the

TABLE 4.1.

Charge transfer band energies for 8-hydroxyquinoline and metal 8-hydroxyquinolinate π complexes. (kK).

Acceptor \ Donor.	Cu^{II}	Pd^{II}	Ni^{II}	8-hydroxy-quinoline.
BTF	21·5	19·7	19·0[b]	-
TFZ	22·7	-	-	26·0
DNBF	15·7	15·4	-	-
NBDF	17·4	-	-	-
CNF	19·6	19·4	-	-
TNB	20·7	-	-	25·0
Picryl azide	19·6	-	-	24·4
TNF	18·2	17·0	-	21·9
TCNB	17·9	17·6	-	23·5
Chloranil	15·9	14·8	14·0[a]	19·6[b]
DDQ	12·9	12·1	-	-
TCNE	13·3[b]	12·1[b]	10·1[b]	-

(a = solution spectrum, b = spectrum of impure solid complex.)

BTF = benzotrifuroxan; TFZ = benzotrifurazan; DNBF = dinitrobenzfuroxan; NBDF = nitrobenzodifuroxan; CNF = dichlorononitrobenzfuroxan; TNB = trinitrobenzene; TNF = trinitrofluorenone; TCNB = tetracyanobenzene; DDQ = dichlorodicyanobenzoquinone; TCNE = tetracyanoethylene.

TABLE 4.2.

Charge transfer band energies for benzotrifuroxan, benzotrifurazan, tetracyanobenzene and dinitrobenzfuroxan organic molecular complexes.

(kK)

Acceptor / Donor	BTF	TFZ	TCNB	DNBF
Naphthalene	27·4	-	24·5	22·2
Anthracene	21·5	-	19·7	16·0
			25·5	
Pyrene	22·9	23·3	19·8	16·7
			25·4	
Phenanthrene	-	27·0	23·4	-
Chrysene	23·8	25·0	21·7	-
Perylene	-	19·2	-	-
Durene	-	27·4	24·4	-
Diphenyl	26·9	-	25·8	-
Azulene	21·7	21·6	19·3	-
β-naphthol	24·1	-	22·0	17·9
Hexamethylbenzene	26·3	26·2	-	-
1,4-diphenylbutadiene	-	24·1	21·5	-
1,5-diaminonaphthalene	-	-	15·9	-
			22·8	
			28·8	
Dimethyl aniline	-	-	17·9	-
			24·5	
			29·0	
Aniline	-	-	21·0	-
			29·2	
2,7-dimethoxynaphthalene	-	-	23·4	-
			29·8	

TABLE 4.3.

Charge transfer bands of other organic molecular complexes. (kK).

Picryl azide/pyrene 21·3, Picryl azide/naphthalene 25·8,

Nitrobenzodifuroxan/naphthalene 24·1,

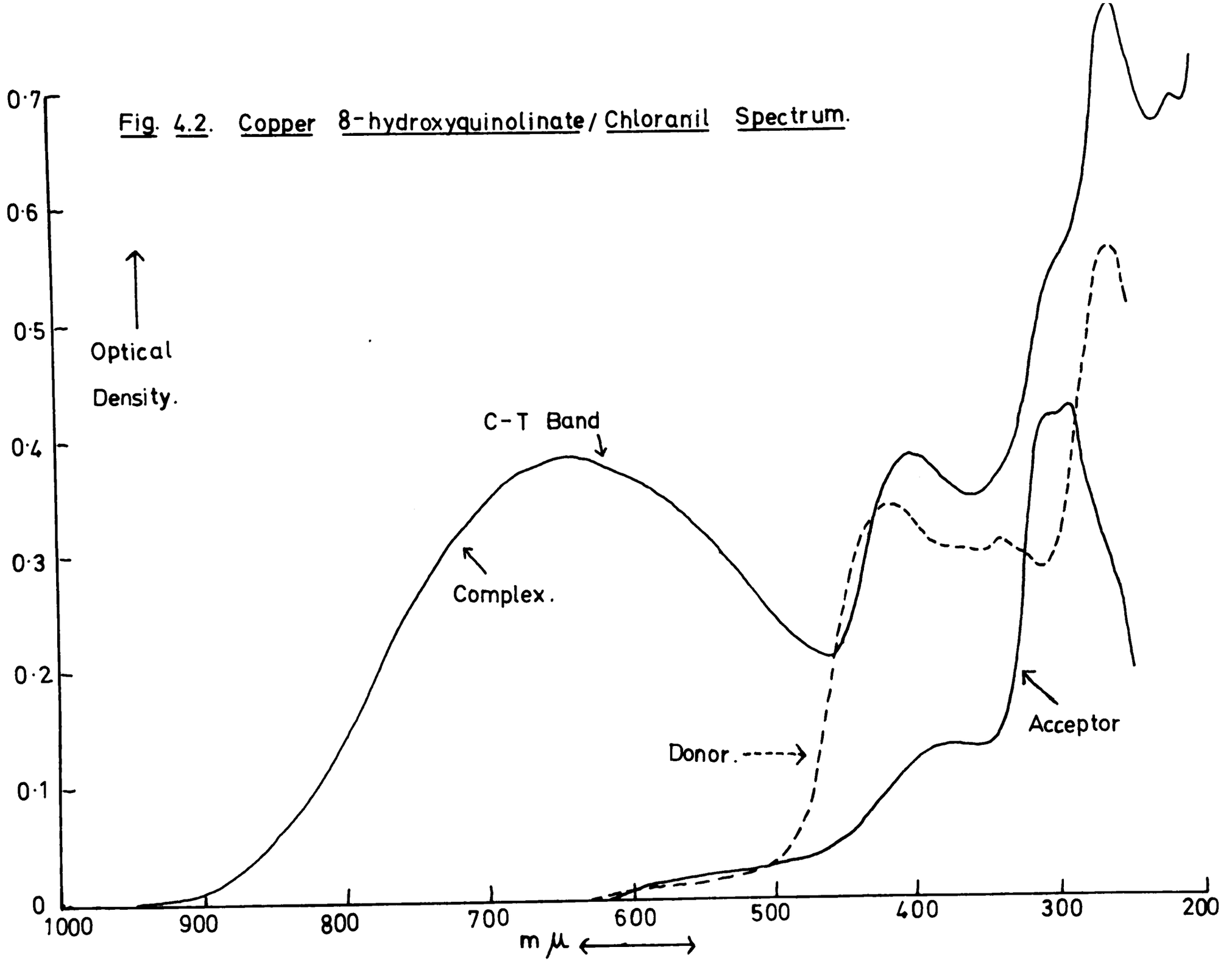
Dichlorodicyanoquinone/pyrene 12·9

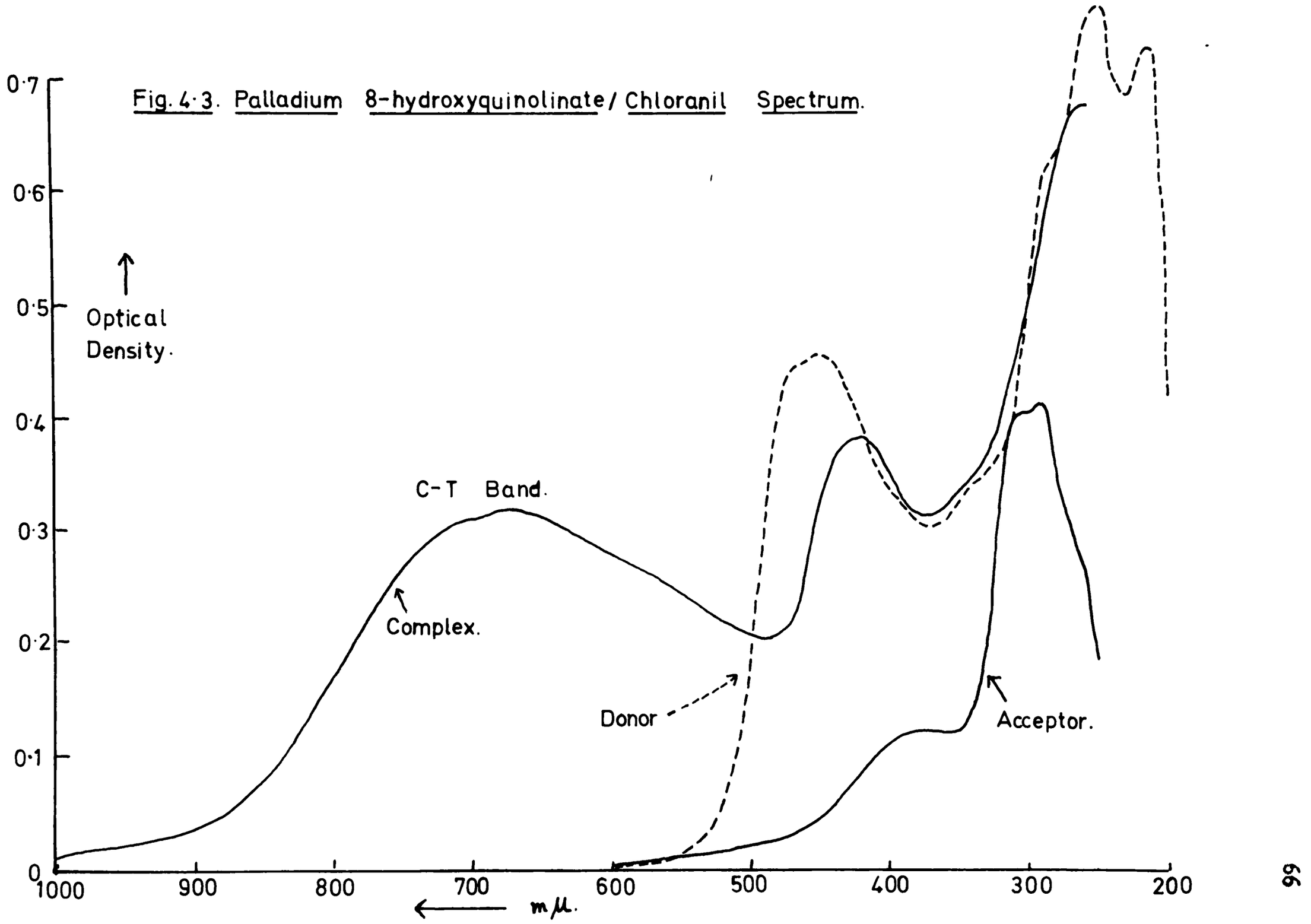
Dichloromononitrobenzfuroxan/pyrene 20·6.

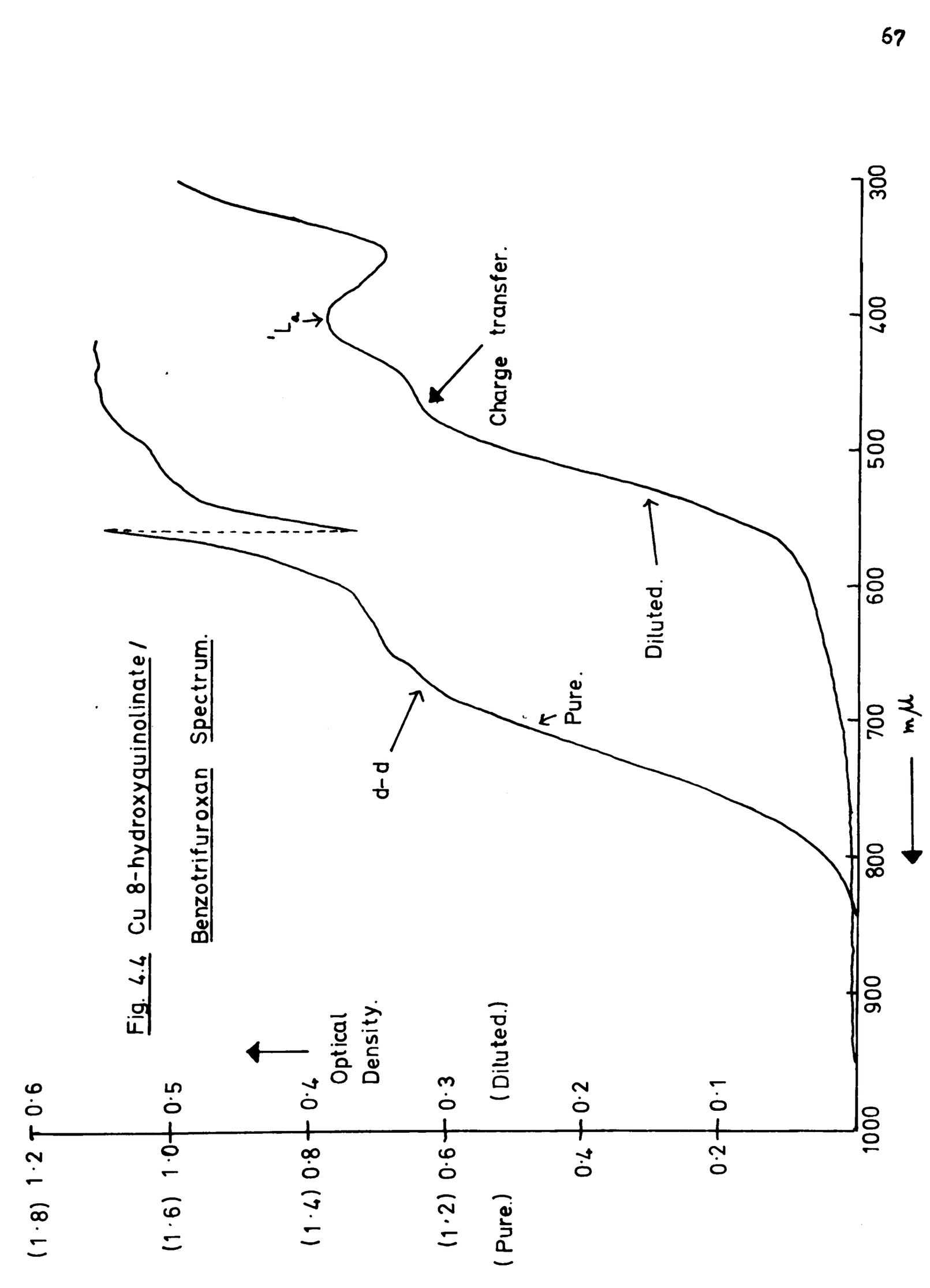
TABLE 4.4.

Inter- and intra- molecular charge transfer bands for chloranil complexes of Cu^{II}, Pd^{II} and Ni^{II} 8-hydroxy- and 5-methyl-8-hydroxy-quinolinates. (kK).

	Inter-molecular.	Intra-molecular.
Cu^{II} 8-hydroxyquinolinate	15·9	24·3
Cu^{II} 5-methyl-8-hydroxyquinolinate	15·3	23·4
Low spin Pd^{II} 8-hydroxyquinolinate	14·8	23·1
Low spin Pd^{II} 5-methyl-8-hydroxyquinolinate	14·3	22·2
Low spin Ni^{II} 8-hydroxyquinolinate	14·0	22·0


Fig. 4.2. Copper 8-hydroxyquinolinate / Chloranil Spectrum.
0·7
0·6
0·5
0·4
0·3
0·2
0·1
0
Optical
Density.
C-T Band
Complex.
Donor.
Acceptor
1000
900
800
700
600
500
400
300
200
mμ


Fig. 4·3. Palladium 8-hydroxyquinolinate / Chloranil Spectrum.
0·7
0·6
0·5
0·4
0·3
0·2
0·1
0
Optical Density.
C-T Band.
Complex.
Donor
Acceptor.
1000
900
800
700
600
500
400
300
200
mμ.


Fig. 4.4 Cu 8-hydroxyquinolinate / Benzotrifuroxan Spectrum.
Optical Density.
(Pure.)
(Diluted.)
(1·8) 1·2 0·6
(1·6) 1·0 0·5
(1·4) 0·8 0·4
(1·2) 0·6 0·3
0·4 0·2
0·2 0·1
1000 900 800 700 600 500 400 300
mμ
d-d
Pure.
Diluted.
Charge transfer.
^1L_a

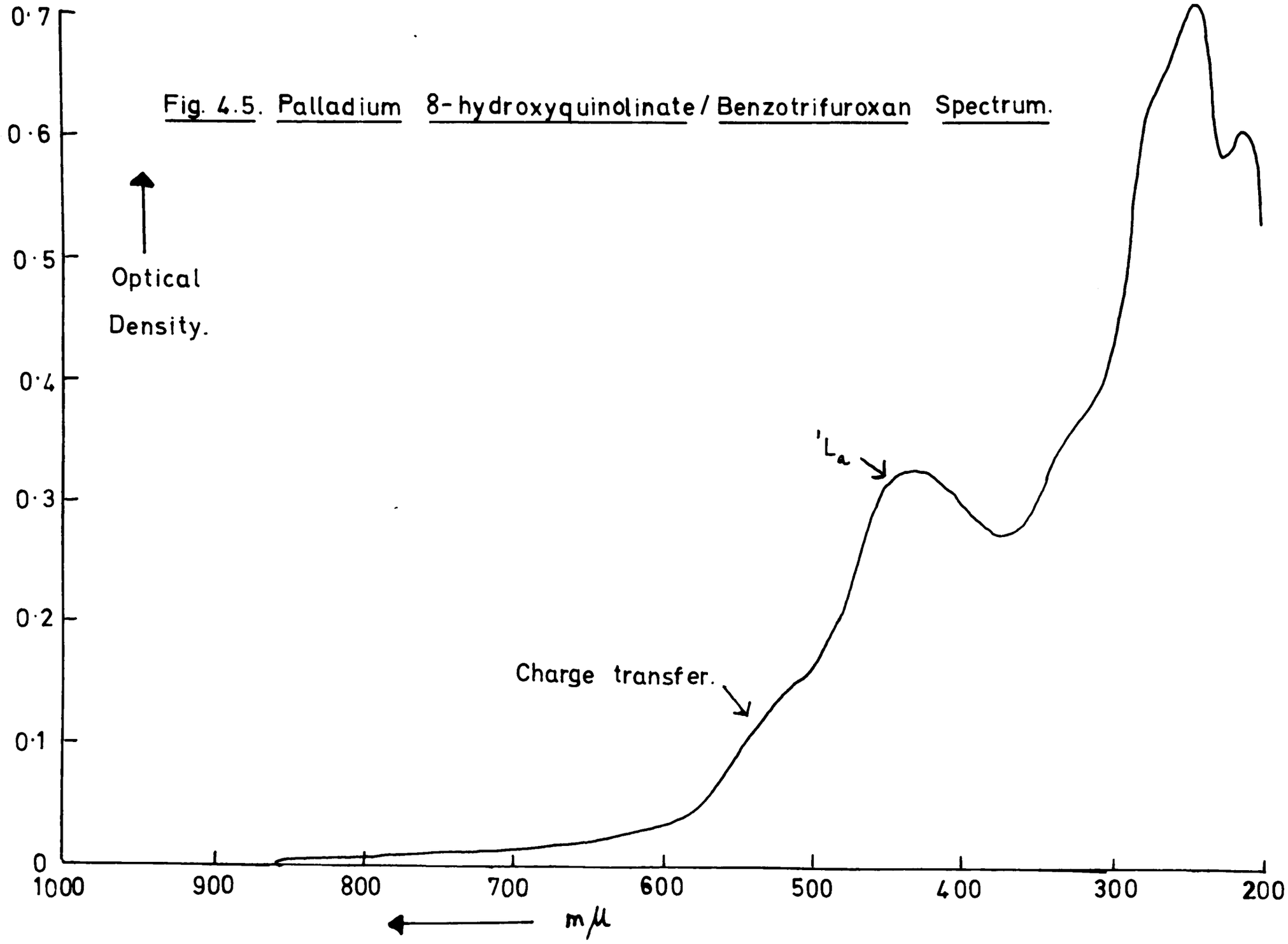


Fig. 4.5. Palladium 8-hydroxyquinolinate / Benzotrifuroxan Spectrum.

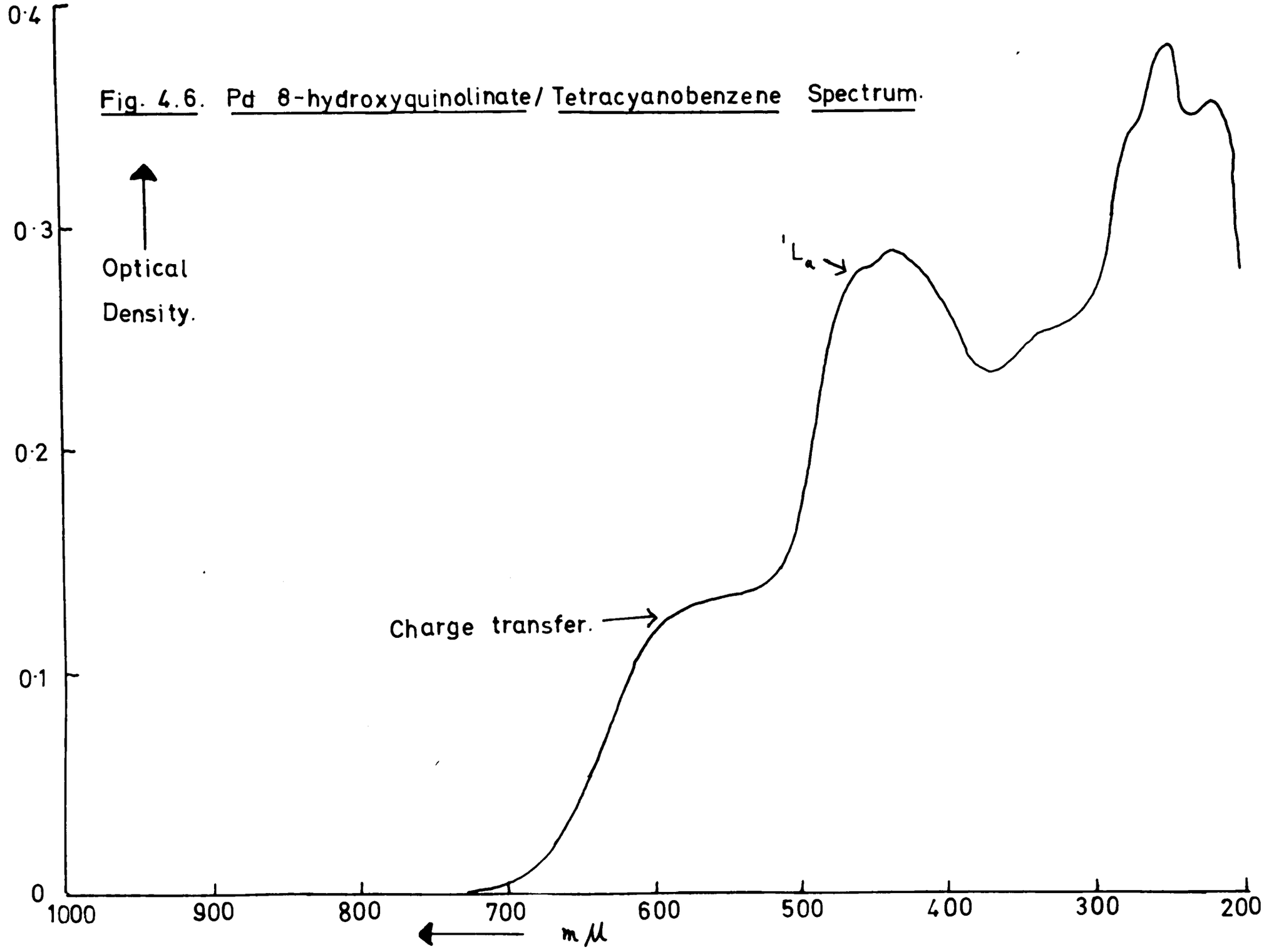


Fig. 4.6. Pd 8-hydroxyquinolinate/ Tetracyanobenzene Spectrum.

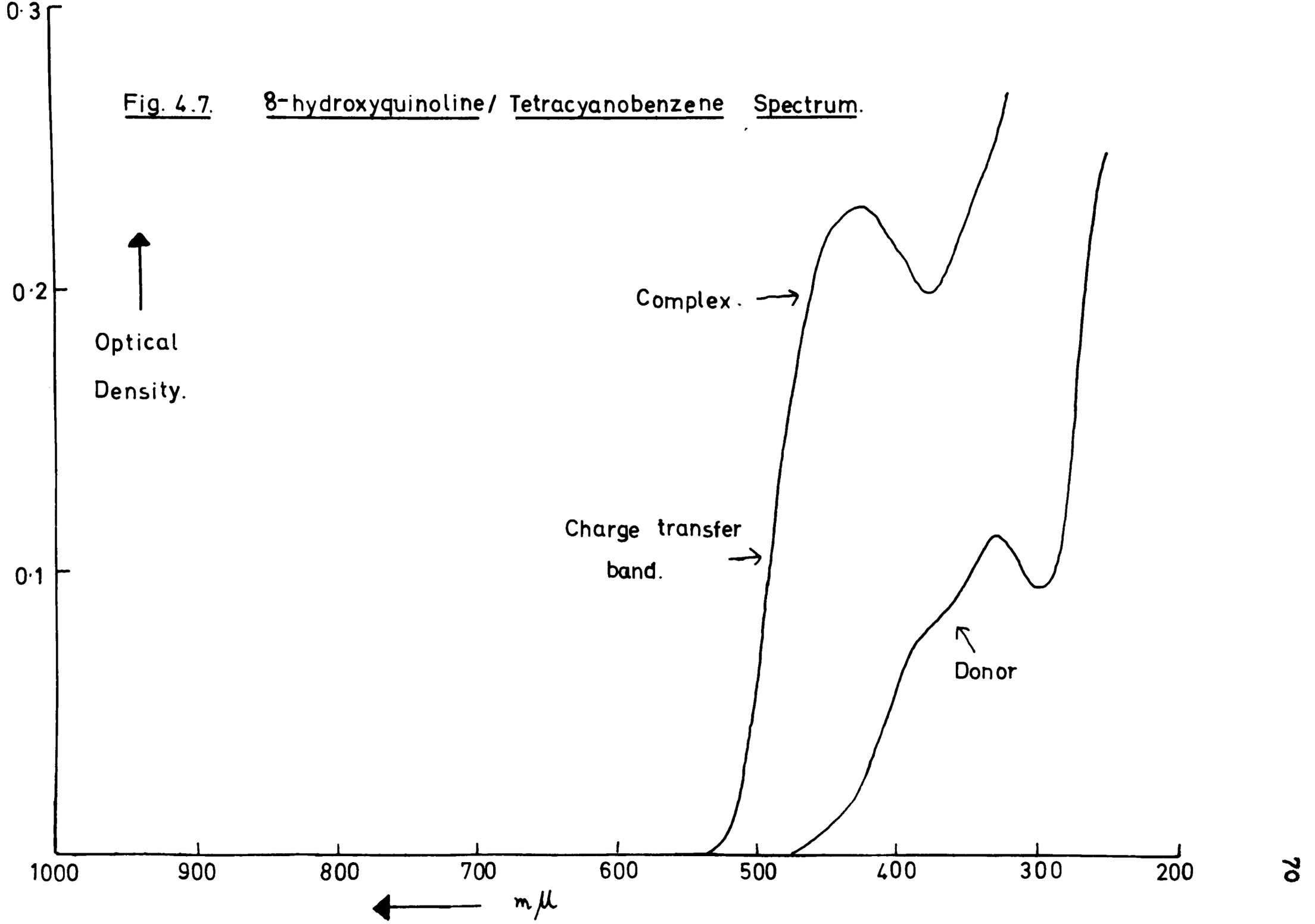


Fig. 4.7. 8-hydroxyquinoline/ Tetracyanobenzene Spectrum.

octahedral positions are occupied by nitrogen atoms of the electron acceptor).

(ii) Small changes in the electron distribution in filled π orbitals of the ligands linked through d orbitals of the metal will affect the energies of the d levels slightly. These changes may be caused by charge transfer perturbations, but, since the molecules are largely in the ground state (which only involves a small amount of charge transfer character c.f. section 4.1), effects of this type will be small, and almost certainly not detectable from the spectrum, even if the d-d bands were isolated as separate bands in the spectrum.

Figures 4.2 to 4.7 show typical spectra, with the different types of band labelled, as illustrations of the general form of the spectra.

4.3.2. Spectroscopic studies of the reactions between strong donors and strong acceptors.

(The following notes are intended as a guide to further investigations, and not as a full discussion of all the species involved, which is beyond the scope of the present work.)

(i) 8-hydroxyquinoline + 2,3dichloro-5,6-dicyanoquinone in $CHCl_3$.

The following sequence of observations was made:

(a) On mixing the warm solutions of the two components, a transient olive-green colour is produced, lasting approximately 15 minutes. The visible spectrum of the solution, recorded rapidly on a Unicam SP700 spectrophotometer, using a freshly filtered sample of the solution, shows a new peak at 16,900 cm^{-1}, which fits exactly on the linear plot of charge transfer bands for 8-hydroxyquinoline against those for corresponding Cu 8-hydroxyquinolinate complexes. This suggests that the transient colour is due to the formation of a charge transfer complex in solution.

(b) Soon after mixing the solutions, a light green-yellow solid begins to precipitate, and precipitation is complete in 30 minutes, with complete fading of the deep olive-green colour of the solution. The reflection spectrum of this solid (undiluted) shows an inflection at 22,000 cm^{-1} and a peak at 25,600 cm^{-1}, but no peaks at lower energy.

(c) The solid dissolves in acetone, giving a red solution, with a weak absorption peak at 19,500 cm^{-1}. On evaporation of the acetone, a rust-red solid is left.

These results show that the product is not a charge transfer complex, and that reaction has occured, probably followed by more complex secondary reactions in acetone.

(ii) 8-hydroxyquinoline + tetracyanoethylene in ethyl acetate.

(a) On mixing cold solutions of the two compounds, a red-mauve colour is produced in solution.

(b) After standing in light for about one hour, the colour fades to give a green-brown solution, with absorption peaks at 15,600 and 17,200 cm^{-1}. If the corresponding copper complex is left in solution in light for 24 hours, it gives a similar solution, with absorption peaks at 16,400 and 18,700 cm^{-1}.

This may be due to reaction of the TCNE with the donor molecule (possibly a Diels-Alder reaction enhanced by charge transfer interactions) and/or polymerisation of the TCNE, induced by light.

(iii) Nickel 8-hydroxyquinolinate + 2,3-dichloro-5,6-dicyanoquinone in chloroform.

(a) On mixing hot solutions of the compounds, a deep magenta colour appears in solution.

(b) This begins to fade after 30 seconds, at the same time becoming cloudy. A yellow precipitate coagulates and settles as the solution cools. This solid does not melt when heated to above 350°C, but decomposes.

(c) The yellow solid is insoluble in CCl_4, benzene and water, sparingly soluble in acetone, ethanol and dioxan, and soluble in 2-methoxyethanol, α-chloronaphthalene and o-dichlorobenzene. The solutions in the last three solvents are deep green, light brown (hot) or deep blue (cold), and purple-brown (hot) or blue (cold), respectively.

The spectra of these solutions show the following features:

29·3 kK (peak, EtOH 2-methoxyethanol)

26·8 kK (peak in EtOH)

25·7 - 25·0 kK (2-methoxyethanol EtOH, inflexion in cold o-dichlorobenzene)

17·2 - 16·8 kK (α-chloronaphthalene o-dichlorobenzene 2-methoxyethanol EtOH).

No band is observed at 11·5kK, the expected position for a charge transfer band of a normal π complex between these molecules.

(d) On warming the solution in α-chloronaphthalene, the band at 16·8 kK diminishes in intensity, while a new band at 21 kK appears, with isosbestic points at cross-over positions of the spectral curves. This suggests that the species responsible for these two peaks are in equilibrium with each other.

(e) The reflection spectrum of the undiluted yellow solid shows a peak at 16·9 kK, followed by a sharp rise in absorption at higher energy. There is a slight rise in absorption towards 10 kK, suggesting that there may be a peak in the near infra-red region.

(f) After standing the residual chloroform solution for five days in light, a light brown solid is produced in small quantities. This gives a red solution in dimethyl sulphoxide (spectrum:- peak at 20·4 kK, inflections at 17 and 14·6 kK), as opposed to the initial yellow solid produced, which gives a green solution in dimethyl sulphoxide.

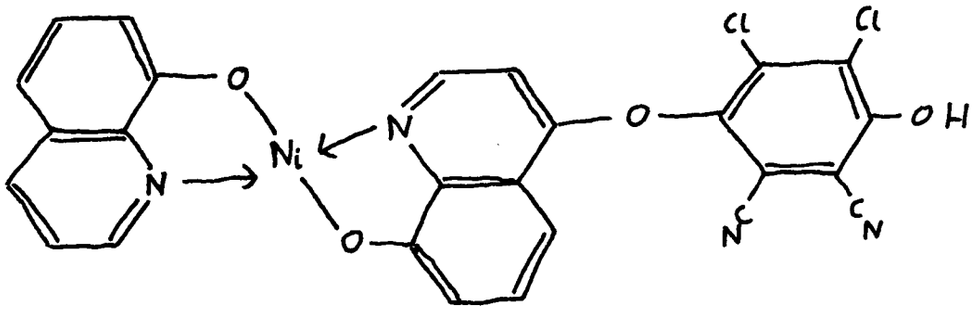
These results show that the two compounds react after transient formation of what is probably a charge transfer complex. They react more rapidly than the corresponding system involving 8-hydroxyquinoline, which suggests that increased electron donor power aids the reaction. One possible reaction scheme for the processes observed is outlined below:

$$Ni(ox)_2 + DDQ \rightleftharpoons Ni(ox)_2^+ + DDQ^-$$

$$\downarrow$$

insoluble product by nucleophilic attack.

One possible formula for the final product is



To discover if the product could be of this type, a sample of the crude material was analysed for C, H, N, and Cl. The postulated product requires

C, 54·5; H, 2·09; N, 9·8; Cl, 12·4 %

The analysis showed

C, 48·2; H, 3·0; N, 10·0; Cl, 13·3 % .

Considering the impure state of the product, this is not inconsistent with the proposed formula.

The infra-red spectrum of the final product shows no band at 1675 cm^{-1}, where the pure acceptor has a strong absorption band probably due to a quinone C=O group[36]. This is consistent with the structure proposed above.

Reactions of the type described above have only been observed with acceptor molecules capable of easy secondary reactions under the influence of charge transfer interactions. This suggests that the transition from formation of stable charge transfer complexes to redox and other processes cannot be predicted merely from ionization potential and electron affinity data, but that actual electron distributions within molecules, in both ground and excited states, must also be taken into consideration.

4.4. Discussion.

4.4.1. Validity of the theories of charge transfer spectra for complexes with metal chelates as donors.

Before the theory outlined in section 4.1 may be used to interpret the significance of the charge transfer band positions, it is necessary to show:

(a) that the complexes formed by metal 8-hydroxyquinolinates

with electron acceptors have spectra following the same trends as those established for organic molecular complexes,

and (b) that the approximations involved in the theory are valid for these complexes.

(a) Spectroscopic similarities between metal 8-hydroxyquinolinate π complexes and organic molecular complexes.

If two electron donors both form a series of similar complexes with a variety of electron acceptors, there will be a simple relationship between the spectra of corresponding complexes of the two donors with common acceptors. In figure 4.8, D_1 and D_2 are the energy levels of the highest filled π orbitals of the two donor molecules, and A is the energy level of the first vacant π orbital of the electron acceptor molecule.

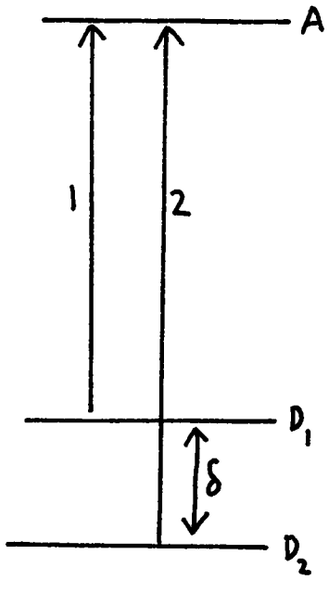
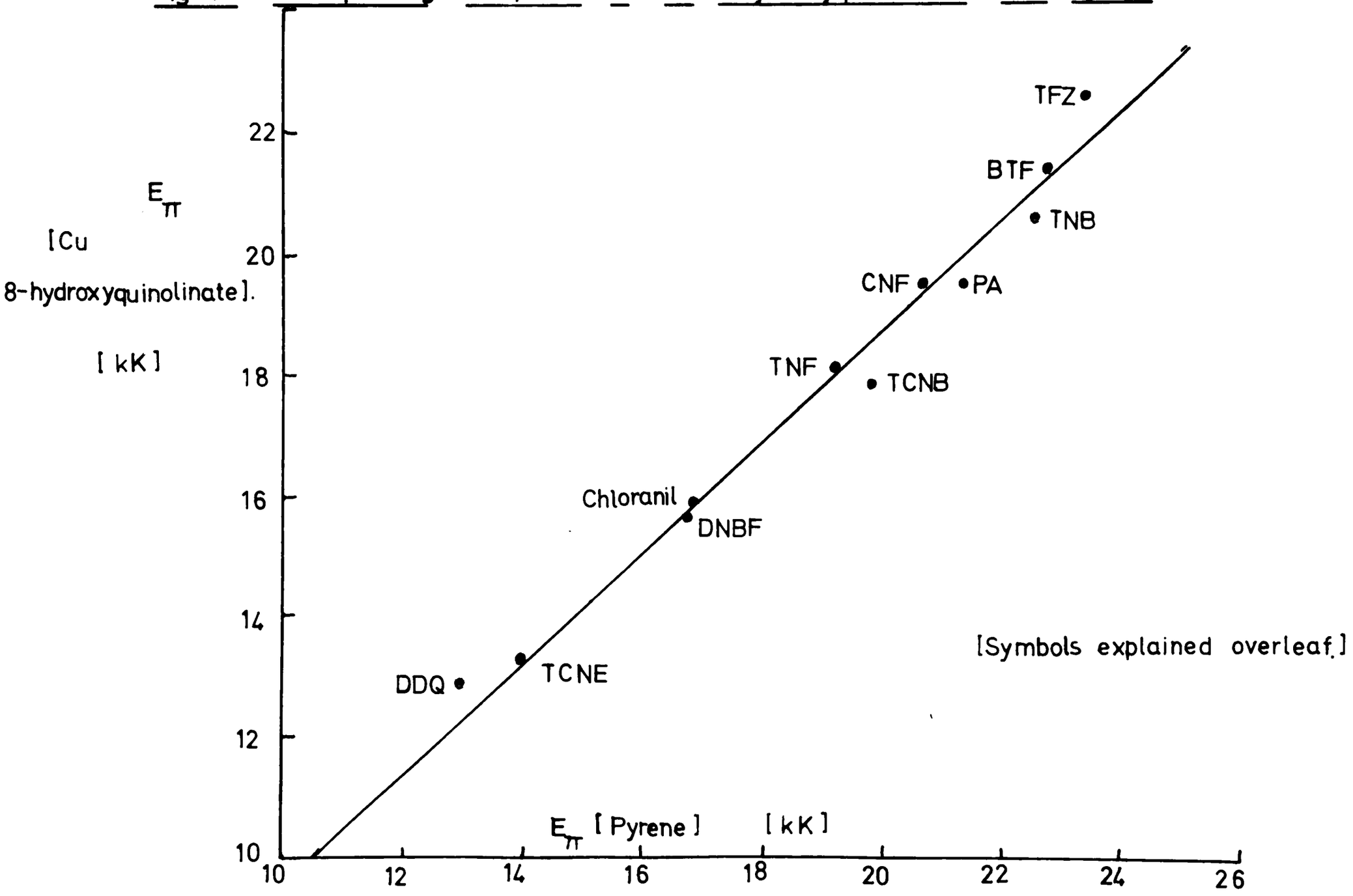


Figure 4.8.

Fig. 4.9. Corresponding Complexes of Cu 8-hydroxyquinolinate and Pyrene.



KEY TO FIGURE 4.9.

TFZ = Benzotrifurazan.

BTF = Benzotrifuroxan.

TNB = 1,3,5-trinitrobenzene.

PA = Picryl azide.

CNF = Dichloromononitrofuroxan.

TNF = Trinitrofluorenone.

TCNB = 1,2,4,5-tetracyanobenzene.

DNBF = dinitrobenzfuroxan.

TCNE = Tetracyanoethylene.

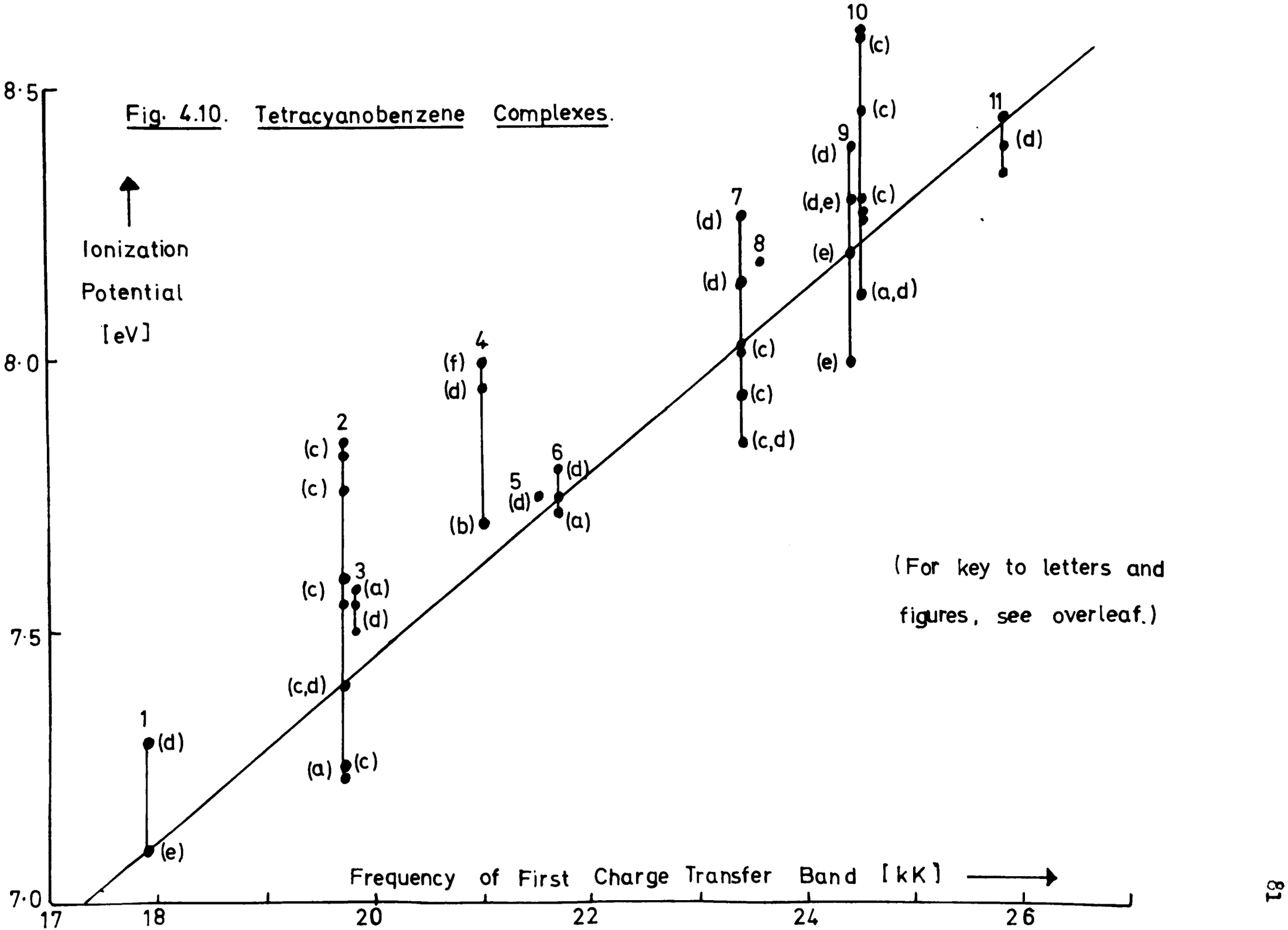
DDQ = 2,3-dichloro-5,6-dicyanobenzoquinone.

For complexes with different acceptors, A will vary, and the perturbation effects causing further separation of D_1 and D_2 from A will therefore vary. If these small perturbation effects are neglected, then a plot of transition 1 against transition 2 should be linear, with unit slope and intercept δ (the difference between the energy levels of the highest filled π orbitals of the two donors).

This may be used to show that any new donor is forming complexes of the normal type. If this is so, a plot of the supposed charge transfer bands of its complexes against the charge transfer bands of corresponding complexes of a donor known to form normal charge transfer complexes will be linear, with unit slope. This plot is shown for corresponding complexes of bis-8-hydroxyquinolinato Cu^{II} and pyrene, in figure 4.9. The slope of the least-squares best straight line drawn is 0·94, thus proving that the complexes formed by metal chelates of this type are of the same type as other π-complexes.

(b) Validity of charge transfer theory approximations for metal 8-hydroxyquinolinate π complexes.

There are two ways to test the validity of the approximations discussed in section 4.1. In the first place, the approximate relationships involving spectra and other physical quantities, such as ionization potential, may be tested, using experimental data. Secondly, other predictions, based on a simple model incorporating all the approximations used, may be compared with


Fig. 4.10. Tetracyanobenzene Complexes.
Ionization Potential [eV]
8·5
8·0
7·5
7·0
17
18
20
22
24
26
Frequency of First Charge Transfer Band [kK] ⟶
1 (d) (e)
2 (c) (c) (c) (c,d) (a) (c)
3 (c) (a) (d)
4 (f) (d) (b)
5 (d)
6 (d) (a)
7 (d) (d) (c) (c) (c,d)
8
9 (d) (d,e) (e)
10 (c) (c) (c) (a,d) (e)
11 (d)
(For key to letters and figures, see overleaf.)

KEY TO FIGURE 4.10.

1 = Dimethylaniline.

2 = Anthracene.

3 = Pyrene.

4 = Aniline.

5 = 1,4-diphenylbutadiene.

6 = Chrysene.

7 = Phenanthrene.

8 = Acenaphthylene.

9 = Durene.

10 = Naphthalene.

11 = Diphenyl.

(a) F.A. Matsen, J. Chem. Phys. 1956 24 602.

(b) K. Watanabe, J. Chem. Phys. 1957 26 542.

(c) M.E. Wacks and V.H. Dibeler, J. Chem. Phys. 1959 31 1558.

(d) G. Briegleb and J. Czekalla, Z. Elektrochem. 1959 63 9.

(e) R. Foster, Nature 1959 183 1253.

(f) H. Hartmann and M.B. Svendsen, Z. Phys. Chem. 1957 NF 11 16.

experimental results.

The relationship between charge transfer band positions and ionization potentials of donors (eqn. 4.8) has often been used to test the validity of the approximations for particular systems[37]. However, experimental values of ionization potentials from different sources show such a wide spread of values that this is not a useful method for detecting small effects due to the breakdown of the approximations (c.f. section 4.1.1.) An example of the type of plot which can be obtained is shown in figure 4.10 for complexes of tetracyanobenzene with organic donors[4,32].

The method based on a simple model of charge transfer, incorporating all approximations, is therefore necessary if some more quantitative estimate of the accuracy of the approximations is required. The approximations of equations 4.7 and 4.8 amount to neglecting the differences in the small perturbations due to charge transfer (implicit in equations 4.1 and 4.2) for series of complexes with common donors or acceptors. If it can be shown that relationships based on the further approximation of negligible perturbations are obeyed reasonably well, the validity of the assumption of negligible differences in perturbations of different related complexes will be beyond doubt.

For a series of complexes with two electron acceptors, an energy level diagram using unperturbed energy levels for donor and acceptor orbitals is shown in figure 4.11. This diagram predicts that a plot of transition 1 against transition 2 should

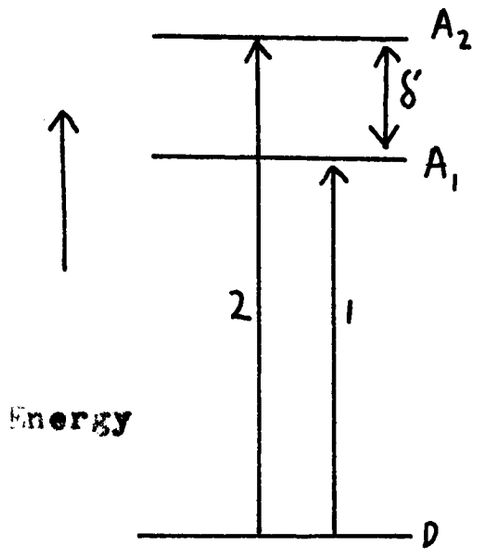


Figure 4.11.

be linear, with unit slope and intercept equal to δ', the difference in the energies of the lowest vacant orbitals of acceptors 1 and 2. This plot is shown in figure 4.12, for complexes of benzotrifuroxan and tetracyanobenzene. (The fact that the points for bis-8-hydroxyquinolinato Cu^{II} and Pd^{II} complexes fit on this line is further proof that they are conventional molecular complexes.) The least squares line has a slope of 0·97 and intercept of 2,700 cm^{-1} on the benzotrifuroxan axis (δ'). δ' may also be obtained by halving the energy difference of the first singlet transitions of the acceptors (making the approximation that the highest filled and lowest vacant orbitals are spaced symmetrically about a convenient origin, as in aromatic hydrocarbon energy levels[38]). These transitions are at 315·6 and 258 mμ for tetracyanobenzene and benzotrifuroxan, so that δ' = 3,500 cm^{-1}. This is remarkable agreement, considering the approximations involved, and justifies the use of equations such as 4.8 and 4.9. However, before general

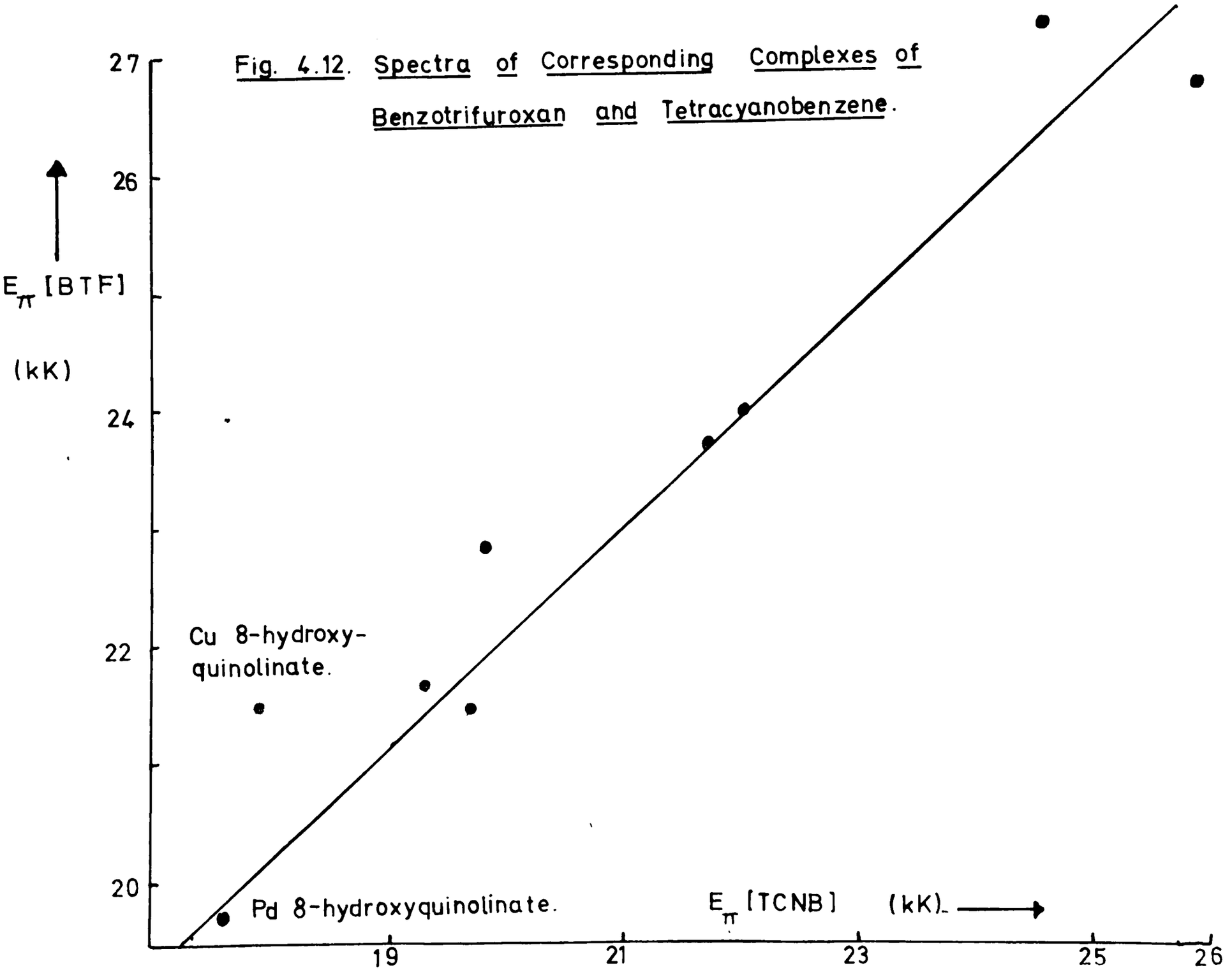


Fig. 4.12. Spectra of Corresponding Complexes of Benzotrifuroxan and Tetracyanobenzene.

use is made of these equations, likely effects due to perturbations must be considered briefly. These may be divided into overlap and energy effects, and will be discussed in terms of the system of corresponding complexes of two donors (figure 4.8).

(1) Overlap effects.

Two cases arise:

(a) D_1 and D_2 have similar shapes, so overlap factors are similar for both, but vary with the acceptor. Acceptors providing better overlap therefore perturb transitions 1 and 2 by similar amounts, to higher energy, so giving a point still on the line, but higher up than in the absence of perturbations.

(b) D_1 and D_2 have different shapes, so overlap changes on changing the acceptor are different for the two donors. This gives a scatter of points, with complexes of acceptors overlapping better with D_1 than with D_2 on one side of the line, and complexes with better overlap for D_2 than D_1 on the other side.

(2) Energy effects.

Two factors are involved:

(a) As the height of A increases, perturbations decrease.

(b) If δ is large, perturbations are greater for D_1 than for D_2.

These effects shift points at low energy to higher energies than predicted by a model involving no perturbations, and (b)

means that the shift along the axis for transition 1 is greater than along the transition 2 axis.

In the absence of accurately known unperturbed orbital energies, it is not possible to demonstrate these effects from experimental data, especially since the scatter of points from the true positions may be due to experimental error as well as to perturbation effects. However, these considerations show that maximum accuracy of the approximate relationships is expected for complexes of similar shape and orbital energy. The various planar metal 8-hydroxyquinolinate complexes satisfy this requirement well, so that relative energy levels deduced from intermolecular charge transfer bands of π complexes of these donors should be reliable.

The use of spectral data obtained from solid complexes, where perturbation effects might be expected to be larger than in solution interactions, does not detract from the validity of the conclusions, since it has been shown that the charge transfer band maximum for the nickel 8-hydroxyquinolinate/chloranil complex in solution is at the same position, within experimental error, as in the solid complex (see table 4.1). If this is true for the low energy transition of this compound, where perturbation effects are likely to be at their largest, it will also be true for the other complexes.

4.4.2. Ionization potentials, electron affinities and orbital energies from spectra.

(a) Electron affinities of acceptor molecules.

Using equation 4.9 and the method of Jortner and Sokolov[39], the following electron affinities have been deduced from the data of tables 4.2 and 4.3 :- (all values are in electron volts)

Benzotrifuroxan	1·9(8) ± 0·03	(mean of 6 values)
Benzotrifurazan	1·9(2) ± 0·10	(mean of 5 values)
Tetracyanobenzene	2·3(0) ± 0·06	(mean of 7 values)
Dinitrobenzfuroxan	2·6	(mean of 3 values)
Nitrobenzodifuroxan	2·3	(single value)
Dichloronitrobenzfuroxan	2·2	(single value)
Picryl azide	2·2	(mean of 2 values)

Published values[39] for some of the other acceptors used are given below for comparison:

Tetracyanoethylene	2·8(9) ± 0·10
Chloranil	2·5(9) ± 0·17
Trinitrobenzene	1·8(6) ± 0·13.

In the series of increasing electron affinity: trinitrobenzene < benzotrifuroxan ≏ benzotrifurazan < dichloronitrobenzfuroxan ≏ picryl azide < nitrobenzodifuroxan < dinitrobenzfuroxan, there are some interesting points:

(i) Trinitrobenzene is a much poorer electron acceptor than would have been predicted from the trend benzotrifuroxan < nitrobenzodifuroxan < dinitrobenzfuroxan, as it appears before benzotrifuroxan and not after dinitrobenzfuroxan. This may be due to steric effects, which are known to push nitro groups out of the plane of the ring[23a], which will prevent conjugation of the π electrons of the nitro groups with those of the ring.

(ii) Picryl azide is a better electron acceptor than trinitrobenzene. This may be because of an interaction between the azide group and one adjacent nitro group, which ensures that at least this part of the substituent system is held in the plane of the ring and therefore able to conjugate with the ring π system. (See chapter 3, where the picryl azide conformation in its copper 8-hydroxyquinolinate complex is shown.)

(iii) If one of the nitro groups in dinitrobenzfuroxan is replaced by two chlorine substituents, the acceptor power is reduced. This agrees with the general observation that chlorine is not a good substituent for enhancing electron acceptor power. (e.g. Trinitrobenzene is an electron acceptor and forms complexes with electron donors, whereas trichlorobenzene is not a good electron acceptor.)

Using the molecular orbital theory equation 4.12, ($h\nu_{C.T.} = a + b\chi$), as described in section 4.1, for a series of tetracyanobenzene complexes, gave the predicted linear plot[4], whose slope gave the value of β (the carbon-carbon resonance integral) as -3·03 eV. This agrees well with other estimates[25],

and is further proof that the approximations of the theory are valid. From the intercept, assuming that a Hückel type expression is still valid for tetracyanobenzene, the energy of the lowest vacant orbital of the molecule is given by

$$E = \alpha - 0{\cdot}37\beta$$

(where α = Coulomb integral for carbon

β = carbon-carbon resonance integral).

This compares with values of

$E = \alpha - 0{\cdot}46\beta$ for trinitrobenzene

and $E = \alpha - 0{\cdot}11\beta$ for tetracyanoethylene[25,40]

which is the same order of acceptor strength as given by the electron affinities.

(b) Ionization potentials and orbital energies of the metal complex donors.

Since the 8-hydroxyquinoline complexes behave as normal donors, the relationships of equations 4.8 and 4.12 may be used to deduce ionization potentials and Hückel χ parameters (assuming the Huckel theory is still valid for a planar metal complex of this type) for the highest filled π orbitals of the complex. These values are as follows:

Compound.	Ionization potential (eV)
8-hydroxyquinoline	7·9(4) ± 0·10 (mean of 3 values).
Cu complex	7·3(3) ± 0·07 (mean of 4 values).

Compound	Ionization potential (eV)
Pd 8-hydroxyquinolinate	7·1(3) ± 0·11 (mean of 3 values)

Compound	Hückel χ value.
8-hydroxyquinoline	0·57 ± 0·01 (mean of 5 values)
Cu complex	0·42 ± 0·03 (mean of 6 values)
Pd complex	0·37 ± 0·02 (mean of 4 values)

These results show that the energy levels of the highest filled orbitals of 8-hydroxyquinoline metal chelates are much higher than in metal-free 8-hydroxyquinoline. Energy changes of this type are associated with extension of the delocalised π orbitals over a larger area, and, in the metal complexes, this must involve linking the π systems of the two 8-hydroxyquinoline groups through the central metal atom. The degree to which the t_{2g} orbitals of the metal are exposed to the ligand π orbitals will control

(i) the ease with which this extension of delocalisation occurs (as shown by the energy of the intermolecular charge transfer band in the π complex)

and (ii) the ease with which transitions corresponding to intramolecular ligand-metal charge transfer processes occur (as shown by the energy of the intramolecular charge transfer band).

Thus, if the energy of filled ligand π orbitals is proportional to the extension of conjugation, and if this in turn is

proportional to the energy of ligand-metal charge transfer transitions, a direct proportionality between inter- and intramolecular charge transfer bands in the spectra of a series of related complexes of this type is a possibility.

To test this possibility, the two types of charge transfer band were plotted against each other for complexes of chloranil with 8-hydroxyquinoline complexes of copper, palladium and nickel and 5-methyl-8-hydroxyquinoline complexes of copper and palladium. This plot is shown in figure 4.13, and clearly shows that the relationship is as predicted.

A relationship such as this would be expected if the donor bands considered were pure π-π^* transitions. The reason why it also applies to the bands which have so far been described as ligand-metal charge transfer bands is clear if the true nature of these bands is considered. Internal π-π^* transitions of the 8-hydroxyquinolinate anion may be divided into two types, according to whether the transition moment is polarised along the long or short axis of the molecule. These transitions are known as the ^1L_b and ^1L_a transitions, respectively (using the Platt notation[41]). The ^1L_a transition can mix in states involving charge transfer in the anion (i.e. resonance hybrids with negative charge on the ortho and para positions of both rings as well as on the oxygen), and also states with back donation from the t_{2g} orbitals of the metal to the ring π system. Thus, the donor band involved in this relationship may be regarded as a ligand π-π^* transition modified by combination with states involving charge transfer between

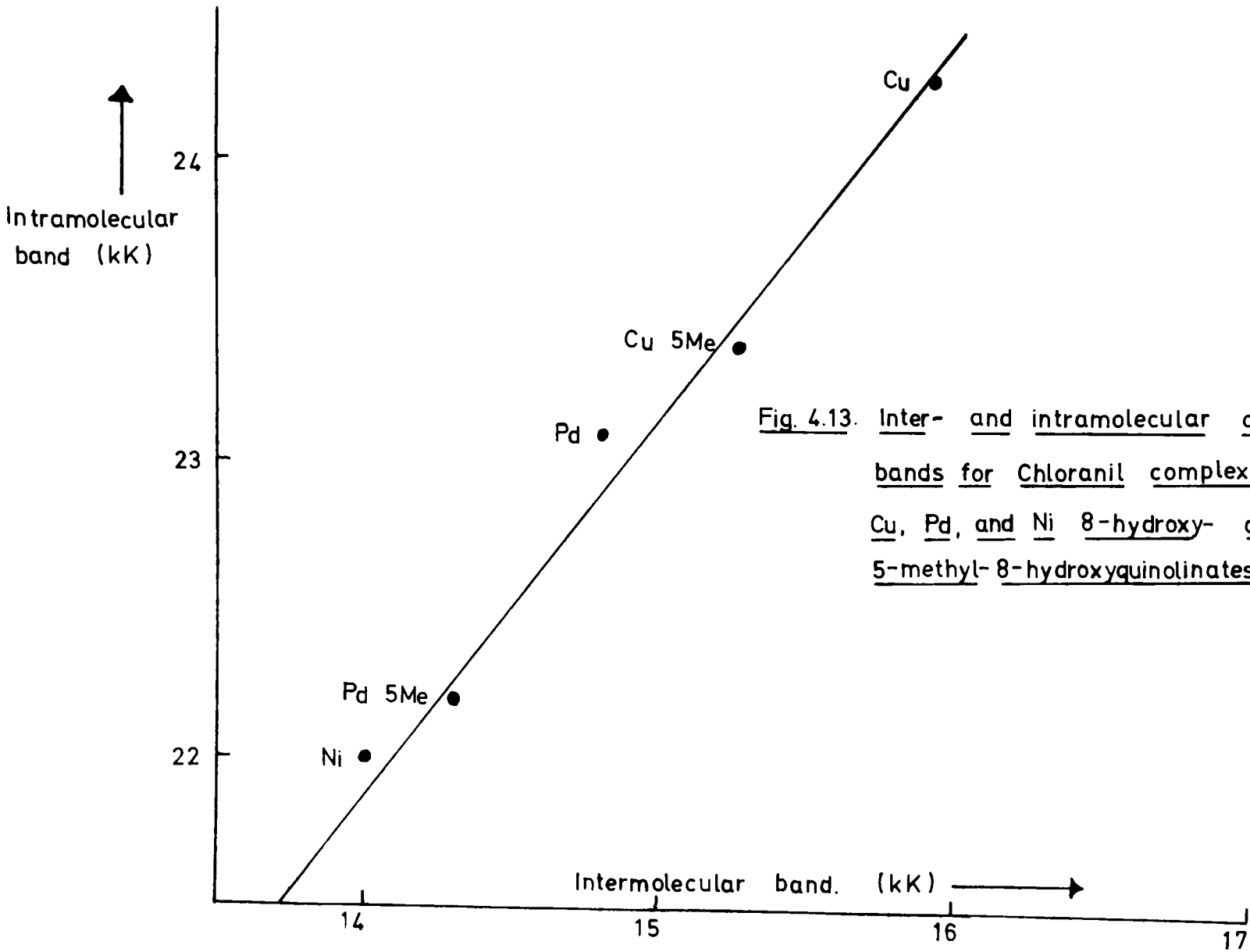


Fig. 4.13. Inter- and intramolecular charge transfer bands for Chloranil complexes of Cu, Pd, and Ni 8-hydroxy- and 5-methyl- 8-hydroxyquinolinates.

the metal and the ligand. It will therefore follow the same relationships as are followed by pure π-π^* transitions.

Studies of the above type provide direct experimental results showing the effect of different metal ions on ligand π orbital energies. Molecular orbital calculations on such metal complexes are difficult, as the values of resonance and overlap integrals for metal-ligand bonds are largely empirical. However, some Hückel calculations have recently been made for 8-hydroxyquinoline and its nickel complex[21]. The calculated value of χ for the highest filled orbital of neutral 8-hydroxyquinoline is +0·552, which agrees well with the experimental value of 0·57 deduced above. For the nickel complex, the χ values for the highest and second highest filled orbitals are 0·200 and 0·580. Deduction of Hückel χ parameters from charge transfer spectra of single complexes is not a satisfactory procedure, but the value deduced from the spectrum of Ni 8-hydroxyquinolinate/chloranil is 0·34. The difference between experimental and theoretical values here suggests that the assumptions used to deduce overlap and resonance integrals in the calculations may have been invalid. Experimental values of energy levels obtained in this way could be useful as an indication of which values of the resonance and overlap integrals are most appropriate for bonds involving metal atoms.

4.4.3. Infra-red spectra.

In using theory which neglects perturbation effects, it has been assumed that the percentages of charge transfer character in the ground states of the complexes are small. One direct method of confirming this is to compare the infra red spectrum of a complex with the infra red spectra of its separate components. An important contribution to the ground state from intermolecular charge transfer will be reflected in changes in infra red frequencies of vibrations which are sensitive to the changes in electron distribution thus produced.

Infra red spectra of the copper 8-hydroxyquinolinate complexes with chloranil and benzotrifuroxan, and of the free components of these complexes, were recorded from 600 - 4000 cm^{-1} using a Perkin Elmer Model 21 spectrophotometer. (Samples were in the form of nujol mulls between NaCl plates, and the NaCl prism was used).

The spectra of the complexes closely resembled the superimposed spectra of the two components, with small shifts of 20 cm^{-1} or less for some of the bands. Empirical assignments of the bands were made (using Bellamy's "The infra red spectra of complex molecules"[36]), and from these it was deduced that the small changes in the spectra of the complexes represented the weakening of certain vibrations as a result of charge transfer from filled bonding orbitals to anti-bonding orbitals. For example, in the chloranil complex, the C-Cl stretch frequency of the chloranil

molecule is moved from 710 to 692 cm^{-1}, and the C=O stretching vibration bands have a different intensity pattern. However, in both complexes these shifts are small, and suggest that the ground state electron distribution is not changed appreciably by charge transfer perturbations.

CHAPTER 5.

ELECTRON SPIN RESONANCE.

5.1. Introduction.

Copper (II) complexes give an electron spin resonance spectrum consisting of four lines of equal intensity, due to interaction between the unpaired electron of the d^9 ion and the nuclear spin of copper (3/2).[42] If this unpaired electron is delocalised over a ligand which contains atoms with a nuclear spin near to the metal atom, each of the four lines will be split into hyperfine lines, the number and intensity of such lines depending on the nuclear spins and number of atoms of each type in the environment of the metal. Copper 8-hydroxyquinolinate contains two nitrogen atoms, with nuclear spin 1, co-ordinated to copper, and two hydrogen atoms, with nuclear spin 1/2, on the ring carbon atoms adjacent to the nitrogen atoms. The E.S.R. spectrum may therefore yield valuable information on the nature of the bonding between copper and this ligand.

In a crystalline copper complex, the magnetic dipole interactions between neighbouring paramagnetic species lead to a broadening of any hyperfine structure[ref.42, p.90], but, if the copper complex can be diluted by doping into a known matrix of a similar complex containing no paramagnetic species, this broadening is very much reduced. Further information on the

bonding may then be obtained by measuring the dependence of the spectrum on the orientation of the paramagnetic species with respect to the applied magnetic field.

This chapter reports preliminary investigations of this type on crystals containing 0·1, 1·0 and 10 percent of copper 8-hydroxyquinolinate/chloranil doped into a matrix of the corresponding palladium complex.

The main objectives of the work were:

(a) To determine the concentration of copper complex giving the best resolution of the spectrum consistent with a low noise level, and to observe any hyperfine structure in the spectrum.

(b) To obtain qualitative estimates of the influence of copper concentration on line width.

(c) To mount a crystal giving sharp hyperfine structure in three mutually perpendicular directions, using simple techniques, and, if possible, to deduce parameters concerning the degree of covalent bonding (both σ and π) from the variation of the spectrum with angle in these three planes.

5.2. Experimental.

E.P.R. spectra were recorded using a Varian spectrometer, kindly made available by Dr. L. Merriwether of the Department of Chemistry, Imperial College, London. Crystals

were mounted on a quartz rod (approximately 1/4" diameter), using non-paramagnetic wax. The rod was clamped to a rotating mount, with a dial calibrated from 0 to 360°, which could be screwed into the cavity of the instrument. A crystal could therefore be positioned at any desired orientation with respect to the field. (Thanks are due to Dr. G. Horsfield of Varian Associates Ltd., who provided this attachment.)

Preliminary experiments showed that a 1 % doped crystal gave well resolved hyperfine lines and a reasonable signal strength. A crystal, about 2mm. long, with well defined faces (as drawn in Appendix A, section 3, Optical goniometry), was therefore mounted in the following three orientations (judged visually, using a binocular microscope):

(i) Needle axis vertical

(ii) Needle axis horizontal, line on end face vertical

(iii) Needle axis horizontal, line on end face horizontal.

In each orientation, spectra were recorded at 10° intervals over a 180° range, at room temperature. The direction of a reference line on the crystal with respect to the scale zero was noted in each case, so that the exact orientation of the crystal with respect to the field at each position was known.

Crystals of the 0·1 and 10% doped complexes were mounted in the same way, and spectra were recorded at known orientations for comparison of line widths, the modulation being unchanged throughout so as to give a valid comparison.

(In all the above measurements, a dual cavity was used, with

a standard manganese salt in one cavity, giving 6 lines for calibration purposes. Before changing any sample after a series of measurements, the field positions of each of these lines were checked.)

Thanks are due to Dr. H. A. O. Hill for assistance and instruction in the techniques used.

5.3. Results and Discussion.

Figure 5.1 shows typical E.S.R. spectra for the 0·1, 1·0 and 10% copper doped crystals. (The orientation of the crystal for these spectra was as follows: needle axis vertical, end line at an angle of 83° to the field for 0·1 and 10% crystals and at 77° to field for the 1·0% crystal).

The spectrum for the 10% crystal in figure 5.1 shows four sets of lines, resulting from the interaction of the unpaired electron with the copper nucleus. Each of these sets consists of five lines, due to interaction of the electron with the two equivalent nitrogen nuclei, each with a spin of 1. Comparison with the spectra for the 1·0 and 0·1% crystals shows that these five hyperfine lines each consist of at least two, and sometimes three, components. This extra splitting is caused by interaction of the unpaired electron with the nuclear spins of the hydrogen atoms attached to the carbon atoms adjacent to the nitrogen atoms in the ring system of the ligand. Two equivalent protons should give an extra-hyperfine splitting of each line into three (spin 1, 0 or -1). As seen from the 0·1% compound spectrum, this occurs

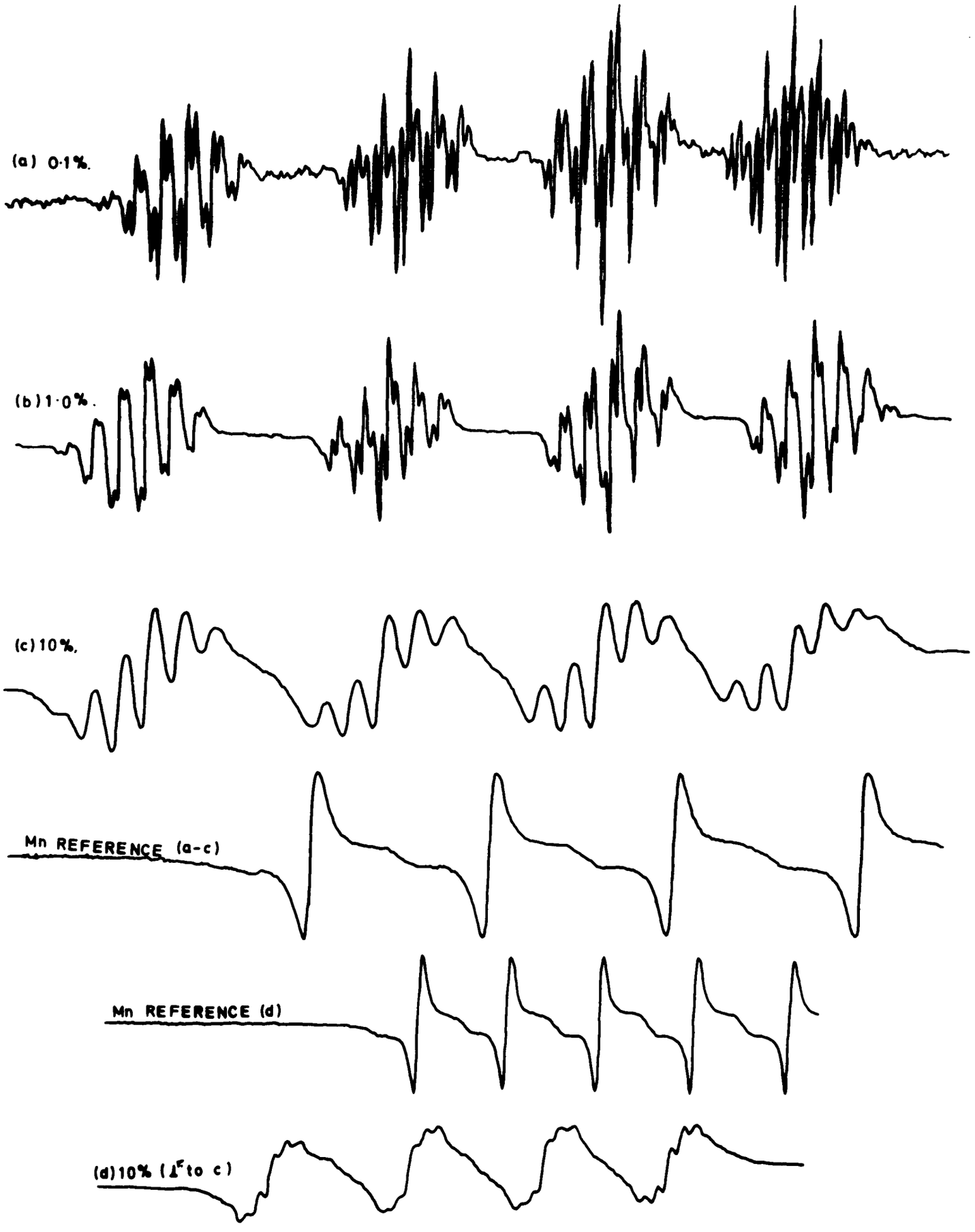


FIG. 5.1. E.S.R. SPECTRA.

most clearly at the high-field end of the spectrum, whereas at the low-field end the extra-hyperfine splitting is smaller and overlap between adjacent lines reduces the number of lines actually observed. This field-dependent splitting arises from the fact that the external applied field exerts a larger effect on the electron, relative to that produced by its environment in the crystal, when the electron is near the hydrogen atom than when it is near the copper and nitrogen atoms. Thus, an effect not normally noticed if the external field is much less than the effect of nuclei in the crystal becomes noticeable when this is not so.

In addition to these features, figure 5.1 shows a small sixth line on the outside edge of the two extreme sets of nitrogen hyperfine lines. This is due to the presence of two main isotopes of copper, Cu^{63} and Cu^{65}. These isotopes have the same nuclear spin, but slightly different nuclear moments[ref.42, p.159], and therefore give slightly different splittings, which only become apparent in the two extreme lines.

These features of the spectra confirm that charge is delocalised between the copper atom and the ligand, as shown by the spectroscopic work of chapter 4.

Figure 5.1 shows that line width varies only slightly in the concentration range 0·1 to 1·0% of copper complex, but increases considerably when there is 10% of copper complex in the lattice. Comparison of the two spectra shown for the 10% compound in two orientations also shows that this broadening effect is

angle-dependent. Line shape theory[ref.42, p.90] shows that the mean square line width is proportional to

$$\left[\frac{1-3\cos^2\theta}{r^3}\right]^2$$

where θ is the angle between the line joining the interacting magnetic dipoles and the direction of the magnetic field, and r is the distance between the dipoles.

The angle term accounts for the angular variation in broadening seen in figure 5.1, and the r^{-6} term means that normally only near-neighbour interactions need be considered. The crystal structure of this compound (Appendix A) is such that there are ten similar molecules (2 in the same plane, 4 above, and 4 below) surrounding each metal 8-hydroxyquinolinate molecule in the lattice. Thus, if the copper complex is distributed evenly through the lattice, each copper 8-hydroxyquinolinate will have at least one more as a near neighbour when the copper concentration reaches 10% . With even distribution, crystals containing only 1·0 or 0·1% of copper complex will have very few sites where there are two copper 8-hydroxyquinolinates as near neighbours. Line broadening is therefore only really effective at concentrations approaching 1% or greater, as observed. This result shows that the copper complex is evenly distributed through the lattice, and that there is very little, if any, tendency for the copper complex molecules to cluster together.

Using the dependence of the spectra on the orientation of the crystal with respect to the field, it is in principle possible

to determine the g-tensor and to deduce parameters indicating the degree of σ and π covalency of the ligand-metal bond[43,44]. For a triclinic system, the calculations become very involved unless either

(a) the crystal is mounted on a goniometer head and orientated so that the planes of the molecules are horizontal or vertical,

or (b) the crystal is mounted in three mutually perpendicular directions, when the solid geometry required to deduce, for example, the g-tensor, is greatly simplified.

The former procedure was not practicable using the simple rotation device available, so the second procedure was attempted. Before any calculations were made, however, the results were examined to see if they were consistent with the assumption that measurements were in three mutually perpendicular planes. Figures 5.2 to 5.4 show the field strength at the centre of the spectrum (proportional to the g value) as a function of angle of rotation in the three planes used. Figure 5.5 shows the three pairs of orientations in which the magnetic field makes the same angle with the molecules of the lattice, and which should therefore give three pairs of g values which are the same in each of the two equivalent orientations. Figure 5.5 also gives the field strengths of the centres of the appropriate spectra (deduced from figures 5.2 to 5.4), which are proportional to these g values. In each case, the two g values are clearly not equal, and this means that

Fig. 5.2. Needle axis horizontal, end line horizontal.

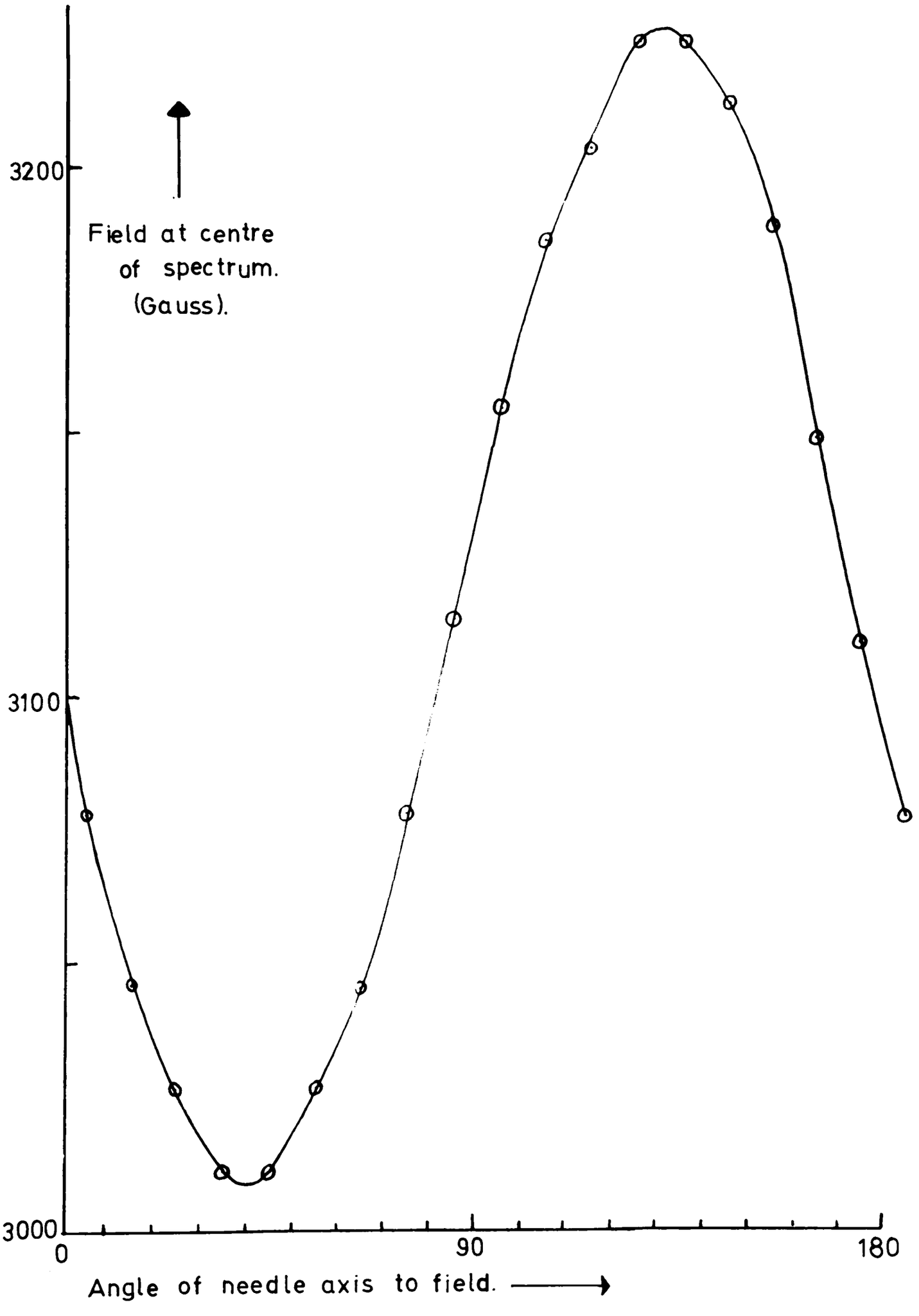


Fig. 5.3. Needle axis horizontal, end line vertical.

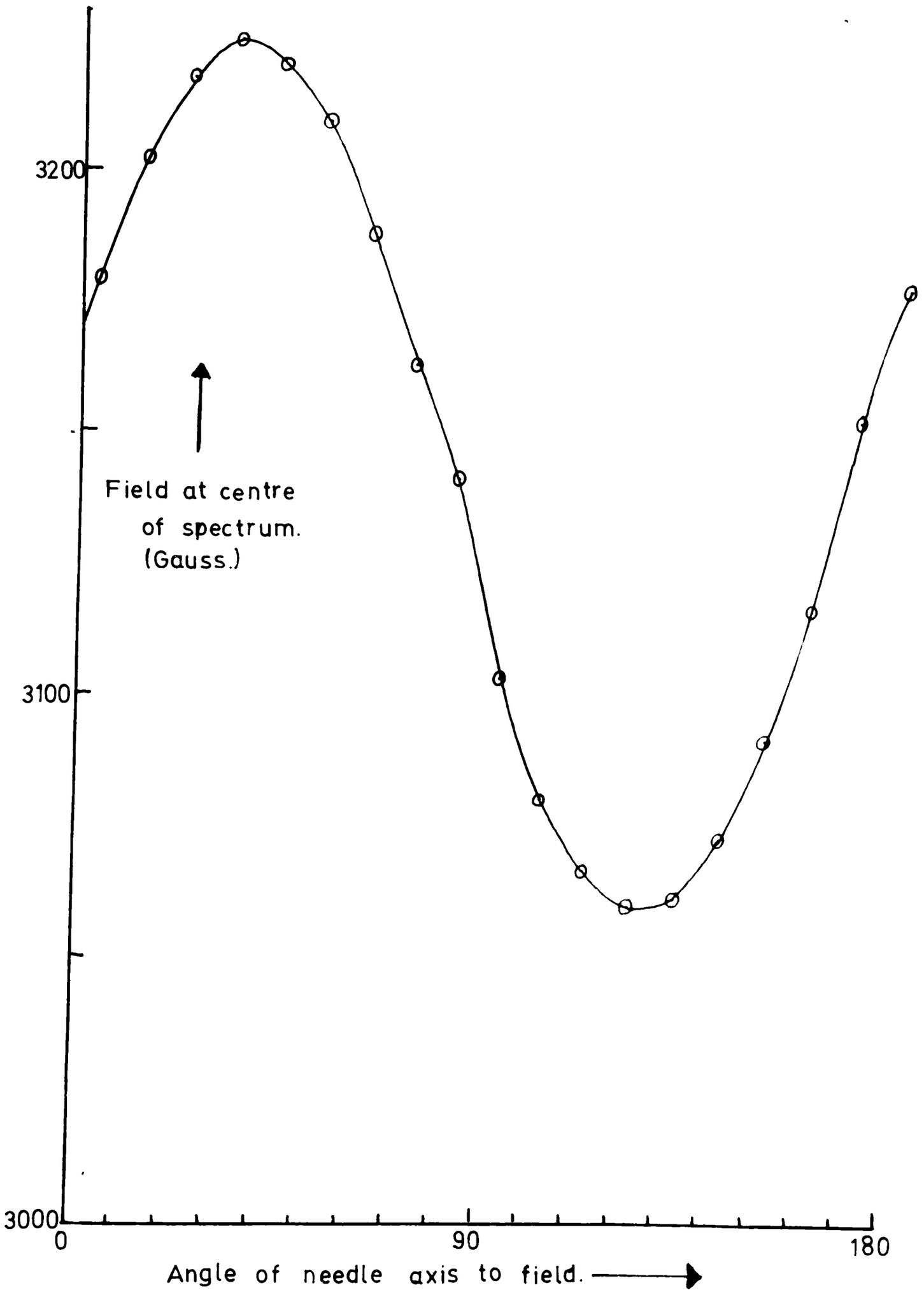
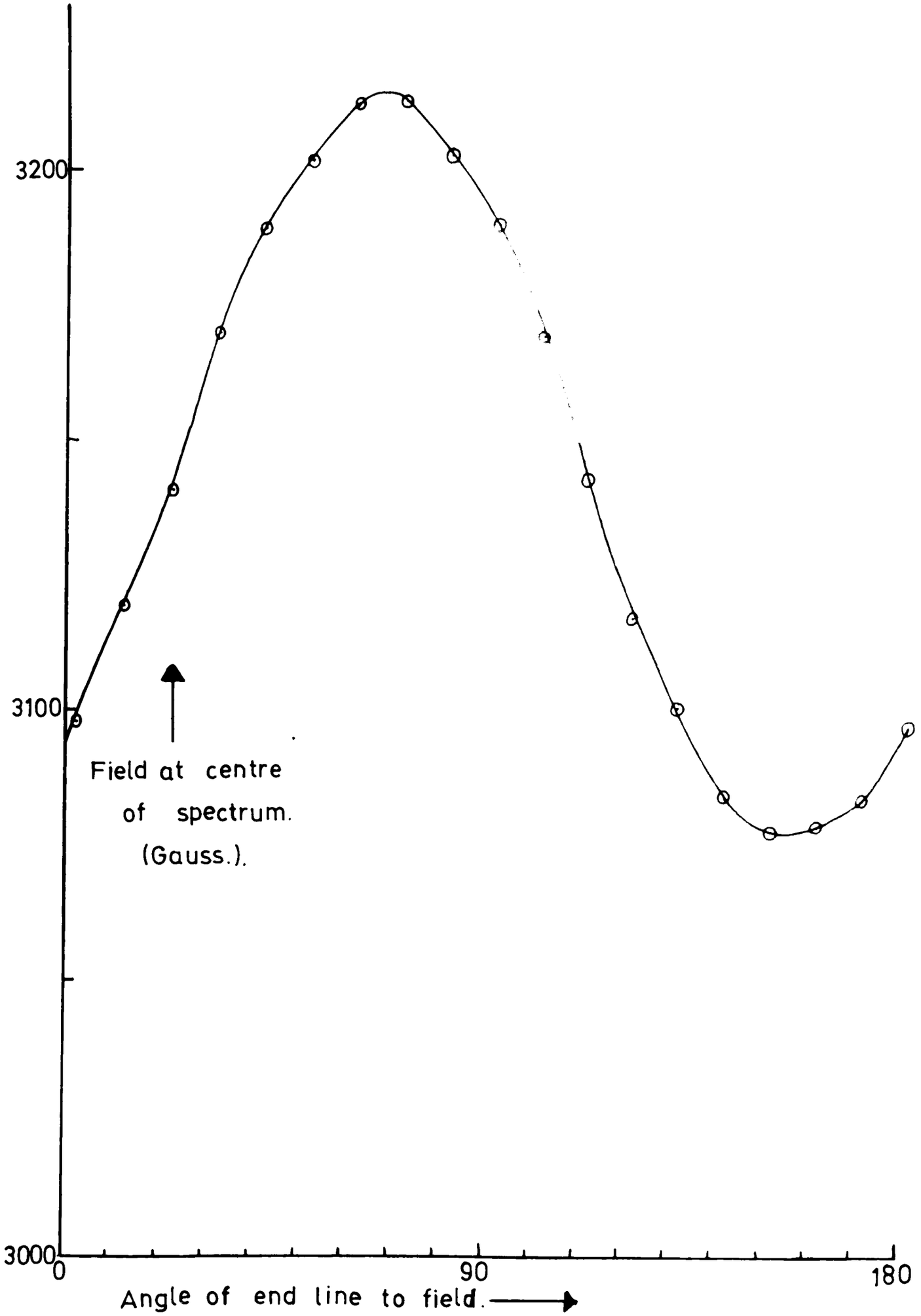


Fig. 5.4. Needle axis vertical.



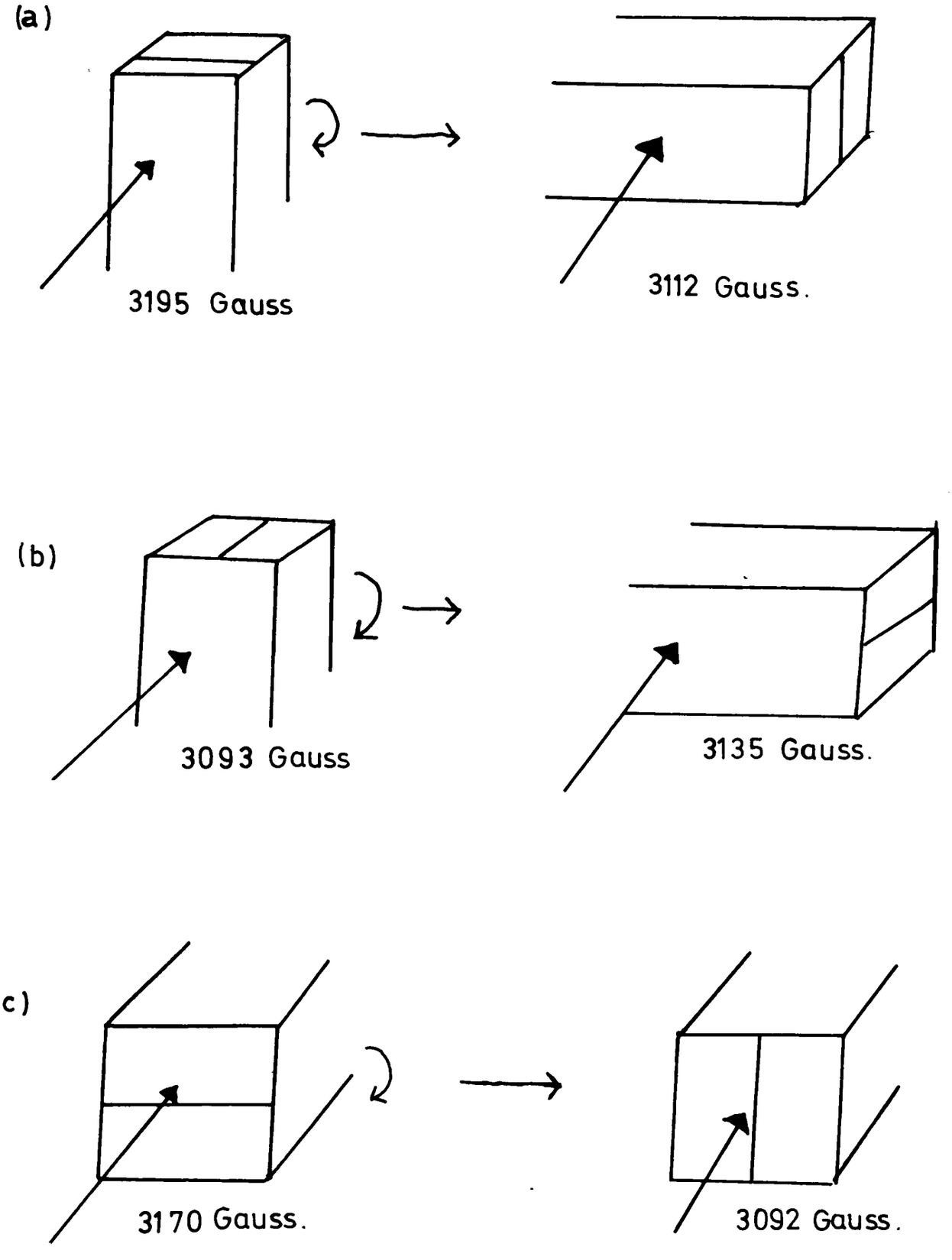

(a)
3195 Gauss
3112 Gauss.
(b)
3093 Gauss
3135 Gauss.
(c)
3170 Gauss.
3092 Gauss.

Figure 5.5.

the planes of measurement cannot have been mutually perpendicular.

These preliminary investigations therefore show that a more accurate means of mounting the crystals is necessary, but that, if this can be done, results of interest can be obtained. In particular, the study of a series of complexes of these donors with different electron acceptors might provide some information on the changes in the percentages of charge transfer character in the ground state of the complexes.

(Thanks are due to Dr. F.I.B. Williams and Rev. D.P. Breen, of the Clarendon Laboratory, Oxford, for their help in assessing the value of these results.)

CHAPTER 6.

ELECTRICAL CONDUCTIVITY.

6.1. Introduction.

In molecular complexes using complexes of metal ions with aromatic ligands as donors, the cations may

(i) affect the energy levels of ligand π orbitals, as observed in absorption spectra and discussed in chapter 4,

and (ii) exert influences, not apparent from spectroscopic investigations, affecting movement of electronic charge through the crystal lattice of the solid complexes, which may be studied by investigations of semiconductivity and photoconductivity properties of the solid complexes.

This chapter describes the construction and development of apparatus to measure these properties, and the results which have been obtained by this method.

6.2. Apparatus and techniques.

Investigations of photoconductivity properties of molecular complexes require apparatus capable of:

(i) measuring very large electrical resistances accurately,

and (ii) providing illumination of known wavelength and intensity onto the sample whose resistance is being measured.

6.2.1. Apparatus for electrical measurements. - A circuit designed

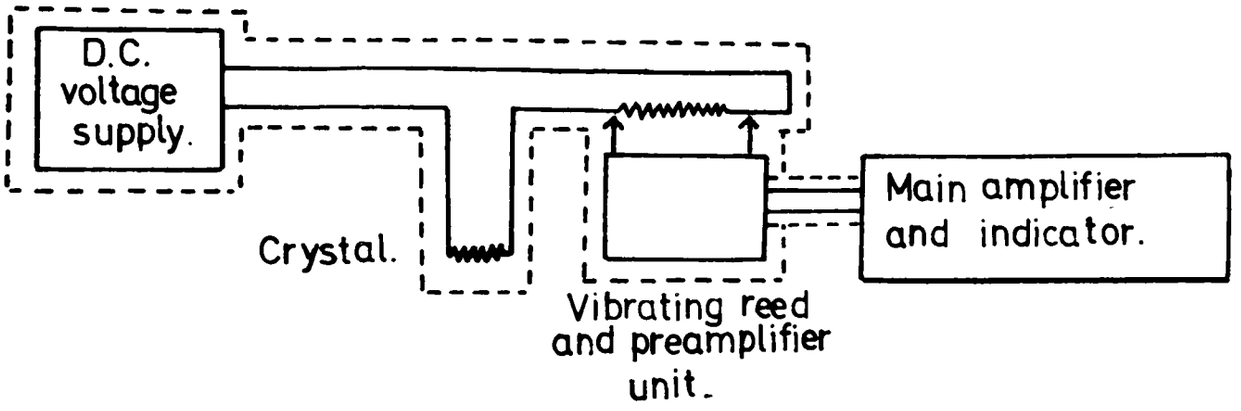


Fig. 6.1 Circuit diagram of Photoconductivity Apparatus.

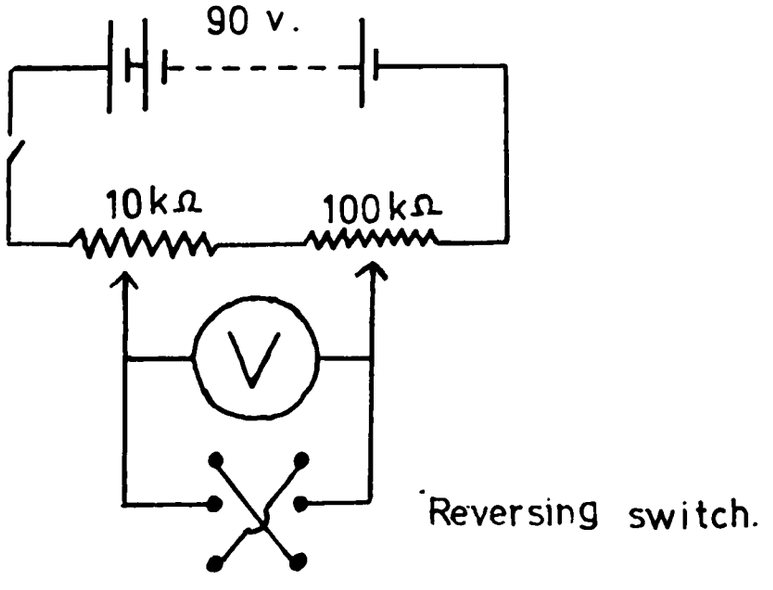


Fig. 6.2 Circuit diagram of D.C. voltage supply.

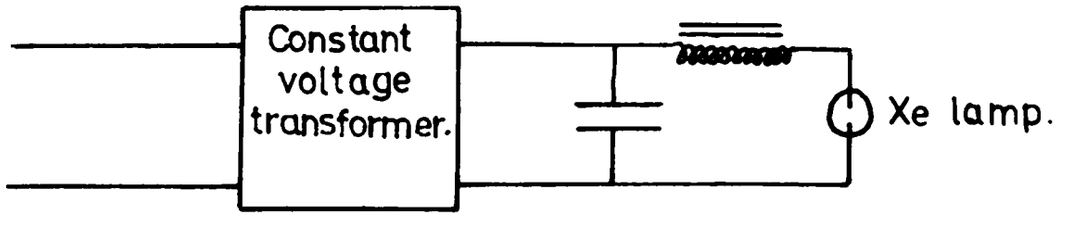


Fig. 6.4 Circuit diagram of Xe lamp power supply.

to measure currents down to 10^{-15}amp. D.C. with up to 90v. applied to the sample was constructed, incorporating the following units and design features. (A circuit diagram is shown in figure 6.1).

(a) A stable D.C. voltage supply.

This was achieved by using 90v. (Exide D.M.526) dry batteries in the circuit shown in figure 6.2. Noise was reduced by building the supply into a screening metal box, using wire-wound potentiometers in the potential divider, and replacing the batteries when their voltage fell to below 70v. Useful battery life was prolonged by using high resistance potentiometers and a high resistance voltmeter, as these consume the bulk of the current from the battery when high resistance samples are being used.

(b) A stabilised high-sensitivity D.C. Ammeter.

An Ekco vibrating reed electrometer, type 616B, was used to measure currents down to 10^{-15}amp. This instrument applies the voltage developed across a large standard resistor (10^{8}, 10^{10} or 10^{12} ohms), in series with the sample, to the plates of a vibrating condensor, the impedance of the resistor in the circuit being negligible by comparison with the resistance of the sample. The resulting alternating signal is amplified by a tuned amplifier, stabilised by feedback loops, and rectified before presentation. Full scale deflection on the most sensitive scale is 3×10^{-15}amp., and the noise level and zero stability of the instrument are below 10^{-15}amp. The overall accuracy claimed by the makers is ±5%. The effect of random noise from other parts of the circuit may be reduced by changing the time constant

of the instrument to reduce its sensitivity to rapid signal changes.

(c) Complete electrical screening.

To eliminate the effects of stray currents induced by movements near the apparatus, which would cause serious disturbances to the low currents flowing in the circuit, the sample compartment, power supply and electrometer input compartment were screened with metal containers, and all electrical connections were made through screened coaxial cable. Careful attention was given to obtain good electrical contact between the separate sections of the screening, and to obtain an efficient earthing system, and this resulted in a noise level of $\pm 0{\cdot}5 \times 10^{-15}$ amps. under operating conditions.

(d) Insulation.

To ensure that leakage across the insulation of the circuit did not prove a limiting factor in determining the maximum resistance which could be measured, great care was taken to keep all insulating materials clean during assembly of the equipment. Electrical connections to the sample compartment were made via copper rods passing through a polytetrafluoroethylene ("Teflon") cone, which was washed several times with distilled CCl_4 and dried well before assembly. Periodic maintenance included dismantling and cleaning this and other key insulation points as necessary. In this way, the insulation was maintained at a level which gave no measurable current when the maximum voltage used was applied across the apparatus in working conditions but with no sample in the sample compartment (i.e. $>10^{+17}\Omega$).

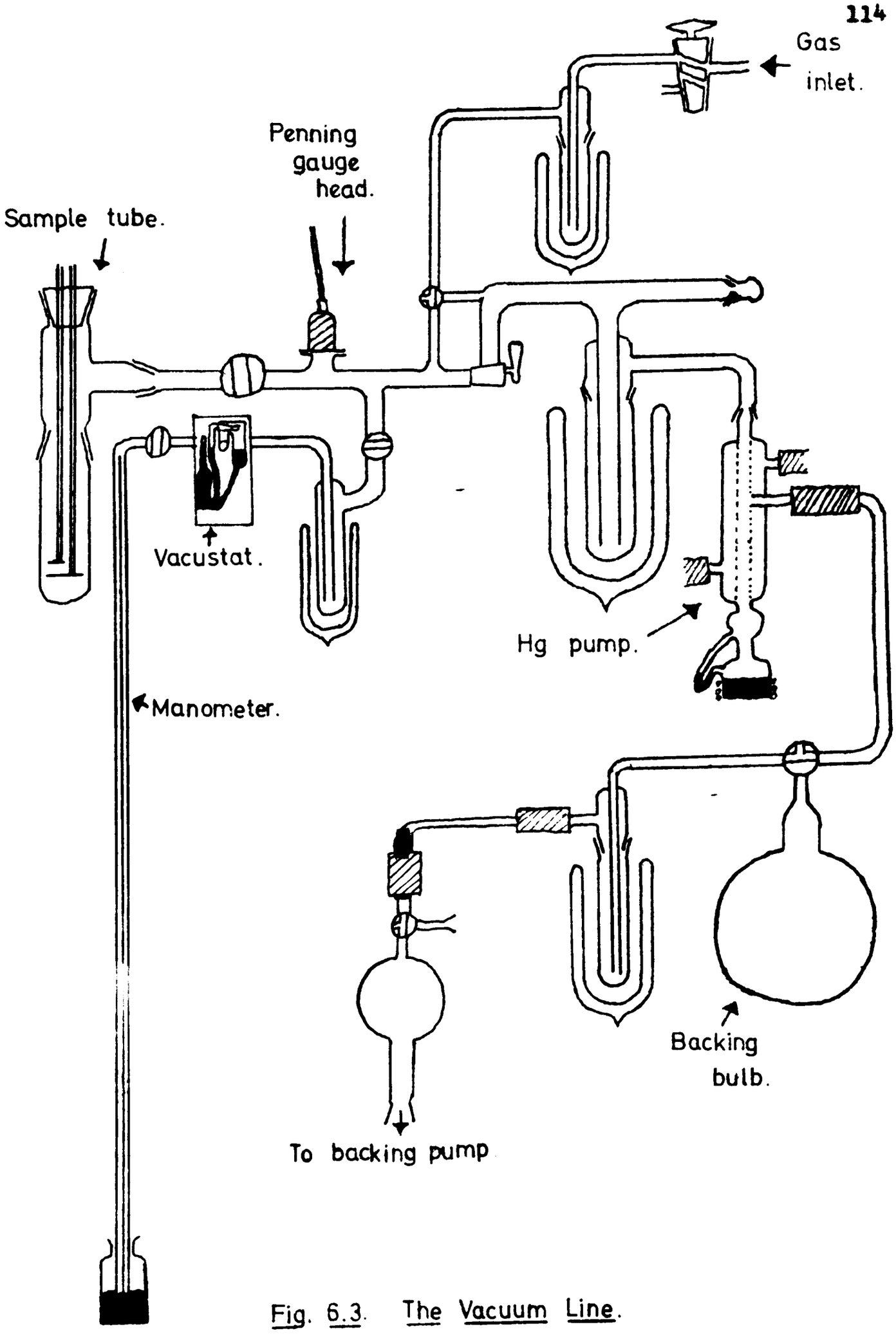


Fig. 6.3. The Vacuum Line.

(e) Evacuated sample compartment.

To minimise surface conduction effects and to prevent gas effects on conductivity measurements, the sample compartment was evacuated to a pressure of about 10^{-5} mm. Hg. for all measurements except those where specific gas effects were being studied. Figure 6.3 shows the vacuum line design. All tubing on the low pressure side of the mercury diffusion pump was at least 1·5cm. internal diameter, to increase pumping effeciency. Pressure was monitored continuously using a Leybold Elliot Penning gauge, reading from 10^{-1} to 10^{-6} mm. Hg. This was dismantled and the electrodes were cleaned at intervals of approximately 2 months during heavy use, to remove deposits which produced optimistic pressure readings. The vacuum line also incorporated an Edwards "Vacustat" gauge for intermediate pressures, and a mercury manometer for higher pressures up to atmospheric.

All the above apparatus was assembled by the late Mr. G. Scregg.

6.2.2. Apparatus for illuminating the sample. - A Beckmann DU monochromator was used to provide monochromatic light at wavelengths from 200-2000 mμ, for illuminating the sample. The apparatus centred on this instrument was developed through the following stages:

(a) A tungsten filament projector lamp was used as source. Tables of monochromator slit widths, calculated from the published dispersion curve for the instrument, for several different band widths, were prepared. Using the slit widths for a chosen bandwidth, the spectrum was scanned, with light entering the monochromator directly from

the lamp, and passing out onto the sample, contained in an evacuated glass tube, via a small quartz lens. The photoresponse curve was then corrected to constant incident energy using the slit width table and published output curves for the tungsten lamp (see ref. 4, the author's Part II thesis, Oxford, 1963).

This method suffered from four important disadvantages:

(i) It assumed that the intensity dependence of the photoresponse was the same in all regions of the spectrum. This is not always the case, and, in cases where it is not so, the correction to constant incident energy is not valid.

(ii) Ageing of the tungsten lamp may lead to changes in its output curve, and, in the absence of a good colour temperature meter, the makers' output curves cannot be applied properly. This again leads to failure of the correction factors.

(iii) The glass envelope of the tungsten lamp, the glass sample tube, and the rapid fall off in intensity of the output of a tungsten lamp below 400 mμ, limit measurements in the ultraviolet region severely.

(iv) The quartz lens focusses light of different wavelengths at different positions, so that the patch of light in the plane of the sample is not of constant area, and the intensity of illumination therefore varies with wavelength as a result of this effect.

(b) The following improvements were incorporated:

(i) A Mazda 500 watt high-pressure Xenon lamp, in a quartz

envelope, using the supply unit whose circuit is shown in figure 6.4, was used in place of the tungsten lamp, and provided a much-improved light output in the ultra-violet region. The lamp was fitted in a metal container with a quartz window, and cooled by a fan, the ozone produced being carried out of the laboratory via a flexible metal pipe. The light produced by this lamp was focussed onto the entrance slit of the monochromator by two surface aluminised mirrors, one plane and the other concave, made by Barr and Stroud Ltd., Glasgow. The glass sample tube was replaced by a quartz tube.

(ii) A Hilger and Watts compensated Schwartz vacuum thermopile, with elements of area 2 x 0·2 mm. and a saphire window, was used to monitor the output. This was fixed in the space normally occupied by the sample, and its output was measured by a Tinsley galvanometer (type SS 6/4500, sensitivity 190mm/μA, resistance 10·6 ohms), connected directly across the thermopile output. Slit widths giving certain standard galvanometer deflections were determined and tabulated. The thermopile was then removed and replaced by the sample assembly. Use of slit widths corresponding to a constant galvanometer deflection from the thermopile should then give equal energy input at all wavelengths of light reaching the sample.

This method is in theory more satisfactory than that used in stage (a), but it was found that when the thermopile was replaced to check that

the calibration had not changed, a different set of slit widths was obtained. This "slit programme" method was therefore unsuitable, because of (i) changes in the lamp output during the course of a run and (ii) the difficulty of re-positioning the thermopile to check the calibration.

(c) The final design incorporated the same lamp and entrance optics as in stage (b), but two surface aluminised mirrors were incorporated on the exit side of the monochromator. A rigid but adjustable mount was made, to hold the thermopile alongside the sample assembly, at the same height as the sample. Light emerging from the exit slit of the monochromator first hit a plane mirror, which was fixed rigidly with respect to the monochromator, on an adjustable mounting. It then travelled to a concave mirror, on a mount which allowed it to be moved to focus an image of the exit slit onto the sample. This mirror could be fixed once the focussing adjustment had been made, and could swivel in a horizontal arc, whose limits were defined by two stops, adjustable to bring the image of the exit slit onto the sample or thermopile at the two ends of its travel. The whole of this optical system was enclosed in a hardboard container, painted matt black on the inside, with openings only at points where light from the monochromator emerged and where the lever operating the swivel mirror projected. A diagram of this optical system is shown in figure 6.5.

With all the mirrors aligned by trial and error to give maximum response on both thermopile and sample, this arrangement

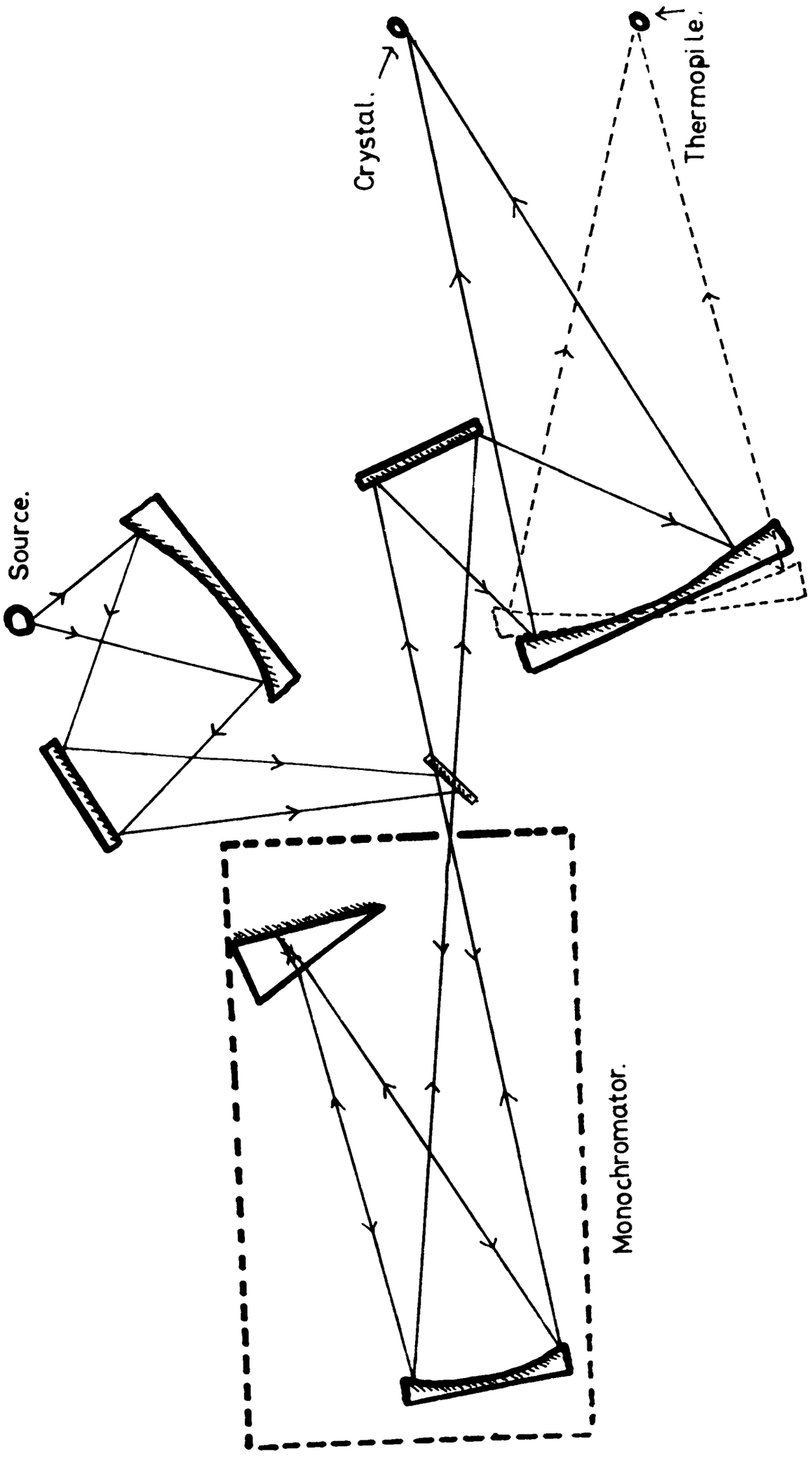


Fig. 6.5. OPTICS OF THE PHOTOCONDUCTIVITY APPARATUS.

could be used in the same way as a manual spectrophotometer, as follows:-

(1) Select the wavelength.

(2) With the swivel mirror in the "thermopile" position, adjust the monochromator slit width until the chosen galvanometer deflection from the thermopile is reached.

(3) Move the swivel mirror to the "sample" position, and observe the increase in conductivity on illumination of the sample.

(4) Repeat for other wavelengths as required.

Since the thermopile has a sensitive area of a similar size and shape to the sample, this method ensures that the photoresponse curves are obtained under conditions of constant incident intensity at all wavelengths, since the thermopile is a black body, with sensitivity independent of the wavelength of the radiation reaching it.

(Thanks are due to Mr. G. Twidle, of the light division of the National Physical Laboratory, for helpful discussions concerning the application of a thermopile to this problem, and to Professor H.W. Thompson, for lending us the thermopile actually used).

6.2.3. Technique. - Previous workers[45,46] have shown that the most useful measurements of electrical conductivity properties of solid samples are obtained when single crystal samples are used. These eliminate uncertainties due to possible inter-particle boundary effects

such as are present in compressed pellet samples, and they also provide the possibility of measuring directional properties of the conductivity and studying the effect of using polarised light.

A suitable well-formed and large crystal of the sample to be studied was selected, using a binocular microscope. Johnson Matthey silver paste preparation F.S.P.3 was used to cement the ends of the crystal firmly to the two parallel copper electrodes of the sample holder, with care being taken to ensure that the crystal was mounted with its needle axis vertical. The silver paste was left for at least 2 hours in air to set and dry, to prevent cracking of the contacts by too rapid evaporation of the solvent in vacuo. The vacuum was then applied, and, when a pressure of about 10^{-5}mm. Hg had been reached, ohmic runs and photoconduction measurements were made.

To facilitate measurements of small photocurrents in the presence of large dark currents, a backing-off device was used. This supplied a stable D.C. voltage (from a dry battery supply) of opposite polarity to that displayed on the electrometer due to the dark current, and was adjustable to bring the meter to zero reading with no light reaching the sample. The most sensitive scales could then be used to measure small photocurrents accurately. When the dark current was appreciable by comparison with the photocurrent, it was necessary to check that no drift of the dark current had occured between readings of the photocurrent (e.g. due to small changes in room temperature or in the vacuum applied to the sample.)

6.3. Results.

6.3.1. Tests of the apparatus.

To test the apparatus, a series of investigations were made of the photoconductivity properties of twice-sublimed copper phthalocyanine crystals, prepared by Dr. P. Day. The photoconductivity of copper phthalocyanine has been studied previously by the methods of stage (a), described above in the development of the present apparatus[47], and this is therefore a good material to test improvements in the design.

Performance of stage (b) apparatus.

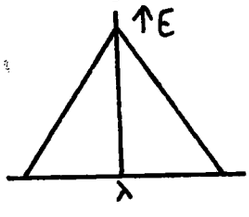
A crystal of copper phthalocyanine was mounted, with the needle axis vertical between the electrodes, and left for two hours for the electrode paste to dry. Ohmicity tests and spectral response curves were obtained in air at atmospheric pressure, using the Xenon lamp. Slit widths calculated to give a constant band width of 200 cm^{-1} were used above 400 mμ, (band widths of 400 cm^{-1} were necessary below 400 mμ to give measurable thermopile output). The observed photocurrents at different wavelengths were corrected to a common energy level by dividing by the thermopile output under the same conditions, obtained by replacing the crystal by the thermopile after the measurements were completed. Figure 6.6 shows the ohmicity of the dark current, and figure 6.7 shows the photoresponse curve, with the 400 cm^{-1} and 200 cm^{-1} bandwidth portions of the curve normalised to give one continuous curve. These measurements were repeated after evacuating the sample, this time

using a tungsten lamp in a repeat run after using the Xenon lamp. These results are also shown in figures 6.6 and 6.7.

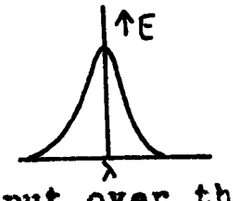
These experiments show:

(i) The main features of the response curves are similar for the different methods used, but details are different.

(ii) The differences are greater in regions where the lamp output is low or changing rapidly, (as shown by comparison with the curves of output energy of the two lamps in the conditions used, which are superimposed on figure 6.7.) This indicates that the correction factors used are not adequate. The reasons for this are (a) the intensity dependence of the photocurrent may not be the same in all regions of the spectrum, and (b) the theoretical band shape for a level source output and wavelength λ at the centre of the band is



If there is a sharp change in the lamp output over the band width, the band shape will change. Thus, if there is a peak in the output, centred at λ, the band shape will be



The integrated output over the band will be recorded by the black-body thermopile. However, if the crystal response is also changing rapidly over the band width, it may only use a small fraction of the integrated output for efficient

production of carriers, and a correction based on the integrated output will therefore be too large.

These two difficulties are both eliminated if a method providing equal incident intensity at all wavelengths is used. No correction factors are necessary, and the output peaks of the lamp automatically lead to smaller slit widths and narrower band widths, thus reducing the problem caused by (b) above. "Slit programmes" giving constant intensity at different wavelengths were therefore obtained for the tungsten lamp, using the thermopile as described in section 6.2, for six different intensity levels. However, on repeating some of the earlier readings after completing this calibration, it was found that reproducible results were not obtained, due to (i) changes in the lamp output, due to ageing processes, and (ii) possible movement of the thermopile during the measurements. The performance of stage (b) was therefore not satisfactory.

Performance of stage (c) apparatus.

The design of stage (c) ensures that the lamp output is measured accurately immediately before each photoconductivity reading. All the optical components and the detector are fixed rigidly, and the mirror system of the monochromator output side ensures that light of all wavelengths is focussed at a single plane onto an area of constant size. Therefore, all the criticisms applicable to previous designs are satisfied, and any failure of this system to provide adequate correction for lamp output

variations represents a problem which cannot be dealt with by improving the apparatus design further.

The photoresponse curve for copper phthalocyanine was determined on this apparatus, using the method of section 6.2.3, after first showing that the crystal was ohmic. This curve is shown in figure 6.8. The curve is not a great improvement on earlier curves, but does show a smaller change around 850 mμ (where a lamp output variation occurs). The measurement was repeated using a different light level, and the shapes of the two curves, shown in figure 6.8, agree well, showing that although the stage (c) apparatus does not provide complete correction for intensity fluctuations in the lamp output, the resulting irregularities in the curves are reproducible. The absorption spectrum of copper phthalocyanine[48] contains peaks which are much sharper than those in the spectra of molecular complexes, and this means that the photoconduction response curves for the complexes to be studied here can be expected to be smoother than the copper phthalocyanine curves, for reasons discussed above (see discussion of performance tests for stage (b) apparatus). Since the only further improvement to the equipment would consist in using a lamp with a smoother output curve (which is not available unless ultraviolet output is sacrificed), it was decided to proceed with measurements on the molecular complexes, subject to the proviso that small features on photoresponse curves thus obtained cannot be interpreted with certainty unless they occur in regions where the lamp output is reasonably flat.

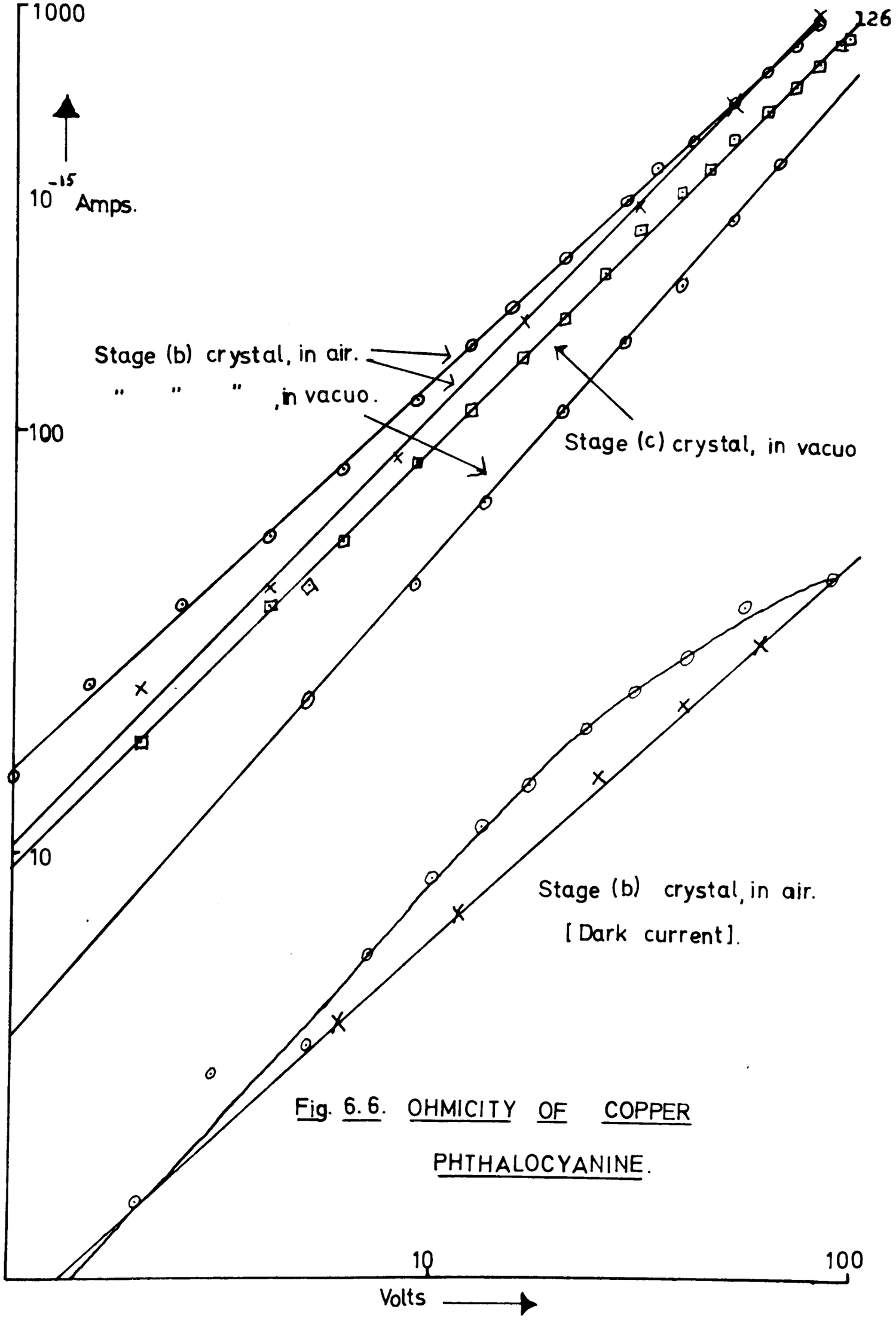
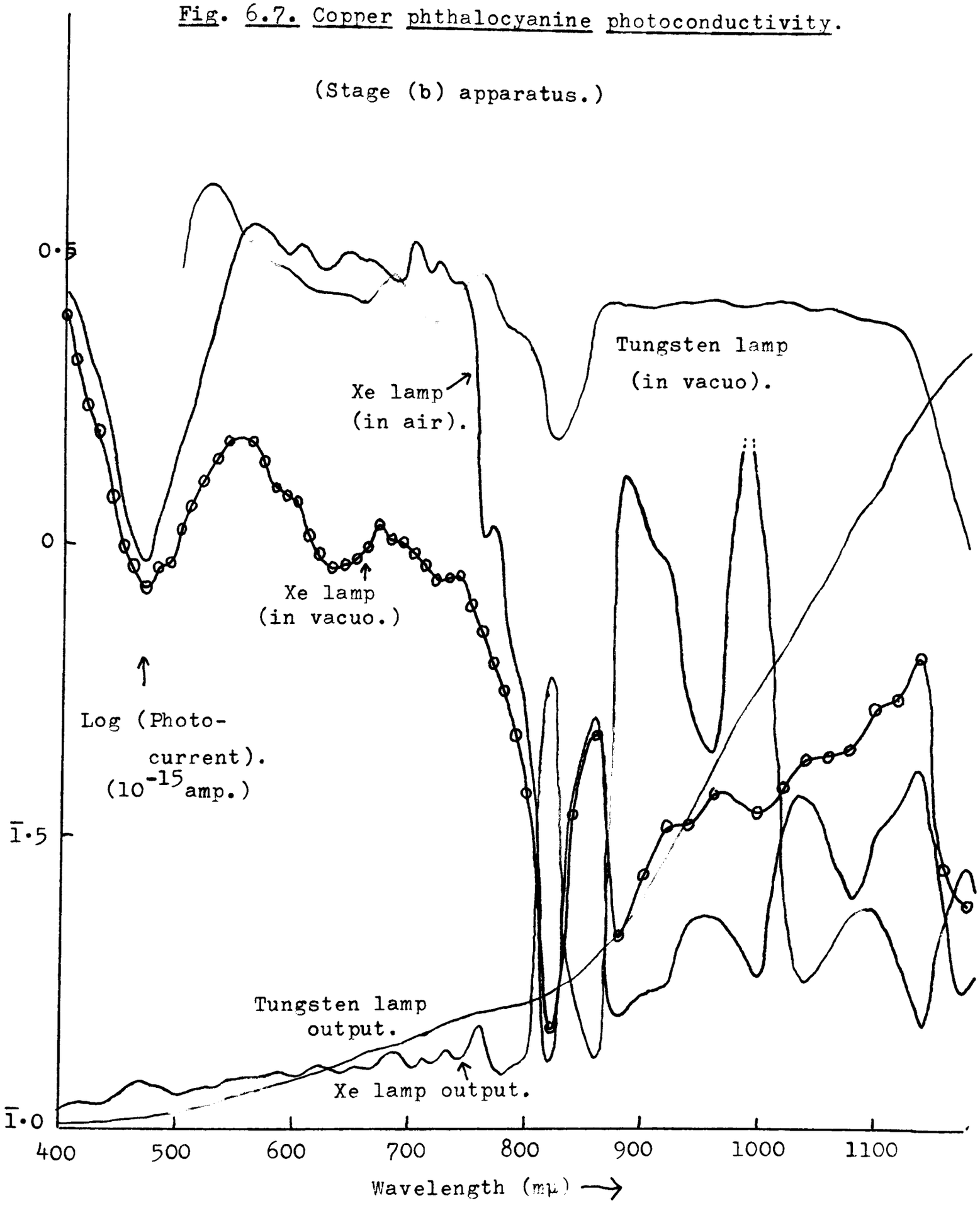


Fig. 6.6. OHMICITY OF COPPER PHTHALOCYANINE.

Fig. 6.7. Copper phthalocyanine photoconductivity.

(Stage (b) apparatus.)



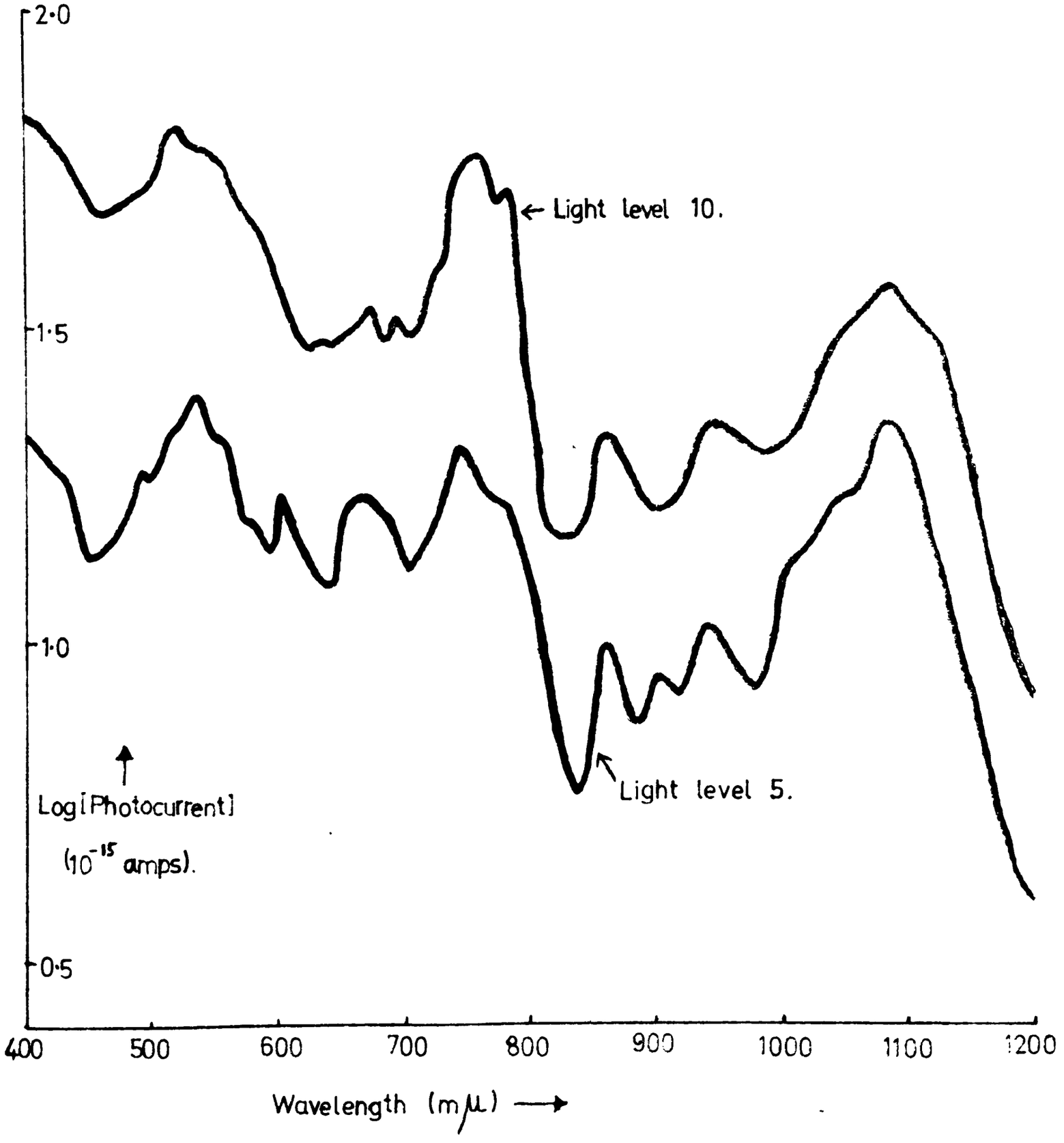


Fig. 6.8. Cu Phthalocyanine Photoconductivity

[Stage (c) apparatus]

6.3.2. Investigations of photoconductivity in molecular complexes of 8-hydroxyquinoline and its metal complexes with electron acceptors.

The apparatus and technique developed as described above was used to investigate the photoconductivity properties of the complexes listed below, which were the only materials obtained as crystals of a suitable size for electrical measurements. This list shows that some of the materials did not photoconduct and that others gave photoconduction phenomena of varying degrees of interest.

(a) Materials showing measurable photoconduction.

Palladium 8-hydroxyquinolinate/chloranil.

Copper 8-hydroxyquinolinate/chloranil. (Photovoltaic in vacuo, but not in air.)

8-hydroxyquinoline/tetracyanobenzene.

(b) Materials showing photocurrents of zero or too small for useful measurements.

Palladium 8-hydroxyquinolinate/tetracyanobenzene.

Copper " " / " "

" " " /trinitrobenzene.

" " " /picryl azide.

8-hydroxyquinoline/trinitrobenzene.

All the materials showed photovoltaic effects rising below 270 mμ. These results will now be described in more detail.

(1) Palladium 8-hydroxyquinolinate/chloranil.

Three crystals of the complex were studied in the following ways:

(a) Ohmicity.

The ohmicity of the crystals with voltages of up to 99v. was studied for conductivity in the dark and with light of 460 mμ, with the monochromator slits wide open (2·0mm.) The resulting plots of log (current) v. log (applied voltage) are shown in figures 6.9 to 6.11. The dark current was small (approximately 3×10^{-13}amp.) and non-ohmic, but in all cases the combined dark+photo-current was ohmic. The non-ohmic behaviour of the dark current may be due to electrode barrier effects, but these do not appear to influence the photoconductivity, and, since this is large compared to the dark current, the effect does not invalidate measurements of photoconduction.

Specific resistances were calculated for the first crystal (using crystal dimensions measured with a microscope with a transparent scale incorporated into the optical system), for conductivity in the dark and with illumination with light of wavelengths 460 and 905 mμ, corresponding to two positions of strong response of photoconductivity, (using slit widths giving galvanometer deflections of 10 cm. from the thermopile). These were as follows:

Specific resistance in the dark = $2{\cdot}7 \times 10^{12}$ ohm/cm.

" " with light of 905 mμ = $2{\cdot}2 \times 10^{12}$ ohm/cm.

" " " " " 460 mμ = $3{\cdot}9 \times 10^{11}$ ohm/cm.

Fig. 6·9. Ohmicity of 1st. crystal of Pd 8-hydroxyquinolinate/Chloranil.

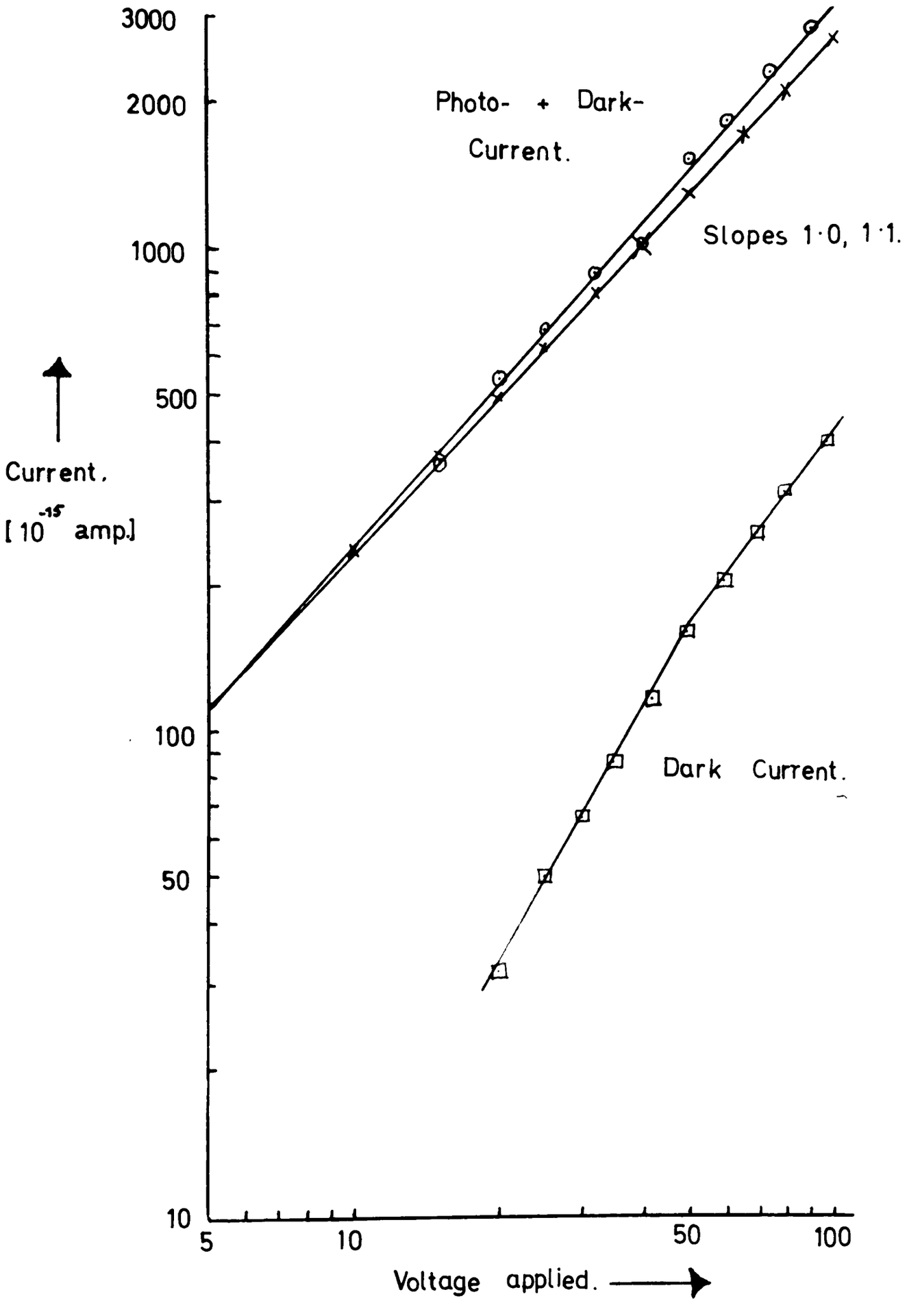


Fig. 6·10. Ohmicity of 2nd. crystal of Pd 8-hydroxyquinolinate/Chloranil.

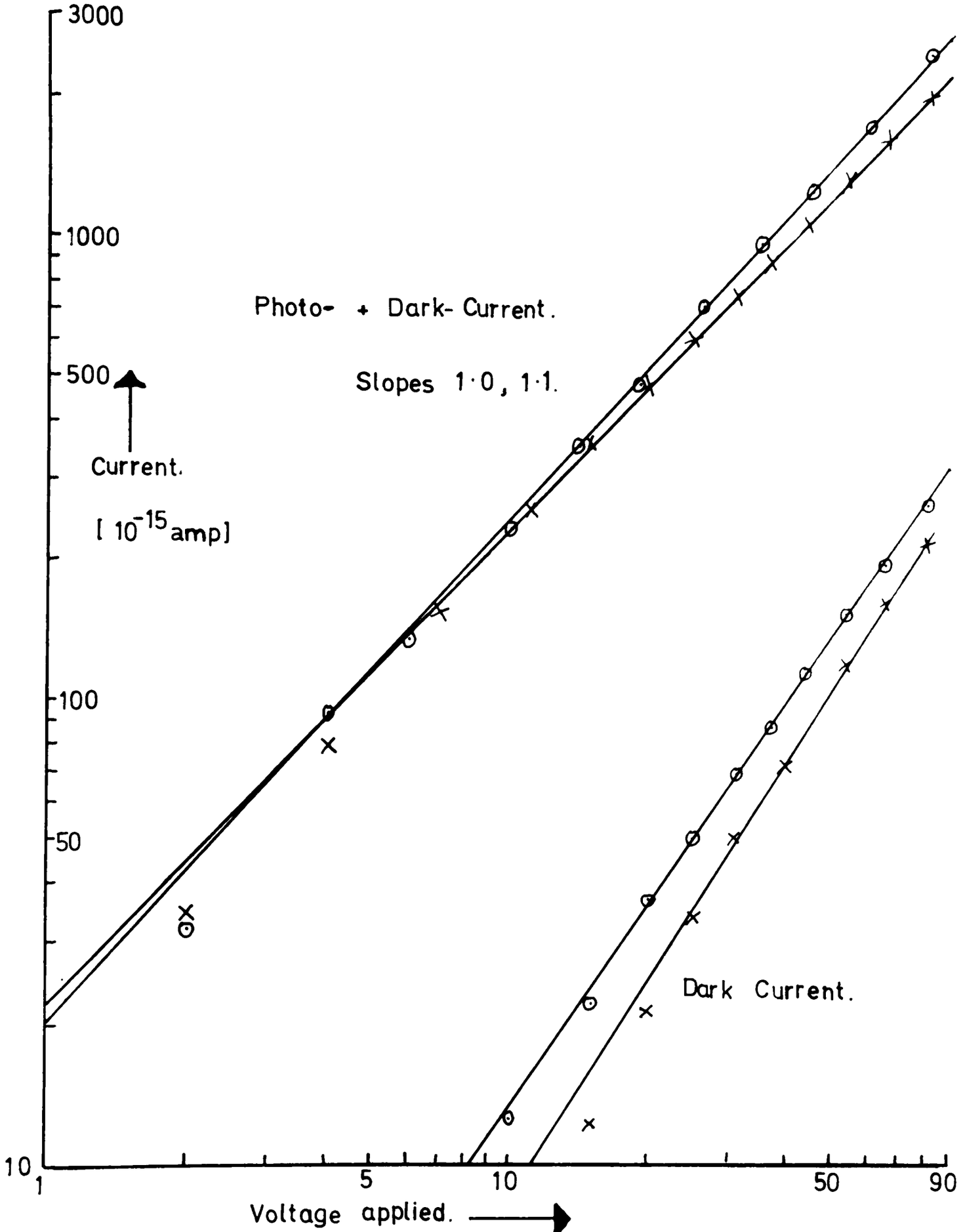
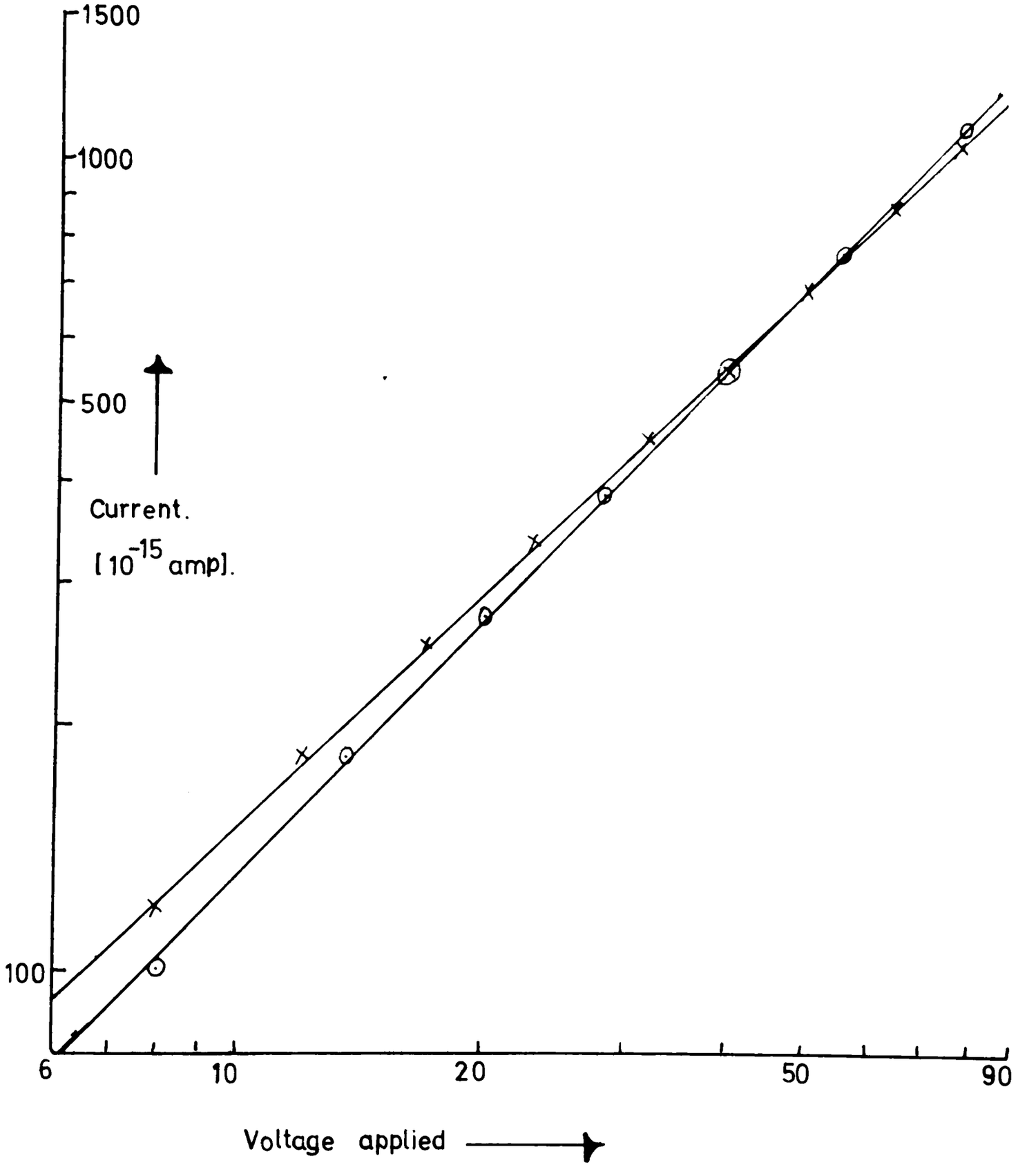
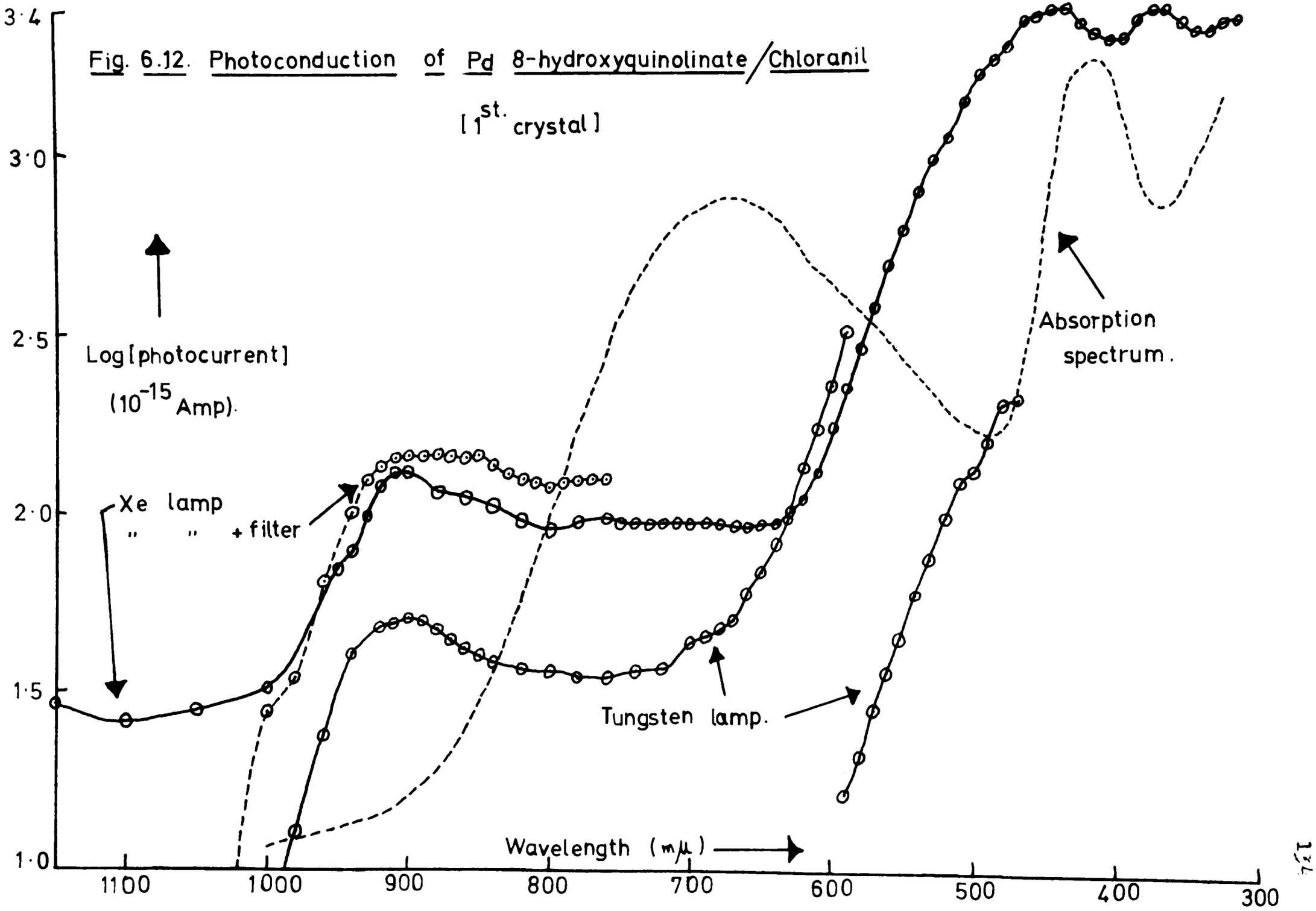


Fig. 6.11. Ohmicity of 3rd. crystal of Pd 8-hydroxyquinolinate/Chloranil

[Photo- + Dark- Current.]




Fig. 6.12. Photoconduction of Pd 8-hydroxyquinolinate/Chloranil
[1st. crystal]
3·4
3·0
2·5
2·0
1·5
1·0
Log [photocurrent]
(10^-15 Amp).
Xe lamp
" " + filter
Tungsten lamp.
Absorption spectrum.
Wavelength (mμ)
1100
1000
900
800
700
600
500
400
300

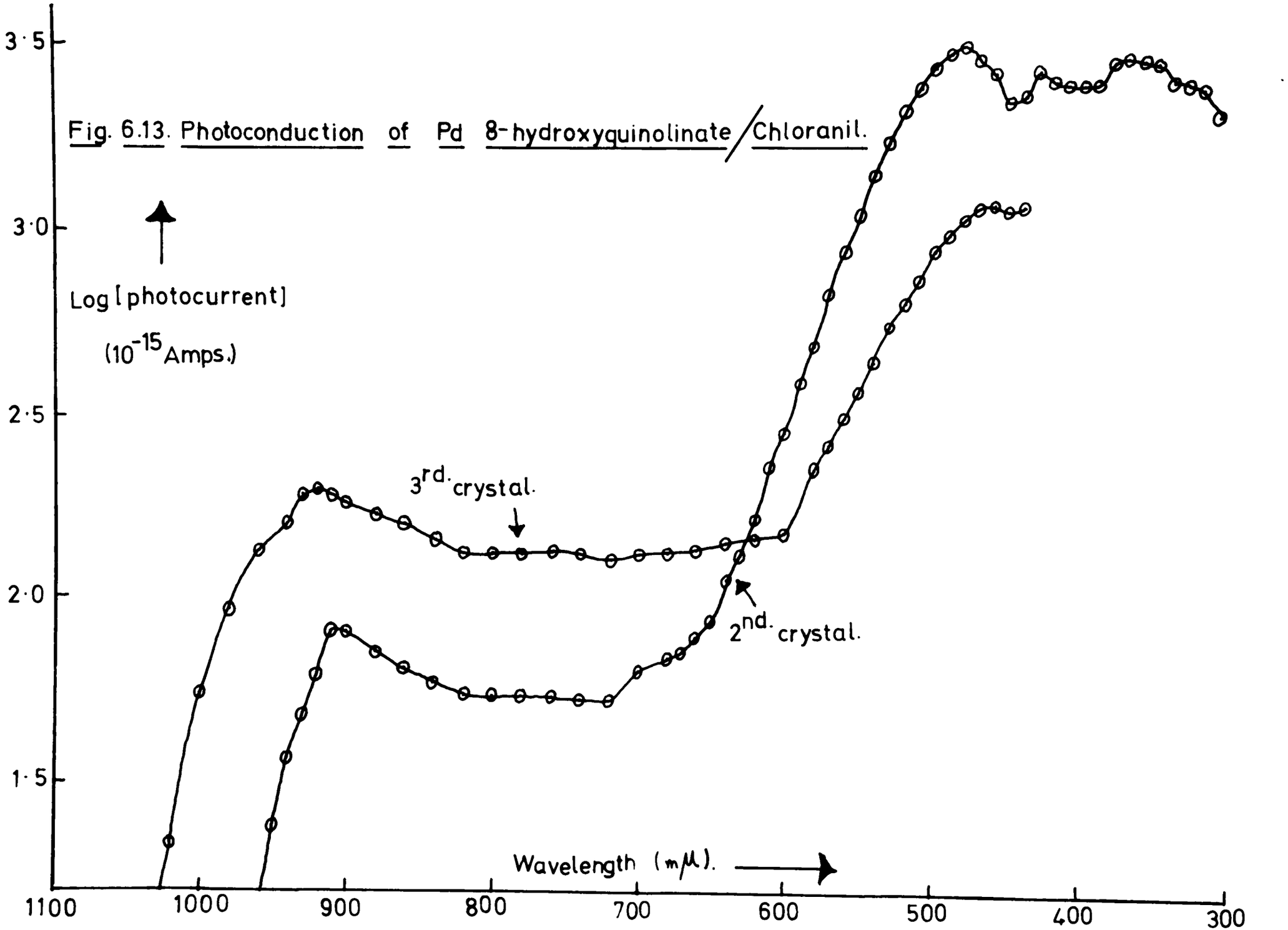


Fig. 6.13. Photoconduction of Pd 8-hydroxyquinolinate/Chloranil.

(b) Spectral response of photoconductivity.

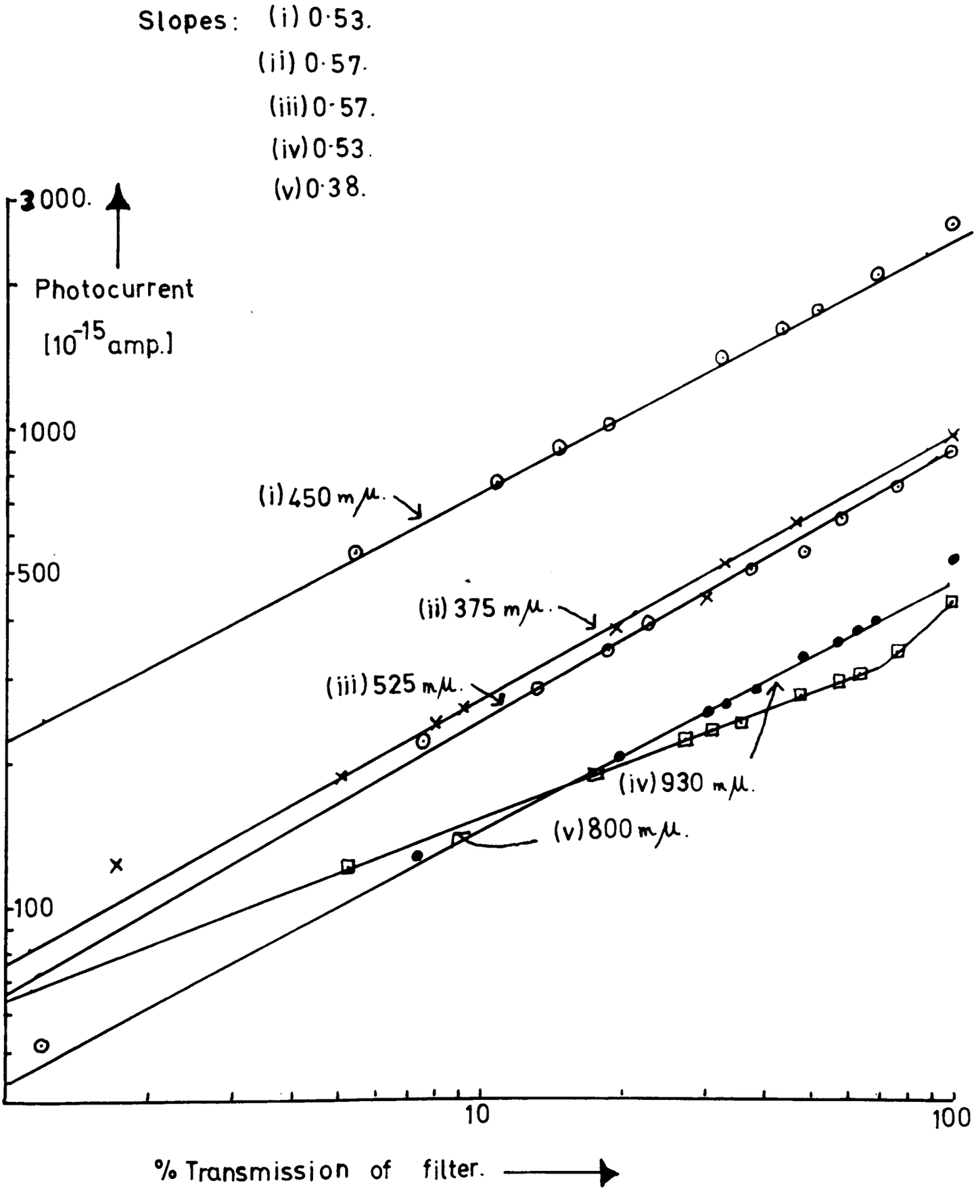
Curves showing photoconduction as a function of wavelength were obtained for the three crystals by the methods previously described, using tungsten and xenon lamps. These are shown in figures 6.12 and 6.13, together with the absorption spectrum of the complex for comparison. They are smooth curves, and the main features of all curves obtained are similar.

The response in the infra-red region between 850 and 2000 mμ is of especial interest, and the possibility that this is due to stray light from the visible and ultraviolet regions must be eliminated before interpretations of its origin can be made. The response curve from 2000 - 760 mμ was therefore repeated for the first crystal, using a Wratten 88A gelatine filter, mounted in glass, to cut out all light of wavelengths below 750 mμ before it entered the monochromator. The resulting curve, shown in figure 6.12, shows that the response above 1050 mμ is caused by stray light, but that the peak at about 900 mμ is genuine.

(c) Dependence of photoconduction on intensity of illumination.

Using Kodak "Neutral" density filters of nominal optical densities of up to 2·0, calibrated by recording their actual absorption spectra using a Unicam SP 700 recording spectrophotometer, the intensity of the light falling onto the crystal was varied while maintaining the same bandwidth. Plots of log (photocurrent) against log (percent transmission of filter) were made at wavelengths of 930,

Fig. 6·14. Pd 8-hydroxyquinolinate / Chloranil Photoconduction. Intensity dependence.



800, 525, 450 and 375 mμ, and are shown in figure 6.14, where the slopes of the plots (which give the power laws of the dependence of photocurrent on intensity) are also recorded.

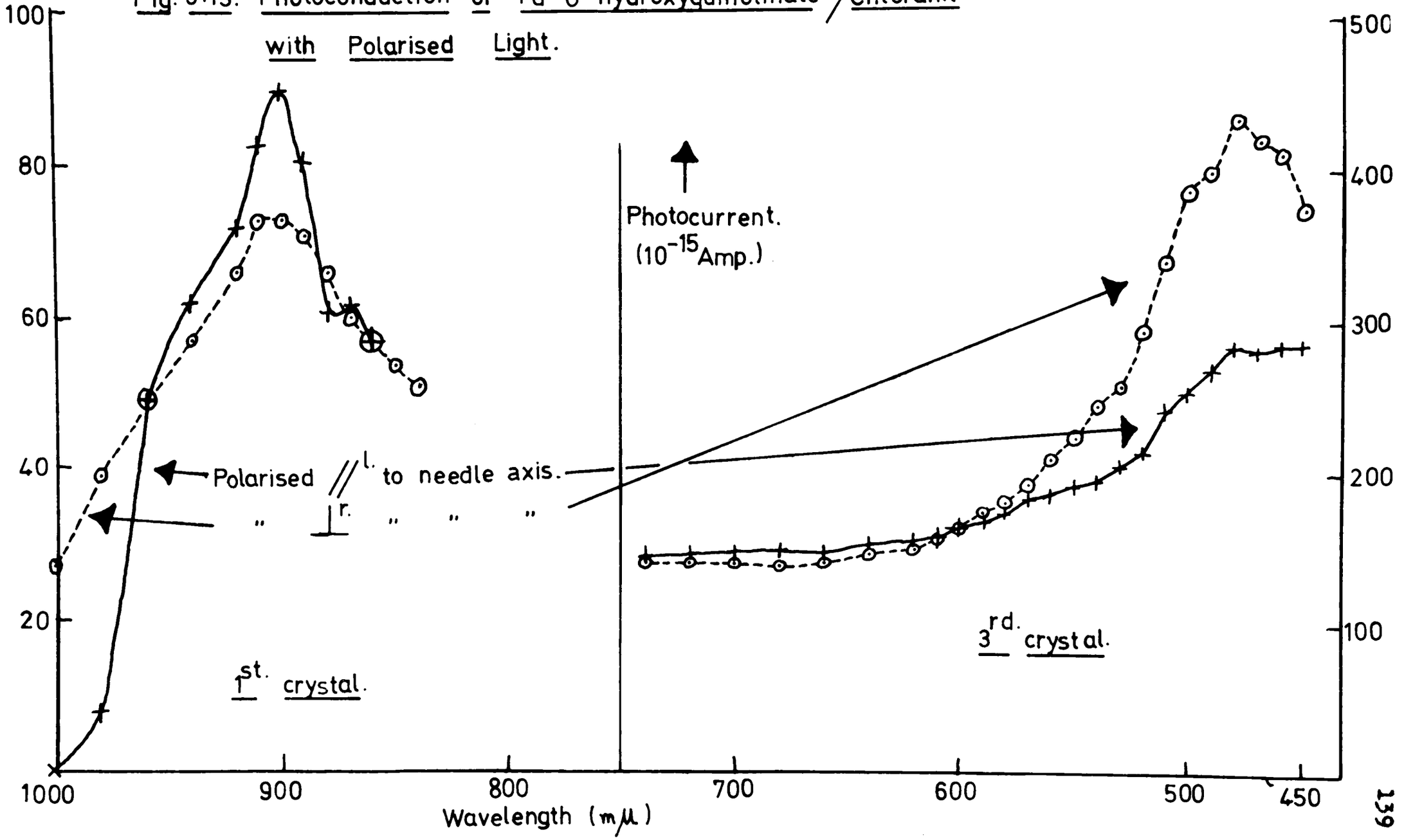
(d) Dependence of photoconduction on polarization of the light.

A simple rotating mount holding a polarizing filter (Polaroid type HR for wavelengths from 770 - 2000 mμ, and Kodak "Pola-screen" from 450 - 750 mμ) was constructed and fitted so as to hold the filter immediately after the final mirror of the monochromator exit optics, in a position where the light would pass through it irrespective of whether the final mirror was in the crystal or thermopile positions. (With this arrangement, residual polarisation from the optical system before the filter does not affect the direction of polarization of light reaching the crystal, which is determined solely by the orientation of the filter. Residual polarizations simply mean that slit widths giving equal intensity for two orientations of the polarizing filter at a single wavelength will not in general be equal.) Very little polarization, too small for the differences between maximum and minimum values to be reliable, was observed between 1000 and 750 mμ. Between 750 and 450 mμ, larger differences were observed. The response curves for light polarised approximately parallel and perpendicular to the needle axis of the crystal are recorded in figure 6.15.

(e) Gas effects.

With illumination of the crystal by the xenon lamp at 420 mμ (slit width 1·98mm., thermopile output 10 units), 700 mμ

Fig. 6.15. Photoconduction of Pd 8-hydroxyquinolinate /Chloranil with Polarised Light.



(slit width 2·0mm., output > 20 units), and 900 mμ (slit width 2·0mm., output ≫ 20 units), the following gas effects were observed, the dark current being zeroed with each gas change and the figures being in units of 10^{-15}amp. :-

	In vacuo.	In N_2.	In H_2.	In air.	In O_2.
420 mμ	2950	2650	2690	2950	2890
700 mμ	300	152	160	205	300
900 mμ	815	665	720	815	916

The dark current was not affected by nitrogen or hydrogen, but fell by a factor of 3 in air, and by a factor of 10 in oxygen. These effects were reversible on re-evacuation, with the exception of the hydrogen case.

(2) Copper 8-hydroxyquinolinate/chloranil.

Three crystals of this complex were studied as follows:-

(a) Ohmicity.

Ohmicity tests were carried out on the photocurrent in air and in vacuo as soon as the sample had evacuated to 10^{-5}mm. Hg. Typical plots are shown in figure 6.16, and indicate that the crystals were ohmic. (The dark conductivity was not measurable as it was less than 10^{-15}amp. with the maximum applied voltage.) Towards the end of the ohmic runs in vacuo, persistent deviations from ohmic behaviour were observed, and, on reducing the applied voltage to zero, a photovoltaic effect was observed. This prevents studies of

Fig. 6.16. Ohmicity of Cu 8-hydroxyquinolinate/Chloranil.

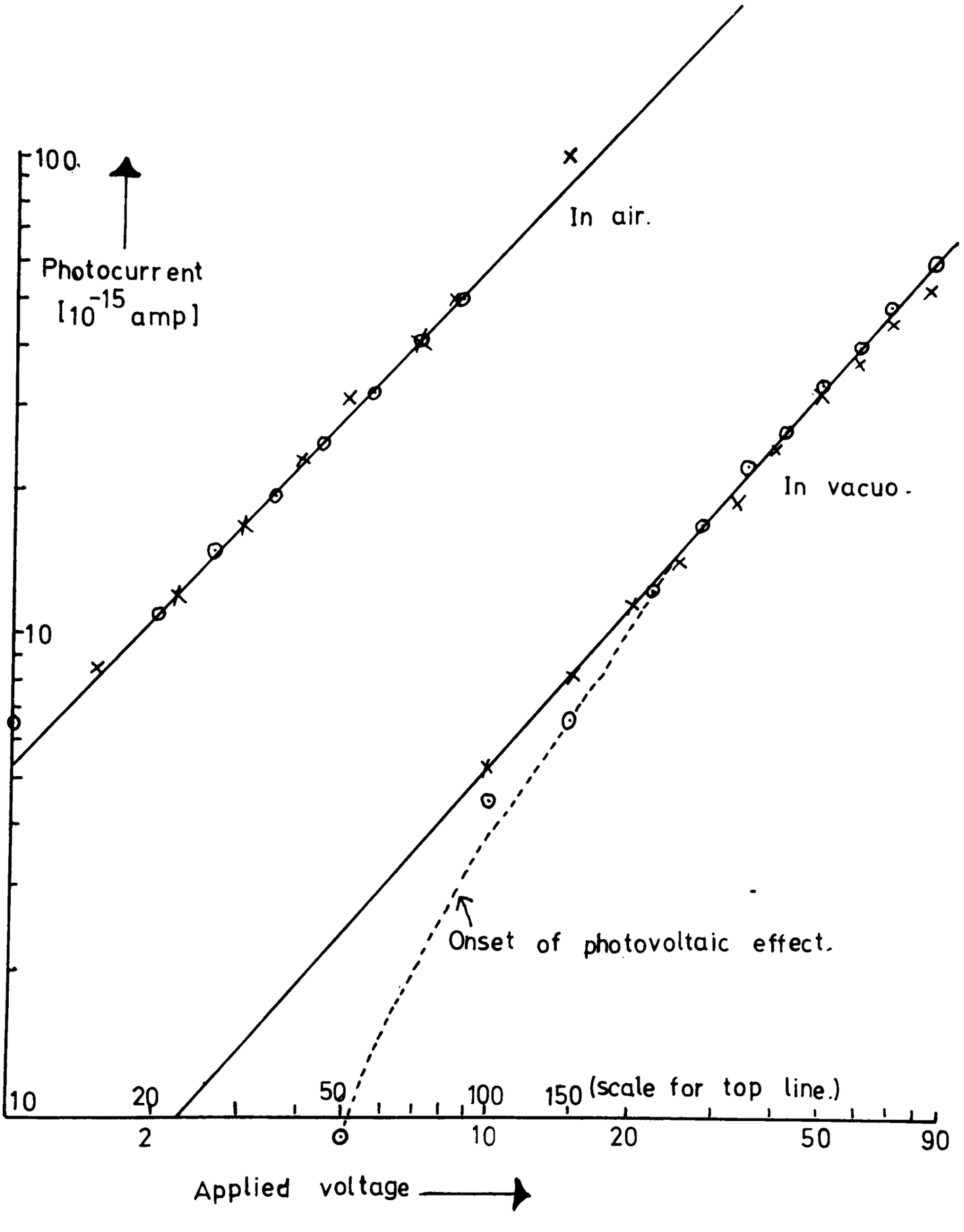
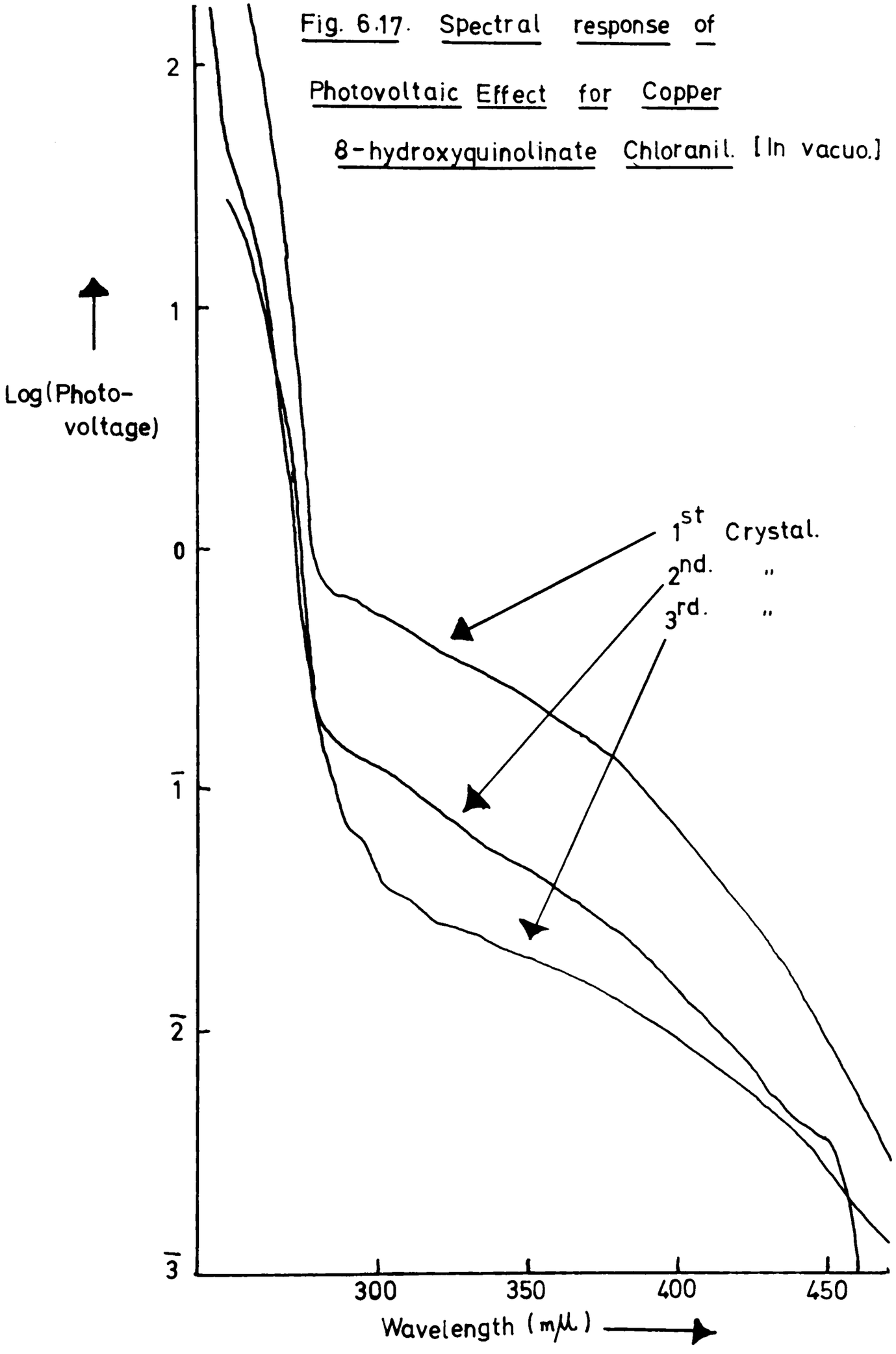
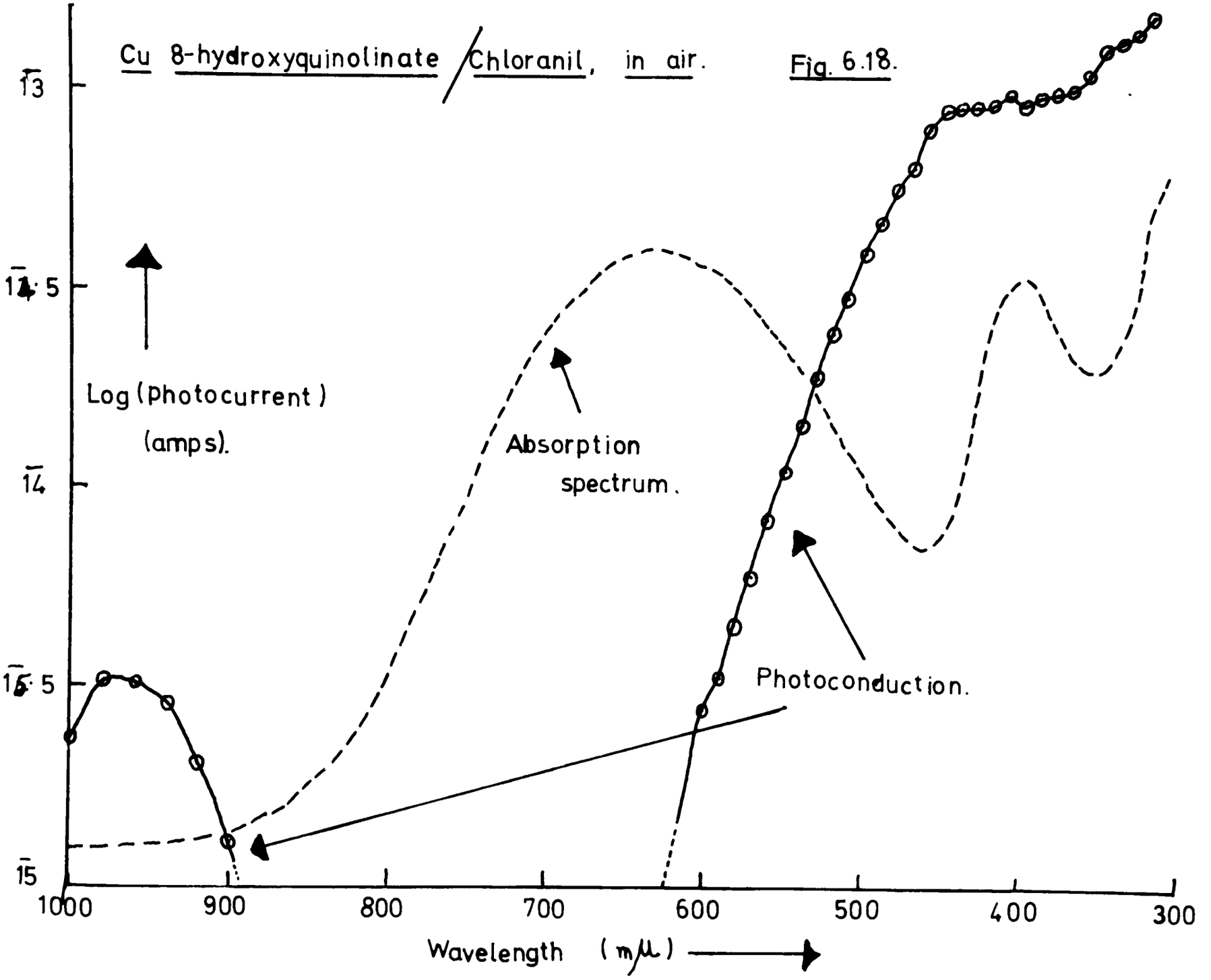


Fig. 6.17. Spectral response of Photovoltaic Effect for Copper 8-hydroxyquinolinate Chloranil. [In vacuo.]




Cu 8-hydroxyquinolinate / Chloranil, in air.
Fig. 6.18.
$\bar{1}3$
$\bar{1}4{\cdot}5$
$\bar{1}4$
$\bar{1}5{\cdot}5$
$\bar{1}5$
Log (Photocurrent) (amps).
Absorption spectrum.
Photoconduction.
1000
900
800
700
600
500
400
300
Wavelength (mμ)

photoconduction in vacuo.

(b) Spectral response of the photovoltaic effect.

This was recorded for each of the three crystals. In all cases, the effect began at about 500 mμ, rising steadily to about 280 mμ, then rising very steeply into the ultraviolet region. These curves are shown in figure 6.17.

(c) Effect of gases.

The following cycle of experiments was carried out to test for gas effects:

(i) Mount a crystal and evacuate for 36 hours to 10^{-5} mm. Hg. Photoconduction occurs on illumination, followed by a slow rise of a positive-polarity photovoltaic effect.

(ii) Admit air at atmospheric pressure. The photovoltaic effect rapidly falls to zero, leaving a photoconductive effect of approximately the same magnitude as in vacuo initially.

(iii) Re-evacuate with the backing pump alone. The photovoltaic effect rises rapidly with positive polarity, increasing as pressure decreases.

(iv) Admit nitrogen at atmospheric pressure. The photovoltaic effect falls rapidly to zero.

(v) Evacuate to about 10^{-2} mm. Hg. The photovoltage rises with negative polarity.

(vi) Evacuate to lower pressures. The photovoltage falls to zero and rises with positive polarity.

(vii) Admit air and re-evacuate. The phenomena of (ii) and (iii) are repeated.

(viii) Admit argon at atmospheric pressure. The photovoltaic effect rapidly falls to zero.

(ix) Re-evacuate. The photovoltaic effect swings to negative polarity, falls to zero, and finally regains its original positive value as the vacuum improves.

(d) Spectral response of photoconduction in air.

After first testing the ohmicity of the photocurrent in air (shown in figure 6.16), the spectral response curve was obtained by the usual methods. This is shown in figure 6.18. The poor photoconductivity of the material prevents measurements such as intensity dependence and polarised light studies. (The specific resistance of the material with illumination by light of 460 mμ with a monochromator slit width of 2·0 mm. is approximately 1·6 x 10^{13} ohm/cm.)

(3) 8-hydroxyquinoline/tetracyanobenzene.

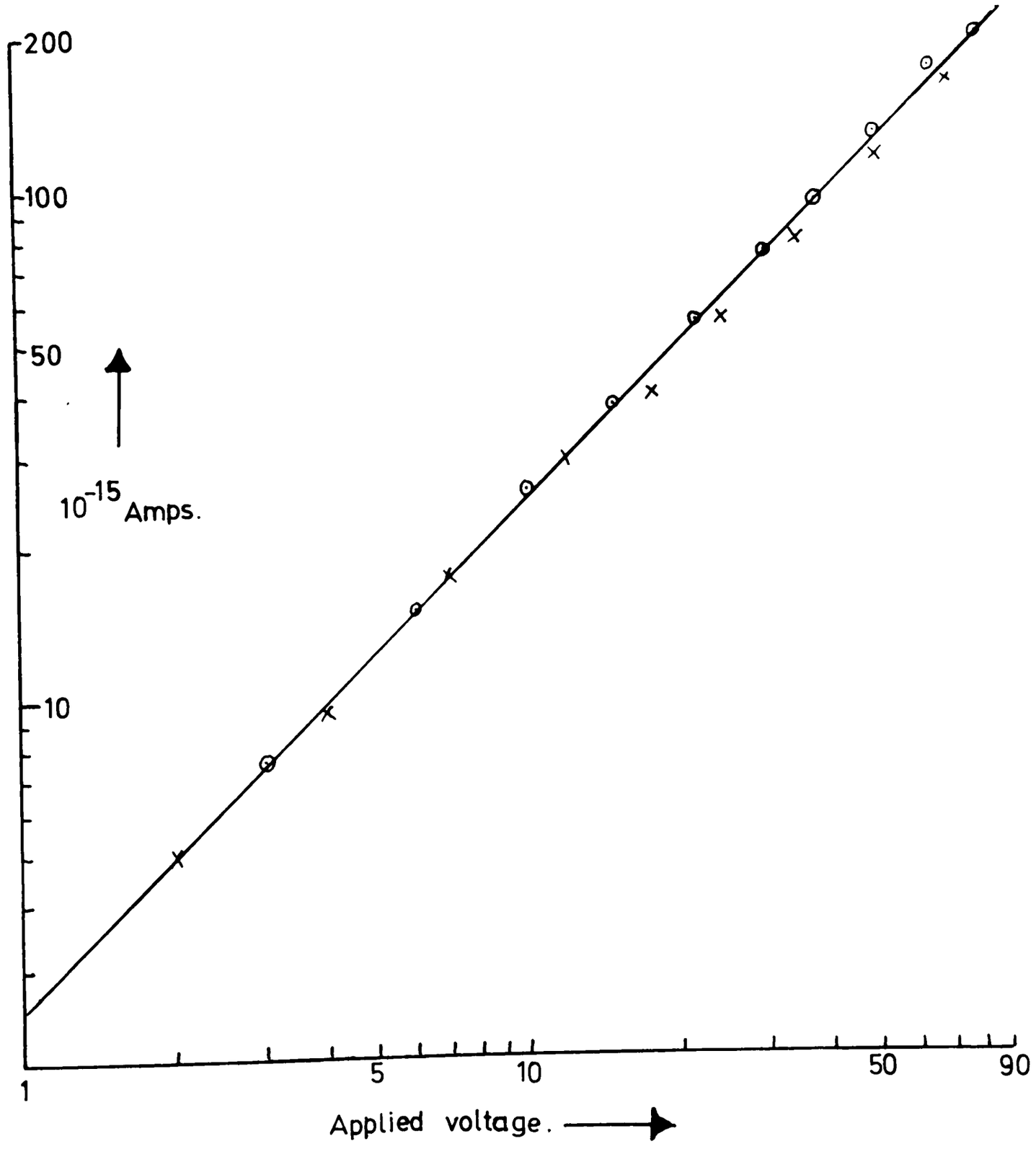
One crystal of this complex was studied as follows:

(a) Ohmicity.

The photocurrent with illumination by light of 750 mμ wavelength and monochromator slit width 2·0 mm., for the evacuated sample, was shown to be ohmic for applied voltages up to 80v. (See figure 6.19). The dark current was only 2 x 10^{-14} amp. with 80v. applied, so ohmicity tests on this were not practicable. Approximate specific resistances were (a) in the dark, 3·8 x 10^{13} ohm/cm., and (b) at 750 mμ, under the conditions of the ohmicity test, 3·8 x 10^{12} ohm/cm.

Fig. 6.19. 8-hydroxyquinoline / Tetracyanobenzene.

Ohmicity of Photocurrent. [In vacuo].



(b) Spectral response of photoconductivity.

Curves showing the spectral dependence of photoconduction were obtained using the xenon lamp at two different intensity levels. These are shown in figure 6.20.

(c) Dependence of photoconduction on intensity of illumination.

Kodak "neutral" density filters were used as described previously to determine the intensity dependence of the photocurrent at 375, 460, 520 and 600 mμ. The resulting plots of log (photocurrent) against log (percent transmission of filter) are shown in figure 6.21.

(d) Gas effects.

The following effects of gases on the photoconduction and dark current were observed:

(Slit width 2·0 mm.)	Dark current (10^{-15}amp.)	Photocurrent (10^{-15}amp).
In vacuo at 380 mμ	20	520
" " " 460 "	"	221
" " " 520 "	"	387
" " " 600 "	"	428
In N_2 at 380 mμ	9	58
" " " 460 "	"	74
" " " 520 "	"	180
" " " 600 "	"	225
In O_2 at 380 mμ	1·7	11
" " " 460 "	"	12
" " " 520 "	"	46
" " " 600 "	"	60.

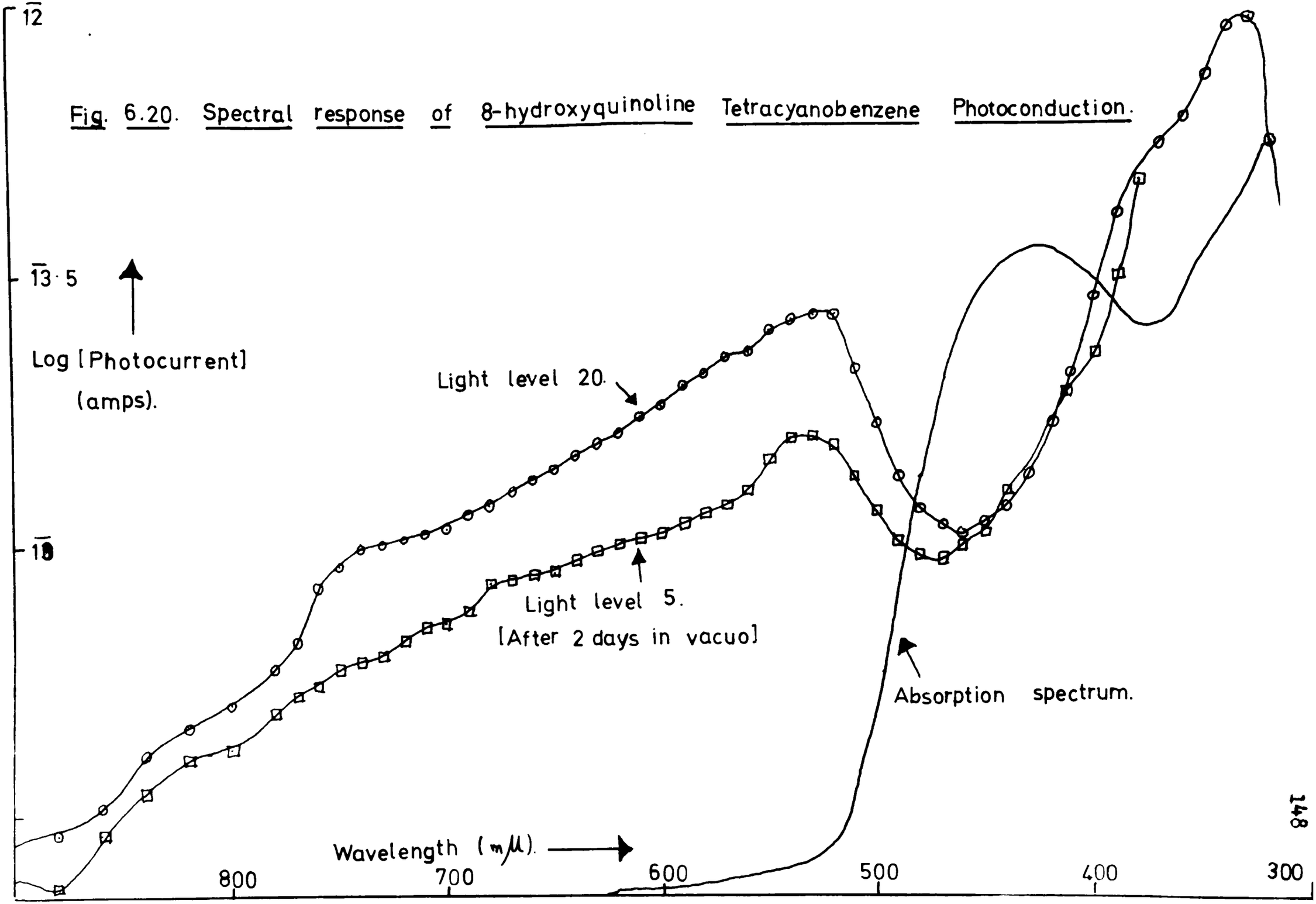
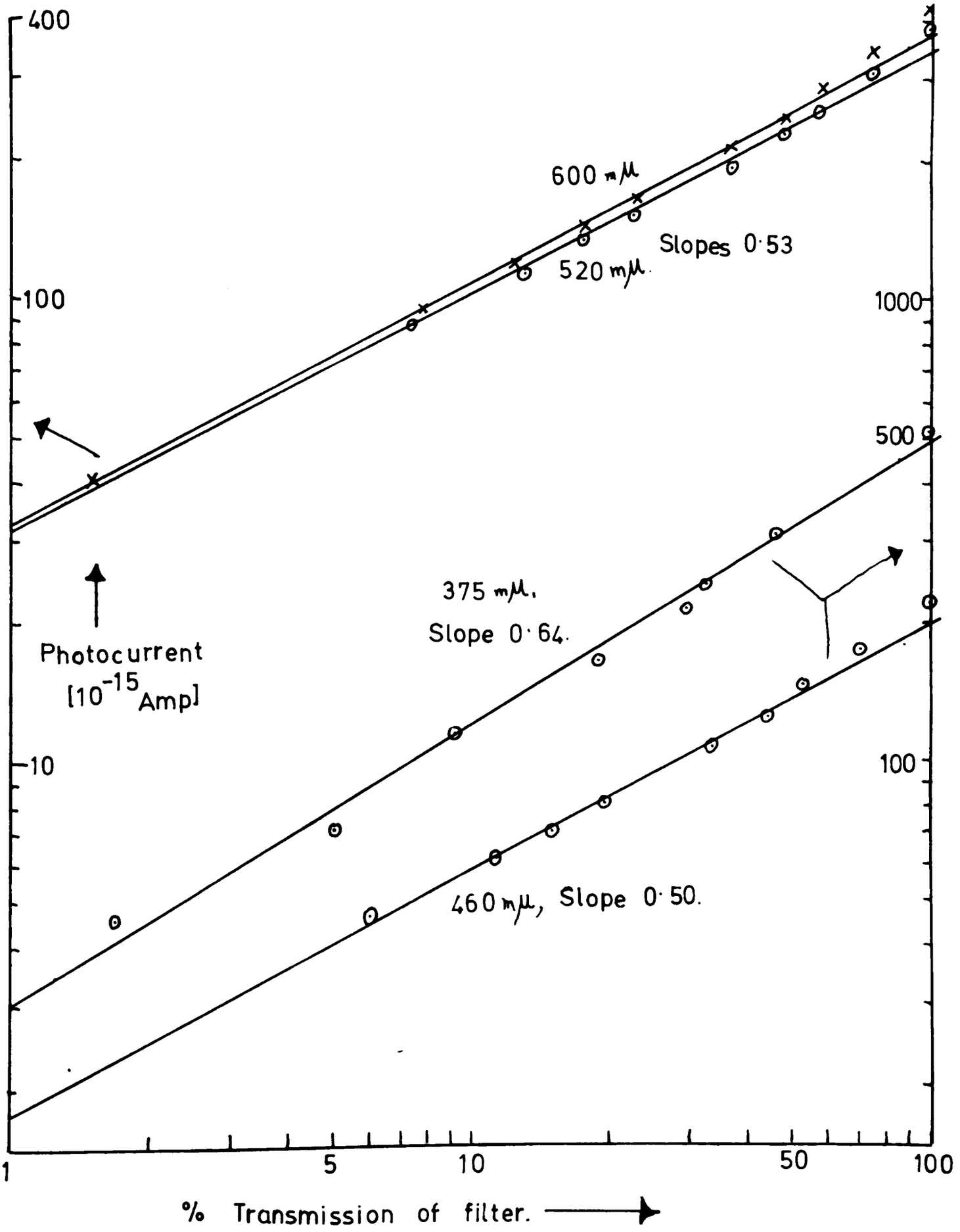


Fig. 6.20. Spectral response of 8-hydroxyquinoline Tetracyanobenzene Photoconduction.

Fig. 6.21. Photoconduction of 8-hydroxyquinoline/

Tetracyanobenzene. Intensity Dependence.



Observation of the crystal after it had been removed showed it to be coated with a thin layer of a pale cream solid, while the bulk of the crystal was still bright yellow. This may indicate either evaporation of 8-hydroxyquinoline from the crystal, or reaction, possibly photoinduced, for example with oxygen. The response curves of figure 6.20 show that this affects the absolute values of photoconduction in the near ultraviolet region, but that the general shape of the curve is unchanged.

(4) Other complexes.

Trinitrobenzene complexes of 8-hydroxyquinoline and its copper complex showed negligible photoconductivity (less than 10^{-15}amp. with 85v. applied) above 300 mμ, with the monochromator slits wide open, and a photovoltaic effect below 270 mμ, rising to a maximum at 232 mμ. The dark current was not detectable.

Copper 8-hydroxyquinolinate/picryl azide gave similar behaviour.

Copper 8-hydroxyquinolinate/tetracyanobenzene gave a photoresponse of less than 10^{-15}amp. with 79v. applied, above 400 mμ. Below 400 mμ, this rose to a peak of about $4{\cdot}3 \times 10^{-15}$amp. at about 330 mμ, before falling to $3{\cdot}6 \times 10^{-15}$amp. at 280 mμ, where a photovoltaic effect, with a maximum at 232 mμ, set in. The crystal used had a cross-section of 0·07 x 0·05 cm. and was the largest obtained for this material in several attempts to grow crystals. The figures quoted above are for measurements with the monochromator slits wide open. It may therefore be concluded that the complex conducts, but so weakly

that measurements of the effect are not possible.

Palladium 8-hydroxyquinolinate/tetracyanobenzene.

Three crystals of this material were investigated. With the largest crystal, no dark current could be detected, but, with the monochromator slits wide open and with 88 volts applied, a photocurrent rising to 10 x 10^{-15}amp. at 680 mμ was observed, beginning at 800 mμ and falling off to 300 mμ, where a photovoltaic effect set in (with a maximum at 233 mμ). Thus, the complex conducts too weakly for significant measurements, although it appears to be a better conductor than the corresponding copper complex.

6.3.3. Photoconductivity of palladium 8-hydroxyquinolinate/chloranil complexes doped with copper 8-hydroxyquinolinate/chloranil.

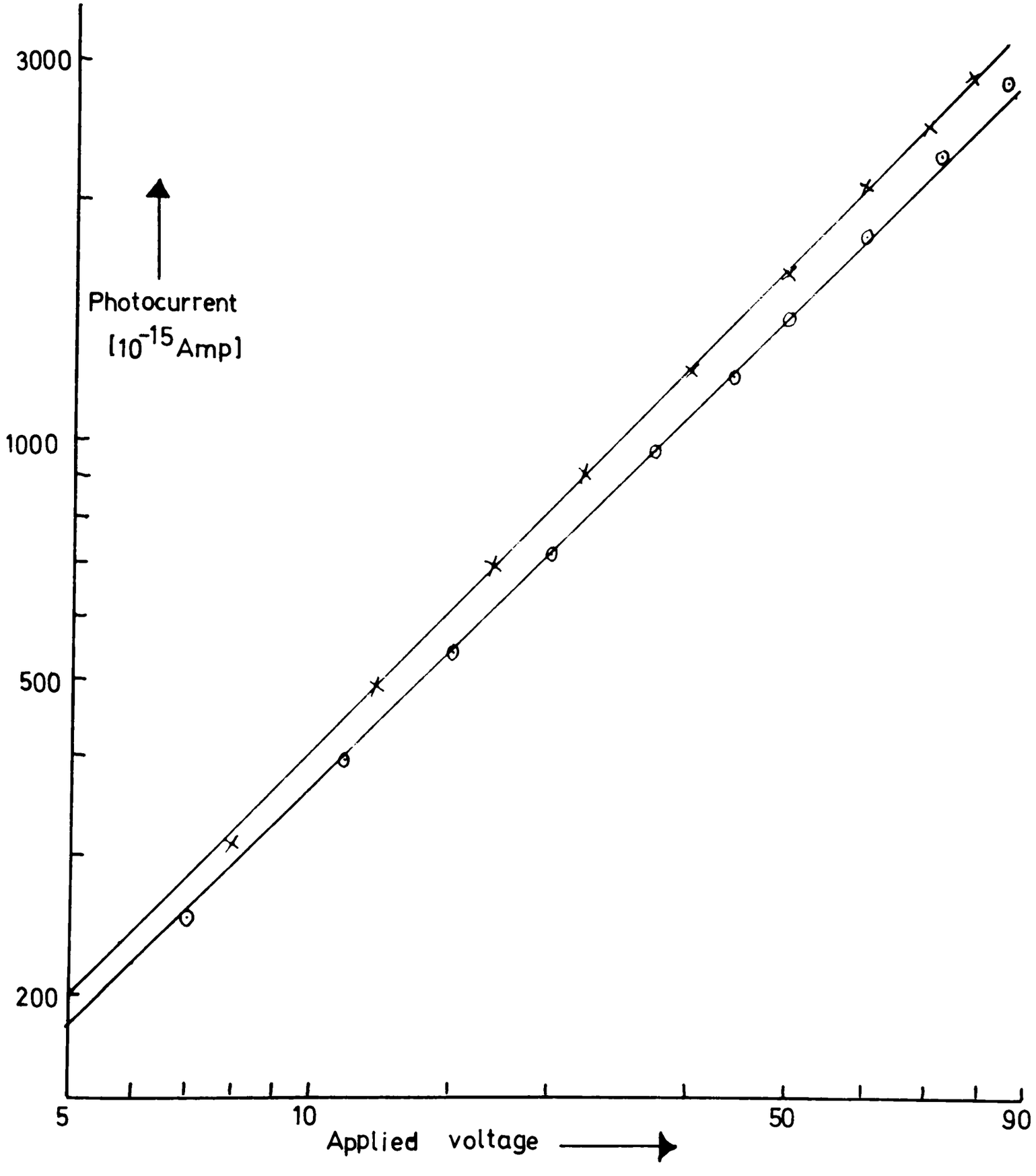
Using weighed proportions of the copper and palladium complexes of 8-hydroxyquinoline, containing up to 30 molar percent of the copper complex, thirteen batches of crystals of palladium 8-hydroxyquinolinate/chloranil doped with different amounts of the copper complex were prepared and analysed as described in chapter 2.

A crystal from the preparation using 10 percent of the copper complex was studied to investigate any differences from the photoconduction properties of the complex containing no copper. With 75 volts applied to the evacuated sample, the dark current was 10^{-14}amp. (at least 30 times smaller than for the complex containing no copper). The crystal was a good photoconductor, with a much larger response

at long wavelengths than in the case of the complex containing no copper. The photo- + dark- current at 1000 mμ, with the monochromator slits at 2·0 mm., was shown to be ohmic for applied voltages of up to 75 volts (see figure 6.22). The spectral response curve was determined in the usual way, and is shown in figure 6.23. The main features of this curve are similar to those of the complex containing no copper, but the long wavelength response is much increased relative to the rest of the curve. Using three different polarising filters (Polaroid type HR, Kodak "Polascreen" and Polacoat type P140) for infra-red, visible and ultraviolet regions, the response curves with light polarised parallel and perpendicular to the needle axis of the crystal were obtained, as described above for the complex containing no copper. These are shown in figure 6.23. A repeat measurement of the response curve at wavelengths above 625 mμ using the tungsten lamp (which gives much less ultraviolet light) showed that the response at wavelengths above 1350 mμ was probably due to stray ultraviolet light, since this curve only began to rise at 1350 mμ. The large peak at 980 mμ is still present, and is therefore a genuine property of the crystal (see figure 6.23).

In view of the marked change in the ratio of the long and short wavelength responses of photoconductivity, it was decided to investigate the dependence of this ratio on the amount of copper present in the crystal, to discover whether any systematic effects due to the copper atoms could be detected. At least two crystals of each composition were investigated as follows:

Fig. 6.22. Ohmicity of 10% Cu doped Pd 8-hydroxyquinolinate.



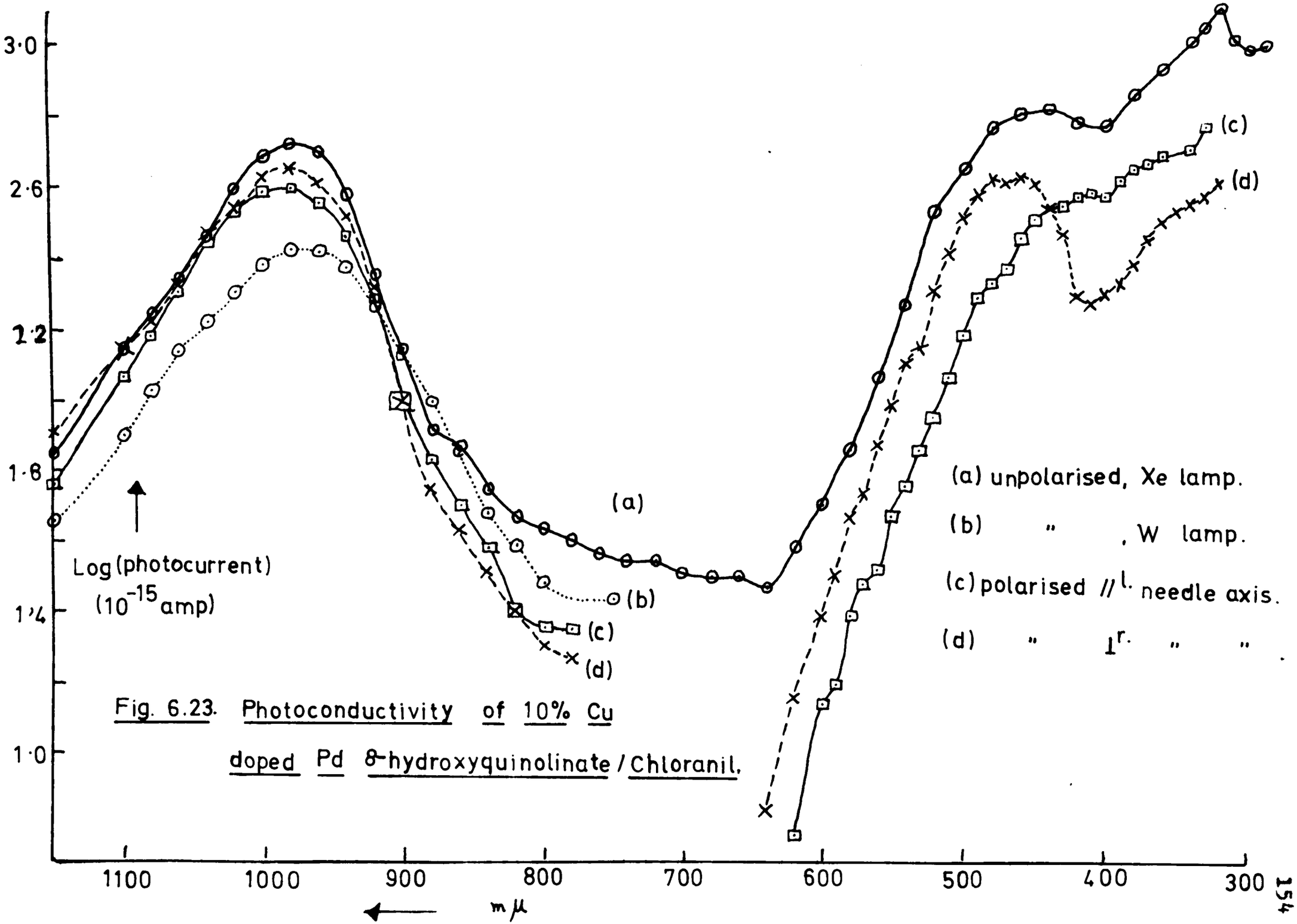


Fig. 6.23. Photoconductivity of 10% Cu doped Pd 8-hydroxyquinolinate / Chloranil.

(i) The evacuated sample was shown to be ohmic when illuminated with light of 460 mμ wavelength.

(ii) After first ensuring that the long wavelength peak was still a maximum at 980 mμ, the ratio of the photoconductivity at 980 mμ to that at 460 mμ (where there is a definite peak in the polarised response curve of the 10% doped crystal, shown in figure 6.23) was determined carefully. The dark current was backed-off to zero before each measurement, and the ratio was measured 3 times for each crystal to obtain a reliable mean value.

(iii) The dark current was noted before removal of the crystal for measurement of its dimensions and for analysis. Removal of the crystals was found to be relatively easy, since the silver paste of the contacts could be removed by gentle rubbing with a soft brush soaked in acetone.

Table 6.1 shows the resulting ratios, together with approximate values of the resistivity at 980 mμ, 460 mμ and in the dark. Figures 6.24 and 6.25 show these quantities plotted as a function of the percentage of copper in the sample, as determined by x-ray fluorescence analysis.

6.3.4. Photoconductivity of copper and palladium 8-hydroxyquinolinates.

Large hexagonal plate crystals of the copper complex, grown from pyridine at 40°C by Dr. G. Morpurgo, were used for conductivity studies. With electrodes about 3mm. square on the flat faces of a

hexagonal plate crystal about 1mm. thick, the dark current with 84 volts applied was only 12×10^{-15}amp. There was no photoconduction above 270 mμ, but a small photovoltaic effect was observed below 270 mμ, with a peak at 235 mμ.

A similar crystal, mounted with the electrodes on opposite edges of the hexagon, with a large area of crystal exposed to the light, gave a dark current too small to measure (less than 10^{-16}amp.) There was no photoconduction above 350 mμ, and only a small photocurrent of 2×10^{-15}amp. between 350 and 270 mμ. Below 270 mμ, a large increase, due to a photovoltaic effect, occured. The light beam was then masked so that the crystal, but not the electrodes, was illuminated. The small photoconduction persisted, but the photovoltaic effect vanished, showing that the latter is probably an electrode effect.

Palladium 8-hydroxyquinolinate crystals were grown from chloroform solution, slowly. Two types of crystals appeared - long needles and small irregular prisms. (X-ray photographs show that these are two different forms, and that the needle crystals have one side of the unit cell very short). A needle crystal was mounted, shown to be ohmic, and tested for photoconductivity. The response curve of figure 6.26 was obtained. The crystal was photovoltaic below 260 mμ. The specific resistance of the compound was found to be $2{\cdot}8 \times 10^{14}$ohm/cm. (dark) and $4{\cdot}8 \times 10^{12}$ohm/cm. (at the photoconduction peak).

TABLE 6.1.

Copper-doped Pd 8-hydroxyquinolinate/chloranil complexes.

Photoconduction ratios and resistivities.

% Cu	Ratio of 460mμ/980mμ conduction.	Specific resistance (ohm/cm.) At 460mμ	At 980mμ	In the dark.
0	20•2	$3•9 \times 10^{11}$	$2•2 \times 10^{12}$	$2•7 \times 10^{12}$
	34•6		(at 905mμ)	
1	11•3	$1•3 \times 10^{11}$	$7•1 \times 10^{11}$	$1•2 \times 10^{12}$
	17•0			
5	5•9			
	15•1			
	9•4			
	27•0	$1•4 \times 10^{12}$	$1•9 \times 10^{13}$	$3•6 \times 10^{13}$
10	1•2	$7•4 \times 10^{12}$	$9•0 \times 10^{12}$	$2•5 \times 10^{14}$
	2•8	$7•3 \times 10^{12}$	$2•0 \times 10^{13}$	$4•0 \times 10^{14}$
	1•8			
	2•5			
12	13•2	$8•8 \times 10^{11}$	$1•3 \times 10^{12}$	$1•4 \times 10^{12}$
	9•9			
14	48•6	$1•1 \times 10^{12}$	$1•7 \times 10^{13}$	$2•3 \times 10^{13}$
	60•2			
16	87•7			
	53•1			
	104•7			
	21•0			
	48•6			
18	77•5			
	63•2			

TABLE 6.1. (Continued)

% Cu	Ratio of 460mμ/980mμ conduction.	Specific resistance (ohm/cm.) At 460mμ	At 980mμ	In the dark.
20	48·6			
	56·5			
22	4[illegible]·5	$3·1 \times 10^{12}$	$5·5 \times 10^{12}$	$5·5 \times 10^{12}$
	29·2	$8·1 \times 10^{12}$	$2·3 \times 10^{13}$	$2·5 \times 10^{13}$
24	9·1			
	13·5			
	11·8			
27	45·2	$5·4 \times 10^{12}$	$5·5 \times 10^{13}$	$6·8 \times 10^{13}$
	51·7			
30	21·8	$4·4 \times 10^{12}$	$9·6 \times 10^{13}$	$>10^{14}$
	19·3			
100	25·5	$1·3 \times 10^{13}$	$3·4 \times 10^{14}$	$>10^{15}$

Fig. 6.24. Photocurrent ratios for Cu-doped Pd 8-hydroxyquinolinate/Chloranil complexes.

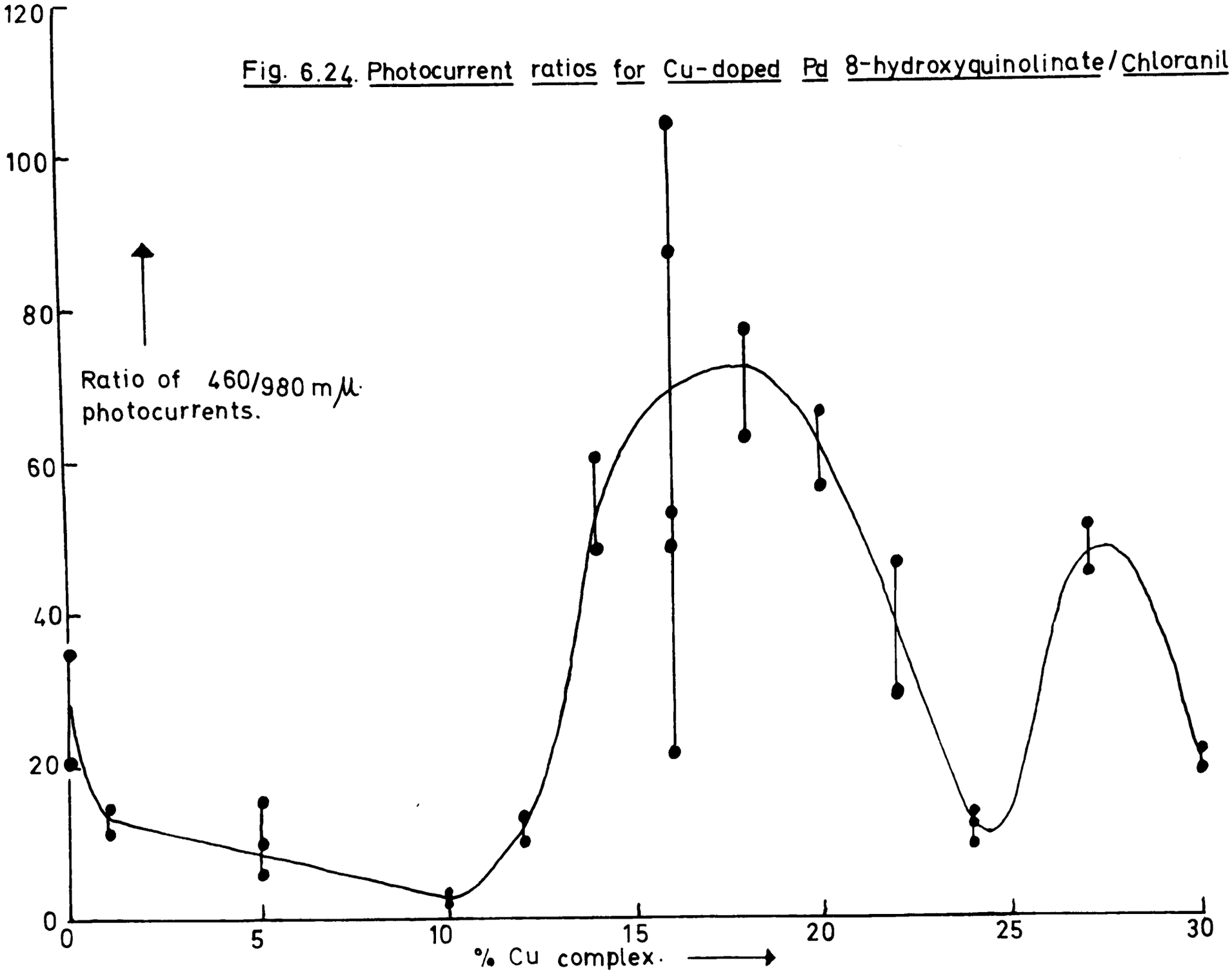
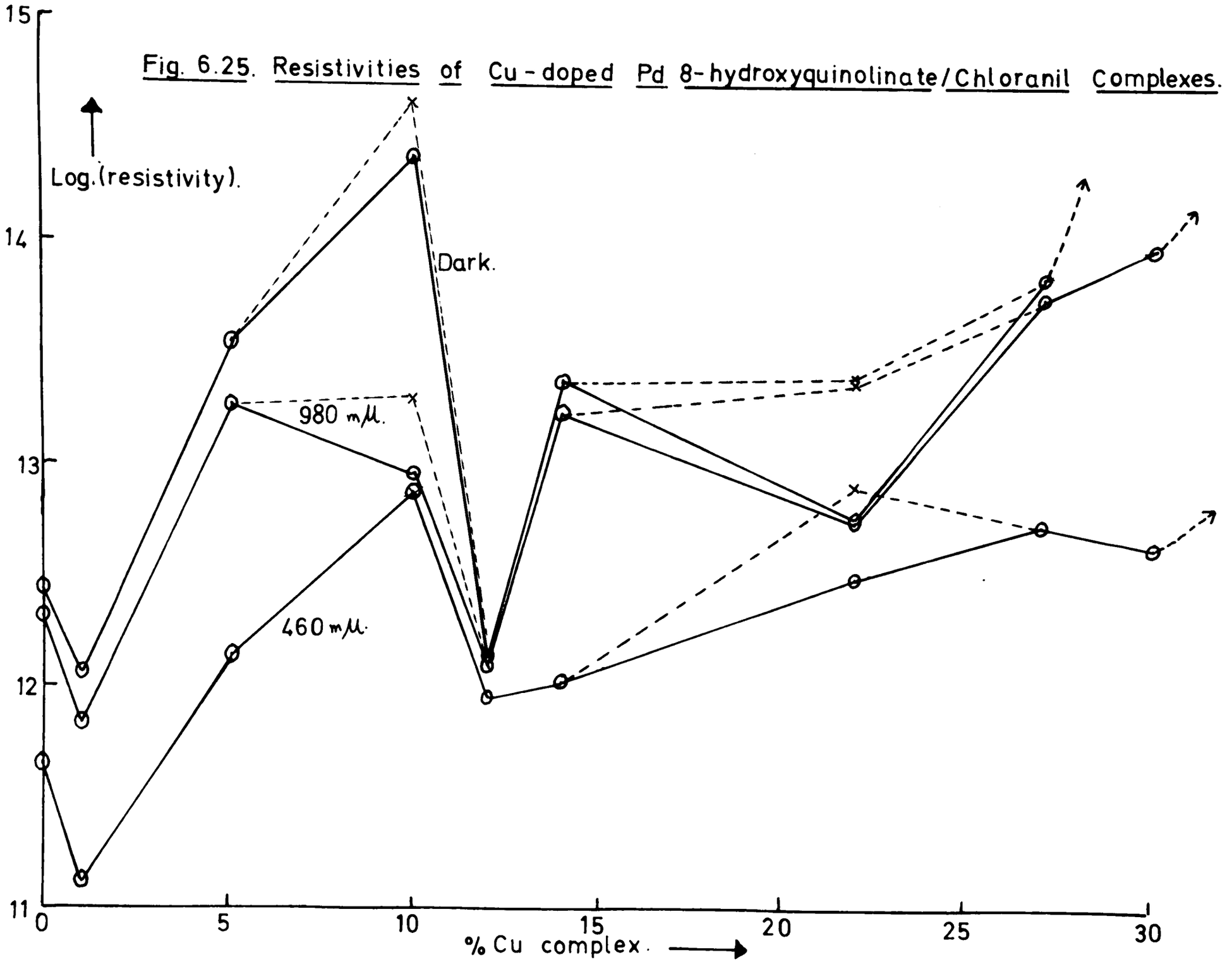
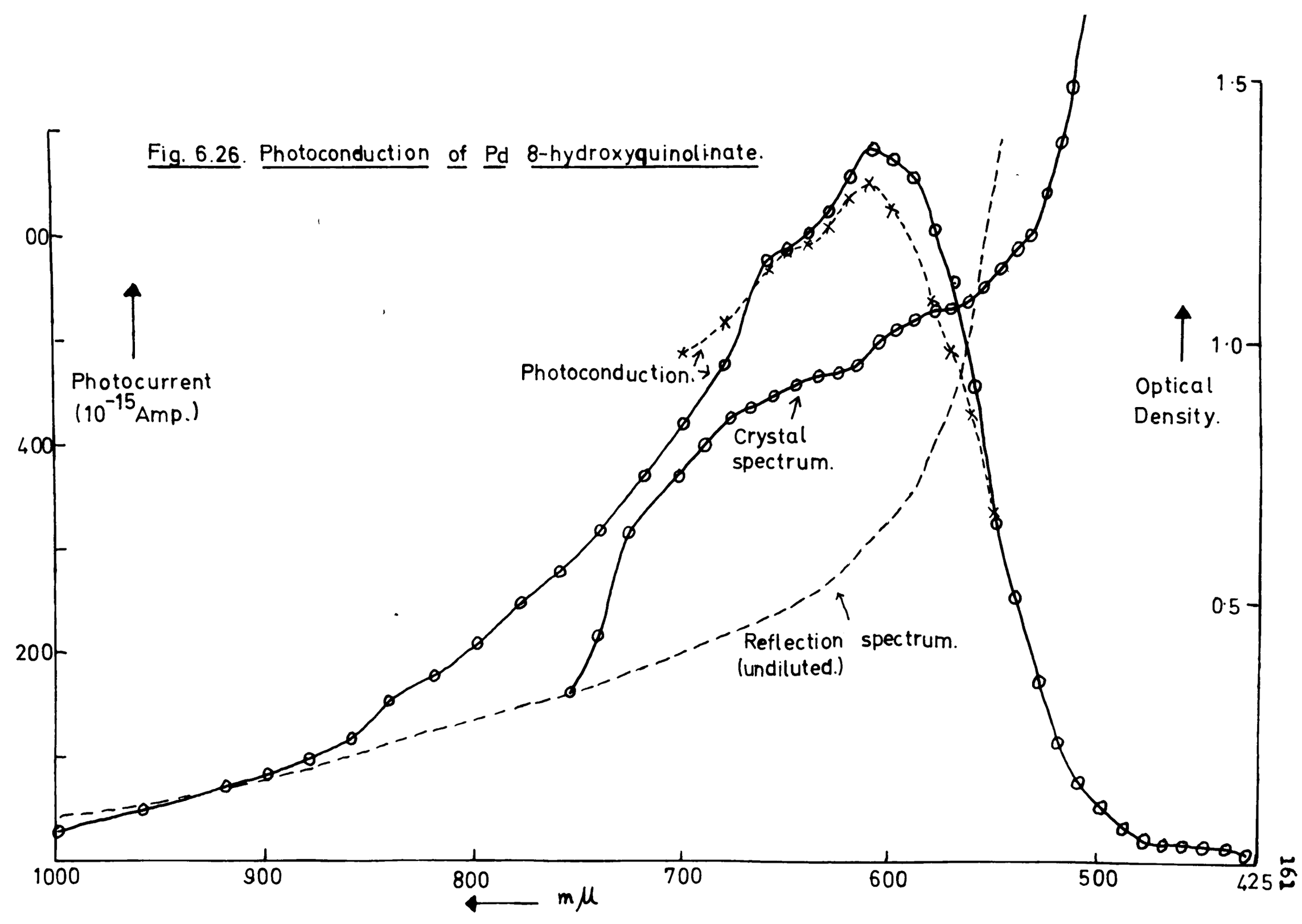


Fig. 6.25. Resistivities of Cu-doped Pd 8-hydroxyquinolinate/Chloranil Complexes.




Fig. 6.26. Photoconduction of Pd 8-hydroxyquinolinate.
00
400
200
Photocurrent
(10^{-15} Amp.)
Photoconduction.
Crystal
spectrum.
Reflection spectrum.
(undiluted.)
1·5
1·0
0·5
Optical
Density.
1000
900
800
700
600
500
425
mμ

6.4. Discussion.

6.4.1. Summary of facts deduced from experimental results.

The present results show the following features:

(a) Spectral response curves for molecular complexes show two response regions related to the charge transfer absorption band, one of low energy and the other of high energy with respect to the peak of the absorption band.

(b) The low energy peak is smaller than the high energy peak, and more sensitive to impurities. In the palladium 8-hydroxyquinolinate/chloranil complex, the dark, but not the photo-, current is sensitive to oxygen. In the 8-hydroxyquinoline/tetracyanobenzene complex, both the dark and photo-currents are sensitive to oxygen and to nitrogen.

(c) The photocurrent varies as (intensity of illumination)^n, where n varies only from 0·4 to 0·6 across the whole spectral range studied.

(d) Studies with polarised light show that the high energy response is polarised, whereas the low energy response is not affected by the direction of polarisation of the light.

(e) Small amounts of stray light from visible and/or ultraviolet regions produce a relatively large effect in extending the low energy response into lower energy regions.

(f) Resistivity values corresponding to the dark current and low and high energy photoconduction maxima, for copper-doped palladium 8-hydroxyquinolinate/chloranil complexes, follow the curves of figure 6.25 when plotted against the percentage of copper in the

crystal.

(g) The corresponding plot for the ratio of high and low energy photoconduction is as shown in figure 6.24.

(h) Pure palladium 8-hydroxyquinolinate is a photoconductor, whereas copper 8-hydroxyquinolinate is not.

(i) Copper 8-hydroxyquinolinate/chloranil shows photovoltaic effects in vacuo, which vanish immediately when gases are admitted.

Other workers, studying purely organic complexes, have deduced the following additional features[49],

(j) Activation energies of the dark current do not correlate with the energy of the charge transfer absorption maxima.

(k) Increasing temperature increases photoconductivity (activation energy approximately 0·2 eV), the increase being greater for the low energy band than for the high energy band.

6.4.2. Mechanisms of photoconduction in molecular complexes.

Facts (b), (d), (f), (g), and (k) suggest that the low and high energy bands are caused by different mechanisms.

The positive activation energy of photoconduction suggests that charge movement is better described by a hopping model than by a band model. The chief problem in deducing a mechanism is therefore the origin of the carriers, and three contributing processes may be distinguished:-

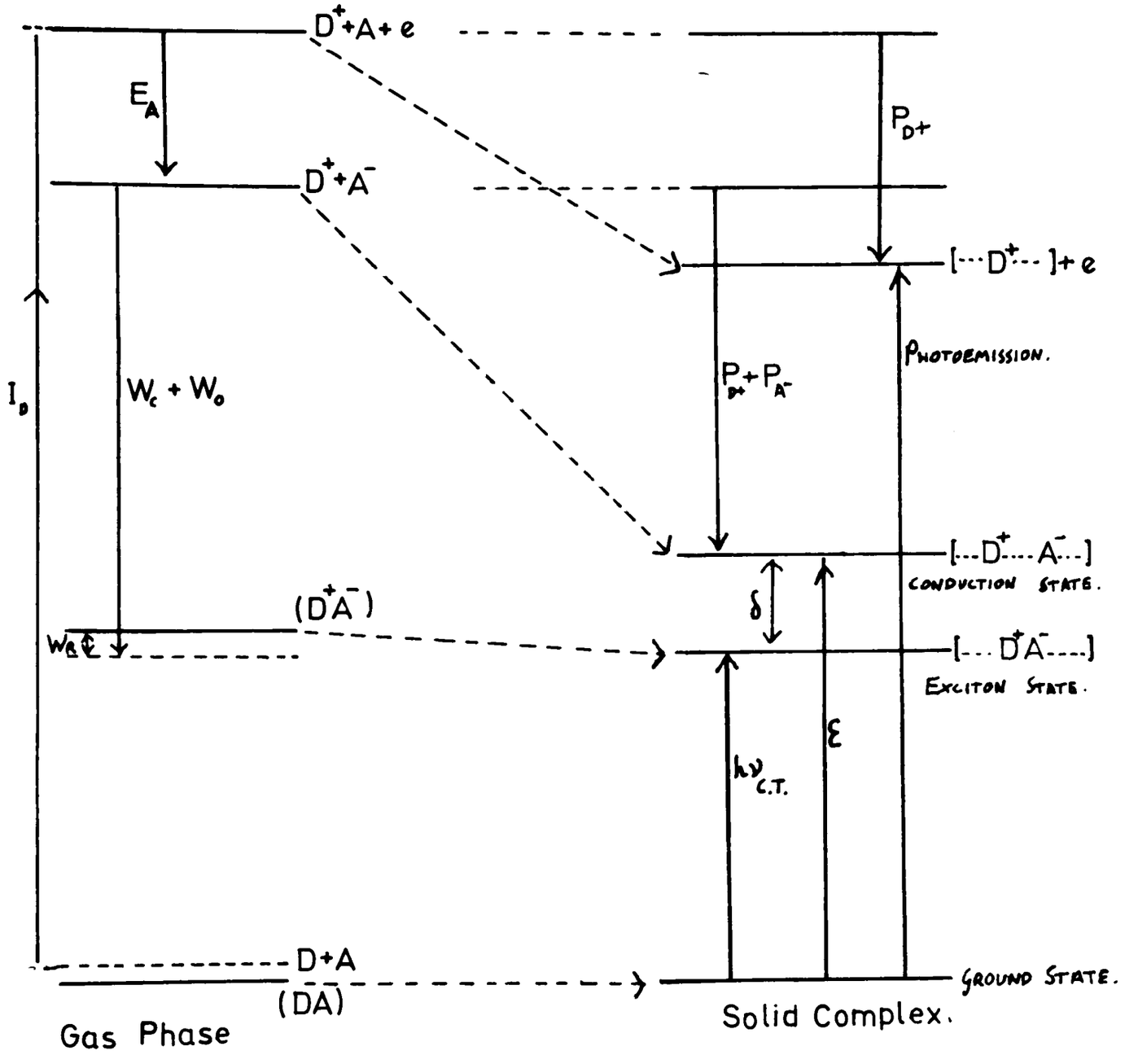


Fig. 6.27. Energy level diagram for electrical conduction in molecular complexes.

(i) The high energy band.

Figure 6.27 is an energy level diagram for donor-acceptor systems in the vapour phase and in the solid state. For electrical conduction, ion pairs from the charge transfer excited state must be separated, to give free, mobile charges. The net energy (δ) required to do this ($= E - h\nu_{C.T.}$) is the sum of three contributions:

(a) The electrostatic energy needed to separate the D^+A^- pair ($= e^2/R_{D^+A^-}$, where $R_{D^+A^-}$ is the average D^+-A^- distance in the charge transfer excited state).

(b) The charge transfer resonance energy (δW) lost in separating the ion pair.

(c) The polarisation energy of isolated D^+ and A^- ions in a slightly distorted environment of near-neutral D and A molecules ($P_{D^+} + P_{A^-}$).

Thus, $\delta = (P_{D^+} + P_{A^-}) - (e^2/R_{D^+A^-} + \delta W)$, and depends on the strength of the complex, the size of the molecules, the polarisability of the molecules, their dipole moments, and the general rigidity of the lattice. Depending on the balance of these quantities, it may be positive or negative.

Whether δ is positive or negative, the photoconduction response peak from this process will usually be on the high energy side of the absorption peak, since:

(a) δ represents only the net energy required, and additional activation energy will usually be required to overcome

activation energy barriers,

and (b) there is frequently a singlet transition of the donor molecule in this region, which can mix with the charge transfer transition. Light of wavelengths where absorptions due to these two transitions overlap is therefore likely to be most effective at producing charge carriers, by the following mechanism:

Ground state of donor $\xrightarrow{h\nu}$ ^1L_a excited state

D D*

^1L_a excited donor + acceptor molecule $\xrightarrow{h\nu_{c.t.}}$ $(D^+A^-)^*$ in excited state

D* A or $\cdots D^+ \cdots A^- \cdots$ separated carriers.

(ii) The low energy band.

If stray light of wavelength corresponding to the ^1L_a singlet excitation of the donor is present when the wavelength of the main illumination is long, charge carriers will be produced on the low energy side of the charge transfer absorption band, by the mechanism outlined above. However, this cannot account for all of the low energy response, as shown by the results obtained using stray light filters.

An alternative mechanism giving free carriers from ion pairs involves the trapping of one half of the ion pair at particular lattice sites, leaving the other half with a net force, due to

interaction with the applied electric potential, greater than that which is experienced by the trapped charge.

In the metal 8-hydroxyquinolinate/chloranil complexes, the different sizes of the donor and acceptor molecules result in a structure where positive charge can move directly over a network of neighbouring donor molecules, whereas the acceptor molecules are completely isolated from one another by intervening donor molecules (c.f. chapter 3 and appendix A). The negative charge on an acceptor molecule in an excited charge transfer ion pair is therefore trapped in a cage of donor molecules, which will not easily accept extra negative charge.

If one of the donor molecules of this cage is a copper complex, any movement of negative charge from the acceptor will tend to be onto this molecule rather than onto a palladium complex, since $copper^{II}$ is more readily reduced (to $copper^{I}$) than $palladium^{II}$. The lattice around the acceptor molecule will take some time to relax from the arrangement adopted around the acceptor anion, so that, if the extra electron now present on the copper complex is to move off again, the most favourable site will be that of the original acceptor molecule. Thus, copper complexes tend to form traps, in which negative charge resonates between copper 8-hydroxyquinolinate and chloranil. (Lattice defects may also trap negative charge in a similar way.)

The positive charge will move by the pathway making least activation energy demands. Since positive hole migration may be regarded as electron transfer from a neighbouring molecule into the

positive hole, and since palladium 8-hydroxyquinolinate has a lower ionization potential than copper 8-hydroxyquinolinate, the pathway requiring least activation energy will be one based entirely on a network of palladium 8-hydroxyquinolinate molecules.

The distribution of positive charge on the positively charged 8-hydroxyquinolinates will differ for the palladium and copper cases. Copper^{III} (d^8) in a planar environment, is more stable than palladium^{III} (d^7), so that the positive charge in the copper complex will tend to concentrate on the metal, whereas in the palladium complex it will concentrate more on the ligand. Since the ring systems of the ligands, but not the metal atoms, of neighbouring 8-hydroxyquinolinates overlap, the positive charge on a palladium 8-hydroxyquinolinate will probably be more mobile than that on a copper complex, which will tend to be trapped at the metal atom. There is a chlorine atom of the acceptor close to the metal atom of the donor, so this provides an easy pathway for electron transfer in the ion pair recombination process, and further reduces conductivity in crystals containing large concentrations of copper. This charge distribution effect also reduces the probability of the energetically favourable process

$$Cu\ ox^{+} + Pd\ ox \longrightarrow Pd\ ox^{+} + Cu\ ox$$

since the positive charge is not in the region of overlap of the two molecules.

That the charge distribution is as suggested can easily be verified for the copper complex, by illuminating a crystal

containing a small amount of the copper complex doped into the palladium complex, with the sample in an E.S.R. machine. The spectra of the type shown in chapter 5 will vanish if the positive charge is located chiefly on the copper atom, giving a d^8 ion with paired spins.

(iii) Exciton-exciton collisions.

Ion pairs may also be separated by a redistribution of energy occurring at exciton-exciton collisions. (Excitons in this case may be regarded as charge transfer excitation energy migrating from molecule to molecule in the lattice.) It has been shown that there is a finite possibility of energy exchange when excitons collide[50], which could occur as follows:

$$\underset{\text{exciton}}{(D^+A^-)} + \underset{\text{exciton}}{(D^+A^-)} \longrightarrow \underset{\text{neutral molecules.}}{(DA)} + \underset{\text{separated charges.}}{(\cdots\cdots D^+\cdots\cdots A^-\cdots\cdots)}$$

This should give a maximum carrier concentration where charge transfer absorption is maximum, unless the carrier concentration is limited by recombination. The intensity dependence results (figures 6.14 and 6.21) show that recombination occurs to a similar extent over the whole region studied, so this mechanism cannot account for the shapes of the photoresponse curves. It is nevertheless a contributing factor, and may be important in the low energy region if trapping can lead to increased probability of energy redistribution at exciton-exciton collisions.

6.4.3. Interpretation of resistivity data for copper-doped palladium 8-hydroxyquinolinate/chloranil complexes.

Crystal structure evidence (c.f. chapter 3 and appendix A) shows that

(a) the doped complexes have the same structure as the palladium complex with no copper present.

and (b) each metal 8-hydroxyquinolinate molecule has 10 near neighbours of the same type (2 in the same plane, 4 above, near the ends of the molecule, and 4 similar ones below). Thus, if the copper complex is distributed evenly through the lattice, there will be one neighbouring copper 8-hydroxyquinolinate for any other one when the concentration of the copper complex reaches 10 percent. Similarly, when the concentration reaches 20 percent, there will be two such neighbours if the distribution is even.

Electron spin resonance results (c.f. chapter 5) show that the broadening of the hyperfine lines increases more markedly on going from 1 to 10% of copper complex present than on going from 0·1 to 1·0%. This would not be the case if the copper complex molecules tended to cluster together, and suggests an even distribution of the complex through the lattice.

Analytical results (c.f. chapter 2) show that the copper concentrations in the crystals are the same as those in the solutions used for their preparation. Thus, the binding energy of a copper

complex in the lattice must be similar to that of a palladium complex, in the concentration range used. This suggests that the distribution of copper complex molecules will be even throughout the lattice, and not as irregular clusters, from entropy considerations.

This evidence, in conjunction with the hypothesis that copper complexes act as electron traps, explains the main features of the resistivity curves of figure 6.25 as follows:

(a) The resistance for both dark and photoconduction is high with 0 and 10% of copper complex present. At these concentrations there are either no traps apart from lattice defects, or no particularly favourable trapping sites, since every copper or palladium 8-hydroxyquinolinate molecule has one other copper 8-hydroxyquinolinate molecule as a neighbour. Thus, there are no points in the lattice where the negative charge of the anion of an ion pair is stabilised with respect to all neighbouring sites. The probability of positive hole migration without the migration of the associated negative charge is therefore reduced, less carriers are produced, and the resistance is high.

(b) The resistivity falls rapidly for copper concentrations slightly greater than 0 and 10%. Here there are widely-spaced "super-traps", consisting of regions containing more copper than the surrounding regions. (For example, a 12% copper-doped crystal has super-traps consisting of copper 8-hydroxyquinolinate molecules with at least two similar neighbours, as opposed to the average copper trap with

only one similar neighbour.) A negative charge in one of these super-traps is stabilised with respect to all neighbouring sites, leaving the associated positive charge still free to migrate under the influence of an applied voltage.

(c) The resistivity of the dark current is exceptionally high, for example, with 10% of copper complex present. In the dark, the rate of production of ion pairs is low, and not sufficient to overcome the rate at which they drop back to the near-neutral ground state, unless conditions for separation of the ion pairs are good. This is not so for the 10% doped compound, so the equilibrium concentration of carriers is small and the resistivity is high.

With large applied voltages, positive charge may migrate more rapidly, so that ion pairs are "torn apart". If the rate of production of ion pairs is comparable with the rate of recombination, as is likely in the dark, this may lead to a large increase in the number of carriers as the applied voltage is increased. This may account for the non-ohmic dark currents e.g. in the pure palladium 8-hydroxyquinolinate/chloranil complex (see figures 6.9 and 6.10).

(d) In the range 12-14% of copper complex, there is a steep rise in the resistivity for the dark- and 980 mμ photo- currents. Super-traps are now closer together and therefore less effective. The rate of production of ion pairs at 980 mμ and in the dark is low, and not sufficient to prevent the equilibrium concentration of carriers falling as trap efficiency decreases. At 460 mμ, the rate of production of carriers is much faster, by a different mechanism,

and this does not occur.

(e) There is a general rise in resistivity as the copper complex concentration increases towards 100%. This is expected as a result of the transition from 100% Pd complex to 100% Cu complex (which has a much higher resistivity). It is due to

(i) an increased recombination rate as traps become more common,

(ii) decreased mobility of negative charge in a lattice full of traps,

and (iii) decreased mobility of positive charge, due to the onset of trapping by copper complexes with the positive charge located near the copper atom.

Given these resistivity trends, the shape of the curve showing the ratio of photocurrents at 980 and 460 mμ is also explained in the same way.

6.4.4. Photoconduction in metal 8-hydroxyquinolinate crystals.

Figure 6.26 shows that pure palladium 8-hydroxyquinolinate photoconducts strongly in a region where there is only weak absorption. (The extinction coefficient of the weak band observed in the crystal spectrum is approximately 70). This behaviour has also been observed in phthalocyanines (see results section and reference 47) and in anthracene[51]. The position of the weak absorption band in this case

is such that it is most likely to be due to a triplet of a transition of the ligand π electrons. Triplet states are long-lived, and therefore probably more effective at giving rise to conductivity than shorter-lived transitions, and the perturbing effect of the heavy palladium atom could increase the intensity of absorption due to this normally forbidden type of transition.

Further work, particularly polarised crystal spectra and photoconductivity work on palladium phthalocyanine, is needed before definite conclusions can be drawn about this, or about the very poor conductivity of copper 8-hydroxyquinolinate.

6.4.5. Photovoltaic effects.

At certain electrode surfaces, or at boundaries between domains of different crystal structure, photovoltages can be set up[52] (e.g. in ZnS). This may be the origin of the photovoltaic effect observed in copper 8-hydroxyquinolinate/chloranil, since attempts to obtain x-ray diffraction patterns of the crystals always gave photographs showing several sets of patterns, which suggests a domain structure with different lattice arrangements. The effect in pure copper 8-hydroxyquinolinate vanished when the electrodes were not illuminated, suggesting that electrode barriers are also important. The rapid, reversible nature of gas effects on this phenomenon suggests that gas-induced surface effects may short-circuit these boundary potentials.

6.4.6. Relevance to the role of quinones in chloroplasts.

The mechanism of photoconduction discussed above involves the acceptor molecule only in the initial stage of the process, when ion pairs are produced, the negative halves of which are trapped at the acceptor sites. Positive charge moves over a network of donor molecules, virtually independently of the presence of the acceptor. Chloroplasts contain large stacks of chlorophyll molecules, with a smaller number (about 1 per 5 chlorophyll molecules) of quinone molecules, such as plastoquinone[53a]. These molecules may act as the acceptor does in the complexes studied in this work, producing ion pairs, and allowing the positive charge to migrate through the lattice of donor chlorophyll molecules until it reaches the site of the oxidation reaction. Reduction reactions could occur at the sites of trapped electrons on quinone molecules.

The large increase in photoconduction of phthalocyanines when a layer of o-chloranil molecules is put on the surface of the crystals, observed by Calvin et al.[53b], shows that a limited number of acceptor molecules can produce a large effect on charge transfer through stacks of donor molecules of this type.

APPENDIX A.

DETERMINATION OF THE CRYSTAL STRUCTURES OF THE COMPLEXES OF BIS-8-HYDROXYQUINOLINATO PALLADIUM^{II} WITH CHLORANIL AND 1,2,4,5-TETRACYANOBENZENE.

A.1. X-ray photography.

A small, well-formed crystal of each of the complexes was mounted, and single-film zero-layer Weissenberg photographs were obtained about two principal and one non-principal axes, using Cu K_α radiation. These were used to obtain unit cell dimensions for the crystals.

The x-ray intensities of 1880 (palladium 8-hydroxyquinolinate/chloranil) and 1920 (palladium 8-hydroxyquinolinate/tetracyanobenzene) independent reflections were estimated visually from sets of multiple (5) film equi-inclination Weissenberg photographs about the a axis, using a calibrated intensity strip. Because of the space group, it was necessary to take two 220° Weissenberg photographs of each layer, apart from the zero layer, in order to record the complete 360° rotation of the reciprocal lattice. The data from individual layers were placed on a common scale, using the exposure time to x-rays from a stabilised source, and carefully standardised development conditions.

A.2. Cell dimensions and crystal data.

The lateral distance in mm. of a reflection (h,k,l), as recorded on a Weissenberg photograph taken in a camera of 5·73 cm. diameter, from its equivalent $(\bar{h}, \bar{k}, \bar{l})$ on the other half of the film, is the angle θ in degrees given by the Bragg equation

$$\sin\theta = \lambda/2d$$

where d is the distance of the reciprocal lattice point producing that reflection from the origin of the lattice.

For a reflection (h, k, l),

$$\mathrm{Sin}^2\theta = R_{11}h^2 + R_{22}k^2 + R_{33}l^2 + R_{12}hk + R_{13}hl + R_{23}kl \qquad (A.1)$$

where $R_{11} = \lambda^2 a^{*2}/4$

$R_{12} = \left(2\lambda^2 a^* b^* \cos\gamma\right)/4$ etc. (A.2)

where a*, b* etc. are reciprocal cell dimensions.

Using values of θ for several reflections of high index on the three single-film zero-layer photographs, and equation A.1, R_{ij} values were calculated and cell dimensions and angles were deduced.

The density of the crystals was determined by flotation in a mixture of dibromobenzene and tetrabromoethane, whose density was measured on a density balance.

At this stage in the structure determinations, the following crystal data were known:-

Palladium 8-hydroxyquinolinate/chloranil.

Triclinic pinacoidal; optically biaxial; $\underline{a}$ = 8·17 ± 0·02, $\underline{b}$ = 8·18 ± 0·02, $\underline{c}$ = 9·69 ± 0·02 Å; α = 99·5 ± 0·2, β = 77·8 ± 0·2, γ = 66·0 ± 0·2°; $\underline{U}$ = 546·5 Å^3, $\underline{D_m}$ = 1·931, z = 1, $\underline{D_c}$ = 1·946 gm/ml. Space group $P\bar{1}$ (C_i^1; no. 2).

Palladium 8-hydroxyquinolinate/tetracyanobenzene.

Triclinic pinacoidal; optically biaxial; $\underline{a}$ = 8·73 ± 0·02, $\underline{b}$ = 7·97 ± 0·02, $\underline{c}$ = 9·38 ± 0·02 Å, α = 109·6 ± 0·2, β = 72·8 ± 0·2, γ = 107·6 ± 0·2°; U = 572·2 Å^3, D_m = 1·671, z = 1, D_c = 1·661 gm/ml., Space group $P\bar{1}$ (C_i^1; no. 2).

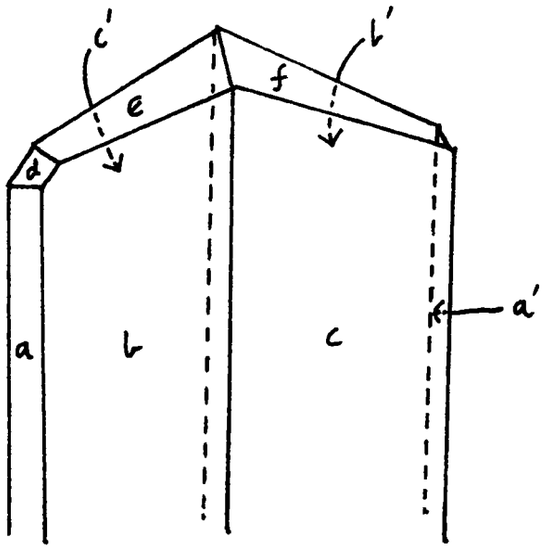
A.3. Optical Goniometry.

(The actual measurements involved in this part of the work were made by the author, but the results were interpreted by Dr. C.H. Prout. The work is described here largely for the benefit of future workers on these systems).

To show that crystals of the complexes of palladium 8-hydroxyquinolinate with chloranil and benzotrifuroxan, containing small percentages of the copper complexes, are isomorphous with the pure palladium complexes, and to identify particular faces of the crystals as known crystallographic planes, optical goniometry studies of two complexes were carried out.

(a) Palladium 8-hydroxyquinolinate/chloranil, containing 1 percent of the corresponding copper complex.

The following angles were recorded for directions perpendicular to the faces labelled as shown in figure A.1.



	θ	ϕ
a	219°4'	127°20'
b	280°58'	"
c	354°24'	"
a'	38°16'	"
b'	100°59'	"
c'	174°27'	"
d	194°9'	183°21'
e	251°11'	204°18'
f	151°16'	246°19'

Using these figures, the stereographic projection was constructed, and the faces were identified as the following:-

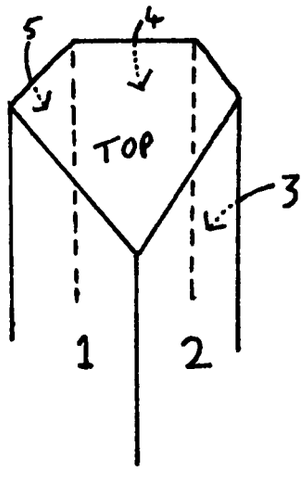
(a) 010 (b) $01\bar{1}$ (c) $0\bar{1}\bar{1}$ (e) 100

(a') $0\bar{1}0$ (b') $0\bar{1}1$ (c') 011

These results imply that the copper-doped complex has the same structure as the pure palladium complex.

(b) Palladium 8-hydroxyquinolinate/benzotrifuroxan, containing approximately 1 percent of the corresponding copper complex.

The following angles were recorded for directions perpendicular to the faces labelled as shown in figure A.2.



	θ	ϕ
1	251°7'	127°20'
2	7°6'	"
3	70°53'	"
4	129°55'	"
5	186°40'	"
Top	219°47'	232°3'

Figure A.2.

Using these figures, the stereographic projection was constructed and the faces were identified as the following:

(2) = $\bar{1}01$ (3) = 101 (4) = 001 (5) = $10\bar{1}$

Top = 010.

A.4. Calculations.

A.4.1. Palladium 8-hydroxyquinolinate/chloranil.

(i) Data corrections.

The intensity I_{hkl} of a reflection (hkl) is a function of the square of the amplitude of the beam reflected by the lattice planes (hkl), $|F_{hkl}|^2$. Corrections dependent on the magnitude of θ for the particular reflection must be applied to obtain $|F_{hkl}|^2$ from I_{hkl}. The corrections applied to the data in this case were as follows:

(1) A correction to account for partial polarisation of the x-ray beam on reflection by a crystal plane. This reduces the intensity by a fraction $(1 + \cos^2 2\theta)/2$, so that

$$I \alpha |F|^2.(1 + \cos^2 2\theta)/2 \qquad (A.3)$$

(2) A correction to account for the fact that reciprocal lattice points at different distances from the origin take different lengths of time to pass through the reflecting angle. This is known as the Lorentz effect, and the correction factor is $1/2\sin\theta$ for the zero layer, and $\frac{1}{2}\cos\theta$ for other layers, where the reflecting plane is not parallel to the axis of rotation of the crystal.

Corrections for absorption or extinction of x-rays by the crystal were not attempted. A small crystal was used, and these effects are therefore likely to be small (ref.54, p.209).

These data corrections were calculated on a Ferranti Mercury

computer, using Dr. C.K. Prout's DRO 4 programme.

(ii) Fourier synthesis.

The electron density at a point (x,y,z) in a cell of space group $P\bar{1}$ can be represented as a Fourier series of the form

$$\rho_{xyz} = 1/V \sum_h \sum_k \sum_l F_{hkl} \exp.-2\pi i\,(hx + ky + lz) \qquad (A.4)$$

The terms F_{hkl} are known as the structure factors of the plane (hkl), and are defined as

$$F_{hkl} = \sum_{n=1}^{N} f_n \exp.2\pi i(hx_n + ky_n + lz_n) \qquad (A.5)$$

where f_n is the scattering factor of the atom concerned at the angle θ of the reflection.

These structure factors, being complex quantities, can be represented as

$$F_{hkl} = A' + iB' \qquad (A.6)$$

where $A' = \sum_{n=1}^{N} f_n \cos 2\pi(hx_n + ky_n + lz_n)$

and $B' = \sum_{n=1}^{N} f_n \sin 2\pi(hx_n + ky_n + lz_n)$

This represents the contribution of each atom at (x_n, y_n, z_n) to the intensity of each reflection. In the space group $P\bar{1}$, which has a centre of symmetry at the origin, for each atom at the point (x_n, y_n, z_n) there is an equivalent atom at the point $(\bar{x}_n, \bar{y}_n, \bar{z}_n)$. The contribution of these two atoms to the structure factor is therefore

$$f_n \exp.2\pi i(hx_n + ky_n + lz_n) + f_n \exp.-2\pi i(hx_n + ky_n + lz_n)$$

$$= 2f_n \cos 2\pi(hx_n + ky_n + lz_n) \qquad (A.7)$$

Thus, all structure factors in $P\bar{1}$ are real, and

$$F_{hkl} = 2\sum_{n=1}^{N/2} f_n \cos 2\pi(hx_n + ky_n + lz_n) \qquad (A.8)$$

The Fourier series for the electron density at point (x, y, z) also includes a phase angle, and the initial problem in carrying out a synthesis of electron density contours by this method is to determine the phase angles of all reflections with respect to a reference point in the lattice. Fortunately, the crystal data deduced from preliminary photographs imply that:

(i) there is a heavy atom in the cell, with diffracting power much greater than all the other atoms in the cell,

(ii) there is only one such atom in the unit cell,

and (iii) this atom may be chosen as the origin.

In these conditions, all the phases with respect to the palladium atom as origin are zero (see, for example, ref.55, p.341).

Using this assumption, a three-dimensional electron density map was computed from the corrected intensity data, using Mills' general Fourier programme "OSH 4"[56] on the Mercury computer. This gave a series of electron density contour maps at intervals of 1/30 of the unit cell length, from which seventeen significant maxima were obtained, corresponding to the seventeen independent atoms, excluding hydrogen, of the two centric molecules.

(iii) Refinement of atomic positions.

To calculate the structure factors corresponding to any set of atomic co-ordinates, equation (A.8) is used. For this work, the

published scattering factor (f_n) curves of Berghuis et al.[57] were used for nitrogen, oxygen, carbon, and chlorine, while that of Thomas and Umeda[58] was used for palladium. A correction was applied to allow for the effects of anomalous dispersion by the palladium atom at low $\sin^2\theta$ values[59].

Thermal vibrations of the atoms in the lattice also affect the observed intensities of reflections, and must be taken into account in calculating the expected structure factors. These vibrations are of much lower frequency than x-rays, so that an atom may be displaced from its mean position at a particular instant, and lead to some interference in the diffracted x-ray beam, with loss of intensity. This effect becomes increasingly important as the amplitude of vibration approaches the spacing of the planes. Thus, there is a temperature factor, involving both the amplitude of vibrations and the spacing of the planes. For isotropic vibrations this has the form

$$I_{obs.}/I_{calc.} = \exp.-2B_{iso}\sin^2\theta/\lambda^2. \qquad (A.9)$$

($B_{iso.}$ is a constant, equal to $8\pi^2\bar{u}^2_{iso.}$, where $\bar{u}^2_{iso.}$ is the mean square amplitude of vibration of the atoms.)

For anisotropic vibrations, B is a tensor defining the vibrational ellipsoid of the atom, and, using equation (A.2) for $\sin^2\theta$, equation (A.9) may therefore be written as

$$I_{obs.}/I_{calc.} = \exp.-(b_{11}h^2 + b_{22}k^2 + b_{33}l^2 + b_{12}hk + b_{13}hl + b_{23}kl) \qquad (A.10)$$

where $b_{11} = a^{*2}/4.B_{11}$, $b_{12} = 2a^*b^*/4.B_{12}$ etc., and B_{ij} ($= B_{ji}$) represent the six independent components of each B in reciprocal space.

Using these temperature factor expressions and the atomic co-ordinates obtained from the first Fourier synthesis, structure factors were calculated. For both complexes, the initial R value at this stage (where $R = \sum(F_{obs.} - F_{calc.})/\sum F_{obs.}$) was 0·39. (Initial temperature factors in the calculation were deduced from a Wilson plot.)

To obtain more accurate atomic positions than those obtained from the electron density map produced in the first Fourier synthesis, it is necessary to calculate small shifts in the atomic co-ordinates, which give calculated structure factors $F_c(hkl)$ which minimise the function

$$\sum w\Delta^2 \quad \text{that is,} \quad \sum_u w_1(hkl)(\,|F_o(hkl)| - |F_c(hkl)|\,)^2 \qquad (A.11)$$

For each reflection, an equation of the type

$$\Delta F_c = \frac{\partial F_c}{\partial x_n}\Delta x_n + \frac{\partial F_c}{\partial y_n}\Delta y_n + \frac{\partial F_c}{\partial z_n}\Delta z_n = F_o - F_c \qquad (A.12)$$

may be set up, and from the total number of equations available it is possible to calculate Δx_n, Δy_n, and Δz_n values for all atoms to give the best agreement between ΔF_c and $(F_o - F_c)$. The number of such equations is very large (1880 reflections but only 17 atoms), and the calculations were performed on a Ferranti Mercury computer, using Rollett's "SFLS" programme[55] (which uses a block diagonal approximation to the normal matrix). Temperature factors were also included in these calculations.

In three cycles of refinement, using isotropic temperature factors and unit weight for all reflections, the R factor fell to 0·18. The scale factors were then checked and found to be correct, and three more cycles of refinement were carried out, using anisotropic temperature factors and the weighting scheme

$$\sqrt{w} = \sqrt{\frac{1}{1 + \left(\frac{|F_o| - b}{a}\right)^2}}$$

with $a = b = 120$ on the same scale as table A.1, and w as used in equation (A.11). The final R factor was 0·108.

A.4.2. Palladium 8-hydroxyquinolinate/1,2,4,5-tetracyanobenzene.

Data correction and Fourier synthesis of the initial electron density map were carried out for this material by the same methods used for the chloranil complex.

The refinement of the structure was carried out as the first complete test of the full-matrix least squares programme (SAMTAPE) by J.S. Rollett, on the English Electric KDF 9 computer. This programme takes into account the effect on all other positional and temperature factor parameters of the lattice produced by a small change in any one such parameter, whereas the block diagonal approximation used in the "SFLS" programme only considers changes produced in the other positional or temperature factor parameters for the particular atom for which a small position or temperature factor change, respectively, is made. The power of the full matrix

least squares method is shown clearly by the fact that, using only isotropic temperature factors and giving unit weight to all reflections the R value fell from 0·39 at the end of the preliminary Fourier synthesis structure to 0·108 in a single cycle of refinement taking 70 minutes. A second cycle of refinement by the same procedure reduced the R value to 0·102.

Tables A.1 to A.8 give final space parameters, temperature factor parameters, interatomic distances, and observed and calculated structure factors for these structures.

A.3. Description of the Pd 8-hydroxyquinolinate/chloranil structure.

The crystal is made up of planar bis-8-hydroxyquinolinato-Pd^{II} molecules and planar chloranil molecules in sheets approximately parallel to the crystallographic (111) plane. Each sheet contains equal numbers of the two molecules, and the sheets are arranged with respect to each other in such a way that donor and acceptor molecules in adjacent sheets form stacks of alternate donor and acceptor molecules, characteristic of π complexes. These stacks are staggered along the a axis. (c.f. figures 3.1 and 3.2, p.24-7).

Figure 3.3. shows the chloranil molecule projected onto, and parallel to, the least squares best plane of the metal complex. Two chlorine atoms at 3·44Å complete an octahedron about each Pd atom. This distance is shorter than the non-bonded Pd-Cl distance of 3·85Å found in $PdCl_2$[60], but much longer than can be expected from any

bonding interaction. The π system of the chloranil molecule lies far from the position of best overlap with the donor molecule π system, but near the area of maximum π electron density of the donor π system.[21] The best plane of the chloranil molecule makes an angle of 15·5° with the best plane of the palladium 8-hydroxyquinolinate molecule.

Since the peripheral atoms of chloranil carry partial negative charge, they will tend to be attracted to the palladium atom, which carries partial positive charge. The attraction between palladium and chlorine is stronger than that between palladium and oxygen, since van der Waals forces are greater for the former, (although electrostatic forces are probably greater for the latter). The octahedral position minimises repulsions between ligands and is therefore adopted.

Given these structural features, the molecular packing is ultimately determined by a compromise between maximum π overlap of donor and acceptor orbitals and minimisation of free space in the crystal. This results in a tilting of the chloranil molecule with respect to the 8-hydroxyquinolinate plane, due to repulsions between peripheral atoms of the chloranil molecules and those of neighbouring 8-hydroxyquinolinate molecules.

A.6. Description of the palladium 8-hydroxyquinolinate/tetracyanobenzene structure.

The crystal is made up of planar bis-8-hydroxyquinolinato Pd^{II} molecules and planar tetracyanobenzene molecules, in sheets approximately parallel to the crystallographic (021) plane.

Each sheet contains equal numbers of the two molecules, and the sheets are arranged with respect to each other in such a way that donor and acceptor molecules in adjacent sheets form stacks of alternate donor and accepter molecules, characteristic of π complexes. These stacks are staggered along the a axis. (c.f. figures 3.4 - 3.6, p.29-31)

Figure 3.7 shows the tetracyanobenzene molecule projected onto, and parallel to, the least-squares best plane of the metal complex. Two carbon atoms, of cyanide groups, lie above and below the palladium atom, displaced laterally from the octahedral position by about 0·75Å, and at a distance of 3·40Å from the palladium atom. This distance is much longer than can be expected from any bonding interaction, and probably represents a van der Waals contact distance. The π syetem of the acceptor lies much closer to the position of best overlap with the donor π system than in the chloranil complex, although it is still displaced from the ideal position towards the region of maximum π electron density of the donor molecule[21]. The best plane of the tetracyanobenzene molecule makes an angle of 4·5° with that of the palladium 8-hydroxyquinolinate molecule.

Since the cyanide groups of tetracyanobenzene carry partial negative charge, they will tend to be attracted to the palladium atom, which carries partial positive charge. The actual position adopted by the tetracyanobenzene molecule is a compromise between (i) maximum π overlap of donor and acceptor orbitals, (ii) close approach of a cyanide group of the acceptor to the palladium atom, (iii) minimisation of repulsions between palladium 8-hydroxyquinolinate molecules in adjacent sheets, and (iv) minimisation of free space in

the crystal lattice. The weaker van der Waals interaction between carbon or nitrogen and palladium than between chlorine and palladium, and the larger size of the tetracyanobenzene molecule, account for the closer approach to the position of maximum π overlap in the tetracyanobenzene complex than in the corresponding chloranil complex. Repulsions from palladium 8-hydroxyquinolinate molecules above and below the tetracyanobenzene molecule, and on opposite sides of it, result in the tilting of the tetracyanobenzene molecule with respect to the 8-hydroxyquinolinate planes. The angle of tilt is less than in the chloranil complex, since the acceptor lies in a position of better overlap with the donor than in the chloranil complex.

Note on the portions of this work carried out by the author.

The x-ray photography was carried out by Dr. B. Kamenar, and the interpretation of stereographic projections by Dr. C.K. Prout.

Indexing of the photographs, measurement of intensities, preparation of the data for computing, computing, and interpretation of the results was done by the author, under the constant supervision of Dr. C.K. Prout.

TABLE A.1.

Observed structure amplitudes and calculated structure factors for (*hkl*)

h	*k*	*l*	$5\|F_o\|$	$5F_c$
0	-7	1	143	21
		2	176	181
		3	157	152
		4	156	149
		5	48	-23
		6	67	63
		7	90	94
		8	112	126
		9	115	139
		10	95	109
0	-6	1	72	62
		2	30	47
		3	135	103
		4	258	255
		5	253	266
		6	176	197
		7	84	83
		8	85	85
		9	49	51
		10	100	111
		11	79	76
0	-5	1	220	204
		2	193	170
		3	195	164
		4	235	233
		5	210	190
		6	142	134
		7	69	71
		9	53	53
		10	99	99
		11	128	103
0	-4	1	46	-14
		2	169	163
		3	85	63
		4	45	55
		5	195	188
		6	203	211
		7	247	249
		8	180	170
		9	129	110
		10	71	74
		11	65	70
		12	101	117
0	-3	1	140	100
		2	280	334
		3	261	307
		4	164	158
		5	112	86
		7	164	157
		8	155	145
		9	264	279
		10	45	51
		11	100	112
0	-2	1	42	-3
		2	174	180
		3	131	106
		4	65	48
		5	36	32
		6	109	86
		7	180	149
		8	274	288
		9	293	300
		10	180	171
		11	101	104
		12	39	57
0	-1	2	67	36
		3	170	161
		4	249	292
		5	258	310
		6	155	128
		7	58	48
		8	63	51
		9	196	165
		10	179	175
		11	114	123
0	0	2	145	121
		3	111	-72
		4	220	188
		5	134	132
		6	79	61
		7	132	105
		8	132	100
		9	110	99
		10	138	166
		11	132	155
0	1	1	185	163
		2	171	178
		3	191	159
		4	257	276
		6	288	231
		7	201	233
		7	240	233
		8	40	33
		9	27	-3
		10	55	58
0	2	0	167	137
		1	244	300
		2	313	417
		3	279	311
		4	121	96
		5	114	95
		6	125	104
		7	156	133
		8	107	92
		9	124	132
		10	93	105
0	3	0	198	-192
		2	114	111
		3	190	168
		4	220	189
		5	250	248
		6	255	213
		7	199	192
		8	168	169
		9	136	144
		10	87	86
0	4	0	117	79
		1	176	172
		2	207	207
		3	223	218
		4	151	128
		5	278	304
		6	118	111
		7	77	86
		8	30	44
0	5	0	290	272
		1	150	134
		2	85	78
		3	124	-87
		4	119	110
		5	171	173
		6	141	159
		7	115	121
		8	89	102
0	6	0	143	129
		1	156	132
		2	157	134
		3	173	169
		4	139	120
		5	97	90
		6	99	88
0	7	0	155	145
		1	133	143
		2	147	166
		3	75	83
		5	44	-29
0	8	0	34	40
		1	44	57
		2	75	82
		3	136	183
0	9	0	122	143
1	-9	2	46	53
		3	56	63
		4	95	112
		5	105	135
1	-8	-2	32	43
		-1	34	39
		0	67	76
		1	87	85
		2	119	117
		3	169	175
		4	138	156
		5	103	105
		8	99	103
1	-7	-4	169	136
		-3	153	157
		-2	128	141
		-1	201	214
		0	164	153
		2	53	51
		3	31	35
		4	114	96
		5	30	37
		6	143	140
		7	148	147
		8	100	100
		9	97	112
		10	112	128
1	-6	-6	110	141
		-5	163	190
		-4	145	167
		-3	96	101
		-2	44	54
		-1	94	82
		0	144	120
		1	169	173

41152—2

TABLE A.I. (*Continued*)

h	k	l	$5\|F_o\|$	$5F_c$
		2	168	179
		3	171	148
		4	63	47
		5	32	26
		6	206	210
		7	75	81
		9	46	-32
		10	123	139
		11	147	169
1	-5	-7	46	65
		-6	68	75
		-5	49	60
		-4	106	101
		-3	141	127
		-2	165	133
		-1	219	197
		0	238	212
		1	294	261
		2	198	186
		3	50	52
		4	128	-78
		5	30	-5
		6	135	113
		7	206	210
		8	149	140
		9	97	101
		10	90	110
		11	93	105
1	-4	-8	49	59
		-7	155	164
		-6	110	117
		-5	177	154
		-4	31	17
		-3	189	167
		-2	190	185
		-1	60	54
		1	119	96
		2	242	228
		3	270	265
		4	250	233
		5	163	153
		6	137	124
		7	147	132
		8	167	159
		9	115	108
		11	40	54
		12	74	97
1	-3	-9	107	115
		-8	196	191
		-7	184	190
		-6	144	127
		-5	69	-43
		-4	166	-144
		-3	195	187
		-2	208	174
		-1	302	303
		0	141	118
		1	294	264
		2	238	225
		3	238	214
		4	278	314
		5	228	194
		6	67	-26
		7	66	69
		8	182	174
		9	284	258
		10	93	103
		11	61	83
		12	51	61
1	-2	-10	84	93
		-9	68	86
		-8	116	119
		-7	117	114
		-6	181	164
		-5	210	166
		-4	213	187
		-3	196	157
		-2	282	287
		-1	265	254
		0	177	156
		1	37	-15
		2	118	-79
		3	144	147
		4	360	472
		5	260	295
		6	239	233
		7	103	99
		8	202	195
		9	118	100
		10	30	15
		11	119	119
		12	63	79
1	-1	-10	153	172
		-9	163	164
		-8	142	124
		-7	166	137
		-6	268	239
		-5	292	285
		-4	164	151
		-3	41	30
		-2	47	41
		-1	254	264
		0	237	270
		1	213	236
		2	229	336
		3	167	158
		4	132	128
		5	127	104
		6	230	203
		7	165	121
		8	123	105
		9	32	5
		10	170	168
		11	166	179
		12	167	199
1	0	-11	131	150
		-10	206	221
		-10	200	221
		-9	89	101
		-9	102	101
		-8	70	71
		-8	77	71
		-7	53	56
		-7	53	56
		-6	93	76
		-5	294	264
		-4	353	404
		-3	262	264
		-2	236	283
		2	136	161
		3	72	-64
		4	46	-12
		5	146	124
		6	326	309
		7	266	225
		8	181	146
		9	147	140
		10	112	120
		11	114	117
		12	73	120
1	1	-10	146	109
		-10	113	109
		-9	122	125
		-9	126	125
		-8	118	162
		-8	175	162
		-7	207	183
		-6	141	109
		-5	272	257
		-4	181	152
		-3	250	269
		-2	165	-150
		2	251	450
		3	250	323
		4	320	359
		5	18	76
		6	100	80
		7	84	68
		8	147	121
		9	187	165
		10	165	161
		11	96	108
		11	116	108
1	2	-11	121	136
		-10	152	104
		-10	92	104
		-9	103	86
		-9	82	86
		-8	163	138
		-7	205	183
		-6	60	57
		-5	34	-2
		-4	46	39
		-3	244	244
		-2	251	290
		-1	340	521
		1	232	190
		2	59	43
		3	295	309
		4	230	231
		5	109	92
		6	111	91
		7	158	120
		8	191	164
		9	292	270
		10	128	143

TABLE A.I. (*Continued*)

h	k	l	5|F_o|	5F_c
		11	95	115
1	3	-11	93	100
		-10	39	-1
		-9	93	88
		-8	113	102
		-7	237	221
		-6	240	219
		-5	256	249
		-4	165	141
		-3	149	123
		-2	58	48
		-1	200	183
		0	270	249
		1	135	89
		2	160	140
		3	251	264
		4	303	350
		5	274	250
		6	150	121
		7	83	71
		8	100	97
		9	98	100
		10	93	107
1	4	-11	37	57
		-10	190	195
		-9	198	200
		-7	122	108
		-6	186	171
		-5	284	271
		-5	75	271
		-4	88	84
		-2	151	127
		-1	277	251
		0	357	330
		1	324	317
		2	190	141
		3	70	60
		5	92	83
		6	154	135
		7	177	173
		8	123	126
		9	131	122
1	5	-11	58	66
		-10	179	190
		-9	129	121
		-8	70	70
		-6	244	197
		-5	286	273
		-4	268	237
		-3	260	244
		-2	175	146
		-1	88	-50
		0	138	115
		1	121	104
		2	213	191
		3	99	-79
		4	88	78
		5	199	205
		6	225	236
		7	168	175
		8	96	93
1	6	-11	49	53
		-10	125	115
		-9	166	181
		-8	170	179
		-7	125	122
		-6	70	59
		-5	69	61
		-4	128	115
		-3	172	152
		-2	124	97
		-1	117	89
		0	174	139
		1	258	246
		2	184	158
		3	32	30
		4	131	133
		5	58	67
		6	91	103
		7	20	42
1	7	-10	31	38
		-9	53	66
		-8	119	122
		-7	84	85
		-4	137	129
		-3	235	212
		-2	249	243
		-1	191	174
		0	118	111
		3	97	103
		4	106	126
		5	148	151
		6	104	110
1	8	-9	66	73
		-8	104	107
		-7	178	200
		-6	48	56
		-5	77	71
		-4	67	73
		-3	67	67
		-2	90	84
		-1	126	125
		0	142	129
		1	127	127
		2	140	159
		3	179	189
		4	148	156
1	9	-7	35	50
		-5	123	116
		-4	102	100
		-3	112	117
		-2	80	89
		-1	147	153
		0	150	156
		1	83	72
		2	76	93
2	-10	-3	5	98
		-2	4	85
		-1	3	98
2	-8	0	140	159
		1	131	134
		2	69	60
		4	60	60
		5	79	72
		6	90	92
		7	45	57
2	-7	-3	120	136
		-2	76	67
		-1	47	49
		0	44	51
		1	47	48
		2	79	72
		3	63	50
		4	80	72
		5	162	152
		6	164	177
		7	131	138
		8	58	68
2	-6	-4	117	122
		-3	55	62
		-2	78	84
		-1	94	93
		0	86	70
		1	194	188
		2	221	214
		3	156	129
		5	54	-18
		6	152	138
		7	125	121
		8	145	140
		9	69	83
		10	86	90
2	-5	-5	101	87
		-4	164	166
		-3	215	226
		-2	165	169
		-1	133	117
		0	54	39
		1	91	86
		2	96	95
		3	205	189
		4	74	55
		5	190	181
		6	150	138
		7	165	153
		8	161	140
		9	116	115
		10	92	95
2	-4	-7	135	129
		-6	130	118
		-5	113	106
		-4	98	89
		-2	114	101
		-1	198	185
		0	190	167
		1	168	147
		2	204	189
		3	278	297
		4	264	264
		5	149	146
		9	135	141
		10	145	146
		11	117	129
		12	76	89
2	-3	-8	65	62
		-7	107	106

41152—3

TABLE A.I. (*Continued*)

h	k	l	$5\|F_o\|$	$5F_c$
		-6	171	174
		-5	140	129
		-3	186	182
		-2	228	211
		-1	263	286
		0	188	161
		1	133	115
		2	82	60
		3	128	129
		4	140	127
		5	189	186
		6	191	190
		7	126	126
		8	88	78
		9	98	86
		10	169	166
		11	123	129
		12	38	55
2	-2	-9	70	64
		-8	134	144
		-7	170	179
		-6	291	311
		-5	119	99
		-4	203	194
		-3	111	110
		-2	34	25
		-1	122	-94
		0	40	-1
		1	274	324
		2	221	235
		3	141	153
		4	221	228
		5	169	186
		6	209	220
		7	143	128
		8	123	96
		9	62	56
		10	84	79
		11	135	139
		11	140	139
		12	138	135
		12	129	135
2	-1	-10	129	140
		-9	157	161
		-8	160	157
		-7	18	129
		-6	111	98
		-5	86	82
		-4	189	169
		-3	210	211
		-2	172	147
		-1	84	-52
		0	204	182
		1	243	308
		2	168	195
		3	97	92
		4	58	17
		5	38	-0
		6	183	175
		7	263	259
		8	361	413
		9	99	95
		10	107	113
		11	76	69
		11	67	69
		12	147	163
		12	140	163
2	0	-10	45	60
		-9	60	65
		-8	146	150
		-7	159	154
		-6	157	160
		-5	150	155
		-4	58	265
		-3	250	288
		-2	165	179
		-1	74	64
		3	203	271
		4	181	230
		5	186	176
		6	146	131
		7	268	270
		8	255	235
		9	150	130
		10	83	77
		10	66	77
		11	65	69
		11	55	69
		12	125	142
		12	121	142
2	1	-10	40	44
		-9	81	85
		-8	197	195
		-7	169	165
		-6	95	88
		-5	178	168
		-4	22	22
		-3	125	123
		-2	228	291
		3	185	190
		4	162	180
		5	68	54
		6	45	41
		7	77	65
		8	210	186
		9	215	208
		10	176	179
		11	160	148
		12	28	94
2	2	-11	129	145
		-10	75	82
		-9	51	47
		-8	31	42
		-7	91	62
		-6	247	227
		-5	252	269
		-4	107	104
		-3	161	157
		-2	244	315
		2	130	-93
		3	173	181
		4	173	151
		5	199	192
		6	243	206
		7	145	108
		8	31	37
		9	127	110
		10	137	129
		11	121	122
2	3	-11	159	170
		-10	186	186
		-9	126	113
		-8	113	100
		-7	139	123
		-6	207	188
		-5	152	130
		-4	84	79
		-2	193	202
		-1	191	214
		1	332	347
		2	278	284
		3	222	218
		5	143	141
		6	156	150
		7	31	-13
		8	31	34
		9	118	108
		10	154	161
2	4	-11	131	133
		-11	126	133
		-10	243	216
		-9	184	177
		-8	94	92
		-6	41	-1
		-5	93	81
		-4	228	227
		-3	283	274
		-2	107	91
		-1	99	76
		0	177	144
		1	231	215
		2	164	183
		3	103	89
		4	160	151
		5	170	159
		6	192	170
		7	164	150
		8	174	178
		9	116	105
		10	81	90
2	5	-10	216	194
		-9	131	130
		-8	187	186
		-7	108	111
		-6	142	119
		-5	118	98
		-4	160	145
		-3	153	129
		-2	35	22
		-1	111	-78
		0	118	102
		1	196	171
		2	251	255
		3	267	286
		4	264	278
		5	156	145

TABLE A.1. (Continued)

h	k	l	5|F_o|	5F_c
		6	102	98
		7	99	94
		8	127	112
		9	76	81
2	6	-10	100	99
		-9	99	109
		-8	136	133
		-7	142	130
		-6	171	135
		-5	61	58
		-4	89	75
		-3	189	176
		-2	147	112
		-1	229	202
		0	196	163
		1	138	126
		2	91	78
		3	69	56
		4	214	221
		5	105	104
		6	129	125
		7	113	102
		8	158	167
2	7	-10	47	51
		-9	100	51
		-8	72	73
		-7	170	168
		-6	237	236
		-5	252	233
		-4	143	123
		-3	76	68
		-2	76	74
		-1	155	129
		0	88	84
		1	108	96
		3	164	166
		4	174	180
		5	169	160
		6	108	102
		7	39	63
2	8	-9	102	112
		-8	67	74
		-7	112	112
		-6	140	130
		-5	153	145
		-4	91	78
		-3	81	78
		-2	119	97
		-1	173	156
		0	165	163
		1	137	139
		2	115	115
		5	55	47
2	9	-8	85	94
		-7	54	55
		-5	148	160
		-4	155	172
		-3	159	158
		-2	59	73
		-1	44	55
		0	42	51
		1	90	95
		2	74	76
		4	4	49
2	10	0	66	112
3	-7	-1	27	-5
		0	53	53
		1	134	118
		2	145	144
		3	190	188
		4	140	152
		5	92	83
		6	62	66
		7	104	92
		8	95	105
3	-6	-3	99	97
		-2	126	124
		-1	130	134
		0	80	85
		1	59	62
		2	97	96
		3	102	99
		4	86	88
		5	60	61
		6	64	70
		7	143	149
		8	166	180
		9	174	164
		10	79	87
3	-5	-5	178	208
		-4	126	121
		-3	93	84
		-2	130	135
		-1	79	81
		1	90	92
		2	90	83
		3	151	130
		4	90	73
		5	208	194
		6	139	138
		7	48	52
		9	107	107
		10	158	150
		11	93	107
3	-4	-6	110	113
		-5	96	107
		-4	94	97
		-3	93	91
		-2	149	136
		-1	184	170
		0	239	245
		1	200	196
		2	89	83
		3	136	-102
		4	98	-58
		5	191	191
		6	126	114
		7	99	99
		9	171	185
		10	185	181
		11	157	163
3	-3	-7	82	74
		-6	86	85
		-5	150	147
		-4	173	181
		-3	150	136
		-2	132	119
		-1	104	97
		0	190	160
		1	155	141
		2	105	85
		4	124	105
		5	179	163
		6	222	230
		7	163	140
		8	95	99
		9	49	59
		10	51	56
		11	125	128
		12	179	187
3	-2	-8	162	163
		-7	82	83
		-6	67	64
		-5	95	-62
		-4	119	110
		-3	148	150
		-2	141	134
		-1	147	123
		0	212	202
		1	264	273
		2	269	314
		3	235	260
		4	117	95
		6	43	42
		7	154	156
		8	163	158
		9	90	96
		10	96	94
		11	102	110
		12	157	155
3	-1	-9	114	121
		-8	102	113
		-7	104	114
		-5	28	-19
		-4	231	227
		-3	224	226
		-2	288	309
		-1	107	105
		0	144	129
		1	57	55
		2	154	155
		3	267	365
		4	238	274
		5	73	75
		6	136	133
		7	190	177
		8	209	203
		9	64	62
		10	66	65
		12	79	83
3	0	-9	126	130
		-8	133	135
		-7	207	196
		-6	180	168
		-5	142	125
		-4	42	36

41152—4

TABLE A.I. (*Continued*)

h	k	l	5|F_o|	5F_c
		-3	120	126
		-2	141	133
		-1	161	156
		3	275	442
		4	193	210
		5	190	198
		6	40	38
		7	134	130
		9	40	52
		10	205	179
		11	142	134
		12	109	122
3	1	-10	138	137
		-9	80	86
		-8	67	74
		-7	164	150
		-6	207	194
		-5	176	156
		-4	156	132
		-3	145	144
		-2	180	195
		-1	123	159
		3	62	-26
		4	104	86
		5	276	273
		6	258	238
		7	212	186
		8	63	52
		9	197	172
		10	150	141
		11	171	165
3	2	-10	57	78
		-9	105	109
		-8	125	117
		-7	131	110
		-6	246	229
		-5	275	286
		-4	186	186
		-3	97	91
		-2	116	-85
		2	50	121
		3	151	158
		4	180	178
		5	260	252
		6	180	147
		7	147	118
		8	164	137
		9	104	105
		10	118	115
		11	125	135
3	3	-10	90	109
		-9	152	146
		-8	143	131
		-7	57	50
		-6	130	128
		-5	78	74
		-4	188	195
		-3	64	58
		-2	250	299
		-1	187	199
		0	102	99
		1	216	235
		2	206	203
		3	218	224
		4	30	15
		6	99	87
		7	222	198
		8	266	242
		9	191	190
		10	104	105
		11	78	103
3	4	-9	88	84
		-8	163	152
		-7	140	136
		-6	131	120
		-5	122	115
		-4	187	163
		-3	203	200
		-2	275	310
		-1	87	87
		0	65	61
		2	281	287
		3	262	264
		4	178	165
		5	135	135
		6	126	102
		7	128	107
		8	185	183
		9	77	91
		10	93	98
3	5	-10	114	109
		-9	88	88
		-8	167	158
		-7	183	161
		-6	180	159
		-5	60	56
		-4	43	44
		-3	78	73
		-2	219	217
		-1	266	283
		0	208	193
		1	203	178
		2	183	169
		3	188	165
		4	124	113
		5	63	67
		6	64	53
		7	115	95
		8	116	107
		9	157	146
3	6	-10	132	126
		-8	46	50
		-7	129	127
		-6	227	203
		-5	146	144
		-4	133	117
		-3	144	137
		-2	149	125
		-1	179	162
		0	162	166
		1	83	79
		3	49	41
		4	140	135
		5	181	200
		6	197	197
		7	116	116
		8	86	87
3	7	-9	111	111
		-8	53	67
		-7	141	128
		-6	137	131
		-5	128	120
		-4	151	139
		-3	63	55
		-2	69	-34
		-1	137	122
		0	169	165
		1	215	220
		3	120	118
		4	134	144
		5	130	142
		6	101	91
		7	73	79
3	8	-9	110	116
		-8	69	66
		-5	105	110
		-4	171	163
		-3	149	137
		-2	139	130
		-1	120	11
		0	138	136
		1	39	40
		3	4	129
		4	89	94
		5	116	123
3	9	-7	72	79
		-6	59	73
		-5	85	89
		-4	102	103
		-3	121	121
		-2	106	103
		-1	82	81
		0	42	38
		1	82	85
		2	142	157
		3	147	156
3	10	-5	61	65
		-4	79	75
		-3	103	102
		-2	132	146
		-1	133	129
		0	100	107
4	-7	1	6	72
		2	83	81
		3	78	105
4	-6	-1	93	96
		-1	93	96
		0	77	77
		0	77	77
		3	84	82
		4	138	129
		5	149	160
		6	93	97
		7	40	54
		9	93	97
4	-5	-1	73	76

TABLE A.1 (*Continued*)

h	k	l	5|F_o|	5F_c
		0	131	118
		1	158	146
		2	120	102
		3	91	75
		4	126	105
		5	125	113
		6	102	108
		7	77	79
		9	52	60
		10	108	111
4	-4	-5	133	136
		-4	128	112
		-3	132	134
		-2	114	109
		-1	53	36
		0	129	114
		1	126	133
		2	123	106
		5	189	174
		6	181	178
		7	201	196
		8	117	109
		9	70	71
		10	45	53
		11	107	107
4	-3	-6	129	109
		-5	133	129
		-4	134	140
		-3	96	102
		-2	81	74
		-1	38	38
		0	119	108
		1	163	154
		2	245	254
		3	154	117
		4	203	202
		5	73	75
		6	70	73
		7	89	63
		8	123	108
		9	135	121
		10	51	65
		11	88	93
		12	52	115
4	-2	-7	110	94
		-6	101	93
		-5	84	84
		-4	71	80
		-3	163	157
		-2	229	232
		-1	211	194
		0	145	125
		1	114	103
		2	150	135
		3	151	139
		4	118	114
		5	78	66
		6	56	59
		7	64	47
		8	181	173
		9	200	179
		10	137	139
		11	67	68
4	-1	-8	124	125
		-7	195	200
		-6	143	143
		-5	76	79
		-4	151	147
		-3	116	105
		-2	132	118
		-1	87	76
		0	136	123
		1	117	107
		2	141	145
		3	148	147
		4	212	224
		5	212	213
		6	100	99
		9	161	135
		10	137	130
		11	99	98
		12	60	74
4	0	-8	140	135
		-7	164	171
		-5	152	145
		-4	101	98
		-3	65	59
		-2	41	-4
		-1	148	140
		0	238	334
		0	239	334
		1	197	214
		2	82	91
		3	102	106
		4	30	57
		5	149	146
		6	150	151
		7	203	189
		8	130	118
		9	114	101
		10	135	124
		11	16	140
		12	117	131
4	1	-9	119	112
		-8	107	102
		-7	74	80
		-6	101	101
		-5	205	182
		-4	214	204
		-3	126	134
		-2	57	-9
		-1	81	76
		0	105	122
		3	117	142
		4	92	94
		5	184	184
		6	274	277
		7	330	359
		8	38	41
		9	38	54
		11	159	148
		12	83	97
4	2	-9	151	143
		-8	135	145
		-7	122	125
		-6	97	84
		-5	131	100
		-4	149	137
		-3	152	157
		-2	49	163
		-1	69	86
		0	101	151
		3	141	175
		4	94	91
		5	41	49
		6	211	194
		7	209	160
		8	175	140
		9	149	122
		10	125	120
		11	145	127
4	3	-10	51	60
		-9	118	105
		-8	100	102
		-7	120	101
		-6	168	160
		-5	71	69
		-4	154	156
		-3	234	254
		-2	289	396
		-1	171	204
		0	33	16
		1	65	-18
		2	88	83
		3	138	133
		4	151	146
		5	169	154
		6	136	111
		7	174	147
		8	178	155
		9	152	148
		10	128	116
		11	43	60
4	4	-10	67	70
		-9	60	67
		-8	83	86
		-7	208	201
		-6	194	184
		-5	76	78
		-4	57	58
		-3	134	137
		-2	303	351
		-1	49	72
		0	140	141
		1	93	81
		2	179	175
		3	133	120
		4	157	166
		5	139	137
		6	37	40
		7	27	4
		8	115	103
		9	136	143
		10	164	145
4	5	-10	94	97
		-9	71	71

41152—5

TABLE A.1. (*Continued*)

h	k	l	$5\|F_o\|$	$5F_c$
		-8	42	56
		-7	88	80
		-6	85	80
		-5	125	120
		-4	115	101
		-3	204	182
		-2	152	139
		-1	176	178
		0	198	207
		1	176	154
		2	115	90
		3	53	11
		4	118	116
		5	150	145
		6	81	60
		7	140	131
		8	147	137
		9	137	135
4	6	-9	97	99
		-8	47	55
		-7	26	48
		-6	89	94
		-5	190	170
		-4	190	155
		-3	25	44
		-1	76	74
		0	151	139
		1	210	190
		2	199	181
		3	214	201
		4	147	143
		5	120	102
		6	103	102
		7	125	127
		8	71	70
4	7	-9	132	127
		-8	81	84
		-7	87	81
		-6	37	45
		-5	71	71
		-4	104	98
		-3	110	97
		-2	103	79
		-1	158	146
		0	147	139
		1	179	169
		2	198	175
		3	170	159
		4	69	66
		5	60	72
		6	101	97
		7	130	128
4	8	-8	125	117
		-7	174	147
		-6	105	100
		-5	91	90
		-4	123	123
		-3	84	69
		-2	139	124
		-1	85	85
		0	65	76
		1	46	45
		2	81	81
		3	179	198
		4	120	137
		5	140	133
		6	86	86
4	9	-7	65	148
		-6	146	134
		-5	60	69
		-3	41	51
		-2	125	112
		-1	124	124
		0	128	129
		2	114	114
		3	95	91
		4	93	94
4	10	-5	99	101
		-4	100	101
		-3	88	83
		-2	82	93
		-1	75	84
		0	62	63
		1	53	57
5	-6	1	91	100
		2	104	110
		3	133	149
		4	100	87
		5	101	96
		6	108	107
		7	47	59
5	-5	-1	102	91
		0	129	115
		1	130	113
		2	150	140
		3	93	95
		4	34	45
		5	34	48
		6	128	103
		7	136	134
		8	137	128
		9	63	71
5	-4	-4	6	85
		-3	80	96
		1	80	77
		2	125	112
		3	147	132
		4	145	121
		5	102	93
		6	130	111
		7	120	113
		8	112	117
		9	73	74
5	-3	-5	58	65
		-4	54	57
		-3	118	113
		-2	105	97
		-1	106	92
		0	162	142
		1	92	79
		2	78	55
		3	27	12
		4	167	150
		5	114	106
		6	28	50
		7	28	46
		8	135	134
		9	168	176
		10	144	139
		11	71	81
5	-2	-6	114	114
		-5	139	132
		-4	121	114
		-3	124	108
		-2	107	96
		-1	162	161
		0	119	114
		2	136	-96
		4	216	224
		5	166	172
		6	153	145
		7	62	59
		8	132	137
		9	120	108
		10	133	131
		11	157	128
5	-1	-7	60	63
		-6	112	95
		-5	119	118
		-4	91	84
		-3	83	80
		-2	89	89
		-1	160	155
		0	175	169
		1	164	157
		2	114	95
		3	113	106
		4	82	75
		5	136	129
		6	112	99
		7	105	111
		8	73	72
		9	81	76
		10	151	145
		11	206	193
		12	80	115
5	0	-6	61	-24
		-5	144	131
		-4	175	178
		-3	174	193
		-2	139	137
		-1	129	130
		0	130	133
		0	130	133
		1	168	192
		2	162	189
		3	87	87
		4	34	37
		5	74	77
		6	155	172
		7	172	165
		8	117	105
		9	102	82
		10	61	70
		11	118	94
		12	83	108

TABLE A.1. (*Continued*)

h	k	l	$5\|F_o\|$	$5F_c$
5	1	−8	133	133
		−7	47	46
		−6	27	35
		−5	154	145
		−4	137	135
		−3	166	172
		−2	49	74
		−1	98	104
		0	77	90
		0	78	90
		1	144	186
		2	188	322
		3	165	238
		4	87	94
		5	74	76
		6	68	70
		7	99	91
		8	39	50
		9	115	97
		10	78	69
		11	109	98
5	2	−8	136	129
		−7	107	103
		−6	91	89
		−5	48	47
		−4	122	112
		−3	116	121
		−2	145	161
		−1	126	156
		0	83	125
		3	64	89
		4	146	164
		5	92	80
		6	172	156
		7	46	44
		8	100	98
		9	202	165
		10	137	124
		11	95	92
5	3	−9	74	73
		−8	130	123
		−7	157	154
		−6	161	150
		−5	144	127
		−4	80	87
		−3	51	49
		−1	83	100
		0	110	155
		1	57	76
		2	63	67
		3	136	149
		4	185	243
		5	204	213
		6	169	150
		8	126	109
		9	106	89
		10	144	143
		11	76	85
5	4	−9	108	107
		−8	72	72
		−7	132	127
		−6	152	141
		−5	119	107
		−4	63	65
		−2	96	101
		−1	118	127
		0	154	196
		1	130	133
		2	117	129
		3	82	89
		4	113	117
		5	98	96
		6	161	142
		7	186	174
		8	141	127
		9	140	120
		10	119	118
5	5	−9	96	91
		−8	75	69
		−7	116	121
		−6	91	83
		−5	158	148
		−4	106	102
		−3	213	227
		−2	106	98
		0	108	81
		1	152	143
		2	189	178
		3	80	82
		4	86	85
		5	125	119
		6	175	171
		7	190	182
		8	123	127
		9	61	69
5	6	−9	116	125
		−8	151	133
		−7	109	106
		−6	66	68
		−5	62	67
		−4	122	119
		−3	202	196
		−2	112	103
		−1	97	99
		0	90	83
		1	210	205
		2	170	160
		3	11	103
		4	78	83
		5	39	43
		6	59	59
		7	138	135
		8	109	105
		9	78	117
5	7	−8	116	100
		−7	140	114
		−6	77	77
		−5	77	81
		−4	118	101
		−3	175	158
		−2	180	180
		−1	128	123
		0	91	88
		1	48	55
		2	68	65
		3	92	92
		4	108	103
		5	96	95
		6	116	113
		7	102	98
5	8	−7	145	127
		−6	100	108
		−5	87	87
		−4	59	69
		−3	47	42
		−2	110	98
		−1	140	131
		0	116	107
		1	67	64
		2	75	83
		3	105	118
		4	118	137
		5	117	116
		6	61	68
5	9	−6	78	76
		−5	127	114
		−4	75	72
		−3	41	40
		−2	117	118
		−1	120	124
		0	121	126
		2	88	90
		3	83	91
		4	90	100
5	10	−4	86	84
		−3	85	84
		−2	65	63
		−1	72	77
		1	70	72
6	−5	1	34	31
		2	75	73
		3	100	88
		4	61	51
		5	67	59
		6	48	42
		7	39	56
6	−4	−1	93	87
		0	84	65
		1	76	52
		2	117	98
		3	127	116
		4	128	124
		5	68	66
		8	89	79
		9	84	91
6	−3	−3	64	57
		−2	91	82
		−1	113	104
		0	121	113
		1	87	79
		2	51	52
		3	86	71
		4	106	95
		5	143	129
		6	140	128
		7	78	86

41152—6

TABLE A.1. (*Continued*)

h	k	l	$5\|F_o\|$	$5F_c$
		8	49	56
		9	93	76
		10	125	108
6	-2	-4	106	96
		-3	62	63
		-1	79	80
		0	121	125
		1	156	149
		2	113	89
		3	108	91
		4	151	143
		5	136	128
		6	144	131
		7	86	73
		8	44	54
		10	99	90
		11	86	98
6	-1	-5	100	95
		-4	100	98
		-3	112	94
		-2	93	84
		-1	123	118
		0	126	123
		1	176	155
		2	70	63
		3	138	143
		5	44	56
		6	79	57
		7	155	138
		8	163	152
		9	99	94
		10	75	72
		11	67	68
6	0	-6	106	99
		-5	95	86
		-4	119	109
		-3	146	136
		-2	112	112
		-1	72	70
		0	49	55
		1	75	69
		2	112	19
		3	141	149
		4	129	127
		5	82	76
		6	31	37
		7	26	117
		8	149	131
		9	122	113
		10	73	72
		11	66	45
6	1	-7	94	83
		-6	64	67
		-5	102	90
		-4	62	59
		-3	86	73
		-2	107	99
		-1	127	154
		0	111	126
		1	88	103
		2	63	80
		3	96	122
		4	113	128
		5	75	77
		6	43	59
		7	61	67
		8	153	135
		9	145	135
		10	126	121
		11	96	89
6	2	-7	35	20
		-7	35	20
		-6	139	139
		-5	120	115
		-4	93	86
		-2	105	105
		-1	143	172
		0	83	114
		3	33	60
		4	111	140
		5	176	178
		6	197	206
		7	113	98
		8	52	57
		9	73	66
		10	134	110
		11	102	113
6	3	-8	60	70
		-7	76	74
		-6	121	106
		-5	136	120
		-4	95	98
		-2	76	77
		-1	85	102
		0	87	141
		2	97	137
		3	55	68
		4	79	90
		5	163	174
		6	217	213
		7	23	28
		8	65	66
		9	70	58
		10	160	139
		11	26	89
6	4	-8	89	85
		-7	59	62
		-6	63	64
		-5	117	117
		-4	160	158
		-3	150	164
		-2	82	96
		-1	72	90
		0	70	99
		1	116	131
		2	97	96
		3	88	85
		4	76	82
		5	147	163
		6	138	114
		7	142	126
		8	127	114
		9	112	102
		10	69	74
6	5	-8	122	103
		-7	135	129
		-6	54	63
		-5	99	94
		-4	137	126
		-3	178	190
		-2	97	101
		0	26	38
		1	91	92
		2	125	128
		3	160	156
		3	146	156
		4	137	133
		4	133	133
		5	56	61
		5	56	61
		6	66	66
		6	66	66
		7	100	93
		7	95	93
		8	119	115
		8	117	115
		9	121	107
6	6	-8	128	116
		-6	57	65
		-5	46	51
		-4	99	102
		-3	198	187
		-2	77	88
		-1	132	130
		0	74	77
		1	91	91
		2	44	58
		3	94	103
		4	99	96
		5	57	60
		6	55	62
		7	124	123
		8	142	128
6	7	-7	80	74
		-6	118	109
		-5	93	89
		-4	119	111
		-3	114	58
		-2	81	82
		-1	116	104
		0	133	112
		1	104	100
		2	62	71
		3	116	116
		4	114	116
		5	68	69
		6	117	119
		7	90	92
6	8	-6	103	89
		-5	99	88
		-4	48	58
		-3	55	58
		-2	82	84
		-1	122	111
		0	154	148
		1	139	138

h	k	l	$5\|F_o\|$	$5F_c$	h	k	l	$5\|F_o\|$	$5F_c$	h	k	l	$5\|F_o\|$	$5F_c$
		2	118	126			−3	86	79			3	77	74
		3	52	63			−2	85	91			4	82	88
		5	62	76			−1	57	72	6	10	−2	97	81
		6	98	106			0	81	87			−1	86	88
6	9	−5	91	84			1	112	103			0	88	53
		−4	90	87			2	128	113			1	49	75
												2	6	124

TABLE A.2

Atomic co-ordinates ($\times 10^4$) and standard deviations ($\times 10^4$)

	x/a	$\sigma(x/a)$	y/b	$\sigma(y/b)$	z/c	$\sigma(z/c)$
Pd	0	0	0	0	0	0
C(1)	7662	25	3669	19	2407	14
C(2)	7186	31	4792	21	3859	18
C(3)	8340	30	4219	22	4687	15
C(4)	9948	27	2364	20	4178	14
C(5)	1091	29	1634	23	4945	15
C(6)	2568	33	9817	27	4408	17
C(7)	2920	28	8722	21	2939	16
C(8)	1767	23	9408	17	2101	13
C(9)	284	23	1318	16	2735	14
N(1)	9112	26	1931	19	1895	15
O(1)	2052	26	8532	21	743	16
C(10)	3811	26	1964	19	462	14
C(11)	6209	20	8994	15	767	12
C(12)	4896	19	1132	14	1366	10
O(2)	4869	25	2007	19	2522	13
Cl(1)	2527	10	4357	6	1062	5
Cl(2)	7501	8	8058	7	1820	5

TABLE A.3.

Thermal parameters ($\times 10^4$). The temperature factor, T, is equal to $2^{-(b_{11}h^2 + b_{22}k^2 + b_{33}l^2 + b_{12}hk + b_{13}hl + b_{23}kl)}$

	b_{11}	b_{22}	b_{33}	b_{23}	b_{13}	b_{12}
Pd	95	23	14	−20	4	−28
C(1)	180	73	16	−56	54	27
C(2)	340	35	78	−57	−8	−31
C(3)	332	114	17	−24	−59	−73
C(4)	270	93	6	−20	−4	−120
C(5)	291	157	20	39	−33	−173
C(6)	339	205	43	1	−36	−187
C(7)	269	74	37	24	32	−115
C(8)	142	21	25	−21	66	81
C(9)	181	8	29	−59	11	31
N(1)	165	25	40	−20	−62	−3
O(1)	274	45	19	−44	−33	40
C(10)	192	48	45	−34	21	64
C(11)	179	106	44	71	33	−6
C(12)	252	50	17	−89	68	−10
O(2)	454	184	46	−17	−139	−229
Cl(1)	503	51	105	−3	−108	−31
Cl(2)	295	203	89	19	−140	−139

TABLE A.4.

Palladium 8-hydroxyquinolinate/chloranil complex.

Interatomic distances (in Å), with standard deviations.

(a) Bis-8-hydroxyquinolinato palladium^{II}.

Pd - N(1)	1·97 (0·02)	C(4) - C(9)	1·42(0·02)
Pd - O(1)	1·98 (0·02)	C(5) - C(6)	1·39 (0·05)
C(1) - C(2)	1·42 (0·03)	C(6) - C(7)	1·45 (0·03)
C(1) - N(1)	1·31 (0·04)	C(7) - C(8)	1·38 (0·03)
C(2) - C(3)	1·35 (0·03)	C(8) - C(9)	1·45 (0·03)
C(3) - C(4)	1·46 (0·04)	C(8) - O(1)	1·31 (0·02)
C(4) - C(5)	1·33 (0·03)	C(9) - N(1)	1·44 (0·03)

(b) Chloranil.

C(10) - C(11)	1·32 (0·02)	C(11) - C(12)	1·55 (0·03)
C(10) - C(12)	1·43 (0·02)	C(11) - Cl(2)	1·67 (0·02)
C(10) - Cl(1)	1·72 (0·03)	C(12) - O(2)	1·22 (0·01)

(c) Between bis-8-hydroxyquinolinato palladium^{II} and chloranil.

Pd - Cl(2)	3·44 (0·01)	C(8) - C(11)	3·44
C(1) - O(2)	3·09	C(8) - C(12)	3·40
C(3) - O(2)	3·37	C(9) - C(10)	3·52
C(7) - C(11)	3·12		

(d) C(4) - C(6) ····· 3·45, where C(6) is in a second bis-8-hydroxyquinolinato palladium^{II} molecule, plane-to-plane with, and slightly overlapping, the first containing the atom C(4).

TABLE A.5.

Palladium 8-hydroxyquinolinate/1,2,4,5-tetracyanobenzene.

Observed structure amplitudes and calculated structure factors for (hkl).

h	k	l	50|F|$_o$	50 F$_c$
0	0	-1	2734	3161
		-2	474	238
		-3	981	788
		-4	741	548
		-5	1078	955
		-6	1289	1153
		-7	893	774
		-8	1409	1223
		-9	1124	921
0	1	-1	3021	2918
		-2	1200	786
		-3	2115	2027
		-4	1902	1653
		-5	1944	1642
		-6	951	817
		-7	1129	918
		-8	886	792
		-9	941	830
		-10	399	430
0	2	0	1267	-951
		-1	2791	2663
		-2	3042	2971
		-3	1275	1062
		-4	1891	1624
		-5	2502	2274
		-6	969	871
		-7	697	721
		-8	810	695
		-9	794	705
		-10	931	832
		-11	577	628
0	3	0	2082	1740
		-1	606	372
		-2	1316	1030
		-3	1503	1334
		-4	1306	1134
		-5	1554	1509
		-6	1259	1093
		-7	1027	889
0	3	-8	1060	932
		-9	928	832
		-10	680	596
		-11	704	617
0	4	0	1983	1713
		-1	376	359
		-2	719	641
		-3	2342	2129
		-4	900	707
		-5	1071	910
		-6	1010	883
		-7	1179	1116
		-8	1062	908
		-9	742	714
		-10	407	426
		-11	543	502
0	5	0	1219	1023
		-1	1627	1465
		-3	1621	1262
		-4	1446	1155
		-5	1574	1354
		-6	513	466
		-7	465	506
		-8	1004	922
		-9	494	535
		-10	542	498
		-11	406	428
0	6	0	1098	855
		-1	1410	1183
		-2	1447	1160
		-3	1613	1239
		-4	1877	1678
		-5	1398	1210
		-6	552	493
		-8	759	797
		-9	576	492
		-10	592	493
0	7	0	503	536

TABLE A.5. (continued)

h	k	l	50|F|$_o$	50 F$_c$
0	7	-1	919	820
		-2	1131	982
		-3	830	654
		-4	1364	1139
		-5	1041	906
		-6	706	741
		-7	652	619
		-8	555	532
		-9	449	410
		-10	302	403
0	8	0	615	631
		-1	676	660
		-2	700	680
		-3	368	367
		-4	471	471
		-5	727	747
		-6	626	652
		-7	590	526
		-8	605	507
0	9	0	842	665
		-1	525	455
		-2	455	462
		-3	433	403
		-4	341	349
		-5	398	387
		-6	447	438
		-7	349	356
0	1	1	2480	2371
		2	3196	3110
		3	1287	1108
		4	977	896
		5	428	360
		6	1187	997
		7	1096	913
		8	1369	1095
		9	601	516
0	2	1	701	543
		2	1696	1489
		3	2616	2500
		4	2462	2296
		5	582	579
		6	900	777
		7	1122	945
		8	779	636
		9	350	345
0	2	10	544	454
0	3	1	1598	1389
		2	1267	980
		3	1812	1617
		4	1696	1431
		5	1462	1236
		6	1340	1133
		7	734	592
		8	676	537
		9	699	509
0	4	1	1999	1648
		2	1699	1590
		3	1188	1085
		4	870	711
		5	1189	956
		6	1315	1052
		7	521	493
		8	766	611
0	5	1	1198	954
		2	375	264
		3	1331	1136
		4	1410	1192
		5	797	674
		6	679	566
		7	478	452
0	6	1	772	690
		2	421	-89
		3	1013	785
		4	1121	940
		5	866	684
		6	427	381
0	7	1	513	508
		2	617	570
		3	568	615
		4	605	459
		5	456	381
0	8	1	695	514
		2	637	511
		3	615	541
0	9	1	697	581
1	0	-1	2331	2528
		-2	654	-290
		-3	1753	1903

TABLE A.5. (continued).

h	k	l	50|F|$_o$	50 F$_c$
1	0	-4	991	1001
		-5	1380	1319
		-6	1073	977
		-7	1234	1175
		-8	908	888
		-9	953	958
1	1	0	1197	1261
		-1	1332	1438
		-2	1248	1127
		-3	2327	2476
		-4	711	818
		-5	1607	1719
		-6	1500	1426
		-7	779	789
		-8	786	748
		-9	432	442
1	2	0	832	2455
		-1	1664	1544
		-2	795	741
		-3	1746	1748
		-4	1973	1880
		-5	1960	1995
		-6	1611	1550
		-7	564	545
		-8	642	606
		-9	508	522
1	3	0	2248	2304
		-1	2391	2305
		-2	371	103
		-3	1340	1236
		-4	2120	2124
		-5	1521	1411
		-6	1178	1131
		-7	1268	1217
		-8	826	798
		-9	501	555
1	4	0	1582	1428
		-1	1916	1877
		-2	1135	1108
		-3	1097	1041
		-4	1217	1097
		-5	1531	1420
		-6	1215	1136
		-7	679	731
1	4	-8	778	802
		-9	498	489
		-10	501	478
1	5	0	1375	1343
		-1	1153	1033
		-2	1582	1476
		-3	1312	1243
		-4	960	856
		-5	1131	1058
		-6	827	843
		-7	321	-204
		-8	703	759
		-9	928	837
		-10	673	627
1	6	0	1091	1070
		-1	901	883
		-2	1327	1274
		-3	1087	940
		-4	683	689
		-5	281	311
		-6	380	510
		-7	375	381
		-8	634	673
		-9	716	719
1	7	0	777	782
		-1	888	872
		-2	885	905
		-3	354	349
		-4	257	364
		-5	492	499
		-6	556	594
		-7	807	801
		-8	507	509
1	8	0	854	742
		-1	627	565
		-2	425	518
		-3	386	454
		-4	625	505
		-5	660	650
		-6	491	504
		-7	369	428
		-8	427	519
1	9	0	568	521
		-1	426	391

TABLE A.5. (continued).

h	k	l	50|F|$_o$	50 F$_c$
1	9	-2	528	473
		-3	632	567
		-4	601	518
		-5	382	444
1	0	3	1324	1324
		4	1579	1585
		5	1370	1210
		6	1747	1622
		7	1291	1159
		8	1718	1574
		9	636	550
		10	309	320
		11	514	431
1	1	1	1502	1413
		2	700	646
		3	2809	2836
		4	1871	1818
		5	1533	1500
		6	1485	1309
		7	828	774
		8	1166	994
		9	647	605
		10	533	519
1	2	1	1736	1718
		2	1630	1726
		3	2565	2413
		4	1151	1091
		5	1195	1036
		6	876	829
		7	781	741
		8	642	588
		9	579	486
		10	490	492
1	3	1	2325	2176
		2	2326	2318
		3	1221	1128
		4	697	607
		5	503	462
		7	676	648
		8	894	840
		9	541	497
1	4	1	1721	1662
		2	1316	1097
		3	1281	1240
		4	624	590
		6	273	322
		7	506	489
		8	730	627
1	5	1	459	486
		2	330	360
		3	1675	1565
		4	707	684
		5	609	648
		6	596	612
		7	536	445
1	6	1	357	406
		2	748	727
		3	944	912
		4	722	700
		5	831	706
		6	689	553
1	7	1	868	801
		2	854	820
		3	450	459
		4	619	543
		5	418	407
1	8	1	716	589
		2	400	423
		3	454	441
1	-1	6	1512	1396
		7	1371	1182
		8	1006	882
		9	583	548
		10	546	539
		11	675	549
1	-2	8	573	532
		9	438	500
		10	620	647
		11	579	479
1	-3	11	668	575
1	-4	11	666	611
1	-5	10	649	622
		11	402	435
1	-6	10	611	604
		11	289	377
1	-7	10	528	490

TABLE A.5. (continued).

h	k	l	50|F|$_o$	50 F$_c$
1	-1	-1	1992	2295
		-2	1022	845
		-3	644	580
		-4	1509	1538
		-5	1480	1405
		-6	1218	1150
		-7	1106	1069
		-8	689	670
1	0	2	1598	1724
1	-1	2	2407	2852
		3	354	303
		4	1661	1818
		5	1468	1556
1	-2	0	1293	1397
		1	1338	1232
		2	2424	2555
		3	1634	1689
		4	2547	2771
		5	2150	2174
		6	436	529
		7	827	778
1	-3	0	1952	1979
		1	254	265
		2	1808	1720
		3	2905	2859
		4	2064	2138
		5	1752	1728
		6	1319	1283
		7	999	887
		8	690	758
1	-4	0	2135	2173
		1	409	509
		2	1036	990
		3	1692	1699
		4	1841	1765
		5	1529	1454
		6	1660	1544
		7	1071	1038
		8	569	593
		9	452	476
		10	283	315
1	-5	0	1379	1233
		1	1459	1350
		2	1210	1160
1	-5	3	1009	874
		4	1588	1558
		5	1210	1160
		6	342	-70
		7	1033	1067
		8	1049	973
		9	876	901
1	-6	0	893	882
		1	1444	1440
		2	1383	1236
		3	856	806
		4	688	524
		5	642	683
		6	279	-64
		7	998	976
		8	1105	1142
		9	644	730
1	-7	0	846	898
		1	1086	1077
		2	634	542
		3	514	536
		4	421	409
		5	714	682
		6	952	917
		7	629	643
		8	423	578
		9	513	551
1	-8	0	609	625
		1	595	647
		2	341	390
		3	545	515
		4	787	787
		5	643	664
		6	614	709
		7	518	606
		8	467	451
		9	419	440
1	-9	0	478	405
		1	484	489
		2	679	616
		3	691	587
		4	535	554
		5	328	442
		6	350	376
		7	681	656

TABLE A.5. (continued).

h	k	l	50|F|$_o$	50 F$_c$
1	0	-10	417	400
1	-1	-9	995	930
		-10	445	422
1	-2	-1	2002	2025
		-2	1709	1836
		-3	1037	1138
		-4	2030	1900
		-5	1013	965
		-6	931	898
		-7	879	841
		-8	613	600
		-9	576	473
		-10	323	366
1	-3	-1	2006	2145
		-2	1682	1644
		-3	1911	1952
		-4	1539	1395
		-5	656	624
		-6	496	446
		-7	233	333
		-8	431	520
		-9	531	534
1	-4	-1	1616	1628
		-2	1815	1703
		-3	1521	1355
		-4	825	877
		-5	570	540
		-6	319	379
		-8	400	375
1	-5	-1	1224	1266
		-2	1021	960
		-3	534	531
		-4	1202	1217
		-5	506	513
		-6	361	442
		-7	424	435
1	-6	-1	1120	1108
		-3	417	492
		-4	1077	1064
		-5	545	588
		-6	631	552
1	-7	-1	788	802
		-2	580	591
		-3	673	719
		-4	520	495
1	-7	-5	573	515
1	-8	-1	624	650
		-2	719	644
		-3	544	521
1	-9	-1	591	553
2	1	0	1707	1818
		-1	827	1008
		-2	2049	2255
		-3	1583	1569
		-4	1256	1403
		-5	1302	1352
		-6	1506	1438
		-7	559	592
		-8	514	564
		-9	453	470
2	0	-2	2200	2561
		-3	381	316
		-4	1114	1112
		-5	808	794
		-6	942	918
		-7	665	738
		-8	534	599
		-9	572	660
2	2	0	865	845
		-1	359	147
		-2	1249	1331
		-3	1720	1800
		-4	988	1004
		-5	1023	1112
		-6	1240	1379
		-7	692	746
		-8	504	563
		-9	537	585
		-10	508	509
2	3	0	1533	1582
		-1	1788	1902
		-2	319	284
		-3	543	583
		-4	1263	1373
		-5	700	753
		-6	702	810
		-7	701	789
		-8	690	779
		-9	538	637
		-10	529	557

TABLE A.5. (continued)

h	k	l	50|F|$_o$	50 F$_c$
2	4	0	1418	1329
		-1	1303	1227
		-2	865	877
		-3	854	866
		-4	1596	1591
		-5	707	707
		-6	771	815
		-7	355	455
		-8	461	608
		-9	563	675
2	5	0	771	780
		-1	998	944
		-2	1294	1320
		-3	1141	1145
		-4	1180	1241
		-5	1083	1098
		-6	894	981
		-7	342	348
		-9	685	691
2	6	0	627	644
		-1	754	745
		-2	846	934
		-3	909	932
		-4	767	771
		-5	1155	1207
		-6	773	850
		-7	488	571
		-8	362	396
2	7	0	457	521
		-1	402	524
		-2	609	673
		-3	693	758
		-4	412	430
		-5	647	736
		-6	660	745
		-7	520	590
2	8	0	605	545
		-1	688	660
		-2	456	523
		-3	489	551
		-4	470	409
		-5	194	349
2	0	2	457	393
		3	416	484
		4	963	857
2	0	5	1488	1481
		6	838	851
		7	1773	1699
		8	1194	1051
		9	486	43
		10	414	431
		11	368	373
2	1	1	2483	3075
		2	1865	2011
		3	1597	1687
		4	192	136
		5	1093	1021
		6	1381	1259
		7	1249	1102
		8	355	395
		9	575	543
		10	524	496
		11	188	408
2	2	1	1273	1124
		2	2463	2760
		3	2299	2469
		4	830	855
		5	908	906
		6	1061	955
		7	694	697
		8	541	563
		9	634	582
		10	463	440
2	3	1	1024	1051
		2	1156	1186
		3	1056	1032
		4	1071	1007
		5	1234	1128
		6	618	626
		7	756	723
		8	602	494
2	3	1	1425	1376
		2	1352	1321
		3	1197	1119
		4	1547	1511
		5	1397	1422
		6	570	529
		7	696	720
		8	774	728
		9	498	436

TABLE A.5. (continued).

h	k	l	50|F|$_o$	50 F$_c$
2	5	1	393	-166
		2	1246	1154
		3	1423	1383
		4	915	856
		5	533	571
		6	484	548
		7	555	487
2	6	1	221	255
		2	745	731
		3	810	781
		4	696	692
		5	271	395
		6	521	482
2	7	1	662	686
		2	568	639
		3	443	442
2	8	1	307	406
		2	507	500
2	-1	6	1235	1156
		7	1500	1433
		8	1470	1321
		10	521	507
		11	577	529
2	-2	8	1027	958
		9	1143	1069
		10	850	809
		11	584	536
2	-3	9	1104	1045
		10	830	876
		11	501	501
2	-4	10	660	714
		11	626	570
2	-5	10	575	617
		11	549	541
2	-6	10	486	496
		11	418	440
2	-1	2	2020	1982
		3	1560	1422
		4	1219	1366
		5	1168	1107
		9	276	161

h	k	l	50|F|$_o$	50 F$_c$
2	-2	0	2630	2878
		1	2505	2595
		2	1442	1312
		3	1717	1730
		4	2527	2510
		5	1049	911
		6	1193	1096
		7	956	796
2	-3	0	1344	1216
		1	1853	1794
		2	950	800
		3	1586	1496
		4	2298	2433
		5	1169	1091
		6	768	738
		7	1165	1037
2	-4	0	273	54
		1	716	567
		2	1943	2057
		3	994	824
		4	1117	1053
		5	1341	1259
		6	1537	1410
		7	1298	1175
		8	1060	971
		9	534	461
2	-5	0	1010	1071
		1	1057	1010
		2	2017	1890
		3	1038	904
		4	1544	1433
		5	1067	866
		6	1082	1022
		7	1148	988
		8	687	639
		9	554	540
2	-6	0	1382	1212
		1	1347	1136
		2	1687	1480
		3	1891	1764
		4	1697	1591
		5	358	359
		7	1095	1040
		8	698	643
		9	790	704

TABLE A.5. (continued).

h	k	l	50|F$_o$|	50 F$_c$
2	-7	0	935	850
		1	1168	1060
		2	1177	977
		3	1690	1476
		4	1009	969
		5	578	625
		6	615	553
		7	836	800
		8	561	585
		9	634	583
		10	307	318
2	-8	0	730	719
		1	740	764
		2	345	358
		3	659	633
		4	882	854
		5	809	821
		6	749	701
		7	570	558
		8	416	417
		9	388	407
2	-9	0	485	472
		2	334	354
		1	395	459
		3	341	356
		4	616	584
		5	645	564
		6	483	426
		7	612	570
2	0	-10	665	582
2	-1	-1	4722	6795
		-2	1965	2133
		-3	1709	1682
		-4	857	759
		-5	551	516
		-6	462	465
		-7	774	752
		-8	557	598
		-9	961	811
		-10	530	486
2	-2	-1	336	223
		-2	759	676
		-3	1550	1567
		-4	1495	1479
		-5	1438	1422
2	-2	-6	369	436
		-7	668	620
		-8	643	687
		-9	690	558
2	-3	-1	810	765
		-2	896	884
		-3	728	680
		-4	1536	1430
		-5	1434	1376
		-6	778	812
		-7	797	780
		-9	376	376
2	-4	-1	1734	1695
		-2	1504	1434
		-3	1320	1308
		-4	2098	944
		-5	679	602
		-6	858	788
		-7	939	810
		-8	432	391
2	-5	-1	1183	1060
		-2	1171	1025
		-3	872	788
		-4	896	892
		-5	776	756
		-6	532	505
		-7	605	495
2	-6	-1	932	810
		-2	722	688
		-3	277	-67
		-4	789	717
		-5	1022	850
		-6	534	496
2	-7	-1	562	538
		-2	420	465
		-4	560	526
		-5	541	469
2	-8	-1	432	508
		-2	370	408
		-3	547	494
2	-9	-1	676	611
3	0	0	1429	1194
		-1	1027	1182
		-2	1100	1202
		-3	277	363

TABLE A.5. (continued)

h	k	l	50|F$_o$|	50 F$_c$
3	0	-4	1407	1554
		-5	727	877
		-6	1008	1030
		-7	769	773
		-8	584	702
3	1	0	1057	1060
		-1	1086	939
		-2	851	844
		-3	1119	1117
		-4	1292	1526
		-5	839	899
		-6	1176	1253
		-7	1002	1036
		-8	366	441
		-9	493	450
3	2	0	1624	1568
		-1	2113	2203
		-2	1517	1568
		-3	308	380
		-4	947	1037
		-5	1255	1408
		-6	1059	1147
		-7	841	894
		-8	523	553
		-9	504	476
3	3	0	942	940
		-1	1079	1149
		-2	1587	1747
		-3	456	533
		-4	826	932
		-5	1102	1239
		-6	881	910
		-7	680	731
		-8	643	773
		-9	560	573
3	4	0	942	940
		-1	1079	1149
		-2	1210	1259
		-3	1162	1215
		-4	905	937
		-5	713	742
		-6	876	979
		-7	663	782
		-9	474	514
3	5	-1	1096	1189
3	5	-2	782	805
		-3	1052	1130
		-4	898	925
		-5	637	699
		-6	463	580
		-7	335	516
		-9	399	481
3	6	0	604	631
		-1	763	840
		-2	702	774
		-3	845	937
		-4	506	543
		-5	304	421
		-8	457	493
3	7	0	704	757
		-1	634	730
		-2	615	705
		-3	496	631
		-6	403	457
		-7	351	434
3	8	0	389	419
		-1	683	675
		-2	455	446
		-3	310	390
		-4	391	449
		-5	417	445
3	0	1	1508	1322
		2	1960	2060
		3	1570	1673
		4	1419	1381
		5	1631	1711
		6	1139	1176
		7	1736	1801
		8	736	725
		9	508	500
		10	453	471
		11	537	469
3	1	1	1008	1017
		2	2892	3337
		3	1651	1857
		4	1411	1536
		5	1201	1219
		6	809	784
		7	914	843
		8	770	745

TABLE A.5. (continued).

h	k	l	50|F|$_o$	50 F$_c$
3	1	9	695	717
		10	601	548
3	2	1	1693	1868
		2	1885	1719
		3	981	985
		4	1111	1009
		5	540	593
		6	802	816
		7	889	835
		8	604	582
		9	488	552
		10	677	588
3	3	1	1792	1829
		2	885	890
		3	562	507
		4	339	401
		6	772	735
		7	1056	1010
		8	527	627
		9	622	517
3	4	1	618	603
		2	1499	1578
		3	643	655
		4	357	467
		5	481	494
		6	530	541
		7	519	566
		8	610	576
3	5	1	355	413
		2	1345	1358
		3	718	768
		4	876	823
		5	655	690
		6	429	474
		7	280	306
3	6	1	839	875
		2	524	615
		3	616	668
		4	632	650
		5	660	578
		6	432	497
3	7	1	576	668
		2	462	470
		3	462	499
		4	253	329

h	k	l	50|F|$_o$	50 F$_c$
3	-1	6	1457	1498
		7	1582	1592
		8	670	600
		9	486	467
		10	647	643
		11	426	442
3	-2	8	628	634
		9	780	799
		10	627	614
		11	404	422
		12	426	540
3	-3	9	418	512
		10	713	684
		11	620	573
		12	469	526
3	-4	10	828	849
		11	664	602
		12	296	380
3	-5	10	541	624
		11	439	456
3	-6	10	415	489
		11	413	431
3	-7	10	383	433
		11	336	429
3	-1	0	651	663
		-1	2174	2671
		-2	1828	2136
		-3	215	334
		-4	701	708
		-5	771	891
		-6	947	975
		-7	714	768
		-8	673	730
3	-2	0	1061	1005
		-1	1394	1623
		-2	1548	1733
		-3	1377	1401
		-4	638	710
		-5	1096	1041
		-6	694	724
3	-1	3	1363	1471
		4	1249	1414
		5	1762	1891

TABLE A.5. (continued).

h	k	l	50|F$_o$|	50 F$_c$
3	-2	0	1051	1005
		1	2170	2282
		2	876	966
		3	2330	2532
		4	1946	2098
		5	790	843
		6	1096	1080
		7	645	642
3	-3	0	933	954
		1	1914	1969
		2	2381	2415
		3	2380	2508
		4	2078	2130
		5	780	888
		6	891	859
		7	661	743
		8	240	280
3	-4	0	297	362
		1	1096	1031
		2	626	2036
		3	1904	1864
		4	1567	1664
		5	1859	1907
		6	1044	1026
		7	636	740
		8	383	340
		9	240	289
3	-5	0	687	784
		1	870	902
		2	1015	965
		3	1620	1673
		4	1273	1270
		5	739	637
		6	1165	1236
		7	986	929
		8	1021	993
		9	550	622
3	-6	0	1163	1235
		1	1089	1126
		2	662	662
		3	948	843
		4	863	848
		5	550	-349
		6	1126	1241
		7	1308	1357
		8	887	978
3	-6	9	649	770
3	-7	0	944	1043
		1	708	710
		2	610	629
		3	383	366
		4	671	707
		5	552	583
		6	765	782
		7	729	896
		8	577	711
		9	622	670
3	-8	0	609	693
		1	408	378
		2	506	543
		3	653	707
		4	651	699
		5	815	902
		6	512	586
		7	358	474
		8	504	606
		9	501	497
3	-9	0	445	480
		1	517	520
		2	597	541
		3	580	649
		4	423	531
		5	398	484
		6	703	736
		7	638	610
3	-10	2	418	429
		3	332	419
		4	276	381
		5	344	385
		6	176	576
3	0	-9	510	557
		-10	275	456
3	-2	-7	570	667
		-8	534	639
		-9	390	432
3	-3	-1	1082	1226
		-2	1348	1375
		-3	1114	1213
		-4	1095	1237
		-5	1196	1182
		-6	540	509

TABLE A.5. (continued).

h	k	l	50|F|$_o$	50 F$_c$
3	-3	-7	299	356
		-8	283	369
3	-4	-1	1572	1730
		-2	1319	1403
		-3	1068	1133
		-4	1134	1121
		-5	686	735
		-6	402	457
		-7	233	317
3	-5	-1	1194	1236
		-2	1026	1093
		-3	999	1076
		-4	627	656
		-5	635	715
		-6	333	370
		-7	242	320
3	-6	-1	769	802
		-2	829	912
		-3	386	446
		-4	332	390
		-5	936	882
		-6	371	407
3	-7	-1	658	778
		-2	659	748
		-3	264	352
		-4	444	475
		-5	503	529
3	-8	-1	629	589
		-2	513	514
		-3	535	519
3	-9	-1	436	377
3	1	-7	997	1036
		-8	399	441
		-9	398	450
		-10	235	290
3	2	-7	842	896
		-8	397	553
		-9	398	476
		-10	243	404
3	2	-7	841	894
		-8	507	553
		-9	398	476
		-10	314	404
3	3	-8	612	773
		-9	522	573
		-10	224	341
3	1	3	1622	1857
		4	1415	1536
		5	1557	1219
		6	736	784
		7	909	843
4	-1	0	779	426
		-1	1489	1382
		-2	3993	4410
		-3	1468	1532
		-4	727	805
		-5	713	685
		-6	418	435
		-7	408	426
4	-2	0	1634	1347
		-1	1986	1867
		-2	1899	1552
		-3	849	785
		-4	1024	1097
		-5	748	796
		-6	642	740
4	-3	-1	1472	1521
		-2	405	421
		-3	588	574
		-4	588	602
4	0	0	2286	1767
		-1	2002	1693
		-2	3083	2987
		-3	1585	1659
		-4	688	666
		-5	841	889
		-6	672	712
		-7	744	757
		-8	414	440
4	1	0	1987	1829
		-1	1389	1261
		-2	404	336
		-3	1260	1267
		-4	1114	1242
		-5	760	866
		-6	780	852
		-7	889	945
		-8	398	421

TABLE A.5. (continued).

h	k	l	50|F|$_o$	50 F$_c$
4	1	-9	287	335
4	2	0	1216	1066
		-1	982	1011
		-2	991	932
		-3	605	666
		-4	778	878
		-5	811	850
		-6	593	649
		-7	542	676
		-8	452	531
		-9	399	449
4	3	0	1112	1141
		-1	1242	1210
		-2	1213	1255
		-3	498	510
		-4	557	510
		-5	977	1022
		-6	476	520
		-7	474	507
		-8	385	437
		-9	371	482
4	4	0	271	315
		-1	901	876
		-2	770	832
		-3	812	880
		-4	722	793
		-5	887	1007
		-6	558	620
		-7	499	611
4	5	0	243	-51
		-1	595	618
		-2	780	775
		-3	775	910
		-4	716	808
		-5	625	732
		-6	665	789
		-7	568	602
		-8	266	332
4	6	0	556	540
		-1	466	545
		-2	490	556
		-3	572	654
		-4	533	635
		-5	374	411
		-6	646	723
4	6	-7	533	585
4	7	0	480	535
		-1	423	473
		-2	399	484
		-3	405	470
		-4	447	523
		-5	324	348
		-6	324	439
4	0	1	1350	762
		2	1196	945
		3	1041	697
		4	1467	1397
		5	1037	931
		6	1681	1598
		7	847	774
		8	221	335
		9	644	565
		10	375	426
		11	459	428
4	1	0	2433	1829
		2	2204	1864
		3	221	212
		4	905	864
		5	1383	1325
		6	993	895
		7	344	361
		8	830	741
		9	591	596
		10	653	575
4	2	1	1914	1888
		2	1773	1681
		3	1269	1127
		4	1063	1019
		5	777	693
		6	735	789
		7	936	852
		8	648	613
		9	526	477
		10	436	440
4	3	1	1017	984
		2	1023	937
		3	1448	1418
		4	1513	1435
		5	570	519
		6	839	802

TABLE A.5. (continued).

h	k	l	50|F|$_o$	50 F$_c$
4	3	7	818	753
		8	513	485
		9	399	392
4	4	1	1152	1123
		2	1205	1250
		3	1058	977
		4	1043	985
		5	671	706
		6	713	687
		7	383	436
		8	256	294
4	5	1	979	920
		2	1112	1120
		3	894	860
		4	440	504
		5	510	579
		6	430	445
		7	273	379
4	6	1	543	614
		2	547	550
		3	423	489
		4	220	349
		5	536	529
4	7	1	549	557
		2	431	408
4	-1	5	1025	989
		6	1914	2007
		7	1743	1592
		8	570	-185
		9	575	503
		10	582	563
		11	577	509
4	-2	7	1443	1292
		8	922	842
		9	925	838
		10	725	692
		11	632	561
4	-3	9	1150	1048
		10	572	556
		11	670	560
		12	327	344
4	-4	10	690	644
		11	617	500
4	-4	12	396	415
4	-5	10	717	706
		11	406	409
4	-6	10	533	559
		11	272	330
4	-7	10	468	451
		11	349	387
4	-8	10	355	389
4	-1	3	1206	1026
		4	1423	1272
4	-2	0	1629	1347
		1	1845	1387
		2	1841	1288
		3	647	1648
		4	1169	996
		5	1575	1445
		6	1137	1130
4	-3	0	1921	1720
		1	786	579
		2	1762	1404
		3	2935	2489
		4	996	891
		5	745	705
		6	979	917
		7	1220	1157
		8	1646	1506
4	-4	0	934	796
		1	1442	1364
		2	1242	1030
		3	1437	1351
		4	1254	1172
		5	1251	1130
		6	1382	1313
		7	1128	1144
		8	786	644
		9	907	882
4	-5	0	695	695
		1	1630	1592
		2	763	689
		3	1209	1156
		4	1369	1266
		5	1601	1450
		6	1094	955

TABLE A.5. (continued).

h	k	l	50|F$_o$|	50 F$_c$
4	-5	7	687	681
		8	371	387
		9	791	772
4	-6	0	898	863
		1	1430	1310
		2	1348	1364
		3	1660	1654
		4	602	477
		5	387	397
		6	1047	974
		7	735	665
		8	807	789
		9	684	649
4	-7	0	950	914
		1	1201	1090
		3	1053	1029
		2	1494	1466
		5	243	320
		6	1084	1032
		7	770	725
		8	799	741
		9	409	430
4	-8	0	753	739
		1	467	459
		2	753	751
		3	674	732
		4	719	766
		5	759	712
		6	634	620
		7	434	499
		8	481	530
		9	294	322
4	-9	0	390	428
		2	345	373
		3	696	690
		4	623	644
		5	564	490
		6	543	532
		7	337	386
		8	304	362
4	-10	3	305	328
		4	321	386
		5	286	360
		6	449	522
4	0	-9	317	374
4	-1	-8	390	477
		-9	304	382
4	-2	-7	244	341
		-8	436	432
4	-3	-5	905	946
		-6	859	968
		-7	1127	426
		-8	469	488
4	-4	-1	471	346
		-2	1072	1116
		-3	834	919
		-4	657	755
		-5	689	752
		-6	536	559
		-7	536	533
4	-5	-1	494	576
		-2	1021	968
		-3	908	862
		-4	748	885
		-5	514	617
		-6	468	427
4	-6	-1	847	934
		-2	673	663
		-3	646	617
		-5	596	538
4	-7	-1	760	748
		-2	477	485
		-3	357	406
4	-8	-1	688	653
		-2	379	392
		-3	258	299
4	-9	-1	436	457
4	1	-6	755	852
		-7	863	945
		-8	372	421
		-9	269	335
4	2	-7	542	676
		-8	430	531
		-9	373	449
4	3	-8	282	437
		-9	349	482
5	-1	0	1332	1158
		-1	973	924

TABLE A.5. (continued).

h	k	l	50|F$_o$|	50 F$_c$
5	-1	-2	1354	1519
		-3	1088	1250
		-5	560	640
		-6	485	612
		-7	555	640
5	-2	0	1468	1401
		-1	587	696
		-2	1343	1479
		-3	1219	1373
		-4	633	783
		-5	379	479
		-6	440	531
5	-3	0	1751	1580
		-1	898	1009
		-2	723	869
		-3	841	883
		-4	780	904
5	0	0	1281	1103
		-1	1059	1050
		-2	410	511
		-3	394	515
		-4	402	535
		-5	728	1008
		-6	502	636
		-7	576	715
		-8	508	548
5	1	0	996	1066
		-1	704	749
		-2	1005	948
		-3	693	756
		-4	555	692
		-5	634	840
		-6	535	682
		-7	500	747
		-8	486	612
5	2	0	1338	1397
		-1	1311	1337
		-2	1369	1480
		-3	1034	1206
		-5	481	651
		-6	649	878
		-7	472	613
		-8	395	477
5	3	0	958	1048
5	3	-1	1121	1268
		-2	800	974
		-3	885	1078
		-4	533	662
		-5	525	679
		-6	530	683
		-7	511	590
5	4	0	262	346
		-1	222	376
		-2	735	903
		-3	636	781
		-4	662	887
		-5	517	667
		-6	359	508
		-7	414	565
5	5	0	416	542
		-2	659	851
		-3	448	595
		-4	520	724
		-5	335	539
		-6	300	438
5	6	0	539	748
		-1	505	656
		-2	426	599
		-3	406	578
		-4	456	602
		-5	181	296
5	7	0	278	418
		-1	419	522
		-2	495	608
		-3	364	485
5	0	1	2456	2191
		2	1865	1450
		3	1250	1236
		4	1329	1353
		5	958	965
		6	1380	1402
		7	805	843
		8	685	726
		9	517	544
		10	666	565
5	1	1	2164	2301
		2	1310	1452
		3	1186	1254
		4	786	855

TABLE A.5. (continued).

h	k	l	50|F$_o$|	50 F$_c$
5	1	5	643	736
		6	740	757
		7	735	771
		8	628	746
		9	759	705
		10	554	521
5	2	1	722	846
		2	650	724
		3	761	837
		4	321	407
		5	741	801
		6	923	1016
		7	534	623
		8	487	576
		9	600	584
5	3	1	881	934
		2	389	447
		5	661	716
		6	751	884
		7	595	658
		8	615	556
5	4	1	1243	1411
		2	568	666
		3	458	567
		4	462	562
		5	393	491
		6	327	439
		7	571	543
5	5	1	640	824
		2	581	676
		3	647	769
		4	536	638
		5	399	469
		6	273	306
5	6	1	305	434
		2	478	533
		3	377	445
		4	477	521
5	7	1	343	438
5	-1	1	1175	584
		2	1920	1125
		3	1482	1233
		4	1676	1714
		5	1278	1356
5	-1	6	1791	1931
		7	651	633
		8	431	442
		9	525	605
		10	474	516
		11	496	455
5	-2	0	1504	1401
		1	857	581
		2	2470	1609
		3	1763	1465
		5	1466	1216
		6	1045	1037
		7	599	616
		8	665	654
		9	668	665
		10	347	467
5	-3	0	1579	1580
		1	1634	1434
		2	2306	1978
		3	2197	1777
		4	651	684
		5	949	885
		6	522	572
		7	1139	416
		8	694	738
		9	726	696
		10	544	606
		11	730	687
5	-4	0	1096	1037
		1	1799	1622
		2	1752	1653
		3	1732	1597
		4	1452	1393
		5	909	801
		6	652	766
		8	409	410
		9	971	941
		10	711	713
		11	426	482
5	-5	0	642	687
		1	1033	1036
		2	1329	1352
		3	1120	1132
		4	1184	1193
		5	1076	1099
		6	879	857

TABLE A.5. (continued).

h	k	l	50|F$_o$|	50 F$_c$
5	-5	7	822	808
		8	482	485
		9	680	806
		10	522	581
		11	475	490
5	-6	0	627	774
		1	521	501
		2	985	932
		3	868	856
		5	1204	1280
		6	1164	1188
		7	997	1040
		8	620	752
		9	469	567
		10	438	503
		11	624	591
5	-7	0	581	652
		1	404	514
		2	523	458
		3	664	698
		5	866	879
		6	985	1071
		7	676	801
		8	730	779
		9	492	533
		10	467	476
		11	305	404
5	-8	0	366	398
		1	472	539
		2	482	514
		3	517	609
		4	664	755
		5	504	526
		6	473	569
		7	592	699
		8	616	598
		9	277	343
		10	326	419
5	-9	0	350	386
		1	443	450
		2	593	602
		3	536	527
		4	550	588
		5	598	643
		6	529	515
5	-9	7	451	485
		8	297	416
5	-10	3	285	392
		4	348	363
		5	570	627
5	-1	-8	437	482
5	-2	-7	390	488
		-8	327	438
5	-3	-5	591	712
		-6	647	721
		-7	314	353
5	-4	-1	504	595
		-2	882	1085
		-3	876	926
		-4	603	659
		-5	612	724
		-6	588	601
		-7	251	332
5	-5	-1	295	385
		-2	859	994
		-3	736	860
		-4	621	773
		-5	490	557
		-6	371	408
5	-6	-1	638	782
		-2	562	663
		-3	552	657
		-4	497	520
5	-7	-1	673	819
		-2	451	588
		-3	545	583
		-4	193	251
5	-8	-1	600	607
		-2	439	476
6	-1	0	1150	823
		-1	913	743
		-2	905	889
		-3	1930	2157
		-4	831	969
		-5	336	466
		-6	382	522

TABLE A.5. (continued).

h	k	l	50|F$_o$|	50 F$_c$
6	-2	0	1202	1015
		-1	722	714
		-2	978	1020
		-3	1545	1582
		-4	570	645
		-5	444	598
6	-3	0	690	569
		-1	998	1099
		-2	1065	1140
		-3	505	504
		-4	392	421
6	0	0	1379	999
		-1	1317	1220
		-2	1028	1043
		-3	883	1017
		-4	936	971
		-5	498	632
		-6	391	549
		-7	387	473
6	1	0	1640	1506
		-1	1134	1025
		-2	916	878
		-3	486	491
		-4	501	667
		-5	558	712
		-6	404	545
		-7	356	469
6	2	0	1063	1036
		-1	972	875
		-2	707	791
		-3	626	803
		-4	305	426
		-5	360	446
		-6	497	600
		-7	257	373
6	3	0	736	779
		-1	420	578
		-2	630	742
		-3	510	692
		-4	368	494
		-5	314	430
		-6	494	625
		-7	276	366
6	4	0	747	858
6	4	-2	457	553
		-3	474	589
		-4	391	611
		-5	423	549
		-6	406	563
6	5	0	505	619
		-1	221	229
		-2	344	457
		-3	389	530
		-4	394	557
		-5	368	490
6	6	0	365	470
		-1	425	503
		-2	311	412
		-3	277	386
		-4	256	409
6	0	1	1560	1093
		2	638	522
		3	1350	1013
		4	1213	950
		5	1361	1042
		6	396	405
		7	636	649
		8	624	649
		9	437	528
		10	433	430
6	1	1	1503	1277
		2	530	440
		3	857	725
		4	1177	995
		5	767	738
		6	521	532
		7	697	704
		8	504	574
		9	648	630
		10	240	356
6	2	1	1015	956
		2	1098	1091
		3	1058	988
		4	465	449
		5	693	802
		6	903	921
		7	516	575
		8	428	454
		9	289	349

TABLE A.5. (continued).

h	k	l	50|F$_o$|	50 F$_c$
6	3	1	859	910
		2	1071	1092
		3	1111	1140
		4	429	549
		5	603	698
		6	494	576
		7	377	433
		8	276	363
6	4	1	894	1053
		2	773	838
		3	600	727
		4	494	657
		5	486	546
		6	264	367
		7	95	208
6	5	1	579	686
		2	550	631
		3	343	388
		4	443	542
		5	285	385
6	6	1	336	388
		3	134	287
6	-1	1	1499	896
		2	1667	829
		3	1486	1091
		4	908	688
		5	1971	1834
		6	1418	1299
		7	397	-26
		8	645	514
		9	426	498
		10	521	530
		11	425	488
6	-2	8	726	710
		9	739	732
		10	604	575
		11	386	379
6	-3	8	1031	1010
		9	547	593
		10	622	609
		11	351	359
6	-4	9	552	586
		10	667	620
		11	478	462
6	-5	10	502	494
		11	478	454
6	-2	0	1286	1015
		1	1585	852
		3	1726	965
		4	1691	1256
		6	1717	1450
		5	1669	1477
		7	262	313
6	-3	0	684	569
		1	1269	964
		2	2325	1619
		3	1432	768
		4	1384	885
		5	1127	810
		6	1491	1157
		7	1605	1467
6	-4	0	863	761
		1	1205	928
		2	1669	1346
		3	1051	800
		4	934	693
		5	1427	1129
		6	1424	1126
		7	1152	979
		8	808	919
		9	560	586
		10	612	620
		11	470	462
6	-5	0	1149	1097
		1	834	612
		2	970	863
		3	1408	1181
		4	1565	1285
		5	1135	911
		6	845	691
		7	297	251
		8	734	822
		9	694	767
		10	478	494
		11	449	454
6	-6	0	985	962
		1	940	875
		2	1447	1279
		3	857	717

TABLE A.5. (continued).

h	k	l	50|F_o|	50 F_c
6	-6	4	823	709
		5	722	695
		6	541	551
		7	599	628
		8	687	718
		9	533	628
		10	284	367
		11	335	358
6	-7	0	812	888
		1	1042	1121
		2	970	1017
		5	978	980
		6	692	713
		7	781	777
		8	489	501
		9	391	495
		10	254	371
6	-8	0	534	525
		1	700	720
		2	436	564
		3	363	506
		4	494	521
		5	620	699
		6	465	549
		7	594	585
		8	339	360
		9	420	441
6	-9	1	344	370
		2	556	584
		3	559	604
		4	495	491
		5	364	420
		6	341	377
		7	393	422
		8	274	331
6	-1	-7	316	352
6	-2	-6	398	469
		-7	297	388
6	-3	-5	360	490
		-6	440	522
6	-4	-1	884	828
		-2	561	566
		-3	453	586
		-4	356	510
		-5	336	415
		-6	455	511
6	-5	-1	515	528
		-2	256	346
		-3	562	712
		-4	518	569
		-5	454	543
6	-6	-1	484	554
		-2	432	563
		-3	469	504
		-4	467	472
6	-7	-1	605	646
		-2	520	551
		-3	356	370
6	-8	-1	574	591
		-2	416	496

TABLE A.6.

Palladium 8-hydroxyquinolinate/tetracyanobenzene complex.

Atomic co-ordinates ($\times 10^4$) and standard deviations ($\times 10^4$).

	x/a	σ(x/a)	y/b	σ(y/b)	z/c	σ(z/c)
Pd	0	0	0	0	0	0
C(1)	-21	24	-2930	23	1403	20
C(2)	411	25	-3510	25	2425	21
C(3)	1263	25	-2335	25	3482	21
C(4)	1706	24	-391	23	3538	19
C(5)	2587	24	986	24	4604	20
C(6)	2908	27	2773	27	4519	23
C(7)	2489	25	3249	24	3434	20
C(8)	1643	23	1929	22	2365	19
C(9)	1226	23	141	22	2472	18
N(1)	340	19	-1180	18	1429	15
O(1)	1222	16	2292	16	1258	13
C(10)	4730	22	1114	21	-733	18
C(11)	4250	24	-813	23	-1235	20
C(12)	4518	25	-1938	25	-544	21
C(13)	4420	27	2280	27	-1423	22
C(14)	3393	27	-1640	27	-2484	23
N(2)	4248	23	3312	24	-1983	20
N(3)	2766	24	-2404	25	-3522	21

TABLE A.7.

Palladium 8-hydroxyquinolinate/tetracyanobenzene complex.

Temperature Factors ($U_{iso.}$)

Atom.	$U_{iso.}$ ($\times 10^4$)	Standard deviation. ($\times 10^4$)
Pd	280	5
C(1)	470	41
C(2)	519	45
C(3)	519	45
C(4)	457	40
C(5)	484	42
C(6)	581	49
C(7)	494	43
C(8)	427	38
C(9)	415	37
N(1)	440	33
O(1)	477	29
C(10)	393	36
C(11)	467	41
C(12)	517	44
C(13)	569	48
C(14)	562	48
N(2)	642	45
N(3)	695	49

TABLE A.8.

Palladium 8-hydroxyquinolinate/tetracyanobenzene complex.

Interatomic distances (in Å).

(a) Bis-8-hydroxyquinolinato palladium^{II}.

Pd - N(1) ····· 2·00	C(4) - C(9) ···· 1·41
Pd - O(1) ····· 2·00	C(5) - C(6) ···· 1·39
C(1) - C(2) ···· 1·37	C(6) - C(7) ···· 1·37
C(1) - N(1) ···· 1·33	C(7) - C(8) ···· 1·38
C(2) - C(3) ···· 1·34	C(8) - C(9) ···· 1·39
C(3) - C(4) ···· 1·44	C(8) - O(1) ···· 1·33
C(4) - C(5) ···· 1·42	C(9) - N(1) ···· 1·39

(b) Tetracyanobenzene.

C(10) - C(11) ····· 1·41	C(11) - C(14) ··· 1·44
C(11) - C(12) ····· 1·37	C(13) - N(2) ···· 1·18
C(10) - C(12)' ···· 1·40	C(14) - N(3) ···· 1·15
C(10) - C(13) ····· 1·42	

(c) Between bis-8-hydroxyquinolinato palladium^{II} and TCNB.

C(14) - Pd ····· 3·48	C(12) - N(1) ···· 3·70
N(3) - O(1)' ····· 3·51	C(12)' - C(8) ··· 3·28
C(10)' - C(4) ····· 3·49	C(14)' - C(6) ··· 3·44
C(10) - O(1) ····· 3·30	C(12)' - C(7) ··· 3·29
C(13) - O(1) ····· 3·16	

The mean standard deviation for bonds involving the palladium atom is 0·02 Å, and for other bonds 0·04 Å. (The programme for computing standard deviations on the new KDF9 computer is not yet working, so standard deviations for each bond are not quoted.)

APPENDIX B.

TECHNIQUES OF SOLID STATE SPECTROSCOPY.

B.1. Reflection spectra.

When light falls onto a crystal of an absorbing material, it is reflected as two components. It may be reflected directly off the front face of the crystal, without penetrating into the interior of the crystal (in which case it is known as the regular reflectance), or it may enter the crystal, reflect off the back face, and emerge diminished in intensity by the absorption due to the meterial in the crystal (when it is known as the diffuse reflectance). The regular reflectance depends on the nature of the surface, the particle size of the material, and the absorption characteristics of the material at the wavelength concerned.

To obtain the true absorption due to absorption occuring in the diffuse reflectance, the regular reflectance must be minimised and compensated for. There are two ways of doing this, as follows:-

(i) Mathematical expressions (e.g. the Kubelka-Munk function[61]), taking into account the variation of regular reflectance with wavelength, may be applied.

(ii) Experimental conditions may be arranged to minimise the regular reflectance and to make it nearly equal to that of the reference blank material.

Reflection spectra of this type can be used to study weak transitions,

using undiluted solid samples, or strong transitions, using non-absorbing solid diluents to reduce the optical density to be measured.

B.2. Transmission spectra of pellets, mulls and films.

Compressed pellets, mulls and films of solid materials will often transmit an appreciable amount of visible and ultraviolet light as well as infra-red light, and can therefore be considered as sample forms for transmission spectra measurements. However, in addition to transmitting light, they scatter it strongly in many cases. This scattering increases strongly towards the ultraviolet region, and must be eliminated to give a flat baseline. This is done by inserting a scatter-plate (e.g. a grease spot on a filter paper) into each beam of a double beam instrument, to introduce such scattering into both beams that the scattering due to the sample becomes negligible by comparison. This reduces the amount of light transmitted to the detectors, and means that in practice these methods are chiefly used for infra-red or near-infra-red spectra, where scattering is weaker, rather than for visible and ultra-violet spectra.

B.3. Transmission spectra of single crystals.

The methods described above make no use of the important structural features of solids (which orientate molecules at definite angles to the crystal faces), since the samples are randomly orientated particles not aligned in any particular direction.

However, if single crystal transmission spectra can be recorded, using polarised light, the directions of transitions relative to the molecules, as well as their position and intensity, may be determined. This can be very useful in assigning particular bands in spectra to particular transitions.

Owing to the high concentration of absorbing centres in crystals, studies are limited to thin crystals and relatively weak transitions, which do not call for the measurement of very large optical densities (which would require a lower level of stray light than can usually be achieved). A useful modification is to incorporate a microscope with reflecting objectives in the sample beam, to focus monochromatic light onto very small crystals, thus allowing the use of much thinner samples and consequently increasing the maximum extinction coefficient that can be measured[62].

B.4. Reflectance spectra.

As the absorption of a solid passes through a maximum, the amount of light reflected from the surface varies in a way which is related to the absorption change[63]. This provides an alternative method for studying spectra of single crystals. Since strong absorption leads to increased surface reflectivity, this method is ideal for studying intense transitions, and may be regarded as a complementary technique to transmission spectroscopy of single crystals.

REFERENCES.

1). G. Briegleb, "Elektronen Donator-Acceptor Komplexe", Springer, Berlin, 1961.

2). M. Calvin, in "Recent progress in photobiology", ed. E.J. Bowen, p.233-4, Blackwell, Oxford, 1965.

3). A.S. Bailey and J.R. Case, Tetrahedron 1958 3 113.
A.S. Bailey, J. Chem. Soc. (1960) 917.
A.S. Bailey, B.R. Henn and J. Langdon, Tetrahedron 1963 19 161.
A.S. Bailey and J.M. Evans, Chem. and Ind. (1964) 1425.
J.J. Merer, Part II thesis, Oxford, 1964.

4). J.D. Wright, Part II thesis, Oxford, 1963.

5). F. Pick, Part II thesis, Oxford, 1965.

6). L.R. Melby, R.J. Harder, W.R. Hertler, W. Mahler, R.E. Benson and W.E. Mochel, J. Amer. Chem. Soc. 1962 84 3374.

7). F. Corsini, Q. Fernando and H. Freiser, Analytical Chem. 1963 35 1424.

8). G. Peyronel and N. Gallo, Atti e relaz. accad. pugliese sci., Part II, 1955 13 7.

9). Y. Muto, Bull. Chem. Soc. Japan 1960 33 604

10). R.D. Gillard, D. Rogers, R.D. Diamand and D.J. Williams, Acta Cryst. 1963 16 A67.

11). P.H. Emslie, R. Foster and T.J. Thomson, Rec. Trav. Chim. 1964 83 1311.

12). J.A. Barltrop and B. Hesp, Proc. Chem. Soc. (1964) 195.

13). M. Banks and E.T. Hall, Archaeometry 1963 6 31.

14). R.S. Mulliken, Rec. Trav. Chim. 1956 75 845.

15). A.S. Bailey and C.K. Prout, J. Chem. Soc. (in press).

16). C.K. Prout and H.M. Powell, J. Chem. Soc. (in press).

17). T.S. Cameron, Part II thesis, Oxford, 1965.

18). G.J. Palenik, Acta Cryst. 1964 17 687.

19). L. Pauling, "The nature of the chemical bond", p.260, O.U.P. 3rd. edition, 1960.

20). R.E. Merrifield and W.D. Phillips, J. Amer. Chem. Soc. 1958 80 2778.

21). R.E. Burton and W.J. Davis, J. Chem. Soc. (1964) 1766.

22). S.C. Wallwork and R.M. Williams, personal communication.

23). (a) D.S. Brown and S.C. Wallwork and A. Wilson, Acta Cryst. 1964 17 168.

(b) A.W. Hanson, Acta Cryst. 1963 16 1147.

24). R.S. Mulliken, J. Amer. Chem. Soc. 1952 74 811.

R.S. Mulliken and W.B. Person, Ann. Rev. Phys. Chem. 1962 13 107.

25). M.J.S. Dewar and A.R. Lepley, J. Amer. Chem. Soc. 1961 83 4560

M.J.S. Dewar and H. Rogers, J. Amer. Chem. Soc. 1962 84 395.

26). C.A. Coulson, "Valence", p.74, O.U.P. 2nd. edition, 1961.

27). "Dictionary of π-electron calculations", C.A. Coulson and A. Streitwieser, Pergamon, 1965.

"Supplemental tables of molecular orbital calculations", Volumes 1 and 2, A. Streitwieser and J.J. Brauman, Pergamon, 1965.

28). G. Briegleb and J. Czekalla, Z. Elektrochem. 1954 58 260.

29). R.S. Mulliken, J. Chim. Phys. 1964 61 20.

30). J.N. Murrell, "The theory of the electronic spectra of aromatic molecules", p.270-283, Methuen, 1963.

31). A. Sweig, Tetrahedron Letters, (1963) 89.

32). A.S. Bailey, R.J.P. Williams and J.D. Wright, J. Chem. Soc. (1965) 2579.

33). H. Kuroda and H. Akamatu, J. Chem. Phys. 1964 40 3748.
B.G. Anex and L.J. Parkhurst, J. Amer. Chem. Soc. 1963 85 3301.

34). R.M. Rochstrasser, S.K. Lower and C. Reid, J. Chem. Phys. 1964 41 1073.

35). K. Sone, J. Amer. Chem. Soc. 1953 75 5208.

36). L.J. Bellamy, "The infra-red spectra of complex molecules", Methuen, 1958, 2nd. edition.

37). H. McConnell, J.S. Ham and J.R. Platt, J. Chem. Phys. 1953 21 66.

38). A. Streitwieser, "Molecular orbital theory for organic chemists" Wiley, 1961.

39). J. Jortner and U. Sokolov, Nature 1961 190 1003.
M. Batley and L.E. Lyons, Nature 1962 196 573.

40). A.R. Lepley, J. Amer. Chem. Soc. 1962 84 3577.

41). J.R. Platt, J. Chem. Phys. 1949 17 484.

42). D.J.E. Ingram, "Spectroscopy at radio and microwave frequencies", Butterworth, 1955.

43). A.H. Maki and B.R. McGarvey, J. Chem. Phys. 1958 29 35.
G.F. Kokoszka, H.C. Allen and G. Gordon, J. Chem. Phys. 1965 42 3730.

44). D. Kivelson and R. Neiman, J. Chem. Phys. 1961 35 149.

45). P.L. Kronick and M.M. Labes, J. Chem. Phys. 1961 35 2016.

46). C.M. Huggins and A.H. Sharbaugh, J. Chem. Phys. 1963 38 393.

47). P. Day, Part II thesis, Oxford, 1961.

G. Scregg, Part II thesis, Oxford, 1962.

48). M. Whalley, J. Chem. Soc. (1961) 866.

J.M. Assour and S.E. Harrison, J. Amer. Chem. Soc. 1965 87 651.

49). H. Akamatu and H. Kuroda, J. Chem. Phys. 1963 39 3364.

50). S. Choi and S.A. Rice, Phys. Rev. Letters 1962 8 410.

51). J.H. Sharp and W.G. Schneider, J. Chem. Phys. 1964 41 3657.

52). J. Tauc, "Photo- and thermo- electric effects in semiconductors" Pergamon, 1962.

53)a R.B. Park and J. Biggins, Science 1964 144 1009.
(b) G. Tollin, D.R. Kearns and M. Calvin, J. Chem. Phys. 1960 32 1020

54). M.J. Buerger, "X-ray crystallography", Wiley, 1942.

55). C.W. Bunn, "Chemical crystallography", O.U.P. 1961, 2nd. edition.

56). O.S. Mills and J.S. Rollett, "Computing methods and the phase problem in x-ray crystal analysis", Pergamon, 1961, p.107.

57). J. Berghuis, I.M. Haanapel, M. Potters, B.D. Loopstra, C.H. MacGillavry and A.L. Veenendal, Acta Cryst. 1955 8 478.

58). L.H. Thomas and K. Umeda, J. Chem. Phys. 1957 26 293.

59). C.H. Dauben and D.H. Templeton, Acta Cryst. 1955 8 841.

60). A.F. Wells, "Structural inorganic chemistry", O.U.P.

61). P. Kubelka and F. Munk, Z. Techn. Physik. 1931 12 513, J. Opt. Soc. Amer. 1948 38 448

G. Kortum, Trans. Faraday Soc. 1962 58 1624.

62). A.J. Thomson, D.Phil. thesis, Oxford University, 1965.

63). B.G. Anex and W.T. Simpson, Rev. Mod. Phys. 32 466 (1960)

B.G. Anex and A.V. Fratini, J. Mol. Spectr. 1964 14 1.

B.G. Anex and R.S. Umans, J. Amer. Chem. Soc. 86 5026 (1964)

ABSTRACT.

The range of materials known as charge-transfer or molecular complexes has been extended to include compounds having metal complexes, with aromatic ligands, as electron donors.

8-hydroxyquinoline and its copper^{II}, palladium^{II} and nickel^{II} chelates were found to be suitable stable, planar donor molecules. They are conveniently soluble in solvents which also dissolve organic electron acceptor molecules. Solid complexes of these donors with thirteen electron acceptors have been prepared and analysed. Experiments testing the suitability of other metal complexes as donors are described, but none of the materials tested was satisfactory, with the exception of copper and palladium 5-methyl-8-hydroxyquinolinates.

Attempts to prepare dichlorodicyanobenzoquinone complexes of 8-hydroxyquinoline or its nickel chelate, and the tetracyanoethylene/8-hydroxyquinoline complex, gave transient charge transfer interactions, followed by further reaction. Spectroscopic work on these systems is reported briefly, and suggests that electron distribution as well as ionization potential and electron affinity data are needed to explain the transition from complex formation to complete electron transfer and redox reactions.

The solid complexes have been studied by x-ray crystallography, visible, ultraviolet and infra-red spectroscopy, electron spin resonance, and electrical conductivity measurements.

Three-dimensional crystal structures of the palladium 8-hydroxy-

quinolinate complexes with chloranil and tetracyanobenzene have been determined by the x-ray diffraction method. The multiple film Weissenberg technique was used to photograph 1880 and 1920 reflections, respectively, the intensities being estimated visually. A three-dimensional Fourier synthesis, phased on the palladium atom, located all atoms apart from hydrogens. The chloranil complex structure was refined using six cycles of a programme involving a block diagonal approximation to the normal least squares matrix, with anisotropic temperature factors and weighted data. The final R value was 0·108. The tetracyanobenzene complex structure was refined using two cycles of a full-matrix least squares programme, with isotropic temperature factors and unit weight for all data. The final R value was 0·102.

These structures, and those of four more of the complexes, determined by other workers, are discussed, and show the following features:

(i) They contain stacks of alternate donor and acceptor molecules, in a plane-to-plane arrangement, the inter-planar spacing being close to the van der Waals distance of 3·40Å found in aromatic hydrocarbons.

(ii) Molecules in adjacent stacks frequently form approximately planar sheets.

(iii) Van der Waals attractions and repulsions frequently lead to the acceptor molecule being tilted with respect to the 8-hydroxyquinolinate plane.

(iv) The Mulliken "Overlap and Orientation" principle is rarely

obeyed, particularly if interactions between atoms of the acceptor and the metal atom are strong.

(v) The stoicheiometries of the compounds depend on the possibility of specific interactions between atoms of the acceptor and the metal atom, the complexing strength of the acceptor molecule, and the relative lattice packing efficiencies of alternative stoicheiometries.

Apart from effects specifically due to the metal atoms, these structures are of the same type as those of organic molecular complexes

Reflection spectra of the complexes show broad, intense bands in the visible region of the spectrum, not present in the spectra of the components. These are due to charge transfer from the filled π orbitals of the donor to the vacant π orbitals of the acceptor. Comparison of these bands with those of organic molecular complexes shows that the charge transfer transitions are of the same type as the latter. Spectra are therefore interpreted using the theories developed for organic complexes. Ionization potentials and orbital energies deduced from charge transfer spectra, using these theories, show that the linking together of two 8-hydroxyquinolinate groups through a metal atom raises the energy of the highest filled π orbital, to an extent proportional to the ease with charge transfer between the metal and ligand occurs. Thus, the order of donor power is low spin Ni^{II} > low spin Pd^{II} > Cu^{II} and 5-methyl-8-hydroxyquinolinates > 8-hydroxyquinolinates.

Several of the electron acceptors used are new, and in these

cases spectra of a selection of organic molecular complexes have also been recorded, and the electron affinities of the acceptors have been deduced. The order of electron acceptor power for these acceptors (including trinitrobenzene for comparison) is tetracyanobenzene $\simeq$ dinitrobenzfuroxan $>$ nitrobenzodifuroxan $>$ picryl azide $\simeq$ dichloronitrobenzfuroxan $>$ benzotrifurazan $\simeq$ benzotrifuroxan $>$ trinitrobenzene. This series shows that electron withdrawing groups, such as the cyano or nitro groups, increase electron acceptor power, unless steric factors prevent them from exerting their full influence by preventing conjugation with the rest of the molecule.

Infra-red spectra of the complexes closely resemble the superimposed spectra of the component molecules, showing that the percentage of charge transfer character mixed into the ground states of the complexes is small. Small shifts of 20 $cm.^{-1}$ or less in some of the bands of the complex are attributable to this small amount of charge transfer character in the ground state.

Electron spin resonance spectra of single crystals of palladium 8-hydroxyquinolinate/chloranil doped with 0·1, 1·0 and 10 percent of the isostructural copper complex, have been recorded. These show four sets of lines, due to interaction of the unpaired electron with the nuclear spin of copper (3/2), each set comprising five hyperfine lines, due to delocalisation of the electron onto the nitrogen atoms of the ligands. In the most dilute sample, the five hyperfine lines are each resolved into three extra-hyperfine lines, possibly due to further delocalisation onto the hydrogen atoms on the carbon atoms

adjacent to the nitrogens. The line width increases more rapidly between 1 and 10 percent of copper complex present than between 0·1 and 1 percent. This is a consequence of the structure, in which each 8-hydroxyquinolinate molecule has ten near neighbours of the same type, and suggests that the copper complex molecules are distributed evenly in the lattice. A regular dependence of the shape and position of the spectrum on the orientation of the crystal with respect to the field was observed, but a more accurate means of orientating the crystal is required before these results can be interpreted with certainty.

An apparatus capable of measuring the photoconductivity of single crystals with resistances of up to $10^{15}\Omega$ at different wavelengths at room temperature has been constructed and tested. All the complexes which could be obtained as large single crystals were examined for photoconductivity properties, and 8-hydroxyquinoline/tetracyanobenzene and copper and palladium 8-hydroxyquinolinate/chloranil complexes were found to photoconduct. The spectral response curves of photoconductivity show two regions of response related to the intermolecular charge transfer absorption band of the complex, one to high energy and the other to low energy of the absorption band. To elucidate the mechanism of photoconduction, a series of crystals containing from 0 to 30 percent of copper 8-hydroxyquinolinate/chloranil doped into the corresponding palladium complex was prepared. The copper content of these crystals was determined using the milliprobe x-ray fluorescence technique. The resistivities of

the crystals vary considerably as the copper content changes. From these results, it has been deduced that the two regions of response are caused by different mechanisms. The high energy response is due to formation of highly energised ion pairs, produced by charge transfer from an excited donor molecule to an acceptor molecule, induced by light of energy corresponding to the region of overlap between inter- and intra- molecular charge transfer transitions. The low energy response is caused by the trapping of the negative charge of a normal ion pair, produced by the intermolecular charge transfer transition, leaving the positive hole free to migrate over a network of neighbouring donor molecules. The copper complex donors act as electron traps, and, at high copper concentrations, as positive hole traps. The possible relevance of these results to the mechanism of the primary quantum conversion act in photosynthesis is discussed briefly.